

MESENCHYMAL STEM CELLS IN AN OVINE MODEL OF KIDNEY TRANSPLANTATION

A Thesis submitted to the University of Adelaide as the requirement for the degree of Doctor
of Philosophy in medicine (PHMED)

By

Bron D Lett (BSc, MSc)

Department of Medicine, University of Adelaide, Adelaide Australia

November 2018

Table Of Contents

Abstract.....	9
Declaration.....	10
Abbreviations.....	11
Chapter 1.....	17
General Introduction.....	17
Part 1.....	19
1.1 Transplantation History.....	19
1.2 Transplant Immunology.....	20
1.2.1 The ABO Blood System.....	20
1.2.2 The Major Histocompatibility Complex.....	21
1.2.3 Human Leukocyte Antigen.....	24
1.2.4 Tissue Typing.....	24
1.2.5 Sheep MHC.....	27
1.3 Rejection Immunology.....	28
1.3.1 Cellular Immunity.....	28
1.3.2 The Humoral Immune System.....	33
1.3.3 The Innate Immune System.....	35
1.4 Immunosuppressant Drugs.....	38
1.4.1 Calcineurin Inhibitors.....	39
1.4.2 Antiproliferative Drugs.....	40
1.4.3 Glucocorticoid Steroids.....	40
1.4.4 mTOR Inhibitors.....	42
1.5 Non-Immune Organ Damage.....	43
1.5.1 Ischemia.....	44
1.5.2 Reperfusion.....	45
1.6 Organ Preservation.....	46
1.6.1 Preservation Solutions.....	47
1.6.1.1 Collins Solution.....	47
1.6.1.2 University of Wisconsin Solution.....	47
1.6.1.3 Histidine-Tryptophan-Ketoglutarate Solution.....	49
1.7 Donor Sources.....	50
1.8 Cellular Therapies.....	53

1.9	Mesenchymal Stem Cells.....	54
1.9.1	History.....	54
1.9.2	Characteristics.....	56
1.9.3	Immunosuppression By MSCs.....	56
1.9.4	Pathways Of MSC Immunosuppression	57
1.9.4.1	Adenosine Accumulation.....	57
1.9.4.2	PD-L1/PD1	58
1.9.4.3	Cyclooxygenase	58
1.9.4.4	PGE2.....	58
1.9.4.5	Transforming Growth Factor Beta (TGF- β)	59
1.9.4.6	Inducible Nitrous Oxide (iNOS).....	60
1.9.4.7	Indolamine 2,3-Dioxygenase (IDO).....	60
1.9.5	Impact On Immune Cells.....	61
1.9.5.1	Dendritic Cells	62
1.9.5.2	Regulatory T-cells.....	62
1.9.5.3	T Helper Cells.....	63
1.9.5.4	CD8 Cytotoxic T-cells	63
1.9.5.5	B-cells	64
1.9.5.6	NK Cells.....	64
1.9.6	MSCs In Different Species	66
Part 2.....		68
MSCs as a Therapy to Improve Kidney Transplantation		68
1.10	Animal Models.....	68
1.11	Clinical Trials Of MSCs In Kidney Transplantation	72
1.11.1	Pilot Studies	72
1.11.2	Clinical Trials.....	76
1.12	Safety	79
1.13	Concluding Summary	80
1.14	Thesis Aims	82
Chapter 2.....		83
General Methods and Materials		83
2.1	Ethics	83
2.2	Animals.....	83
2.3	Animal Handling.....	83

2.4 Animal Procedures.....	84
2.5 Central Venous Lines.....	85
2.6 Magnetic Resonance Imaging.....	85
2.7 Necropsy.....	86
2.8 Stimulation Of PBMC.....	87
2.8.1 MLR.....	87
2.8.2 ConA.....	87
2.9 Isolation Of MSCs.....	88
2.10 Tripsinizing Adherent Cells.....	89
2.11 Expansion of MSCs.....	89
2.12 Freezing Cells.....	89
2.13 Thawing Frozen Cells.....	90
2.14 Flow Cytometry.....	90
2.14.1 One Colour Analysis.....	90
2.14.2 Cell Surface Markers.....	91
2.15 MSC Differentiation.....	92
2.15.1 Adipogenic Differentiation.....	92
2.15.2 Chondrogenic Differentiation.....	92
2.15.3 Osteogenic Differentiation.....	92
2.16 Viability.....	93
2.17 DNA Extraction.....	93
2.18 Primer Design.....	94
2.19 PCR Optimisation.....	95
2.20 Agarose Gel Electrophoresis.....	96
2.21 Sequencing.....	97
2.22 Pharmacology.....	97
2.23 ELISA.....	97
2.24 Banff Grading.....	98
2.25 Appendix A: Pharmaceuticals.....	98
2.26 Appendix B: Reagents used.....	100
2.27 Appendix C: Formulations and solutions.....	102
Chapter 3.....	106
MSC Characterisation.....	106
3.1 Introduction:.....	106
3.1.1 MSC Characteristics.....	106

3.1.2 Differences Between Species	107
3.1.3 Ovine Mesenchymal Stem Cells	108
3.1.4 Chapter Aims	111
3.2 Materials and Methods:.....	112
3.2.1 MSC Isolations.....	112
3.2.2 MSC Expansion	113
3.2.3 Freezing Cells	113
3.2.4 Thawing Frozen Cells	113
3.2.5 Flow Cytometric Analysis	114
3.2.6 Adipogenic Differentiation	114
3.2.7 Chondrogenic Differentiation	115
3.2.8 Osteogenic Differentiation.....	115
3.2.9 Immunosuppression Of Stimulation Assays	115
3.2.10 Immunosuppression Of Mixed Lymphocyte Reactions (MLRs).....	116
3.2.11 Morphology.....	116
3.2.12 Staining With SPIO.....	117
3.2.13 Viability	117
3.2.14 Prussian Blue	118
3.2.15 Iron Spectrophotometry	118
3.3 Results:.....	120
3.3.1 General Results	120
3.3.2 Flow Cytometry	120
3.3.3 Morphology.....	120
3.3.4 Differentiation.....	124
3.3.5 Viability	124
3.3.6 Immunosuppression Of MLRs.....	126
3.3.7 Staining With SPIO.....	128
3.3.8 Prussian Blue Staining	128
3.3.9 Spectrophotometric Analysis	130
3.3.10 Impact Of SPIO On Viability.....	136
3.3.11 Flow Cytometry Analysis Of SPIO-MSCs	136
3.3.12 Differentiation Of SPIO-MSCs.....	136
3.3.13 Immunosuppression Of Con-A Stimulation Assays	140
3.4 Discussion:.....	142

Chapter 4.....	146
Optimisation of the Ovine Heterotopic Kidney Transplant Model	146
4.1 Introduction:.....	146
4.1.1 Large Animal Models	146
4.1.2 Animal Models Of Ischemic Reperfusion Injury.....	148
4.1.3 Large Animal Models Of Kidney Allotransplantation.....	150
4.1.4 Ovine Major Histocompatibility Complex.....	151
4.1.5 The Ovine Heterotopic Kidney Transplant Model.....	152
4.1.6 Chapter Aims:	152
4.2 Materials and methods:	153
4.2.1 Tissue Mismatching Sheep	153
4.2.2 Blood Collection	153
4.2.3 Mixed Lymphocyte Reaction.....	153
4.2.4 DNA Isolation.....	153
4.2.5 Design Of Primers.....	154
4.2.6 PCR	154
4.2.7 Sequencing	155
4.2.8 Pharmacokinetics	155
4.2.9 Transplant Procedure	156
4.3 Results:.....	161
4.3.1 MLR.....	161
4.3.2 PCR	161
4.3.3 Sequencing	165
4.3.4 Pharmacology	171
4.3.5 Development Of Surgical Protocol	173
4.3.5.1 Sheep Grey 7, Occluded Right Hand Jugular Subsequent To Venepuncture	173
4.3.5.2 Sheep Pink 3, Occlusion Of The Right Hand Jugular Around The CVC Resulting In Facial Oedema	174
4.3.5.3 Sheep Pink 5, Excessive Swelling Of The Transplant Site, Reopening The Wound..	177
4.3.5.4 Sheep Pink 6, Incorrect Kidney Placement.....	180
4.3.5.5 Sheep Pink 8, Infection Of The Kidney Post Biopsy	180
4.2.5.6 Sheep Pink 14, Post Transplant Wedge Biopsy Causing Haemorrhage	181
4.4 Discussion:	181
Chapter 5:.....	185

MSC Tracking in Autotransplantation.....	185
5.1 Introduction:.....	185
5.1.1 Tracking MSCs	185
5.1.2 The Ovine Model Of Kidney Heterotopic Autotransplantation.....	188
5.1.3 Detecting The Presence Of Iron Label Using Pixel Intensity	189
5.1.4 Analysis Of MRI Images With ImageJ.....	190
5.1.5 Chapter Aims:	191
5.2 Materials and methods:	191
5.2.1 Preparation Of MSCs.....	191
5.2.2 Labelling MSCs With SPIO.....	192
5.2.3 Surgery.....	192
5.2.4 Administration Of MSCs	193
5.2.5 MRI Tracking.....	193
5.2.6 Kidney Biopsies	194
5.2.7 Histology.....	194
5.2.8 Prussian Blue Staining	195
5.2.9 Quantification Of MSCs	196
5.3 Results:.....	196
5.3.1 Sheep Pink B14.....	196
5.3.2 Sheep Red 15	198
5.3.3 Sheep Red 16	202
5.3.4 Sheep Red 19	206
5.3.5 General Results	210
5.4 Discussion:.....	214
Chapter 6.....	217
Impact of MSCs on Kidney Allotransplants.....	217
6.1 Introduction:.....	217
6.1.1 Benefits Of Direct Arterial Administration Of MSCs	217
6.1.2 Direct Arterial Administration In Small Animal Models Of Kidney Transplantation.....	218
6.1.3 Direct Arterial Administration In Large Animal Models Of Solid Organ Transplantation	220
6.1.4 Chapter Aims:	223
6.2 Materials and Methods:.....	223
6.2.1 MLRs	223

6.2.2 Sequencing	223
6.2.3 Preparation Of MSCs	224
6.2.4 Heterotopic Kidney Allograft Surgery	224
6.2.5 Administration Of MSCs	226
6.2.6 Punch Biopsies Of The Transplanted Kidney	226
6.2.7 Histology	226
6.2.8 Blood Sampling	227
6.2.9 Pharmacology	227
6.2.10 Urine Samples	227
6.2.11 ELISA	227
6.3 Results:.....	228
6.3.1 Mixed Lymphocyte Reactions	228
6.3.2 Tissue Typing.....	231
6.3.3 Control Sheep.....	233
6.3.3.1 Sheep Pink 7	233
6.3.3.2 Sheep Pink 11	236
6.3.4 MSC Sheep	239
6.3.4.1 Sheep Red 21	239
6.3.4.2 Sheep Red 25	244
6.3.5 Results Comparison	248
6.4 Discussion:.....	253
Chapter 7.....	257
Concluding discussion	257
7.1 Ovine Mesenchymal Stem Cells	257
7.2 Ovine Heterotopic Kidney Transplant Model.....	258
7.3 <i>In Vivo</i> Tracking Of Mesenchymal Stem Cells.....	260
7.4 Mesenchymal Stem Cells In Kidney Transplantation.....	262
7.5 Future Directions	263
7.6 Concluding Statement:.....	264
Bibliography	265

Abstract

Mesenchymal stem cells (MSCs) have the potential to address current issues in transplantation with their immunosuppressive and regenerative abilities. MSCs as a therapy to improve kidney transplant outcomes have already been taken to the clinical trial stage. The results of these trials have, unfortunately, been disappointing with no significant improvements seen over current transplant outcomes. A return to basic science will help to answer many of the questions surrounding the best methods for the use of MSCs in transplantation medicine. To this end this thesis has set out to examine the application of MSCs in a sheep model of heterotopic kidney transplantation.

Chapter 3 describes the isolation, characterisation, and labelling of MSCs with a superparamagnetic iron oxide (SPIO) nano particle that can be used to track the cells using MRI and Prussian blue staining. Importantly, labelling the cells with the SPIO did not have an impact on their phenotype or function. In Chapter 5, the SPIO-MSCs then had their migration tracked when delivered systemically in a sheep kidney autotransplantation model, the development of which is described in chapter 4. The observations indicated the cells passed through the transplanted kidney at 15 minutes post administration but had dispersed by 30 minutes. Upon histological study, significantly more cells had been found to localize to the transplanted kidney than to the native kidney.

Lastly, chapter 6 details the effects of MSCs delivered into the artery of kidney allografts. Looking at the creatinine, urea, and kim-1 levels of sheep early after transplantation and later

undergoing rejection, gave suggestions that MSCs could reduce kim-1 levels soon after transplantation and may reduce some aspects of rejection. Additionally, the MSCs did not negatively impact the transplanted kidney, demonstrating the safety of delivering the cells arterially.

Declaration

I certify that this work contains no material which has been accepted for the award of any other degree or diploma in my name in any university or other tertiary institution and, to the best of my knowledge and belief, contains no material previously published or written by another person, except where due reference has been made in the text. In addition, I certify that no part of this work will, in the future, be used in a submission in my name for any other degree or diploma in any university or other tertiary institution without the prior approval of the University of Adelaide and where applicable, any partner institution responsible for the joint award of this degree.

I give permission for the digital version of my thesis to be made available on the web, via the University's digital research repository, the Library Search and also through web search engines, unless permission has been granted by the University to restrict access for a period of time.

I acknowledge the support I have received for my research through the provision of an Australian Government Research Training Program Scholarship.

Bron D Lett

Abbreviations

4EBP1	eukaryotic initiation factor 4e binding protein-1
6-MP	6-mercaptopurine
A2A	A2A adenosine receptor
ABPAS	Alcian blue and Periodic acid–Schiff
AGRF	Australian genome research facility
α -mem	alpha minimum essential media
AP-1	Activator protein-1
APC	Antigen presenting cell
ARF	Acute renal failure
ATP	Adenosine tri-phosphate
BAFF	B-cell activating factor
cAMP	Cyclic adenosine monophosphate
CCL15	Chemokine ligand 15
CD	Cluster of differentiation
CDC-XM	Complement dependent cytotoxicity crossmatch
cGMP	Cyclic guanosine monophosphate
	Chloromethylbenzamido-1,1'-Dioctadecyl-3,3,3,3'-Tetramethylindocarbocyanine
CM-Dil	Perchlorate

CNIs	Calcineurine inhibitors
Con-A	Concavalin-A
COX2	Cyclooxygenase 2
CPM	Counts per minute
CSIRO	Commonwealth Scientific and Industrial Research Organisation
CTL	Cytotoxic T-lymphocyte
CVC	Central venous catheter
CyA	Cyclosporine
DAA	Direct arterial administration
DAPI	4'-6'-diamidino-2-phenylindole
DBD	Donation subsequent to brain death
DCs	Dendritic cells
DLC	Dynamic lung compliance
DMSO	Dimethyl sulfoxide
DNA	Deoxyribose nucleic acid
ECD	Extended criteria donor
EDTA	Ethylenediaminetetraacetic acid
eIF4A	eukaryotic initiation factor-4A
eIF4E	eukaryotic initiation factor-4E
eIF4G	eukaryotic initiation factor-4G
EV	Extracellular vesicle
FACs	Fluorescence-activated cell sorting
FBS	Fetal bovine serum
FGF-2	Basic fibroblast growth factor
FKBP12	FK506 binding protein 12

FOXP3	Forkhead box P3
GPAT	Glutamine-phosphoribosyl phosphate aminotransferase
GR	Glucocorticoid receptor
GREs	Glucocorticoid receptor response elements
GS	Glucocorticoid steroids
H&E	Hematoxylin and eosin
H2O2	Hydrogen peroxide
HES	Hydroxyethyl starch
HIV-1	Human immunodeficiency virus -1
HLA	Human leukocyte antigen
HSC	hematopoietic stem cells
I.M	Intra muscular
I.V	Intra venous
ICAM-1	Intercellular Adhesion Molecule 1
IDO	Indolamine 2,3-Dioxygenase
IF	Interferon
IF- γ	Interferon gamma
I κ B	inhibitor of kappa B
IL-1	Interleukin-1
IL-1B	Interleukin-1B
IL-2	Interleukin-2
IL-3	Interleukin-1
IMPDH	Inosine monophosphate dehydrogenase
iNOS	Inducible nitric oxide synthase
IRI	Ischemia reperfusion injury

ISCT	The International Society for Cellular Therapy
JAK	Janus kinases
LARIF	Large animal research and imaging facility
LoD	Limit of detection
LoQ	Limit of quantification
MAC	Membrane attack complex
MHC	Major histocompatibility complex
MIP	Macrophage inflammatory protein
MIRB	Molday ION Rhodamine-B
MLR	Mixed lymphocyte reaction
MRI	Magnetic resonance imaging
mRNA	Messenger ribose nucleic acid
MSC	Mesenchymal stem cell
mTOR	Mammalian target of Rapamycin
MVs	Microvesicles
NBF	Neutral buffered formalin
NBHD	Non-beating-heart-donors
NF- κ B	Nuclear factor kappa-light-chain-enhancer of activated B cells
nGREs	Negative glucocorticoid receptor response elements
NK	Natural killer cell
NKG2D	Natural killer group 2, member D
NME	New molecular entity
NMR	Nuclear magnetic resonance
NO	Nitrous oxide
OLA	Ovine leukocyte antigen

OPTN	Organ procurement and transplantation net work
PBMC	Peropheral blood mononuclear cell
PBS	Phospahte buffered solution
PCR	Polymerase chain reaction
PCR-SBT	Direct sequencing HLA typing
PCR-SSP	Sequence based primers HLA typing
PD-1	Programmed cell death protein 1
PD-L1	Programmed death-ligand 1
PEPCK	Phosphoenolpyruvate carboxykinase
PGE2	Prostaglandin E2
PKG	cGMP-dependent protein kinases
PVR	Pulmonary vascular resistance
RNA	Ribose nucleic acid
RPMI	Roswell park memorial institute medium
S6K1	S6 kinase 1
SC	Subcutaneously
SCD	Standard criteria donors
SDS	Sodium dodecyl sulfate
SKAR	Polymerase delta-interacting protein 3
SNX9	Sorting nexin-9
SOT	Solid organ transplantation
SOX2	Sex determining region Y-box 2
SPIO	Superparamagnetic iron oxide
SPIO-MSC	Superparamagnetic iron oxide labelled mesenchymal stem cells
SRTR	Scientific registry of transplant recipients

SSO	Sequence based oligonucleotide HLA typing
STAT	signal transducer and activator of transcription
T	Tesla (measurement of magnetic fields)
TAE	Tris base, acetic acid and EDTA.
TAT	Trans-activator for transcription
Tc-99m	technetium-99m
TCR	T-cell receptor
TERT	Telomerase reverse transcriptase
TGF- β	Transforming growth factor beta
Th	T helper cell
TNF	Tumor necrosis factor
T-Reg	T-regulatory cell
USPIO	Ultra small superparamagnetic iron oxide particle
UW	University of Wisconsin solution
VCAM-1	Vascular cell adhesion molecule 1
VEGF	Vascular endothelial growth factor
XM	cross-match
XRII	X-ray image intensifier

Chapter 1

General Introduction

The advent of solid organ transplantation has led to remarkable changes in health outcomes. Conditions that were once fatal are now able to be overcome regularly with excellent quality of life. The continued advancement of transplantation medicine has thus far added 2,270,859 life years to the US population alone in the last 25 years, with kidney transplantation accounting for 60% of this [1]. This representation is unsurprising given that kidney transplantation is by far the most numerous type of solid organ transplantation, with 19,060 being carried out in the US in 2016 (Based on OPTN data as of December 2017). On average a kidney allograft can be expected to survive for 12 years, a significant achievement given the many challenges inherent in the procedure [1]. However, the demand for viable kidneys still vastly outweighs the supply. In Australia, at the beginning of 2017, there were 1067 patients on the wait list for a kidney transplant. That year a total of 794 kidney transplant procedures were performed, unfortunately, 820 new patients were added to the list during this time [2]. This shortfall is predicted to get worse as the population continues to

age, which will result in both a greater incidence of kidney failure, and the potential for poorer transplantation outcomes in the elderly [3-5].

Given the current and predicted deficit of viable organs it is paramount that steps are taken to, not only ensure the survival of kidney grafts, but to also increase the depth of the pool of potential organs. Cellular therapies have the potential to address both of these issues through a combination of immunobiology and regenerative medicine. Mesenchymal stem cells (MSCs) have received a considerable amount of investment as a cellular therapy with ongoing clinical trials using MSCs in a plethora of conditions, from ulcerative colitis and knee cartilage repair to the full gamut of solid organ transplants. www.clinicaltrials.gov currently lists 781 trials involving MSCs, 235 of which involve the application of MSCs to transplantation.

Taking a potential treatment to clinical trials is a major undertaking and requires significant pre-clinical research and investment and large animal models are a valuable resource in the translational steps of this process. Sheep have found a great deal of favour in translational research for a number of reasons. They are easy to handle and have an agreeable disposition, they possess a size comparable to humans in both body and internal organs, and they are able to replace the use of primates, which have fallen out of favour.

This chapter will focus on the application of MSCs to kidney transplantation including their intersection with transplant immunology, the current information garnered from animal studies, and the contemporary state of human pilot studies and clinical trials. Overviews of several topics such as transplant immunology, the history of transplantation, and the history of mesenchymal stem cells are included as background information. Where applicable, information relevant to ovine research is also discussed, as sheep are the model animal made use of in this work.

Part 1

1.1 Transplantation History

The first successful solid organ transplant was carried out in 1954 by Joseph Murray [6, 7]. Until this procedure all other solid organ transplants had failed, if not due to surgical complications then the eventual rejection of the graft. Murray managed to prevent rejection by having an identical twin donate his kidney to his sibling. The impetus for performing what, at the time, was a radical procedure was provided by the observations of skins grafts carried out between identical twins, which were able to survive permanently, unlike skin grafts carried out between genetically diverse individuals [8]. Additionally, their work with kidney autografts in dogs provided evidence that a transplanted kidney could function for prolonged periods [8]. The years following the first kidney transplant heralded the beginning of an era of significant progress for solid organ transplantation, with the first lung transplant in 1963 [9-11], the first pancreas transplant in 1966, and 1967 being the year of both the first liver and the first heart transplant [10, 11].

Today, transplantation is a common occurrence at many centres all over the world with 33,610 transplants being carried out in the USA in 2016 alone (Based on OPTN data as of December 2017). There are several advancements that have made transplantation on this scale, not only possible, but safe and dependable, including a greater understanding of immunology, tissue typing, the discovery of immunosuppressants, and organ preservation techniques.

1.2 Transplant Immunology

1.2.1 The ABO Blood System

When seeking to understand how the immune system impacts graft survival it is first important to understand some of the key immune molecules that play a role in allorecognition.

The ABO blood system provides an interesting look at the genetics and physiology of the immune response to allogeneic tissue, cells, and molecules [12]. Using this system the blood type of an individual is denoted as either A, B, O, or AB [13]. This is determined by a single gene, the ABO gene, with 3 allelic variants, *i*, *I^A*, and *I^B*.

This gene encodes a glycosyltransferase which acts upon antigen H, turning it into either antigen A or antigen B. The *I^A* and *I^B* alleles give rise to the variations of the enzyme that create the A and B antigens, respectively, and hence phenotypes, while the *i* allele results in an inactive enzyme, having no impact on antigen H. The *I^A* and *I^B* alleles interact with the *i* allele in a dominant/ recessive fashion, meaning that in order for someone to possess the O phenotype they need to be homozygous for the *i* allele.

The interaction between *I^A* and *I^B* is one of co-dominance meaning that when an individual inherits one of each of these alleles they have the AB phenotype which expresses both proteins. A person with A type blood, and hence producing antigen A, will create antibodies against Antigen B as it is a foreign antigen to them. The same goes for a person with B type blood and antigen A. An individual with type O blood who produces neither antigen A or B will have antibodies against both of these. And finally, someone with type AB blood will not have antibodies against either antigen A or B as both of these are recognized as self [13].

This sets up a system where type O blood is a universal donor, as it will not create an immune response, and a person with type AB blood is a universal recipient as they will not have an immune response to the donated blood. This system gives a useful illustration of the importance of tissue matching and is one of the most important aspects of transplantation biology with ABO incompatible transplants being considered a contraindication until the advent of sophisticated immunosuppressive regimes allowed graft survival rates comparable to ABO compatible transplants [12, 14].

1.2.2 The Major Histocompatibility Complex

The ABO blood system finds its greatest importance in ensuring compatibility of blood donors and recipients and although it does have a role in solid organ transplantation, there is another class of molecules that are central to tissue typing. These are the molecules of the major histocompatibility complex or MHC.

MHC molecules are vital to the functioning of the immune system as they are responsible for the presentation of antigen to immune cells. The molecules are divided into class I, class II, and class III, with class I and class II creating membrane bound antigen presenting proteins while class III produces secreted molecules that are crucial to immune function such as complement factors and cytokines [15, 16].

Class I MHC, which is present in all cells excluding red blood cells unless in a disease state [17], consists of two polypeptide chains, the α and the β 2-microglobulin. The α chain consists of 3 domains and is highly polymorphic while the β 2-m chain is monomorphic. The α 3 domain is a transmembrane protein that interacts with the CD8 co-receptor found on cytotoxic T-cells and acts to hold the t-cell receptor in place as it interacts with the α 1 and α 2 domains which create the groove into which peptides are bound for display [15, 18, 19].

In a healthy cell, the MHC I proteins will display self-antigen generated from normal cellular processes. This will not induce an immune response, in contrast to the scenario that occurs when foreign peptides are presented. In the instances involving foreign peptide, the CD8 T-cells move towards activation, which in the presence of the required co-stimulatory molecules, will result in the t-cell releasing a raft of cytotoxins that cause the apoptosis of the presenting cell [20]. Additionally, it will make the T-cell, with the help of interleukin-2 (IL-2), undergo clonal expansion multiplying the number of T-cells specific for the particular antigen.

The sources of peptides that will result in activation of CD8 T-cells are varied. Primarily, it is a system that acts to detect cells that have been infected by intracellular pathogens such as viruses and several forms of bacteria [21]. The MHC I complex is also able to aid in the detection of aberrant proteins that may be associated with mutated cells such as in the case of cancer [22].

Lastly, there is cross-presentation in which the antigen presenting cell (APC) is able to take up free exogenous antigen and present it through the MHC I complex. Cross-presentation finds a function in the immune response to tumour cells and viruses that do not target APCs [23]. Furthermore, MHC I finds a role as an inhibitory ligand of natural killer (NK) cells. This function comes to the forefront when a cell becomes infected by a pathogen capable of down regulating MHC I expression to avoid detection by CD8 T-cells [22].

Class II MHC is predominantly associated with professional antigen presenting cells such as dendritic cells. MHC II is concerned with the presentation of exogenous antigens acquired through phagocytosis of foreign bodies. This material is then broken down into peptide fragments, attached to MHC II and presented to CD4 T-cells [18].

MHCII is composed of an α and a β chain each with two domains. The $\alpha 1$ and $\beta 1$ domains are responsible for the formation of the binding site the exogenous antigen occupies as it is probed for identification by the T-cell receptor (TCR) of CD4 T-cells [15]. The $\beta 2$ domain acts as an anchoring site for CD4, which is the co-receptor found on T-helper cells. When recognition of a peptide/MHCII configuration is achieved by a naive helper T-cell, in the presence of the correct co-stimulators, it becomes activated. An activated T-helper cell is able to be driven down several pathways depending on the cytokines that are being expressed by the APC.

T-helper cells are able to differentiate into both memory cells and effector cells. Effector cells can further differentiate into several subtypes [24, 25]. Memory T-cells are responsible for mounting a rapid immune response should the antigen that first activated them be encountered again [26], whereas effector cells play a crucial role in the response garnered from the other immune cells [25]. The two major subgroups of effector cells are the Th1 and Th2 cell types, each having an impact on different aspects of the immune system.

Differentiation into Th1 is triggered by IL-12 [27] IL-2 [28] and several other cytokines, and they influence CD8 T-cells and macrophages through the secretion of interferon γ [27]. This results in a targeted stimulation of the cellular immune system with increased proliferation of cytotoxic T-cells and making macrophages more efficacious [25]. Th2 T-cells are created in response to exposure to IL-4. Through a wide variety of cytokines, including IL-4, IL-5, and IL-13, they act upon the humoral immune system stimulating B-cells, eosinophils, and mast cells [29]. Both of these cell types also create positive feedback loops that result in stronger activation of their pathway. Th1 achieves this by the release of INF- γ , which causes a release of IL-12 from dendritic cells and macrophages. While Th2 cells release IL-4, which has a direct impact on undifferentiated T-helper cells, as well as secreting IL-10, a cytokine that suppresses Th1 differentiation [24, 25].

1.2.3 Human Leukocyte Antigen

In humans, the major histocompatibility complex is referred to as the human leukocyte antigen or HLA. As with all MHC complexes, humans have class I and class II HLA proteins, all of which are encoded on chromosome 6 [30]. Both classes have three loci of genes that encode antigen presenting proteins. Class I genes are HLA-A, HLA-B, and HLA-C with HLA-B and HLA-C being in linkage disequilibrium. While the Class II protein encoding genes are HLA-DR, HLA-DQ, and HLA-DP.

All six of these genes are expressed in the body for a possible total of 12 HLA antigen presenting proteins expressed when allelic homozygosity is taken into account [30]. There are also various genes that are involved in the regulation of the HLA system, such as HLA-DM which plays a role in the processing of class II HLA proteins by clearing the antigen binding site [31]. Tissue typing for transplantation relies on the matching of these genes and their relevant proteins between the donor and recipient.

1.2.4 Tissue Typing

Choosing an appropriate donor – recipient pairing has several steps. First, a complete history needs to be taken to look for any potentially sensitising events such as blood transfusions, pregnancy, or previous transplants [32]. All of these can result in the development of allorecognition of donor antigen making a transplant much more high risk.

Next, is determining the HLA type of both individuals, which can be done either by serotyping or by genotyping [33]. Serotyping involves culturing lymphocytes with antibodies specific for certain HLA types, then adding a fluoro-chrome. If the cells are lysed and become permeable to the fluoro-chrome, then it indicates that they express the antigen corresponding to the antibody in the culture [34]. This technique is simple and low cost; however it lacks

resolution and may not distinguish or pick up many HLA groups, and as such has been replaced by allelic sequence based typing techniques [35].

There are several different approaches to sequenced based detection of HLA type, sequence based oligonucleotides (SSO), sequence based primers (PCR-SSP), and direct sequencing (PCR-SBT) [35, 36]. Sequenced based oligonucleotides uses immobilised nucleotide probes specific for a wide variety of HLA alleles, if an individual has a certain allele then PCR products from them will bind to the relevant probe [36]. Sequenced based primer tissue typing uses primers that correspond to the point mutations that distinguish one HLA allele from another. Using PCR is then possible to detect single HLA alleles based on what primers are able to bind and amplify [36]. Finally, there is the direct sequence method in which primers are made to amplify specific parts of HLA genes; these are then sequenced giving the specific allele [37]. Each of these techniques has its advantages and disadvantages. The SSO and PCR-SSP techniques can be done very quickly; however they rely on having the correct probe or primer pair for the individual's alleles and the sequence is inferred based on a positive match [36]. PCR-SBT takes longer than the other two techniques but it gives the exact sequence of the HLA genes, meaning that if an uncharacterized allele is present then it will be detected and there will be no ambiguity on the identity of the allele [37].

Once the HLA type of a donor is confirmed, the recipient must then be screened for alloantibody. This is carried out by incubating serum from a prospective recipient with stationary phase bound antigens corresponding to the HLA type of a prospective donor [32]. The serum is then washed off and a fluorescent-conjugated anti-human IgG added which binds to alloantibody bound to an antigenic target. Thus, if a fluorescent signal is detected it indicates the presence of donor specific alloantibody [32]. In the absence of a sensitizing event it is likely that a transplant candidate will have little or no alloantibody detected. However, if alloantigen screening is positive then it is important to perform crossmatch

testing (XM), which is considered the final test to determine the safety of a prospective transplant [32].

If alloantigen testing results in a negative outcome, then given the sensitivity of current methods, XM is usually not required. If it is required then there are several methods available. The complement dependent cytotoxicity crossmatch (CDC-XM) is a longstanding method that is routinely performed at many centres [32, 38]. In this test donor lymphocytes are cultured with recipient serum and complement which allows the membrane attack complex to form if alloantibody is able to bind to donor cells.

There are several variations of this to improve sensitivity and detect non-complement binding donor specific antibody and class II targeted alloantibody [32, 38]. A more recently developed method is the flow cytometric crossmatch (flow XM) in which donor lymphocytes, recipient serum, and a fluorescent labelled anti-human immunoglobulin secondary antibody are cultured together and then run on a flow cytometer. Detection of the secondary antibody infers presence and binding of donor specific antibody in the recipient serum [32, 39].

Using these steps it is possible to determine if a donor-recipient pairing is at a high risk of rejection. However even with perfect matches at all HLA loci, negative donor specific antigen, and no sensitising events, rejection can still occur between unrelated individuals due to the presence of minor histocompatibility antigens, which are peptides that are processed during normal cellular function. These minor peptides are still able to elicit a strong immune response [40].

1.2.5 Sheep MHC

Like all vertebrates, sheep possess a diverse and highly polymorphic major histocompatibility complex, which is referred to as the ovine leukocyte antigen or OLA. The sheep MHC genes cluster on chromosome 20, and while the complete sheep genome sequence is available, the current understanding of the structure and function of the OLA region is poor in comparison to the knowledge about the MHC regions of other animals including humans [41, 42].

The IPD-MHC database (<https://www.ebi.ac.uk/ipd/mhc/>) is a repository of MHC sequences from a variety of different species, including sheep. They currently only have data on a single class I MHC, Ovar-N [42], and two class II MHC, Ovar-DRA [43] and Ovar-DRB1 [44] (Ovar being the prefix for identifying the sheep, *Ovis Aries*). Currently, Ovar-N has 26 confirmed alleles [42, 45], Ovar-DRA has 3 confirmed alleles [43, 46-50], and Ovar-DRB1 possesses 106 confirmed alleles [44, 47, 49-53] (As per the IPD-MHC database as of August 2018).

As evidenced by the number of alleles, there is considerable polymorphism in the Class II DRB1 loci, this is characteristic of this gene and is similar to its homologues in other species. Exon 2 is often the focus of genotyping of class II DRB genes due to the high level of polymorphic variation and its role in coding a protein domain which is involved in the binding of peptide [19]. In this way, polymorphisms in exon 2 of the DRB genes, directly contribute to the diversity of antigens that can be recognized by the immune system and sheep are no exception to this [50]. The tendency of DRB1 to be expressed at levels several times higher than other class II MHC genes explains why it is often a major focus of tissue typing and why it has been so prominently characterized in the sheep.

There is evidence of other MHC class II genes being present, DQA1, DQB1, DQA2, and DQB2 have all had several alleles discovered [54]. However, as of writing this they are yet to be verified and as such are not included on the IPD-MHC database.

Furthermore, the MHC class I genes of the sheep have additional information about their organisation. Subramaniam (2015) [42] describes the class I OLA genes as clustering into beta, kappa, and a novel block of genes. This structure is similar to that seen in other mammals save for the fact that the alpha block does not contain any peptide presenting genes, unlike the MHC alpha blocks of humans, chimpanzees, horses, and a variety of other animals [42].

As evidenced by the concerted efforts by several groups, there is considerable work going on in the area ovine immune genetics. However, it is still in a nascent state with much of the genomic assembly yet to be fully elucidated or compared to other species.

1.3 Rejection Immunology

1.3.1 Cellular Immunity

The immunology of transplant rejection is complex and invokes aspects of both the innate and adaptive immune system. Cell-based immunity is crucial in the progression of rejection with the ability of T-cells to become activated by donor derived antigens one of the key instigators of the anti-graft immune response. T cells in a transplantation setting can be activated in both a direct and indirect pathway with antigen presenting cells from both the donor and recipient playing a potential role [55-60].

In the direct cellular response, the recipients T-cells are able to react to the donors APCs by recognizing the intact foreign MHC molecules they possess. In order for this to occur, the donors APCs must migrate to the lymphoid tissue to make direct contact with host T-cells,

this is referred to as the passenger leukocyte theory and it results in a robust immune response to the allograft [61]. The most likely candidate to be implicated as the cause of the passenger leukocyte immune reaction is the dendritic cell, a professional antigen-presenting cell.

In a normal immunologic setting DCs act as part of the innate immune response, being tissue bound and one of the first cells to interact with any immune challenge. Their normal function involves the sampling of their environment via pattern recognition receptors until they are able to up take up a presentable antigen upon which time they mature and migrate to the lymph organs and activate T and B cells [62]. In a transplanted graft, donor DCs become activated in response to the abundant inflammatory signals associated with transplantation. The result of this activation is the migration of DCs to the recipient lymphatic organs where they cause the activation of graft specific T-cells [56, 58, 61]. This is possible because T-cells are able to recognise the polymorphic residues of the donor MHC and are able to respond to this even in absence of an alloreactive peptide being bound [63].

Given that the life span of activated dendritic cells is only a couple of days [64] the donor derived APCs will eventually be depleted, meaning that the direct cellular response to an allograft is restricted to this period. The indirect response, which relies on the host DCs, is able to continue unabated. The indirect pathway of transplant rejection follows the system by which the majority of exogenous antigens are detected by the immune system, this allows for a much greater number of antigens to be produced by the grafts as all proteins that are heterozygous to the recipient are able to elicit an immune response.

In the indirect pathway recipient DCs present antigen to CD4 T cells via the peptide/MHC class II pathway, thus allowing the naive CD4 T cells to take the first step to activating and, if the correct co-stimulatory molecules are present, will result in the activation and proliferation of the T helper cell [56, 59]. Interestingly, because immature DCs are able to produce both

peptide/MHC class II complexes and peptide/MHC class I complexes using exogenous antigens they are able to present donor antigens to both T helper cells and to cytotoxic T cells [65].

There are several ways in which APCs are able to obtain the required antigen for activation of T cells from a graft. They are able to take up proteins that have been shed by the graft and are free in circulation [58, 60]; this could be caused by both ischemia reperfusion injury or by mechanical injury, both common occurrences in solid organ transplantation [66, 67]. Similar to the indirect response, donor cells may be able to migrate to areas where they would come into contact with endogenous immune cells. They would be then be phagocytosed by recipient DCs, starting their role as immune stimulating cells. Or finally, the APCs could infiltrate the graft, acquire alloantigen, and then proceed to secondary lymphoid organs for presentation [55, 57].

The ability of T-helper cells to differentiate into either Th1 or Th2 cells upon activation was mentioned in section 1.2.2. However, there are also several other types of T-helper cell including Th9 [68, 69], Th17 [70, 71], Th22 [72, 73], and Tfh [74, 75]. Of these the most relevant to transplant immunology is Th17 which has been shown to play a role in rejection through an IL-17 mediated mechanism [76-79]. T-helper cells are driven toward Th-17 differentiation upon exposure to IL-6, IL-23 [80], IL-21 [81], and possibly TGF- β [70, 82], although there is some conflicting evidence in regards to TGF- β [80]. As the nomenclature suggests, Th-17 cells express the IL-17 family of cytokines which are pro-inflammatory and can induce the production of chemoattractants for neutrophils [83, 84] which, as discussed later, are able to activate both the innate and adaptive immune system in a transplant setting. Additionally, Th-17 cells have some level of resistance to the immunosuppressive abilities of calcineurin inhibitors (CNIs) [85, 86]. The function of Th-17 cells and their ability to not be

impeded by CNIs explains their link to chronic allograft rejection [87] and signifies that Th-17 cells may be a valuable target for improving long term graft survival.

Acting to restrain the effector T-cells are the regulatory T cell (T-regs). T-regs play a crucial part in the shaping of an appropriate immune response and are involved in ensuring tolerance to self antigen and preventing auto-immune disease [88]. They are characterized by their expression of CD4, CD25, and Foxp3 and their impact on immune cells [89]. They are known to express several inhibitory cytokines such as TGF- β and IL-10 which down regulate effector T-cells, and, further to this are able to cause apoptosis of these cells via expression of granzyme B [90]. T-regs also have the ability to disrupt the presentation of antigen to T-cells by direct interaction and suppression of dendritic cells, thus preventing T-cell stimulation [91]. Given these features it is unsurprising that Tregs have received significant attention in attempts to create tolerogenic environments in transplantation [92-94]. Like other immune cells, Tregs are able to differentiate into memory cells that are capable of having a stronger reaction upon exposure to their selected antigen [95, 96]. However, instead of creating a greater and faster immune response, memory Tregs are able to cause greater immune suppression [95, 96], this is of great value in regards to long term tolerance to self antigen. There is difficulty in defining memory Tregs because, unlike memory effector T cells, they do not display significant phenotypic or functional changes upon activation [97]. However, the existence of memory Tregs is well established using various experimental animal models including tissue specific inducible antigen models wherein Tregs were activated by an inducible antigen and then had a stronger response to this antigen upon encountering it again even when these Tregs were transferred to a naive animal [98, 99]. These experiments demonstrated a long term persistence of Tregs in absence of the activating antigen and that these cells have accelerated kinetics upon secondary exposure to the activating antigen.

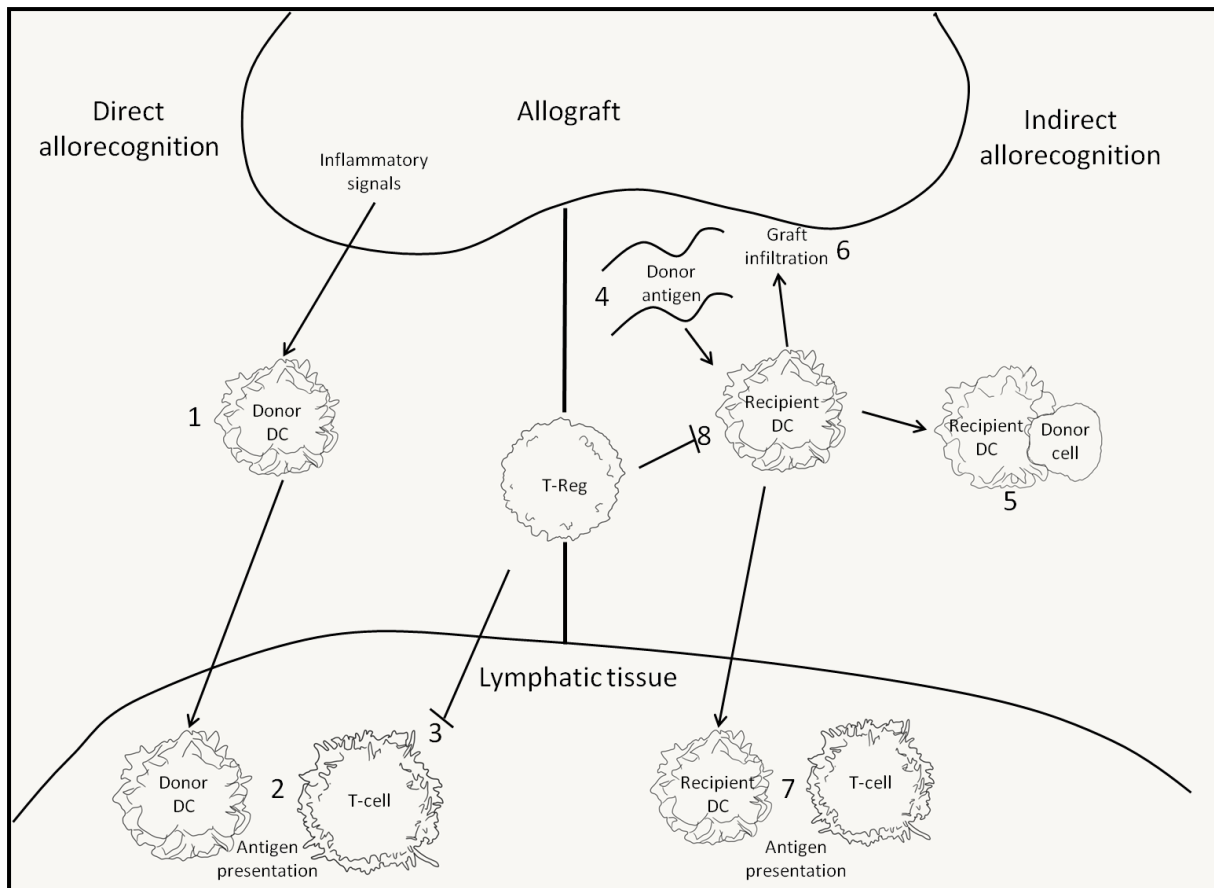


Figure 1.1 The direct and indirect pathways of the cellular response to an allograft. 1) Inflammatory signals from the allograft causes donor derived dendritic cells to move to lymphatic tissues. 2) Once in lymphatic tissue the donor DCs activate the host T-cells resulting in an immune response. 3) T-regs are able to inhibit the activation of host T-cells to donor DCs.

In indirect allorecognition the recipients DCs are able to obtain donor antigen in several ways including 4) taking up free donor proteins, 5) phagocytosing donor cells that have migrated to areas where DCs and resident, or 6) the DCs can infiltrate the graft. Once this occurs the recipient DCs will then 7) move to lymphatic tissue to present to T-cells and trigger an immune response 8) T-regs can also inhibit rejection by preventing the activation of DCs and their subsequent antigen presentation to T-cells.

1.3.2 The Humoral Immune System

A substantial aspect of the immune system is dependent on macromolecules found in the extracellular fluid; this is referred to as the humoral immune system. Of particular importance to solid organ transplantation is the subsection of humoral immunity known as antibody mediated immunity which, as its name suggests, is the actions of the immune system relating to antibodies.

The cellular driver of antibody mediated immunity is the B-cell. B-cells mature in the bone marrow where they acquire a wide array of b-cell receptors each specific for a particular antigen [100]. B-cells then migrate to the lymphatic tissues, once there they may come into contact with an antigen that one of their BCRs recognize, at which point they internalize the antigen and present it on their MHCII molecules allowing for a T helper cell to bind and provide the co-stimulatory signals required for B-cell proliferation and differentiation. At this point the B-cells will rapidly divide and the daughter cells will differentiate into either memory B-cells or plasma cells [100, 101].

Memory B-cells remain in the lymphatic tissue to allow for an immediate and robust immune response should the offending antigen be encountered again [102]. Plasma cells act to produce antibodies specific to the peptide that originally triggered the B-cells [100, 103].

These antibodies are then released into the extracellular fluid where they have several effects including agglutination of specific antigen [104] and acting to effect the destruction of cells displaying the specific antigen [105].

This cellular destruction is achieved through either the complement cascade or complement-independent mechanisms. Activation of the complement cascade results in the formation of the membrane attack complex (MAC) a complex that forms transmembrane channels that disrupt the integrity of the cellular membrane causing cell lysis [106-108].

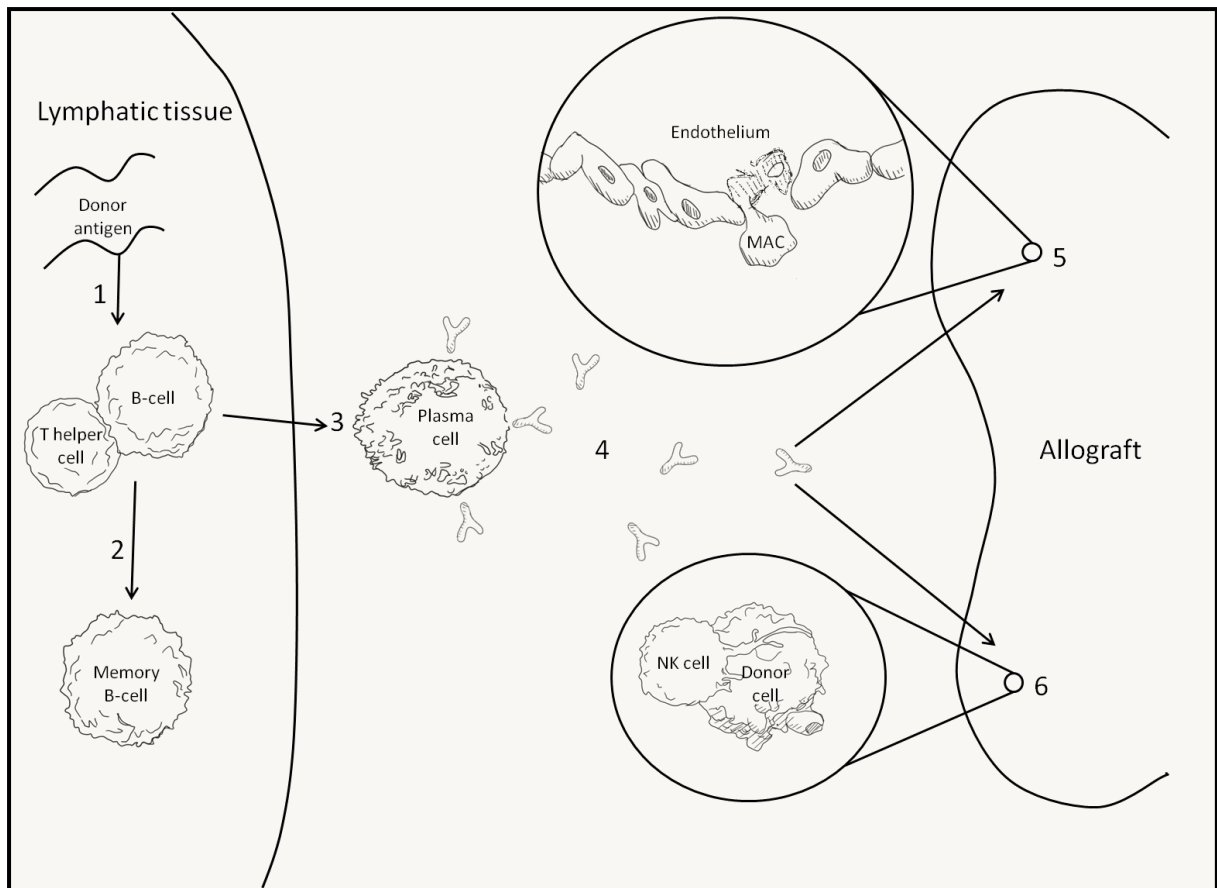


Figure 1.2 The humoral immune response to an allograft. 1) B-cells take up donor antigen and if a T helper cell expressing the correct co-stimulatory molecules is present the B-cell becomes activated. The activated B-cell then differentiates into 2) Memory B-cells, which stay in the lymphatic tissue and act as a rapid response should their activating antigen be encountered again, or 3) Plasma cells which begin to produce antibodies specific to the triggering antigen. 4) These antibodies are released into the extracellular fluid where they will act to allow the immune system to destroy the allograft. This destruction is achieved through either 5) causing the membrane attack complex to bind and disrupt the integrity of allogeneic cell membranes, destroying vascular integrity, or 6) allowing immune cells, such as natural killer cells, to bind to donor cells and carry out their specific cell destruction mechanism.

In a transplanted organ the consequence of this is a loss of vascular integrity. An example of this is found in transplanted kidneys as glomerulitis and capillaritis [109, 110]. Antibodies can also cause tissue lesions via mechanisms that do not rely on the complement cascade and MAC. They are able to do this by allowing NK cells, neutrophils, and macrophages to bind to the antibody coated target cells and triggering their respective cellular destruction methods [111, 112].

As evidenced by the tests that are taken to rule out DSA, the antibodies that represent the most potential harm are targeted to the MHC molecules. However, antibodies directed against other molecules expressed by the donor organ are still able to cause antibody mediated rejection [113].

This can be pertinent when a transplanted organ has undergone cellular damage such as that caused by ischemia reperfusion injury which would result in the release of a wide variety of donor antigens able to trigger a humoral immune response [114]. Even if this is avoided the impact of the antibody mediated immune system can have long term implications and is estimated to be responsible for more than 60% of late graft failure [115].

1.3.3 The Innate Immune System

Some aspects of the innate immune system have already been mentioned as a way in which the humoral immune system can cause cell death in a complement-independent method [111, 112]. Although the adaptive immune system is generally considered the prime mover when speaking about transplant rejection there is mounting evidence that the innate immune system is able to influence rejection and tolerance [116-118].

Inflammation is a key reaction of the innate immune response. It acts to establish a barrier against harmful stimuli and is crucial in initiating tissue repair [119]. Solid organ transplantation has many aspects that result in harmful stressors that will precipitate

inflammation [120]. Oxidative stress is a major cause of cellular damage and is especially prevalent during revascularization of a transplanted organ as returning blood flow after a period of ischemia results in ischemia-reperfusion injury [67], which will be discussed in greater depth later on.

Inflammation caused by the surgical wounds required in transplantation is mainly directed by the granulocytes, in particular mast cells which are tissue resident immune cells that degranulate in response to a variety of stimuli including physical injury [121, 122]. This degranulation results in the release of cell mediator molecules such as histamine, which is responsible for classical inflammatory symptoms such as local edema, warmth, and redness [123]. Mast cells also release powerful chemo-attractants, causing the recruitment of other immune cells to the area of damage [124].

One of the immune cells that migrate in response to these chemokines are the monocytes [125] which give rise to tissue resident dendritic cells and macrophages [126, 127]. High infiltration of macrophages into an allograft is associated with graft loss [117, 128] this is, in part, due the expression of the T-cell chemoattractant, CCL-5 [129, 130]. Macrophages can also play an active role in rejection via phagocytosis, antigen presentation, and production of pro-inflammatory cytokines [128, 131].

Circulating immature DCs are attracted, via a gradient of pro-inflammatory chemokines, to allografts [132]. Once there they mainly act as APCs for donor MHC class II molecules, processing them then migrating to secondary lymphoid tissues where they use the bound allo-MHC peptide to drive T-cell stimulation and differentiation [133, 134]. During their migration they also undergo maturation, causing an up regulation of their co-stimulatory molecules further enhancing their impact on T-cells [132].

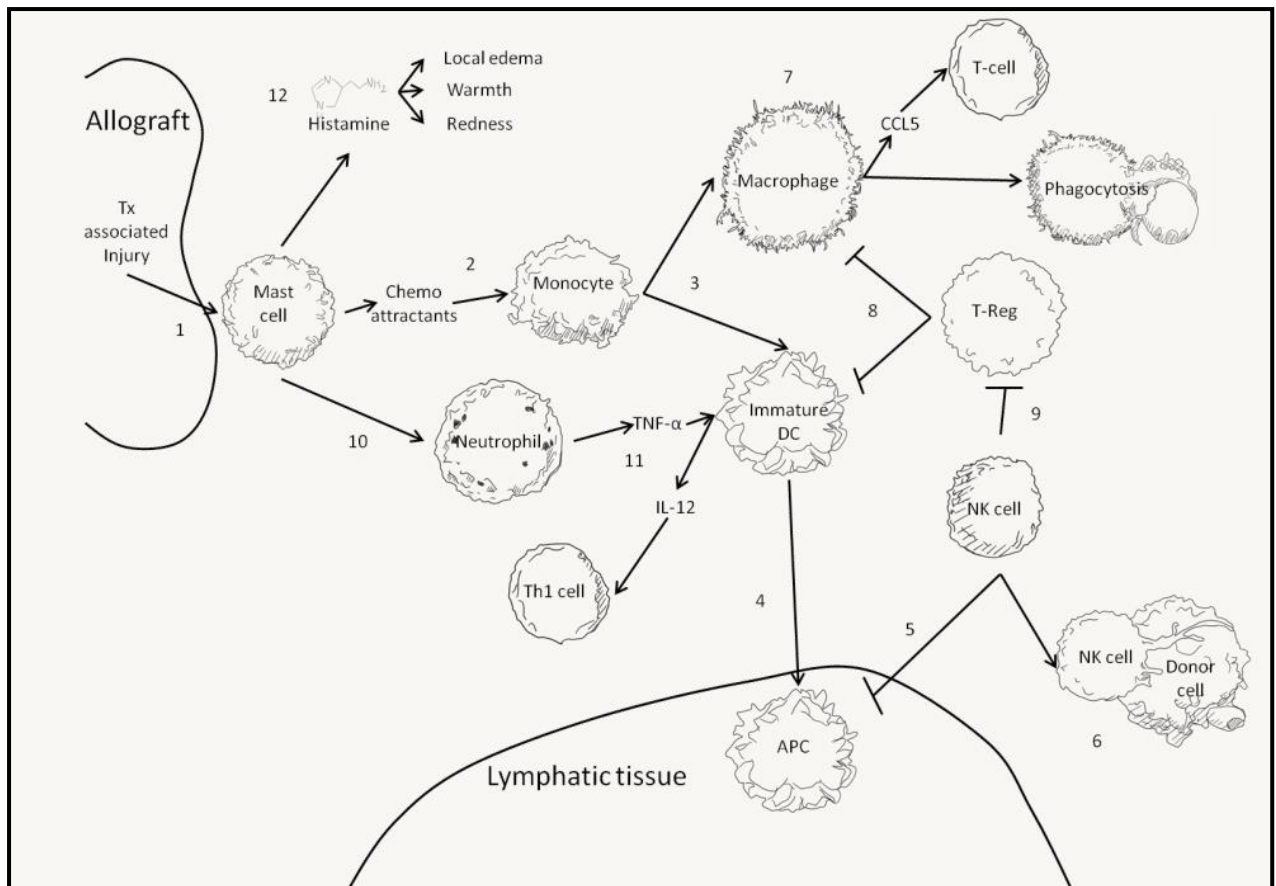


Figure 1.3 The innate immune response to an allograft. 1) Injury associated with the transplant procedure causes resident mast cells to degranulate. 2) These then release chemo attractants that act to recruit monocytes to the area. 3) Monocytes can give rise to dendritic cells or macrophages. 4) DCs in the area of the graft act as APCs and move to the lymphatic tissue after taking up antigen. 5) Natural killer cells are able to inhibit the immune reaction by killing antigen presenting cells. 6) NK cells act to kill donor cells due to their allogeneic MHC. 7) Macrophages are able to cause graft damage in several ways including attracting T-cells via the release of CCL5 and then presenting antigen to them and by the phagocytosis of donor cells. 8) T-regs are able to restrain the immune response by inhibiting the actions of both DCs and macrophages. 9) However, T-regs can be targeted by NK cells, stopping their actions and allowing rejection to occur. 10) Neutrophils also migrate to the tissue in response to transplant associated inflammation. 11) Neutrophils release TNF- α which stimulates DCs to produce IL-12 causing Th1 differentiation and triggering rejection. 12) Mast cells can also release histamine causing classical inflammatory responses.

Natural killer cells, which play a role in the destruction of cells that have been infected by viruses or otherwise mutated [135, 136], have interesting reactions and impacts to allotransplantation. Because they are unable to recognise the MHC of donor cells [137] they treat them like damaged cells as often infected or damaged cells will down regulate MHC class I, a change that marks them for death [138, 139]. Additionally, NK cells can modulate the immune response by killing other immune cells. It has been suggested that they can amplify rejection by killing T- regulatory cells [140] or indirectly aid in the promotion of tolerance by killing donor APCs, thus hindering the direct pathway of cellular rejection [137, 141].

Neutrophils, along with monocytes, are the first cells to migrate to a graft in response to inflammation caused by ischemia reperfusion injury [142, 143]. Once they are situated in the graft they begin to produce chemotaxis inducing chemokines such as INF- γ [118].

Additionally they produce TNF- α which stimulates DCs to produce IL-12 [144] leading to Th1 differentiation of T-cells [27], triggering graft rejection. In this way neutrophils are able to activate both the innate and adaptive immune response in a transplant setting. However, like NK cells their role in allograft rejection is not a requirement and as such any therapy targeting these cells would be unlikely to be effective alone [143].

1.4 Immunosuppressant Drugs

The brief summary of rejection immunology given above presents a complex and multifaceted interaction between the immune system and allografts, with many possible paths to rejection and graft loss. Appropriately, the pharmaceutical interventions required to overcome such dynamic immunoprotective strategies are themselves intricate, with modern immunosuppressant regimes employing a multidrug approach. Each drug in a regimen will have a unique mechanism of action to allow for modulation of several aspects of the immune system while keeping adverse reactions to a minimum [145]. A common immunosuppressant

drug regime for a transplant patient will include the use of a calcineurin inhibitor, an anti-proliferative agent, and a corticosteroid with the most widely used combination being Tacrolimus, Mycophenolate, and prednisone which accounts for between 60%-75% of maintenance regimes at discharge [145]. The calcineurin inhibitors are the foundation of modern immunosuppression and transplantation.

1.4.1 Calcineurin Inhibitors

As their name suggests, calcineurin inhibitors act by inhibiting calcineurin which is a protein phosphatase that is important in the activation of T-cells [146]. It achieves this function by dephosphorylating NFATc or nuclear factor of activated T-cells [146]. Once activated, NFATc moves into the nucleus and acts to increase the transcription of T-cell activating cytokines, in particular IL-2 [147].

Cyclosporine (CyA) works by forming a complex with the chaperonin protein, cyclophilin, this then binds to calcineurin preventing it from triggering T-cell activation [148, 149].

Tacrolimus functions in a similar manner in that it binds to chaperonin protein FKBP12; forming a complex that then binds and inhibits calcineurin [149, 150].

Adverse effects are more likely to occur when blood concentrations exceed the desired range, however even when this range is achieved there is still a risk of adverse events [151, 152].

This therapeutic variability arises because of the highly blood protein bound nature of the drugs and the fact that only the unbound fraction is pharmacologically active [153]. This presents a problem because there are many factors that can alter the amount of bound drugs and the unbound fraction is very difficult to directly measure [153, 154].

1.4.2 Antiproliferative Drugs

The antiproliferative immunosuppressants act to disrupt pathways required in cellular division. Azathioprine is a prodrug that is converted to 6-mercaptopurine (6-MP) and then to thioinosinic acid [155]. Thioinosinic acid interferes with the usual role of inosinic acid by causing product inhibition of glutamine-phosphoribosyl phosphate aminotransferase (GPAT) [156, 157]. This pathway is one of the central aspects of purine biosynthesis and by extension DNA replication [157, 158]. A portion of 6-MP also gets converted into thioguanylid acid, which becomes incorporated into DNA and RNA in place of guanosine resulting in non-functional genetic material [157]. Both of these mechanisms act to stop DNA replication and thus cellular replication. Mycophenolate is metabolized to moiety mycophenolic acid in the liver which acts to reversibly inhibit inosine monophosphate dehydrogenase (IMPDH) [159]. IMPDH acts as the rate limiting enzyme in the de novo synthesis of guanine monophosphate. The end result of mycophenolates mechanism of action is a reduction in the pool of guanine in lymphocytes causing an inhibition of DNA synthesis and thus cellular replication [159]. Mycophenolate is able to somewhat selectively target lymphocytes due to their high cellular replication and because they do not make use of the salvage pathway of nucleotide biosynthesis, an alternative method for acquiring nucleotides utilized by many other cell types [159].

1.4.3 Glucocorticoid Steroids

Glucocorticoid steroids (GS) are a class of drug with potent anti-inflammatory action as well as immunosuppressive properties [160]. The anti-inflammatory mechanisms of action of GS are mediated by the glucocorticoid receptor (GR), a ligand inducible transcription factor.

Although usually located in the cytoplasm, once a suitable ligand has bound the GR moves into the nucleus where it is able to enact changes in gene expression [160, 161]. The GR has two modes of gene regulation, transactivation and transrepression [160, 161].

Transactivation, or transcriptional activation, involves the GR acting as a transcription factor by binding to glucocorticoid receptor response elements (GREs) in the promoter regions of glucocorticoid inducible genes[161]. GR can achieve this binding by either forming a homodimer with itself or through forming a complex with other transcription factors [162]. The Binding of the GR complex to the GREs allows for the recruitment of RNA polymerase II leading to gene transcription and protein expression [162]. GREs have been identified in a wide assortment of operons including those that encode the gluconeogenic enzymes tyrosine amino transferase (TAT), and phosphoenol pyruvate carboxykinase (PEPCK) [162-164].

GR can also act to cause repression of transcription via a direct or indirect method. The existence of negative GREs (nGREs), which cause down regulation of genes upon binding of a GR homodimer, provide a direct path for transrepression while the indirect path requires the binding or blocking of other transcription factors, in effect acting as an antagonist[160, 165, 166].

This antagonistic action results in the a lack of activation of the genes targeted by transcription factors such as NF-kB, nuclear factor of activated t cells, Th1 specific T box transcription factor, GATA3, and AP-1 [162, 167-169]. These particular transcription factors play important roles in the activation and expression of pro-inflammatory molecules TNF, IL-1B, IL-2, IL-3, macrophage inflammatory protein (MIP), granulocyte macrophage colony stimulating factor, nitric oxide synthase, COX2, ICAM-1, and VCAM-1 [162].

By inhibiting their transcription factors there is an eventual reduction in the pro-inflammatory molecules, however this is delayed as it is dependent on the depletion of extant quantities of these molecules.

Based on the types of genes regulated by GREs it was assumed for a long time that the adverse reactions associated with GS, such as diabetes and glaucoma, were caused by transactivation and that the beneficial, anti-inflammatory, outcomes were mediated by transrepression [170]. Ongoing examination of glucocorticoid mechanisms and effects however has shown that GR mediated transactivation is able to contribute to the anti-inflammatory process by inducing the transcription of several potentially beneficial genes including MAPK phosphates 1, GC-induced leucine zipper, and annexin-1 [162].

1.4.4 mTOR Inhibitors

Another major class of mainline immunosuppressant drugs are the mTOR inhibitors, the most notable of which is sirolimus, or rapamycin, for which mTOR (mammalian target of rapamycin) is named for. These drugs are used as a replacement, or in addition, to CNIs and anti-proliferative compounds or to augment a drug regime in hopes of reducing adverse events [171, 172].

mTOR inhibitors act by binding with FKBP12, the same protein that Tacrolimus binds to. However in this instance the resulting complex inhibits the actions of mTOR [173, 174]. The mTOR pathway is vast, complex and plays a role in a wide range of cellular processes. Its immunologically relevant actions are carried out by its impact on S6 kinase 1 (S6K1) and eukaryotic initiation factor 4e binding protein-1 (4EBP1), both of which are important regulators of mRNA translation [175].

S6K1 acts upon a number of substrates including ribosomal protein S6, translation initiation factor 4B, eEF2 kinase, and SKAR all of which are implicated in progressing either

transcription or translation [175, 176]. 4EBP1 acts to inhibit eIF4E, which becomes released upon phosphorylation of 4EBP1 by mTOR [177]. Once free eIF4E is then able to form a complex with eIF4G and eIF4A which bind to the 5' end of mRNA allowing a helicase to remove hairpin folds, opening the mRNA up and allowing its start codon to be recognized by the 40s ribosomal subunit [178].

By creating a complex with FKBP12 that has the potential to inhibit mTOR, rapamycin acts to greatly reduce protein synthesis via the inhibition of mRNA translation, which results in a decline in cell growth, division, and differentiation. Rapamycin therefore has a greater impact on cells with a high level of growth and division such as activated T and B cells [173, 179].

As with all pharmaceuticals, immunosuppressive drugs are prone to adverse events, many of which can be extremely severe to the point that they can result in death. Cancer is common in patients that have been on long term immunosuppression as is diabetes and, of course, opportunistic infection [170, 171, 180, 181]. As such there are always ongoing endeavours to overcome these reactions either by reducing the amount of drug required or with the introduction of new therapies.

1.5 Non-Immune Organ Damage

In addition to the immunological aspects of transplantation, significant attention must be given to other forms of damage that an organ can undergo. There are a multitude of injuries that an organ can endure during retrieval including; traction injuries, capsular tears, loss of vasculature for anastomosis, and vascular injury all of which have the potential to make an organ unsuitable for transplantation [66, 182].

There is, of course, damage that can occur prior to organ retrieval with causes such as extant pathologies affecting the organ, damage accrued during the event that lead to death, and post death biological processes associated with cadaveric organs. These are extremely difficult

complications to address due to their causes being beyond the scope of clinical science to control.

Given the difficulties inherent in controlling many forms of organ damage it is best that research focuses on aspects that can be improved such as ischemia reperfusion injury (IRI). IRI is the result of the deprivation of blood flow to tissue and its resultant injurious processes, followed by the reestablishment of blood flow which, rather than mitigating the previous damage, acts to aggravate it [67]. Dividing IRI into its constituent elements allows for a greater understanding of the physiological processes that occur.

1.5.1 Ischemia

Ischemia acts to deprive cells of oxygen thus disrupting oxygen dependant metabolism [183]. A major consequence of this is a reduction in ATP as a lack of oxygen inhibits the citric acid cycle [183, 184]. This then requires the cells to depend on glycolysis for ATP production [185]. This switch to anaerobic metabolism causes a raft of reactions including lactic acid accumulation and metabolic acidosis resulting in a perturbation of normal cellular ionic composition. In particular there is an increase in intracellular H^+ [183]. In order to correct this, the sodium-proton exchanger is used to move H^+ to the extracellular space the repercussion being an increase in cytosolic sodium [183, 186].

High intracellular sodium would normally be ameliorated by the sodium pump and the sodium/ potassium ATPase, however a dearth of available ATP results in these becoming non-functional. Expulsion of the excess sodium then falls to a reversal of the sodium/ calcium antiporter [183, 187]. This, again, has a consequence in that as sodium is moved out of the cell calcium is moved in. Furthermore calcium channels are opened due to a depolarisation of cell membrane potential caused by the cells inability to control the concentration of ions on

either side of its membrane. This results in a rapid influx of calcium in addition to the already increasing intracellular calcium [188].

This produces a myriad of outcomes including a change in cellular pH, swelling leading to disruption of the cell membrane, and the triggering of apoptosis via activation of both the extrinsic and intrinsic pathways by the activation of the caspase cascade and inducing permeability of the mitochondrial membrane causing the release of pro-apoptotic proteins [183, 188-192].

1.5.2 Reperfusion

The harm caused by the return of blood flow to an ischemia damaged organ can result in vastly greater injury than ischemia alone, this is termed reperfusion injury. The prime movers of this form of injury are oxygen free radicals [183]. Under normal conditions oxygen free radicals are generated at low enough amounts that they can be scavenged and their potential harm negated.

A significant source of these damaging molecules is the xanthine dehydrogenase/ xanthine oxidase pathway [193]. As mentioned, ischemic conditions result in an increase in intracellular calcium, this has the effect of converting xanthine dehydrogenase to xanthine oxidase [194]. While both of these enzymes catabolise hypoxanthine and xanthine to uric acid, xanthine oxidase generates superoxide as a by-product as it uses molecular oxygen as an electron acceptor [195].

However, due to the lack of oxygen inherent in ischemia, xanthine oxidase is unable to function resulting in an increase in the amount of hypoxanthine and xanthine. Once oxygen is reintroduced during reperfusion, xanthine oxidase begins metabolizing its substrates and thus producing superoxide at a rate higher than what the cellular scavenging pathways can regulate [193].

Once superoxide has been produced at high enough levels it begins to react with itself forming hydrogen peroxide (H_2O_2) [196]. H_2O_2 is potently reactive and begins to oxidise polyunsaturated fatty acids in the cell membrane resulting in a loss of cell membrane integrity and cell death [197]. H_2O_2 reacting with lipids and other cellular proteins also generates additional oxygen free radicals creating a chain reaction of cellular destruction [198].

Additionally, oxygen free radicals also cause the production of chemoattractants including leukotriene, $TNF-\alpha$, $INF-\gamma$, and $IL-1$ which cause leukocyte adherence [193, 199, 200]. In the situation of an allograft, IRI will result in cellular break down, producing cellular debris giving abundant antigen for APCs (in place thanks to the chemoattractants) to present thus causing an immune reaction in addition to the damage already sustained [55].

1.6 Organ Preservation

There are several approaches taken to attempt to reduce the deterioration of prospective organ grafts by a lack of homeostasis, and the associated IRI, caused by death or organ retrieval.

Foremost is hypothermic preservation which involves reducing the temperature of an organ in order to slow metabolism and thus metabolic damage. This is achieved by flushing the organ with a cold preservation solution and placing it on ice. By dropping the temperature of an organ from $37^\circ C$ to $0^\circ C$ metabolism is inhibited 12 fold, however this is not enough to halt cellular processes entirely and damage will still accrue, albeit at a slower rate [201].

The delivery of the preservation solution can be achieved by either a simple direct infusion or by a continuous perfusion that allows for substrates to be continually delivered to the cells going some way to ablate the reduction in ATP and the associated negative cellular reactions [202].

1.6.1 Preservation Solutions

1.6.1.1 Collins Solution

Tied to hypothermic preservation and already mentioned, is another important aspect of organ preservation, preservation solutions. The first solutions that showed promise in preserving organ function were the Collins and Eurocollins solutions [203, 204]. These were an attempt to simulate the electrolyte constitution of intracellular fluid and possessed high levels of potassium, magnesium, phosphate, sulphate, and glucose with later compositions removing the magnesium and sulphate [205]. The aim of these solutions was to prevent cellular swelling and loss of metabolically important ions during perfusion and cooling of organs [203]. However this solution still resulted in osmotic shock and eventual lysis of cells possibly due to the breakdown of glucose to lactate resulting in a doubling of intracellular substrate and the requisite influx of fluid [204, 206]. Despite this draw back Collins solution still resulted in significant improvements in delayed graft function as well as other indicators of transplantation success [203].

1.6.1.2 University of Wisconsin Solution

University of Wisconsin solution (UW) was developed by Folkert Belzer and James Southard over a number of years in the 1980s with a view to make a pancreas specific preservation solution [201, 207-210].

Eurocollins solution, although giving good results with other organs, still caused a large amount of oedema and osmotic shock in pancreas preservation [210]. They addressed these issues by replacing the glucose of Collins solution with larger, metabolically inert, sugar molecules to act as impermeants for control of osmolarity. They found a general trend of higher molecular weight molecules having a greater ability to prevent tissue swelling and eventually settled on the use of raffinose and lactobionate with hydroxyethyl starch (HES)

added as oncotic support [210]. Additionally, earlier work by the same authors had shown the beneficial and protective effects of adding adenosine and phosphate to preservation solutions [208]. And finally, they included oxygen radical scavengers' glutathione, and allopurine.

Overtime the formulation of UW was refined to:

Potassium lactobionate	100mM
Potassium phosphate	25mM
Magnesium sulphate	5mM
Raffinose	30mM
Adenosine	5mM
Glutathione	3mM
Allopurinol	1mM
Hydroxyethyl starch	50g/L

With some formulations including the addition of glucocorticoid steroids and insulin [205, 211, 212]. Currently UW is still considered the gold standard of organ preservation solutions. However, it is not without its deficiencies. In particular its high viscosity has been reported to impede its ability to completely wash out blood from organs [213]. This high viscosity has been linked to the use of HES and although the HES does increase viscosity it is not much higher than that of whole blood. The difficulty in removing blood could instead be put down the ability of HES to cause aggregation of blood cells [214], creating a condition in which masses of cells can become stuck in vessels, blocking them, and possibly resulting in delayed perfusion of capillary dependant tissue [215].

1.6.1.3 Histidine-Tryptophan-Ketoglutarate Solution

Although UW has excellent outcomes, research continues into the best formulation to use in different transplantation settings. One solution that has found increasing use is Histidine-Tryptophan-Ketoglutarate solution, also known as custodial. Developed by H.J Bretschneider as a cardioplegic preservation solution, it is based around the histidine/histidine hydrochloride buffer system while using ketoglutarate to aid in ATP production during reperfusion and tryptophan to stabilise the cell membrane [216-219]. One of the key functions of custodial is to induce cardiac arrest. It achieves this by having a low concentration of sodium, magnesium, and potassium, resulting in a depletion of these chemicals in the extracellular space which creates a hyperpolarization stopping myocyte contraction [220]. Additionally, it contains mannitol to act as an impermeate controlling cellular oedema as well as acting as an oxygen free radical scavenger. The final formulation is as follows [205]:

Sodium	15mM
Potassium	9mM
Magnesium	4mM
Calcium	0.015mM
Ketoglutarate	1mM
Histidine	198mM
Mannitol	30mM
Tryptophan	2mM

Although the use of preservation solutions has resulted in improved outcomes in transplantation the organs still accumulate damage and delayed graft function is still a problem.

1.7 Donor Sources

One of the greatest predictors of graft dysfunction is the source of the organ, with deceased donor's contributing to higher levels of complications than live donors [221, 222]. This problem is especially pertinent because of the reality, that outside of kidneys, almost all organ transplants are from deceased donors and as such the majority of organs will accrue at least some injury. Kidney graft failure rates for live and deceased donors are included below:

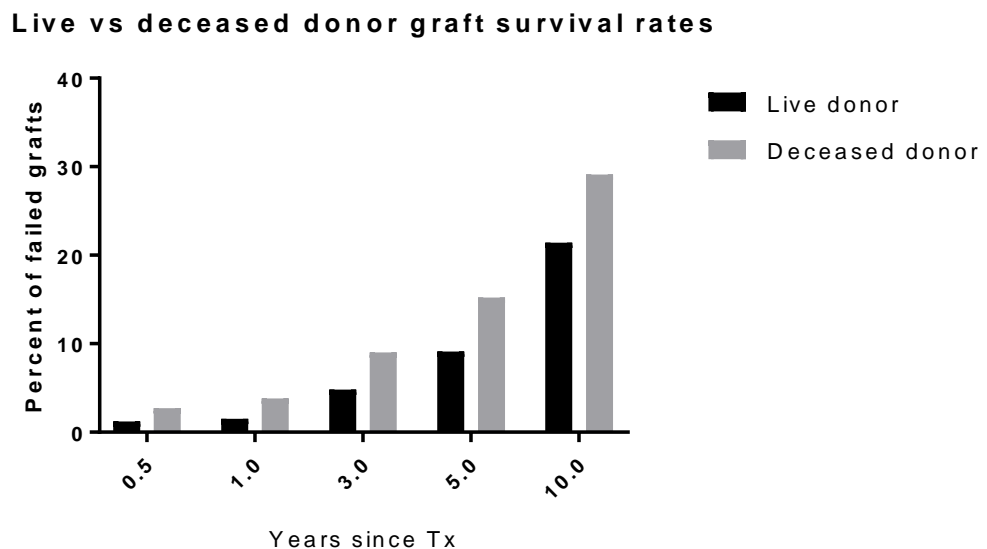


Figure 1.4 Based on data from the organ procurement and transplantation net work (OPTN) and the scientific registry of transplant recipients (SRTR) in 2012, a clear difference in the survival rates between grafts procured from live and deceased donors is observed. [223, 224]

This data shows that grafts from deceased donors have a higher rate of failure at all time points and that this disparity becomes more pronounced the longer the graft is in place [223, 224]. Another important measure of transplant success is delayed graft function, which was briefly mentioned in regards to the effectiveness of preservation solutions. Delayed graft

function is a signifier of long term graft survival and is most commonly defined as the transplant patient having to return to dialysis within 7 days of transplantation [225]. When comparing living and deceased donor kidneys, delayed graft function occurred in only 2.75% of living donors but was much more prevalent in deceased donors at 23.82%.

There are several reasons for this disparity in outcomes [223]. The most obvious is that live donor kidneys are procured under much more controlled conditions than those from deceased donors allowing for shorter ischemia times and a lessened chance of the graft being impacted by co-morbidities. Additionally, tissue matching is able to be more carefully considered in a living donor situation whereas a deceased donor organ has to be used as quickly as possible and as such an optimal match may not be possible.

Deceased donors can also be subdivided into useful groups that can allow some power of outcome prediction. Standard criteria donors (SCD) are mostly defined by not having the signifiers associated with the other classifications [221, 226, 227]. An “ideal” SCD would be a young person with no history of hypertension or diabetes whose cause of death was a motor vehicle accident.

In contrast to this are extended criteria donors (ECD), these are donors who are over 60 years of age or are between 50 – 59 years of age and have at least two of the following indications.

- 1) Their death was caused by a cerebrovascular accident.
- 2) They have a pre-existing history of hypertension.
- 3) Their terminal serum creatinine is greater than 133mmol/L.

These criteria were formulated based on variables that give a 70% or greater risk of graft failure when compared to SCD.

Next are donations subsequent to brain death (DBD) in which a donor has had primary brain death but the respiratory and circulatory systems continue to function either independently or

by medical assistance. This classification can also fall into either SCD or ECD depending on the presence or absence of the corresponding criteria.

Lastly is donation after cardiac death (DCD) in which cardiac function has ceased prior to retrieval of the organs either spontaneously or under medically initiated conditions [221, 226, 227].

Based on these classifications and the multitude of ways in which they differ, it is unsurprising that there are differences in outcomes. In the table below is a summary of various measures of transplant success reproduced from Rao and Ojo., 2009 [221].

	SCD	ECD	DBD	DCD
Acute rejection episode	14%	15%	37%	38%
Delayed graft function	21%	11%	24%	41%
1 year graft survival	90%	82%	91%	89%
5 year graft survival	65%	49%	67%	67%
5 year patient survival	82%	70%	82%	81%

Table 1.1 Prevalence of transplant related complications and morbidity based on differing donor classifications.

This data shows that there are worse outcomes associated with ECD, in particular the 5 year graft survival and the 5 year patient survival. It also shows that both DBD and DCD have higher rates of acute rejection episodes, although their 5 year survival rates still manage to reach parity with SCD. Of course this data may be missing significant information about the

recipients of these organs that may impact transplantation outcome, but it is still a useful representation of the problems associated with non-SCD donation.

1.8 Cellular Therapies

As stated in the general introduction, there is a deficit of viable organs for transplantation and this will become worse as time goes on. As such, all efforts must be taken to address issues that current face transplantation science. Two of the most pertinent were touched on in the immunosuppressant and preservation sections. These are, firstly, the adverse events associated with immunosuppression such as renal toxicity, opportunistic infections, development of malignancy and metabolic complications [145, 151, 152, 171, 181]. And secondly, damage to organs resulting in graft dysfunction or, in extreme cases, the graft being discarded [66, 182, 228].

These complications are being addressed from many angles with one of the more intriguing and potentially useful paths of enquiry being the use of cellular therapies. Depending on the cells used it is possible to modulate several aspects of transplant immunology or to foster a reparative environment to address graft injury and its associated problems. In these ways cellular therapies offer a potential alternative to traditional pharmacological interventions applied to transplantation.

The basic concept of cell therapy is to implant cells with desired properties into a patient in an attempt to treat or cure. Although this idea has been around since the 19th century, it was not until the 1960s that it became a viable treatment with the first bone marrow transplants [229]. Since then, there has been a steady expansion in the type of cells transplanted and the conditions that can be treated. There are several cell types that are being evaluated for preclinical or early clinical trials in solid organ transplantation (SOT), including; T regulatory

cells (Tregs) [230], dendritic cells (DCs) [231], and mesenchymal stem cells (MSCs) [232] which have shown the greatest progress and potential as a cellular therapy and are the focus of this thesis.

1.9 Mesenchymal Stem Cells

1.9.1 History

Early work by Tavassoli and Crosby identified the osteogenic potential of bone marrow [233]. This was validated and expanded upon over numerous years by Friedenstein who found that this osteogenic potential came from a specific subset of cells that were able to be isolated based on their adherence to plastic cell culture vessels and could be identified by their fibroblast like appearance [234-236].

Later work found that these cells had multipotent potential being able to differentiate into several other tissue types including cartilage and adipose tissue [237, 238]. This multilineage differentiation lead to these cells being referred to as Mesenchymal stem cells, although there is some debate about how appropriate this name is based on questions around the “stemness” of these cells [239, 240]. Mesenchymal stem cell is still generally accepted and will continue to be used in this work but they will mostly be referred to by the initialism, MSCs.

As work with MSCs progressed, understanding continued to develop. Vast amounts of work were carried out examining their immunosuppressive abilities as well as the many tissue types that they are able to be isolated from [241-246]. This interest has continued to grow and they have become one of the most widely used cell therapies applied to clinical trials.

However, as work on these cells expanded so did the list of characteristics assigned to them and, owing to the heterogeneous nature of their isolation, there was conflicting information about what constitutes an MSC.

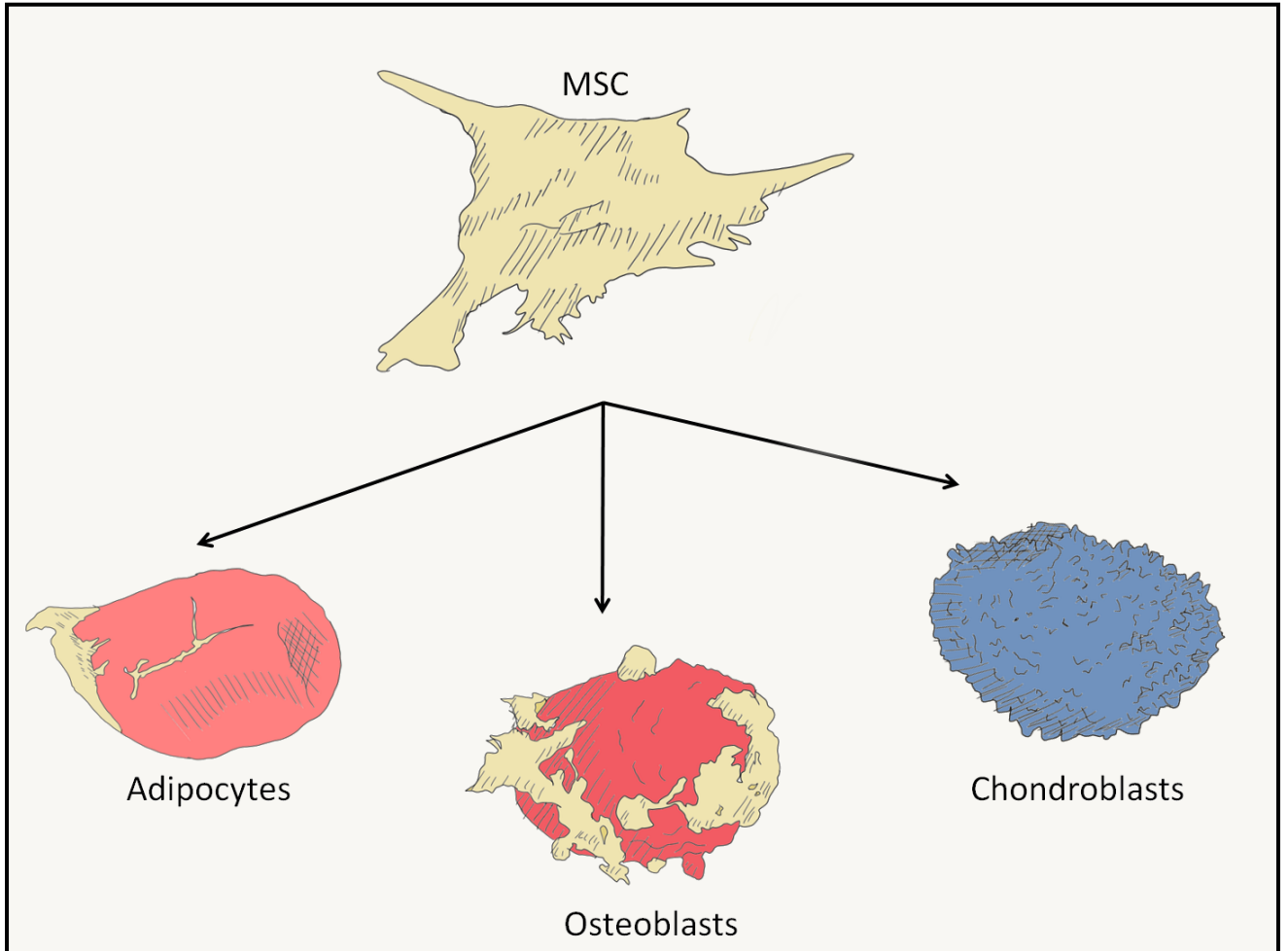


Figure 1.5 One of the defining characteristic of mesenchymal stem cells is their ability to differentiate in fat producing adipocytes, bone producing osteoblasts, and cartilage producing chondroblasts. Although MSCs are capable of differentiation into other cell types it is this tri-lineage differentiation that is used, along with plastic adherence and cell surface markers, to positively identify mesenchymal stem cells.

1.9.2 Characteristics

The International Society for Cellular Therapy (ISCT) has set the minimal criteria for defining MSCs as being plastic adherent, capable of differentiation into osteoblasts, adipocytes, and chondroblasts, and expressing CD105, CD73, and CD90 while lacking expression of CD45, CD34, CD14 or CD11b, CD19, and HLA-DR surface molecules [247]. MSCs are capable of being isolated from many tissues including bone, fat, and umbilical cord [242, 246].

Although this minimal criteria is useful for defining MSCs they also have various other properties such as when they are cultured they adhere to plastic and have a fibroblast-like appearance, possessing a long, thin body and a small number of protrusions [234, 248]. When not adhered to plastic they range in size from 17.9 μ m to 30.4 μ m, large enough to cause vascular obstructions [249]. *In vivo*, MSCs have a role in the formation and homeostasis of connective and structural tissues *via* the production of extracellular matrix, stabilization and regulation of the tissue vascularisation, and the creation of new connective tissue cells [250-252]. In addition to this, they also play a role in the immune system by inducing tolerogenic properties that can be enhanced by *in vitro* treatment [253-256].

These roles are able to be exploited to aid in regenerative medicine and in immunosuppression. Combined with the many tissues from which they can be isolated and their ability to remain stable while being expanded *in vitro* it becomes clear why so much work is now being carried out using MSCs for a large number of clinical applications.

1.9.3 Immunosuppression By MSCs

MSCs have been shown to impact the immune system on several levels and, although it not known whether they exert these effects via cell to cell contact or the excretion of micro vesicles and paracrine factors, it is known that they have potent anti-inflammatory properties

[257-259]and are able to moderate both the adaptive [260-262] and innate [263-265] immune systems. They have demonstrated the ability to foster generation of T-regs [255], inhibit the activation, proliferation, and differentiation of T and B cells [261, 266], and suppress the activity of DCs and NK cells [265, 267, 268]. The ability to shape the immune response in such a wide variety of ways is likely to be dependent on both soluble factors and cell-cell contact and as such the MSC is able to employ a number of molecules and pathways [269, 270].

1.9.4 Pathways Of MSC Immunosuppression

The immunosuppressive abilities of MSCs have been associated with several well established immunosuppressive pathways such as adenosine accumulation [271], PD-L1/PD-1 [272]and either nitric oxide synthase (iNOS) [273-275] in mice, or indolamine 2,3-dioxygenase (IDO) [255, 273, 276] in humans.

1.9.4.1 Adenosine Accumulation

One of the cell markers used to identify MSCs, CD73, is also known as ecto-5'-nucleotidase which is an enzyme responsible for the production of adenosine from AMP [277]. Via this enzyme MSCs are able to create a local increase in adenosine which is then able to bind to the A2A adenosine receptor (A2A) found on many immune cells [271].

The A2A receptor acts to stimulate adenylyl cyclase, elevating intracellular levels of cAMP which then works to increase the levels of inhibitor of kappa B (I κ B), thus, stopping the activation of NF- κ B [278]. NF- κ B is one of the master transcriptional regulators in a plethora of inflammatory genes such as BAFF, CCL15, and TNF- α [279]. In this way MSCs are able to use adenosine accumulation to inhibit immune cell functions.

1.9.4.2 PD-L1/PD1

Programmed death ligand 1 (PD-L1) also known as CD274 is expressed by MSCs while its receptor [272], PD-1, is found on numerous immune cells the most relevant of which are T and B cells [280, 281].

Upon binding of PD-L1, PD-1 becomes clustered with the T cell receptor and acts to block its function via dephosphorylation of the downstream TCR signalling molecules such as zeta-associated protein of 70kD and Protein kinase C θ . This has the resultant effect of stopping T cell proliferation and expression of IL-2 [280, 282].

1.9.4.3 Cyclooxygenase

The Cyclooxygenase or COX pathway is known to generate and maintain immune tolerance [283]. COX-2 in particular plays a role in increasing the production of prostaglandins during inflammation [284]. The products of these pathways are required for the development of functional Tregs and activation of COX also results in reductions in the production of IFN- γ and TNF- α by PBMC [283, 284]. COX-2 is expressed by MSCs and inhibiting it is shown to reduce the immunosuppressive effects of MSCs *in vitro* [285, 286].

1.9.4.4 PGE2

Of the prostaglandins produced in the COX pathway, prostaglandin E2 (PGE2) is the most important prostaglandin in immunology [287, 288]. With 4 receptors that are reactive to differing concentrations of PGE2, this molecule has a wide variety of impacts that may sometimes seem contradictory and has been shown to have both pro-inflammatory and anti-inflammatory actions [287].

Although it supports activation of dendritic cells it also suppresses their ability to attract naive T cells [288]. It also controls chemokine production and acts to stop the recruitment of pro-inflammatory cells while causing a local accumulation of Tregs. Additionally, PGE2 is able to suppress the effector functions of numerous immune cells including Th1, macrophages, and CTLs while promoting the responses of Th2 and Tregs [288].

Of the 4 PGE2 receptors, EP4 is has the greatest impact on immunosuppression and has its effects via PKA and Epas resulting in a decrease in the proinflammatory chemokines IP-10 and MIP1 α , reduced accumulation of CD8 T-cells, and the shifting of macrophage polarization from their pro-inflammatory M1 state to the anti-inflammatory M2 state [287, 288]. MSCs have been repeatedly shown to employ this pathway in achieving immunosuppression and when this pathway is inhibited these immunosuppressive effects are greatly reduced indicating a major role for PGE2 in the function of MSCs [289, 290].

1.9.4.5 Transforming Growth Factor Beta (TGF- β)

TGF- β , which is constitutively expressed by MSCs [291, 292], is known to participate in the regulation of several aspects of the immune system [293]. The function of TGF- β is derived from binding to its receptor, TGFBr. Once bound, TGFBr activates the Smad transcriptional factors [293].

Of prime importance are Smad2 and Smad3 which form homodimers and then create a complex with either Smad4 or TIF1- γ . This complex then translocates to the nucleus and regulates transcription that results in the generation of Tregs, inhibition of proliferation of T and B cells, regulation of differentiation of helper T cells, and suppression of macrophage, DCs, and NK cells [293, 294].

Of significance to transplantation is the action through which Smad, and thus TGF- β , results in the promotion of Treg differentiation. Smad, in its role as a transcription factor, binds to

Smad specific binding sites in the promoter regions of the foxp3 gene. Foxp3 is a master transcription factor in Tregs and is responsible for their immunosuppressive activity [295, 296]. By activating this gene TGF- β producing MSCs are able to drive T cell differentiation towards Tregs and thus promote a tolerogenic situation.

1.9.4.6 Inducible Nitrous Oxide (iNOS)

iNOS results in the production of nitric oxide (NO) which is an immunosuppressive agent in high concentrations [275]. It achieves this via inhibition of the JAK/STAT dependent IL-2 stimulation of T cells [297, 298].

Activation of certain receptors by their ligands such as IL-2r by IL-2 results in receptor associated Janus kinases (JAK) phosphorylating the receptor which allows signal transducer and activator of transcription (STAT) proteins to bind. JAK then phosphorylates the STAT proteins which allows them to form a dimer and translocate to the nucleus where they go on to modulate genes such as FOXP3 and SNX9 which play roles in T cell proliferation and differentiation [299-302].

A High level of nitric oxide, such as what is produced by MSCs, has the capacity to activate guanylate cyclase, resulting in increased levels of cGMP and stimulating cGMP-dependent protein kinases (PKG) [303, 304]. PKG is then able to dephosphorylate STAT, stopping its dimerization and translocation [299].

1.9.4.7 Indolamine 2,3-Dioxygenase (IDO)

IDO is able to interfere with the function of T-cells via the degradation of the essential amino acid tryptophan to kynurenine [305, 306]. Without tryptophan T-cells are unable to proliferate and thus unable to react to immune stimulus. Additionally, kynurenine and its metabolites lead to T-cell apoptosis [307]. Along with iNOS, IDO had long been seen

as one of the major players in the ability of MSCs to cause immunosuppression. Interestingly, these two pathways seem to have a degree of species segregation with human MSCs relying on IDO while murine MSCs rely on iNOS [273, 308].

There have also been additional molecules and pathways implicated in MSC immunomodulation such as HLA-G, Gal 1, IL-10, IL-6, I-CAM, and V-CAM [269, 309-311]. Not all of these molecules act in a directly immunosuppressive manner such as I-CAM and V-CAM which, in their well established adhesion molecule role, allow MSCs to control the proximity of T cells thus allowing the local immunosuppressive environment the best chance to take effect [312].

Using this wide array of strategies allows MSCs to create a comprehensive immunosuppression. The necessity of cell-cell contact was initially questioned as many of the molecules used are able to be excreted. However further evidence has shown that cell-cell contact allows for a more robust MSC induced immunosuppression this could either be due to the ability to deploy a wider range of immunomodulatory techniques or a more interesting idea is that MSC are able to react to the cells they are placed with and tailor their immunosuppressive methods [270, 309]. This would be in line with the evidence that MSCs are much more potent immunosuppressors after being treated with inflammatory cytokines [313].

1.9.5 Impact On Immune Cells.

Having knowledge of the pathways of MSC immunosuppression allows us to understand how they may be able to modulate immune cells in a transplant setting and thus, allow for a graft to survive. The next section will give a brief summation of the interaction between MSC and various immune cells, some of which have already been mentioned with immune pathways and molecules.

1.9.5.1 Dendritic Cells

MSCs have a demonstrated effect on the maturation of DCs as well as their cytokine secretion profiles directing them toward an immunosuppressive state [265]. MHCII, CD86, and CD40 are all markers of DC maturation. When DCs are co-cultured with MSCs, under conditions that would normally drive DC maturation, there is a significant decrease in the expression of these markers [264].

This impediment of DC maturation is the result of several independent, non-redundant pathways including adenosine accumulation, PD-L1/ PD-1, iNOS and IDO with iNOS or IDO usage species dependant [264, 273]. The pathways responsible for halting DC maturation are also implicated in suppression of DC production of TNF- α , a potent activator of T-cells, while either preserving or increasing the production of IL-10, a wide ranging anti-inflammatory and immunosuppressive cytokine [265]. As one of the major antigen presenting cells in transplant rejection, the targeting and inhibition of DC function by MSCs has indirect, downstream repercussions caused by the disruption of the presentation of graft specific antigens to other immune cells [267].

1.9.5.2 Regulatory T-cells

The induction of Tregs appears to be one of the major ways in which MSCs induce a tolerogenic environment [255, 260, 270]. The up regulation of Tregs was mentioned in several of the pathways exploited by MSCs, including TGF- β [291, 296] and PGE2 [314]. The propensity of MSCs to exploit Tregs allows for an amplification of MSC-mediated immunosuppression as Tregs are critical in restraining an immune response, in particular their role in suppressing T cell responses [315].

1.9.5.3 T Helper Cells

The differentiation of naive T helper cells into either Th1 or Th2 cells depends largely on the cytokines present at the time of antigen activation [25, 301, 316]. MSCs are able to impact this cytokine milieu by their secretion of factors such as IL-10 and TGF- β driving differentiation toward the Th2 phenotype [253, 267, 317] which is involved in reactions to extracellular parasites and thus less damaging to a graft than the Th1 phenotype [25]. Additionally, the impact of MSCs on Tregs results in a decrease in the proliferation of T helper cells and, as T helper cells are important in the stimulation of cytotoxic T cells [318], a lessened immune response to an allograft.

1.9.5.4 CD8 Cytotoxic T-cells

Cytotoxic T-cells, as mentioned earlier, are one of the cell types responsible for directly damaging allografts. MSCs are able to reduce CTL reactions [245] with both cell contact mediated mechanisms and via the secretion of soluble factors such as PGE2, IDO, and TGF- β which have already been described.

MSCs are able to inhibit CTL proliferation via the interaction of their MIC A/B molecule with the CTL natural killer group 2, member D (NKG2D) receptor [261]. When NKG2D has an MSC MIC A/B molecule as its ligand it results in a down regulation of the receptor causing a reduction in both CTL proliferation and cytokine production [261]. On top of this the effects of MSC on T-regs, DCs, and Th cells results in a comprehensive disruption of the normal CTL stimulation pathways. This multifaceted approach to immune regulation allows MSCs to have a remarkable impact on CTLs responding to allografts.

1.9.5.5 B-cells

MSCs are able to inhibit the differentiation of B-cells into plasma cells, thus stopping the production of graft specific antibodies in a transplantation setting [319]. MSCs can also alter the chemotactic abilities of B-cells by disruption of various homing molecules [320]. By causing both a reduction in plasma cell creation and inhibiting cell motility, MSCs are able to completely disable B-cells negating their potential impact on graft cells. Of course, this negation is only possible while the MSCs are resident, so the opportunity for the impact of B-cells on long term graft survival is still present.

1.9.5.6 NK Cells

The interaction between MSC and NK cells is interesting. Using IDO and PGE2 MSCs are able to reduce the proliferation of NK cells as well as inhibiting their cytotoxic activity and decreasing their cytokine production [268, 321-323]. This can obviously have an impact on the cytotoxic abilities of NK cells on allograft derived cells but it can also prevent NK cells from eliminating T-regs.

Of particular relevance is the ability of NK cells to target and kill MSCs, as MSCs are often regarded as immunoprivileged and able to evade immune cells [324]. However, their low expression of MHCI makes them a target for activated NK cells; this is counteracted if the MSCs have been stimulated via IFN- γ Part 1 which results in an upregulation of MHCI [313, 324]. This could seemingly be a method in which the immunomodulatory effects of MSCs are prevented by NK induced cytotoxicity until a pro-inflammatory environment stimulates MSCs and their functions are required.

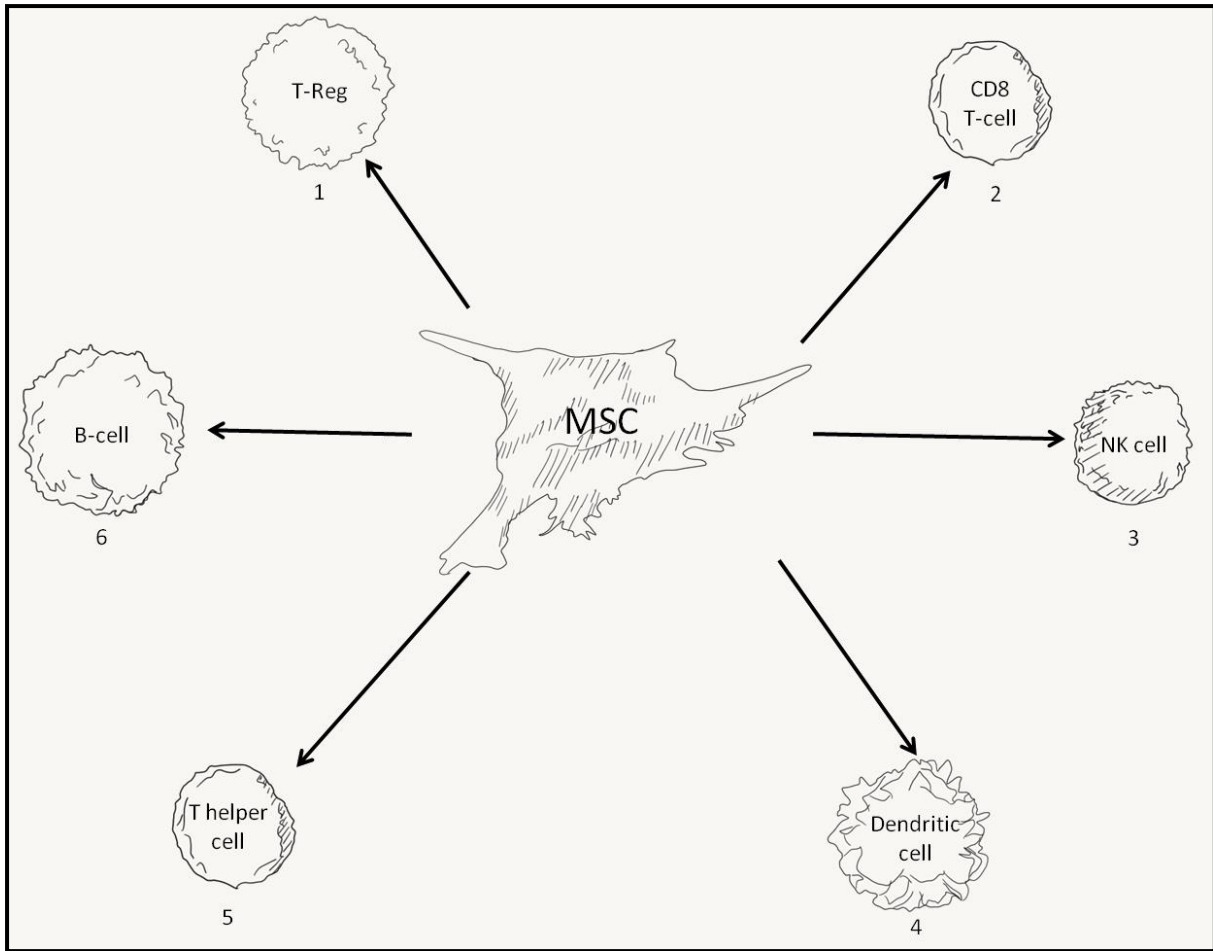


Figure 1.6 The impact of MSCs on immune cells. 1) MSCs are able to up regulate the activity of T-regs using TGF- β and PGE2, this then amplifies MSC immunosuppression by the commandeering of T-reg immunosuppressive abilities. 2) MSCs can reduce CB8 T-cell proliferation and cytokine production directly via the MIC A/B – NKG2D interaction as well as by the impact of MSCs on T-regs, DCs, and Th cells. 3) Using IDO and PGE2, MSCs can reduce NK proliferation, cytotoxic activity, and cytokine production inhibiting their ability to directly damage allografts as well as their ability to destroy T-regs. 4) MSCs are able to prevent DC maturation and move them towards an immunosuppressive state using several pathways including PD-L1/PD-1, iNOS, and adenosine accumulation. 5) Using the secretion of IL-10 and TGF- β , MSCs are able to drive T helper cell differentiation toward the Th2 phenotype which is less damaging to allografts than the Th1 phenotype. 6) By preventing the maturation of B-cells to plasma cells, MSCs are able to stop the production of allograft specific antibodies and the immune pathways they direct.

1.9.6 MSCs In Different Species

The minimal criteria for MSC identification as defined by the International society for cellular therapy was developed in human MSCs, and although MSC from different species all have similar properties and functions there are some key differences.

One of the most important was touched upon in the section of MSC immunomodulatory pathways and that was the use of IDO or iNOS, which is variable depending on the species the MSCs are derived from. Initially this difference was noted in human and mice MSCs. Further work indicated that species could be divided into either IDO or iNOS utilizes. With monkeys, humans, and pigs using IDO while mice, rats, rabbits, and hamsters use iNOS. They noted that the iNOS utilizes all came from the phylogenetic clade, Glires. However their species selection was limited so the results could not be extrapolated [273, 308].

The use of cell surface markers to identify MSCs is also impacted by species specific differences. STRO-1 is a marker used in addition to the minimal criteria to purify human MSCs further, as plastic adherence selection still results in a somewhat heterogenous cell population [325]. Although this marker has shown great promise in humans, rats, and pigs it has been reported that it does not exist in sheep MSCs [326], this has the potential to create translational issues if research is being performed on STO-1 purified cells.

Table 2 has been reproduced from Boxall and Jones' review of MSC characterization [327], which is useful in showing the cell surface expression differences between species, the original table has been updated based on more current information.

For the purposes of this research it is the differences between humans and sheep that are of greatest interest, of which it is notable that the confirmed differences are in markers that fall outside of the minimal definition criteria and any other potential differences are either, not confirmed or have not been examined. Knowing this information allows for antibody panels

to be developed that are able to take into account the lack of availability of species specific reagents, while still confirming the identity of the cells.

	Human	Mouse	Rat	Dog	Pig	Sheep
CD13	+	+-	NA	NA	NA	NA
CD29	+	+	+	+	+	+
CD31	-	-	NA	NA	-	-
CD34	-	-	NA	-	-	-
CD44	+	+	+	+	+	+
CD49e	+	+	+	NA	-	NA
CD45	-	-	-	-	-	-
CD73	+	+	+	-	-	+
CD90	+	+	+	+	+	+
CD105	+	+	+	-	+	+
CD146	+	NA	NA	+	+	+
CD166	+	+-	NA	NA	-	+
CD271	+-	NA	NA	+-	+-	+-
CD117	+-	+-	NA	NA	-	NA
Sca-1	+-	+	NA	-	-	-
SSEA4	+	+	NA	-	-	-
Stro-1	+	NA	+	NA	+-	-
W8-B2	+	NA	NA	+	+	+-

Table 2. Surface antigen expression from different species. + indicates confirmed expression. – indicates confirmed non-expression. +- indicates either low expression or conflicting reports. And “NA” indicates no available information.

Part 2

MSCs as a Therapy to Improve Kidney Transplantation

The application of MSCs to kidney transplantation is a theoretically sound idea. MSCs have properties that may be able to address several of the most pertinent issues facing kidney transplantation. Their regenerative effects offer the possibility of a remedy to ischemia reperfusion injury and the associated inflammatory induced damage. While the immunosuppressive effects of MSC hold the promise of being able to reduce pharmacological immunosuppressive load, thus curtailing some of their more troublesome adverse effects. To this end there have been numerous animal models as well as clinical trials investigating the safety and efficacy of MSCs in a kidney transplant setting.

1.10 Animal Models

Comprehensive animal studies are often a prerequisite prior to the initiation of clinical trials. When examining the application of MSCs to kidney transplantation however, you find relatively few animal experiments in comparison to the number of clinical trials that have been completed or are underway. The majority of these studies were carried out in a rat model of kidney transplantation [328-334]; with only one based in a large animal model with the utilization of a porcine autotransplantation model [335] (A further exploration of animal models of kidney transplantation is included in chapter 4). There have been many other studies looking at the use of MSCs in ischemia reperfusion injury [336-338], however these

tend to use *in situ* clamping and warm ischemia so do not fully replicate the transplant induced IRI experienced by a kidney graft nor does it encompass the intersection of IRI with transplant immunology.

Evidence of a positive effect of MSCs in kidney transplantation was initially demonstrated in a pair of papers by M. Alessianis' group in 2010 in which they used a rat kidney allotransplantation model [328, 334].

Their first paper examined whether a direct arterial administration or a tail vein administrative route of 3×10^6 MSCs was favourable. They found that the direct arterial infusion had better outcomes than the venous infusion, including a faster functional recovery, as measured by serum creatinine, and improved histological features, including tubule and glomerular preservation and reduced inflammatory infiltration [334].

In tandem to this they carried out work looking at the effects of MSCs on syngeneic and allogeneic kidney transplants. They used a direct arterial injection of 3×10^6 MSCs into both the syngeneic and allogeneic test groups and found that the mice that received the MSCs had improved kidney function and attenuated histological damage, similar to the findings of their other paper. Additionally, the allogeneic MSC group had less cellular infiltration thus reducing acute rejection in comparison to the control group [328].

Again using a rat allotransplant model, Hara *et al* in 2011 examined if MSCs were able to prevent the deleterious responses that occur in response to cold preservation and the subsequent IRI of kidneys [331]. The cold ischemia times were either 30 minutes or 24 hours and the test groups received 3 doses of either 2.5×10^6 or 5×10^6 MSCs at 3 time points which were 7 days before Tx, immediately after Tx, and 1 day after Tx. The MSCs were administered via the tail vein and the animals also received cyclosporine. The transplanted kidneys were harvested after 3 days and examined for markers of inflammation.

Their results showed that there was a dose dependent reduction in inflammatory marker RNA including TNF- α , IFN- γ , and IL-1 β as well as a reduction in the recruitment of APCs to the graft [331], consistent with the findings of De Martino *et al* [328] and Zonta *et al* [334].

Further work was carried out in 2012 by Franquesa *et al* [329] looking at the reparative or protective effects of MSCs post Tx. Using a rat model of chronic allograft nephropathy they demonstrated that a single, venous dose of 5×10^5 MSCs at 11 weeks post Tx was able to reduce proteinuria, interstitial fibrosis and tubular atrophy. Furthermore, the MSC group was able to reduce the recruitment of T cells and macrophages as well as reducing inflammatory cytokines and increasing anti-inflammatory factors.

The 11 week time point was chosen as it corresponded to an increase in proteinuria in their model. They concluded that when MSCs were given at this time point they had a protective effect rather than a reparative one, this was based on the expression of several markers of kidney injury, including KIM-1 and N-GAL, which were only seen to increase in the control group indicating that kidney injury did not occur in the MSC group [329].

2017 work carried out by Wu *et al* [332] examined the impact of microvesicles (MVs) derived from human MSCs on IRI experienced by cold perfused deceased donor rat kidneys. Given what is known about how MSCs exert their effects it has been theorized that their extracellular micro vesicles maybe able to induce positive outcomes. In this study donor rats had cardiac arrest induced for 20 minutes, before warm ischemia was carried out on the donor kidney via *in situ* clamping. The kidney was then finally removed, perfused with university of Wisconsin solution and stored at 4°C for 18 hours before being transplanted into a syngeneic recipient. Immediately after the Tx was completed, the MVs were injected intravenously and the animals were then sacrificed at 24h, 48h, 1 week, and 2 weeks post transplant.

Their findings indicated that MVs were able to ameliorate IRI at both the acute and chronic stage. They showed that treatment with MVs resulted in an improved survival rate and improved renal functions. This was attributed to an ability to mitigate renal cell apoptosis, enhanced cellular proliferation, and alleviation of inflammation in the first 48 hours and an abrogation of renal fibrosis in the late period. Additionally, a decrease in the number of macrophages in the renal graft was observed [332].

Yu *et al.*, (2017) [333] carried out work looking at the impact of early administration of MSCs on chronic rejection in an allogeneic rat kidney transplant model. To do this they performed kidney transplants using Dawley rats as donors and wistar rats as recipients then divided them into 3 groups. Group 1 received cyclosporine for 10 days as well as 1×10^7 MSCs at days 0, 3, and 7. Group 2 received cyclosporine for 10 days. And group 3 received no treatment. Histopathology and immunohistochemistry was then examined at week 12. Their results showed that an early administration of MSCs was able to decrease the severity of symptoms associated with chronic renal allograft rejection such as; mononuclear cell interstitial inflammation, tubular atrophy, interstitial fibrosis, and vascular fibrous intimal thickening. Additionally, MSCs greatly reduced glomerulosclerosis [333].

All of these studies showed a definitive beneficial effect of MSCs in kidney transplantation over a variety of scenarios and settings. However, as they were all carried out in rats it is difficult to know how these findings would translate to the clinic. To elucidate this further it is important that large animal models be used.

Thus far there is only one study that has used MSCs in a large animal model of kidney transplantation. Baulier *et al.*, (2014) [335] used a pig model of kidney autotransplantation that mimics deceased donor transplantation though the use of a 1 hour warm ischemic period achieved via clamping of the kidney vessels, followed by 24 hours of cold preservation in

UW solution. After this the kidney is transplanted back into the donor animal and the remaining kidney is removed. As a test group they gave 6 animals 1×10^6 cells/kg of autologous MSCs directly into the renal artery 6 days post transplantation. They then followed the animals for 3 months to examine the development of features associated with IRI damaged kidneys such as plasma creatinine levels and fibrosis.

Their results showed that MSCs improved glomerular and tubular functions leading to improved renal function recovery when compared to the control group that underwent transplantation without MSC infusion [335]. Although these results are promising for the use of MSCs in IRI conditions mimicking deceased donor transplantation, the autotransplant setting removes the immunological impact on the graft and the MSCs as well as eliminating the interplay of MSCs with potential immunosuppressive drugs.

1.11 Clinical Trials Of MSCs In Kidney Transplantation

1.11.1 Pilot Studies

Several clinical trials and pilot studies have already been carried out looking at the application of MSCs in kidney transplantation. Perico *et al.*, (2011, 2013) [339, 340] have performed two pilot studies looking at the use of MSCs in kidney transplantation with a total pool of 4 patients. In their first study they administered intravenous autologous MSCs 7 days after transplantation and followed the patients for 360 days.

From days 7 to 14 post transplant, serum creatinine increased in one of their patients, however acute graft rejection was excluded via biopsy. They also noted an increase in patient Tregs and a decrease in T cell expansion post-transplant. Long term, both patients showed stable graft function and the authors concluded that MSC infusion in kidney transplant

recipients is feasible, allows increase of Treg in the peripheral blood, and controls memory CD8⁺ T cell function [339].

In their second trial, they dosed two living-related kidney transplant recipients with autologous MSCs one day before transplantation. The change in dosing time was an attempt to avoid the acute graft deterioration assumed to be caused by intragraft localization of MSCs when dosing 7 d post-transplant. Although both patients had no side effects to the MSC infusion and both had stable graft function at 12 mo, one of their patients did have an acute rejection episode 14 d post-transplant that was resolved with corticosteroid therapy. The authors attribute the rejection episode to a higher number of HLA mismatches.

They concluded that pre-transplant administration of MSCs avoided the cell induced graft dysfunction associated with post-transplant MSC administration and that this method is favourable for future trials [340].

Peng *et al.*, (2013) [341] examined the effect of autologous MSCs on renal transplants by giving six patients MSCs combined with half doses of tacrolimus. They then compared acute rejection, graft function, and graft survival at 12 mo to a control group of six patients receiving standard dose tacrolimus.

The results of this showed no toxic adverse effects associated with MSC infusion and all patients survived with stable graft function to 12 mo with only one acute rejection episode in the control group. The one difference they did notice was elevated B-cell counts in the MSC group at 3 mo compared to the control. They concluded that MSCs may provide benefits in renal transplantation by reducing the required dose of conventional immunosuppressive drug that is required for long term graft survival [341].

Lee *et al.*, (2013) [342] took a different approach to their administration of MSCs. At the time of transplant, 7 patients received 1×10^6 cells/kg of donor derived MSCs directly into the iliac crest. They found that the MSC group had an increase in several anti-inflammatory cytokines, including IL-10 and IL-6. However they also noted that there were 3 instances of rejection (2 acute, and one antibody mediated) as well as 2 cases of borderline rejection. This was in comparison to the control group of 4 in which 1 case of acute rejection was noted. Unfortunately, they did not include the data for the cytokine levels of the controls, nor did they include the creatinine levels and as such conclusion could not be drawn from them. They concluded that intraosseous injection of MSCs was safe but that further research was needed [342].

Reinders *et al* (2013) [343] applied MSCs as a response to negative findings during protocol biopsies. 6 patients were given 2 intravenous infusions of autologous MSCs when protocol biopsies showed rejection, interstitial fibrosis, or tubular atrophy. In 2 patients who presented with rejection they reported a resolution of tubulitis without interstitial fibrosis or tubular atrophy. They also noted that 3 of the patients developed opportunistic infections and had a decrease in donor specific proliferation in a peripheral blood mononuclear cell proliferation assay. These results were consistent with systemic immunosuppression and they concluded that the use of MSCs in this setting was safe [343].

The application of MSCs as a desensitizing agent was investigated by Saadi *et al* in 2013 [344]. After having trouble with a sensitized patient who required retransplantation they used 2 intravenous infusions of donor specific MSCs at a dose of 5×10^7 cells split over the 2 infusions. 2 months after treatment they found that the cross-match was repeatedly negative. They then used this technique on two more patients and had similarly successful outcomes.

It should be noted that the MSCs were not the only immunoablative therapies given and so the exact extent to which the MSCs contributed to the removal of sensitization cannot be determined. They came to the conclusion that MSCs are a potential treatment for pre-transplantation desensitization but that additional work needs to be performed before this use can be applied with confidence [344].

The most recent pilot study was carried out by Mudrabettu *et al* in 2015 [345]. They tested various doses and dosage timings on 4 patients. Two patients received low doses of MSCs ($.21 \times 10^6$ cells/kg to $.35 \times 10^6$ cells/kg) and two patients received higher doses (2.1×10^6 cells/kg to 2.8×10^6 cells/kg). All patients received an initial dose of MSCs 1 day before their transplantation and then 3 of the patients received an additional dose on day 30 post transplantation while the remaining patient, from the low dose group, received their second dose on day 60.

Mudrabettu did manage to show some positive outcomes associated with the infusion of MSCs. In particular their test group had a lower average serum creatinine over the course of 24 weeks. Additionally they showed that infusion with MSCs corresponded with high regulatory T-cell levels and lower CD4 T cell proliferation and, significantly, they reported no adverse events. Although their results were positive the authors still cautioned that the small size of the study makes extrapolation inadvisable and insist on further clinical trials before drawing conclusions [345].

As is the case with many pilot studies, solid conclusions about the efficacy of the treatment are difficult to make. Most of these pilot studies set out to primarily act as safety studies before further clinical trials. In this respect they were all able to show that MSCs had an acceptable safety profile when applied to kidney transplantation. The one potential concern was highlighted by Perico in which they noted some graft dysfunction due to migration of

MSCs to the transplanted kidney [339]. However this was transient, did not have a long term impact, and was able to be overcome with a change in protocol [340]. This issue was also not noted in any of the other pilot studies indicating that it may be a rare event.

1.11.2 Clinical Trials

Larger clinical trials have also been carried out in addition to the pilot studies. One of the earliest and most substantial trials was carried out by Tan *et al* in 2012 [346]. In their trial they had one hundred fifty-nine kidney transplant patients split into 3 groups, with two groups receiving autologous MSCs with either standard dose calcineurin inhibitors (CNIs) or low dose CNIs and the control group receiving standard dose CNIs and anti-IL-2 receptor antibody.

The major conclusions from this study were that the MSC groups had a lower incidence of glucocorticoid-resistant rejection, a faster recovery in renal function, and significantly decreased risk of opportunistic infections than the control group. This study also addresses safety concerns over the use of MSCs as there were no adverse reactions reported in either of the test groups.

However, this trial was not without its problems. It was noted by the authors that the number of rejection episodes in the control group was higher than what would be expected in a modern transplant centre. This made it appear that the MSC groups performed better than standard immunosuppression when this may not be the case. Additionally, the major differences in graft function were only noticed in the first 2 weeks [346]. It is conceivable that this was due to the regenerative abilities of MSCs repairing the reperfusion injury associated with all kidney transplants. And lastly, the major difference in opportunistic infections was noted in the MSC and low dose CNI group. As there was no control low dose

CNI group, it cannot be determined if the observed reduction in infection is due to MSCs or simply due to the reduced use of immunosuppressive drugs.

Another large study carried out by Vanikar *et al* in 2014 [347] looked at a combination of MSCs with hematopoietic stem cells (HSC). They compared this group to HSC infusion with no MSCs and a control group receiving standard immunosuppression with each arm containing 95 patients.

The major aim of their study was to examine the potential for MSC and HSC treatment to allow a lowering of immunosuppressive drug load. The patients received donor derived stem cells 5 days prior to transplantation at an average dose of $.33 \times 10^4$ MSC/kg and 8.85×10^8 HSC/kg. The two test groups additionally underwent a tolerance induction protocol starting 15 days pre-transplant. This study followed patients out to 7 years, however some data at the 7 year mark is incomplete so this summation will only include out to 5 years.

This study had several significant findings; The MSC group had a better survival rate at 1, 3, and 5 years compared to the HSC alone and the control group. This trend was also found in the death censored graft survival rate. The serum creatinine was initially lower in the control groups but by the 5 year point the MSC group had a better outcome here as well.

Addressing their primary research objective they found that at the time of analysis 3.6% of patients in the MSC group were on no immunosuppression, 13.3% were on prednisone monotherapy, 51.8% were on dual-therapy immunosuppression, and 31.3% were on triple therapy immunosuppression. In the HSC alone group 1.3% of the patients were on no immunosuppression, 5.3% were on prednisone monotherapy, 56.6% were on dual-therapy, and 36.8% were on triple therapy. This is in stark contrast to the control group in which all the patients remained on triple therapy [347].

This study has shown some very promising benefits of the use of MSCs, however, there are several issues that are cause for hesitation. One of the most obvious issues is that the test

groups and the control group received different induction therapies prior to transplantation; this introduces an additional variable that has the potential to have a potent impact on transplant outcomes. In the context of MSCs for kidney transplantation it also has issues in that the MSCs were infused with HSCs and given that the doses of HSCs were far greater than MSCs it is uncertain the extent to which each cell population played a role. Of greatest importance however is the lack of statistical significance. The differences in graft survival did not reach statistical significance and neither did the lower serum creatinine at 5 years in the MSC group. And lastly, the reduced immunosuppression of the test groups is misleading in that the control group did not undergo evaluation for the lowering or discontinuing of their drug regimes.

The most recent clinical trial was comparatively modest in size with only 16 patients in each arm and was carried out by the same group that performed the 2013 Peng *et al* pilot study [348]. The primary focus of this clinical trial was to evaluate if the use of MSCs was able to allow for a reduction in immunosuppressive load.

Both the test and control group underwent identical induction therapy of cytoxan and methylprednisolone. The control group then received a standard dose of Tacrolimus (0.07-0.08 mg/kg/day) while the test group received low dose Tacrolimus (0.04-0.05 mg/kg/day) as well as two infusions of MSCs. The first infusion, numbering 5×10^6 cells, was carried out on the day of transplantation and was directly injected into the renal allograft artery just prior to the completion of the arterial anastomosis. The second infusion was carried out one month later wherein 2×10^6 MSC/kg were administered intravenously.

The patients were followed up for 2 years and had a variety of metrics monitored including graft survival, creatinine levels, urea levels, and lymphocyte levels. Across all tracked elements no statistically significant difference was noted. Graft survival, urea, urine protein, urinary red blood cells, urinary white blood cells, 24-hour urine protein, creatinine clearance

rates, and lymphocyte levels were all similar enough between the two groups that a statistically significant change could be found with this sample size.

The result that they do draw is that because there was no difference MSCs offer the potential for a lowering of immunosuppression [348]. However, they do not have a low dose Tacrolimus control group so it is possible that the lower drug levels could have been sustained even without the use of MSCs, this is supported by evidence showing that many immunosuppressants are able to be lowered without any adverse effects as long as careful monitoring is carried out [349, 350]. Additionally, serum tacrolimus levels are not representative of the actual effective tacrolimus level. This is due to the highly protein bound nature of the drug which results in only a small percentage being responsible for its immunosuppressive impact, so any changes to blood biochemistry can have a dramatic impact on the free, and therefore active, tacrolimus in the blood [351, 352].

1.12 Safety

Although the pilot studies and clinical trials mentioned do not demonstrate any major adverse events attributable to the administration of MSCs in transplantation, there is ongoing concern about the safety of MSCs as a therapy. The primary issues relate to the ability of MSCs to reduce anti-tumour immune functions [353], promote angiogenesis of tumours which can then result in metastasis [354], as well the potential for unwanted differentiation [355]. The tumour supporting functions of MSCs have been demonstrated *in vitro* and in pre-clinical models [353, 354], and, although they have yet to cause detrimental effects clinically, this does not exclude their potential to cause adverse events, requiring continued caution.

The negative impact of unwanted differentiation was clearly demonstrated in 2017 during a trial in which MSCs were used as a treatment for macular degeneration [355]. Three patients received intravitreal injection of mesenchymal stem cells and subsequently had complete

vision loss by one year post administration. It is thought that the MSCs differentiated into myofibroblasts resulting in retinal detachment [355].

These safety issues show the need for careful and considered progress in the use of MSCs, significant gaps persist in the knowledge surrounding how different isolation techniques and transplant environments may impact how MSC react when administered.

1.13 Concluding Summary

Each of these clinical trials has shown some seemingly positive effects, however due to a variety of issues it is not possible to make definitive conclusions about the use of MSCs in kidney transplantation. There are obviously ethical considerations that determine what a clinical trial can and cannot do, these are completely necessary for patient safety but do present problems when it comes to study design. One conclusion that most of the available evidence supports is that MSCs have an acceptable safety profile. But, their potentially beneficial effects for transplantation have yet to be as apparent as initially hoped.

Despite the current lack of positive clinical data, there still remain several very important questions to be answered before the best application of MSCs is known and they can obtain mainstream clinical use.

The issue of whether autologous or allogeneic MSCs are better is significant, with arguments for both being put forward. Tan *et al* employed autologous MSCs because of the issues surrounding MSC isolation from deceased donors [346]. Furthermore, the use of autologous MSCs would avoid any potential for rejection of the cells and a subsequent loss of their function. However, there is some evidence that MSCs are immuno-evasive allowing them to escape recognition by the host immune system [356]. If this is the case, then allogeneic MSCs are promising as obtaining them will not impact the eventual recipient who may have

serious health issues that could be exacerbated by the collection of MSCs or could impact the quality of the cells.

The immuno-evasive status of MSCs also opens up the potential for third party derived MSCs, this would invalidate concerns about obtaining MSCs in the cases of deceased donors. Nevertheless, issues pertaining to the immunogenicity of allogeneic or third-party derived MSCs have not been substantially addressed *in vivo* and have not been addressed in large animal models.

There are preclinical studies demonstrating that allogeneic MSC monotherapy alone failed to prevent allograft rejection [357-359], in contrast, studies reporting on the benefits of allogeneic MSCs have also shown short term prolongation of graft survival [360]. More importantly, in some studies, pre-transplant allogeneic MSC monotherapy accelerated allograft rejection thereby questioning the immunoprivileged status of MSCs [358, 359, 361-363]. There is evidence that allogeneic MSCs can trigger an anti-donor immune response resulting in accelerated allograft rejection [362, 363]. The co-administration of allogeneic MSCs with immunosuppressive drugs however, showed better outcomes of the allograft compared to MSC monotherapy [364, 365]. Therefore, the synergistic effects of allogeneic MSC with immunosuppressive drugs need to be taken into consideration in MSC therapy.

Questions around the dose rate, the timing, the route of administration, what happens to the cells, what exactly the MSCs are doing, and their mechanism of action still remain unanswered. Given the state of the field it is not possible to accurately speculate on the answers to these questions. Additionally there is the potential for the modification of MSCs that further expands their possible applications and potential efficacy.

1.14 Thesis Aims

The primary aim of this thesis was to examine the impact that MSCs have on kidney allograft function in the days following transplantation as well as assessing if MSCs are able to offer prophylaxis against rejection upon the withdrawal of immunosuppressive drugs.

In order to achieve the primary aims, several secondary aims needed to be met. First, development of the ovine heterotopic kidney transplant model needed to be carried out to ensure reproducibility and to reduce possible undesirable variables influencing later experiments.

Second, gaining knowledge about the migration of MSCs when injected intravenously in a large animal model was required in order for an informed decision about the route of administration of the MSCs.

Chapter 2

General Methods and Materials

2.1 Ethics

Ethical approval for this project was granted by both the University of Adelaide animal ethics committee and the South Australia Pathology Animal ethics committee. The University of Adelaide AEC project number was M-2013-118 and was granted for the period beginning the 19th of August 2013 to the 18th of August 2017. The SA pathology AEC project number was originally 88/13 before being changed to SAM18 and was granted for the period beginning on the 19th of August 2013 to the 31st of August 2017. Under both of these project approvals, the use of 36 sheep was approved for the purpose the improvement of human and animal health and welfare.

2.2 Animals

All animals were 2 year old female merino sheep. They weighed between 50 and 60 kg and were sourced via the large animal research and imaging facility (LARIF, 101 blacks road, Gilles Plains, Adelaide 5086). All animals were examined by a qualified vet to ensure they had no pre-existing conditions prior to experimental use.

2.3 Animal Handling

Proper restraint of conscious animals was required to ensure minimal risk to both the sheep and any personnel present. When collecting blood or inducing anaesthesia, the sheep were tipped onto their rumps, this results in the animal becoming docile even while having blood taken. Tipping a sheep is a common practice in live stock handling, it is carried out by

positioning yourself to the side of the sheep, placing your left hand under its jaw, putting your left knee just behind the animals left shoulder, your right knee just in front of its right hip and your right hand on its back above the hips. Next, you begin to turn the animals head away from you while placing pressure downwards on the hips, as you begin to feel the animals weight on your legs you take a step back with your right leg, the hind legs of the sheep should start to go down, continue to bring the head around until the sheep is resting on its rump with its back against your legs. From this position the animal is able to be handled with relative ease and you have access to the major blood vessels in the neck to collect blood or give I.V. drugs.

For procedures that took place within the post operative holding pen it was sufficient to lean on the sheep and secure them against the pen wall, this resulted in them either holding in place or sitting down. When held in either of these positions the animals were sufficiently restrained to allow for biopsy of the transplanted kidney, collection of blood, and the administration of oral pharmaceuticals.

2.4 Animal Procedures

All animal procedures were carried out at the LARIF with assistance from veterinary technicians or veterinarians as required. The Transplant surgeries were carried out by the Surgeons from the Royal Adelaide Hospitals renal transplantation unit.

Many of the procedures carried out required that the animals be placed under general anaesthesia. This was initially induced using a single dose of sodium thiopentone (50mg/ml) at 10-25 mg/kg. However, later on the animal ethics committee deemed that a mixture of ketamine (0.5 mg/kg) and diazepam (0.2-0.3 mg/kg) were better suited for induction and so this was adopted. Isoflurane at 1-2% was used for maintenance during extended procedures with an electrocardiograph used for heart rate monitoring.

Post operative pain relief consisted of 0.01mg/kg buprenofen, given subcutaneously (SC) and local anaesthesia was induced using SC lignocaine, 20mg/ml as needed.

A full list of drugs used and their application can be found in appendix A.

2.5 Central Venous Lines

Central lines were required for several procedures to administer drugs and fluid or for collection of blood samples. Two separate locations were used to place central lines; most commonly they were placed into the jugular vein, however, during the kidney transplant surgery a line was placed into the inferior vena cava. In order to place the jugular line the sheep was put under general anaesthesia, the wool over the jugular clipped back and a 14 gauge catheter attached to a 10 ml syringe inserted. The syringe was drawn back to confirm venous placement, when blood filled the barrel the needle was withdrawn leaving the catheter. A 3 way tap was then connected to the catheter which was sutured to the skin to prevent it from being pulled out.

Details of the inferior vena cava line are covered in more depth in chapter 4. Briefly, after a nephrectomy was performed a line was placed into the stump of the renal vein still attached to the vena cava. This line was then threaded down the vena cava and the venous stump ligated to anchor the line in place. The line was then further anchored to the skin as the nephrectomy wound was being closed.

2.6 Magnetic Resonance Imaging

A Siemens 1.5 Tesla (T) Sonata MRI machine was used to for imaging. General anaesthesia was induced as stated above and the animals placed on a ventilator and heart rate monitor after being shifted on to the MRI table. Radio frequency coils of the correct size were placed over the areas of interest, which were the transplanted kidney, the chest and abdomen, or the *ex vivo* organs. Anatomical scans were taken to identify the organs to be

imaged before a T2* sequence was used with parameters designed to give sufficiently good resolution data in a reasonable time with a good signal to noise ratio. These parameters varied depending on what was being imaged.

2.7 Necropsy

Necropsies were carried out upon euthanasia of sheep that had undergone transplantation and a variety of tissue collected for further analysis. To begin, the transplanted kidney was removed from the neck, dissected medially on the lateral aspect of the kidney. 6 wedges of tissue were then collected from each side of the kidney; these were placed in 10% formalin. Next, the abdomen was opened by making an incision along the ventral aspect of the abdomen from just posterior to the sternum down to the rear flank. This was opened up and the gut, which dominates the cavity, was retracted to allow access to the liver and the spleen. These organs were removed and wedges of tissue cut and placed in formalin. Next, the sternum was separated using repurposed by-pass gardening lopper, giving access to the lungs. The lungs were removed and had sections cut from them that were then placed in formalin. Lastly, a section of ear was cut and placed in a collection container for future DNA extraction if required. The ear tissue was stored at -20°C which allows the DNA to remain stable long term.

40 ml of whole blood was collected into 50 ml falcon tubes with 2ml of heparinised saline. The blood was mixed 1:1 with PBS and was separated into 20ml aliquots in fresh 50ml falcon tubes. 15ml of lymphoprep was underlaid using a glass pipette. The tubes were then spun at 900xg for 45minutes with no brake. The MNC layer and most of underneath was collected, taking care not to aspirate the red blood cells at the bottom on the tube. MNC from two tubes were pooled into a fresh 50ml falcon tube and the volume increased to 40ml total with PBS and centrifuged for 10 minutes at 700xg, break off, in order to wash off the ficoll. The supernatant was discarded and the pellet resuspended in 20ml PBS and centrifuged 400xg for

5 minutes break off. This was repeated to ensure complete removal of any remaining ficoll. The pellet was then resuspended in a known quantity, dependant on the size of the pellet, of PBS and counted using a haemocytometer.

2.8 Stimulation Of PBMC

2.8.1 MLR

Stimulator cells were suspended at 1×10^6 cells/ml in RPMI. These were then irradiated with 30 grays of radiation to stop proliferation. These cells were then plated at a density of 5×10^4 cells per well of a 96 well plate. The responder cells were added at the same density so that each well had a final cell number of 1×10^5 , RPMI was added to each well to give a final total volume of 200 μ l and the surrounding wells filled with PBS to reduce evaporation. The plates were then incubated at 37 $^{\circ}$ c in a 5% CO₂ enriched and humidified incubator for 4 days. The wells were then pulsed with 1 μ Ci (37mBq) of tritiated thymidine and incubated for a further 18 hours under the same conditions. Following incubation the cells were harvested using a skatron cell harvester (Skatron, Norway) onto glass fibre filter mats. The mats were then placed in a scintillation count cassette and had 30 μ l of scintillation liquid added on top of the filter map before being sealed. The counts per minute were then measured using a Beckman LS 2800 beta counter (Beckman, USA). The counts per minute are a representation of the incorporation of tritiated thymidine into the cells. This acts as a measurement of the proliferation of the cells after being pulsed. Each cell pairing is run in five duplicates and the highest and lowest counts are removed. The end result is the mean of the 3 most concordant results +/- standard deviation.

2.8.2 ConA

Isolated PMBC were resuspended in RPMI at a density of 1×10^6 . Cells were then aliquoted into cell culture plates at a density of 1×10^5 cells/well. 10 μ g/ml of Con A was added

to each well. The plates were then incubated and followed the remaining steps as described for the one-way MLR. If MSC were to be added they were irradiated with 30Gy to stop their proliferation and plated out the day before to allow them to adhere. The MSC were added to the wells at 0.1%, 1% or 10% of the number of PBMC to be added.

2.9 Isolation Of MSCs

Female merino sheep were anesthetized using ketamine (0.5mg/kg) and diazepam (0.2-0.3mg/kg) for induction and Isoflurane (1-2%) as maintenance. The right hand side of the sheep was shorn over the hip with enough space to create a sterile field. A small incision was made in the skin over the superior aspect of the right hip. Using a portable image intensifier xray machine, an osteobell "T" needle was forced into the iliac crest until it reached the cancellous bone being careful not to push through the other side of the bone. Next the core of the Osteobell needle is removed and a 60ml leur-lock syringe attached and drawn back to allow the collection of bone marrow aspirate. This aspirate is then placed into a 50ml falcon tube with heparin up to 40ml. Following collect the bone marrow aspirate was filtered through a 70nm cell strainer to remove any bone chips or clots and split across 4 50ml falcon tubes, mixed with an equal volume of PBS and then under laid with 15ml of ficoll. The tubes were then centrifuged at 1000xg for 45 minutes at room temperature with the break off. The resulting mononuclear cell layer was collected and two tubes worth was pooled into one. PBS was then added and a wash spin performed to remove the ficoll. The resulting pellets then underwent 2 additional washes in 20ml PBS. A cell count was performed after the second wash. The final cell pellet was resuspended in complete media (10% FBS, 1% Ascorbate, 1% Glutamate, 1% sodium pyruvate, and .5% penicillin/ streptomycin) at 1×10^6 cells/ml. The cells were then plated out at 30,000 cells per cm^2 or 5.25×10^6 cells per T175 flask. Cells were cultured at 37C 5% CO₂ for 7-10 days during which time they will adhere to the flask before a media change was performed.

2.10 Trypsinizing Adherent Cells

Due to the adherent nature of the MSCs trypsinization is required to remove them from flasks. This was performed by washing the flasks twice with 10ml PBS to remove any trace of the complete media. Trypsin was added at a volume of 1ml per T75 flask and incubated for 5 minutes at 37°C to detach cells. The flasks were lightly tapped and swirled to ensure detachment of MSCs before 5ml of 5% FBS in PBS was added to quench the trypsin. The detached cells were collected in 50ml falcon tubes and the flasks rinsed with 10ml PBS. The flasks were inspected under a light microscope to confirm that all the cells had been collected. PBS was added to each tube to bring the final volume to 30ml and centrifuged at 250xg for 5 minutes at 4°C. The resulting pellets were then resuspended in 5ml of 5% FBS in PBS and a cell count performed.

2.11 Expansion of MSCs

After the first media change, cells were cultured for approximately 3 days, or until they reached 70-90% confluency before being passaged. Care was taken to ensure cells never reached 100% confluency prior to passaging. Once the cells reached 80% confluency they were harvested by trypsinization as described above. After the cell count the falcon tubes were topped up with PBS and spun again at 250xg for 5 minutes and 4°C and the supernatant discarded. The pellets were then resuspended in complete MSC media and plated out at 10,000 cells per cm² or 1.75x10⁶ cells per T175 and allowed to reach 80% confluence before being split again.

2.12 Freezing Cells

If cells were to be frozen they were centrifuged at 250xg for 5 minutes at 4°C then resuspended at 5x10⁶ cells/ml in freezing media which consists of 20% FBS and 10% DMSO in addition to the normal complete media. The suspension was transferred to cryovials, at 1.8ml per vial, placed in a “Mr Frosty” cryobox and frozen in a -80 freezer.

2.13 Thawing Frozen Cells

Cryovials were placed in a water bath at 37°C until the frozen core became moveable then tipped into a 50ml tube containing 10ml of 5% FBS in PBS. This was then centrifuged at 250xg for 5minutes at 4°C. The supernatant was decanted, the pellet resuspended in 5% FBS in PBS and a cell count performed. The suspension was topped up with PBS and washed again then resuspended in complete media and plated at 10,000 cell/ cm². The thawed cells were passaged once prior to being used.

2.14 Flow Cytometry

All washes were carried out by resuspending the cells in 5ml cold FACS wash buffer and centrifuging at 250xg for 5 minutes at 4°C unless otherwise stated

2.14.1 One Colour Analysis

MSC were harvested from flasks by trysinization as previously described. After 2 washes the cells were counted and 1x10⁵ cells aliquoted per cell surface marker to be analysed. The cells were then centrifuged at 500xg, 5 min and the supernatant removed. The remaining cell pellet was then resuspended in 5ml FACS wash containing 10% heat inactivated rabbit serum and incubated on ice in the dark for 10 minutes to block non-specific Fc receptors from binding the antibodies to be used. During the incubation period primary antibodies for each marker were aliquoted into clean flow tubes, antibody amounts used are detailed in table 2.1. The cell suspension was then washed and resuspended in FACS wash at 1x10⁶ cells/ml, 100µl of this was added to each of the antibody tubes and incubated for 30 minutes on ice, in the dark. After this incubation the cells were washed once more and, if the primary antibody was unconjugated, a suitable secondary antibody was added in a final dilution of 1 in 500 in FACS wash buffer. The samples were then incubated for 20 minutes on ice, in the dark. After this incubation the cells were washed once again and then lysed using 10% FACS lysing solution for 20 minutes at room temperature, in the dark. The cells were

then washed twice more before being resuspended in 200µl PBS and stored at 4°C in the dark until being analysed on a BD FACSCantoII (BD Biosciences, San Jose, CA,

<http://www.bdbiosciences.com/>)

2.14.2 Cell Surface Markers

The cell surface markers and the volumes used for the MSC characterization flow cytometry are as follows:

Antibody	Source	Catalogue number	Clone	Amount added
CD11b	Serotec	MCA1425GA	CC126	10µl
CD14	Serotec	MCA920GA	VPM65	10µl
CD31	Serotec	MCA1097GA	CO.3E1D4	10µl
CD45R	University of Melbourne	N/A	SBU 20.96	50µl
VCAM-1	BD biosciences	550547	429	50µl
MHCII	Serotec	MCA2226	37.68	10µl
MHCI	Serotec	MCA2224	41.17	50µl
CD44	University of Melbourne	N/A	25.32	50µl
CD73	BD biosciences	550741	TY/23	10µl
CD90	Bioss	BS-0778R	30-80/161	10µl
CD105	BD biosciences	562759	MJ7/18	10µl
CD166	BD biosciences	559260	3A6	10µl
Unstained	N/A	N/A	N/A	N/A

Table 2.1 Antibodies used in flow cytometric staining of ovine mesenchymal stem cells along with the source, catalogue number, clone, and the amount used to stain 100,000 cells.

2.15 MSC Differentiation

2.15.1 Adipogenic Differentiation

After cell harvesting and counting, cells were resuspended in complete media and seeded on a 12 well plate, at 4×10^4 cells per well. The plate was incubated for 2 days at 36°C , 5% CO_2 to allow the cells to adhere. On day 2 the complete media was removed and the wells washed with PBS before 2ml of complete adipogenesis differentiation media was added. The plates were placed back in the incubator and allowed to undergo differentiation. The media was changed every 4 days for a period of 20 days. After 20 days the cell were stained with Oil Red O stain to visualize lipid vacuoles.

2.15.2 Chondrogenic Differentiation

After cell harvesting and counting, cells were resuspended in complete media and seeded on a 12 well plate at 4×10^3 cells per well and incubated for 1 day at 36°C , 5% CO_2 to allow the cells to adhere. After 1 day the complete media was removed and the cell washed with PBS before 2ml of complete chondrogenesis differentiation media was added. The plates were placed back in the incubator to allow the cells to differentiate with the media being changed every 2-3 days for 20 days. After 20 days the cells were stained with Toluidine blue to stain cartilage purple.

2.15.3 Osteogenic Differentiation

After cell harvesting and counting, cells were resuspended in complete media and seeded on a 12 well plate at 2×10^4 cells per well and incubated for 2 days at 36°C , 5% CO_2 to allow the cells to adhere. After 2 days the complete media was removed and the well washed with PBS before 2 ml of Osteogenesis differentiation media was added. The plate was plated back in the incubator and to allow the cells to differentiate. The media was changed every 3

days for a period of at least 21 days. After 21 days the cells were stained with Alizarin red which labels calcified depositions red.

2.16 Viability

MSC viability was verified using the ThermoFisher LIVE/DEAD fixable dead cell stain kit. Prior to use a vial of the reactive dye and the supplied anhydrous DMSO were thawed out. 50µl of DMSO was added to the vial of dye and vortexed to ensure complete dissolution of the dye. 1×10^6 cells were collected and centrifuged at 250xg for 5 minutes at 4°C. The cells were then resuspended and washed in PBS by centrifugation at 500xg for 5 minutes before being resuspended once more in 1ml of PBS. The cell suspension then had 1µl of the reconstituted dye added before being briefly vortexed. The cell solution was incubated on ice, in the dark for 30 minutes before being fixed. To fix the cells they were washed with 1ml of PBS, the cells were then pelleted by centrifugation and the supernatant removed before being resuspended in 900µl of PBS and 100µl of 37% formaldehyde added. The cells were then incubated in the dark at room temperature for 15 minutes. A final wash was performed using 1ml of PBS with 1% FBS before the pellet was resuspended in 1ml of PBS with 1%FBS. The cells were then analysed on a flow cytometer using the AmCyan-A detection channel.

The dye works by reacting with cellular amines. The permeable membrane of dead cells allows the dye to react with amines on the interior of the cell and not just those on the cell surface, as is the case with live cells. This results in a stronger florescence being produced by dead cells and a distinct right-ward shift when analyzed on a flow histogram.

2.17 DNA Extraction

Blood samples collected in an 8ml green top sodium heparin tube were taken and DNA was isolated using a Qiagen DNeasy blood and tissue DNA purification kit. As per

manufacturer's instructions, 100µl of blood was added to a 2ml microcentrifuge tube with 20µl proteinase K and the volume adjusted to 220µl with PBS. 200µl of buffer AL was added and the tube vortexed before being incubated at 56°C for 10 minutes. The resulting mixture was pipetted into a DNeasy quick spin column in a 2ml collection tube and spun at 8000 rpm for 1 minute. The flow through and collection tube were discarded and the spin column placed in a clean collection tube. 500µl of buffer AW1 was added and the tube spun at 8000 rpm for 1 minute. The flow through and collection tube were discarded and the column placed in a new collection tube. 500µl of buffer AW2 was added and the tube spun at 13,000 rpm for 3 minutes. The flow through and collection tube were discarded and the column placed into a 2ml eppendorf tube. 200µl of buffer AE was added directly to the membrane and incubated for 1 minute at room temperature before being spun at 8000 rpm for 1 minute in order to elute the DNA.

The resulting purified DNA was analysed using a nanodrop spectrophotometer to determine the quality and concentration.

2.18 Primer Design

Ovine genomic sequence for the DRA and DRB1 genes was acquired from the CSIRO ovine genome browser (<http://gbrowse-ext.bioinformatics.csiro.au/gb2/gbrowse/oarv3/>). The target sequences were then put into the primer3 primer design application (<http://bioinfo.ut.ee/primer3-0.4.0/>) and several binding locations tested until a primer pair with acceptable melting temperatures (58°C – 62°C), GC content (30%-60%), and product size (250bp – 800bp) were created. These primers were then ordered from Geneworks through their custom oligos service (<https://www.geneworks.com.au>).

2.19 PCR Optimisation

Once the primers had been designed and diluted they were optimised by altering the annealing temperature and the length of the extension step. The PCR conditions were as follows:

Reagent	Amount per reaction
GoTaq Green master mix	25 μ l
Forward Primer	5 μ l
Reverse Primer	5 μ l
Purified DNA	1-5 μ l
H2O	10-15 μ l
Total reaction volume	50μl

Table 2.2 Components of the PCR reaction mixture

The total volume of the reaction was set as 50 μ l, however the volume of the constituent reagents varied. This variation was based on the concentration of the purified DNA sample as determined by the nanodrop. To counteract this, the amount of H2O added was changed to suit.

When optimising the protocol the two major factors that were altered were the annealing temperature (Step 3) and the length of the extension step (Step 4), these are indicated in bold. The goal of this optimisation was to have a protocol that all three of the primer pairs could run on and still give high quality PCR products for sequencing.

Step	Temperature	Time
1	94°C	2 minutes
2	94°C	30 seconds
3	50-60°C	30 seconds
4	72°C	30 seconds – 2 minutes
5	72°C	5 minutes

Table 2.3 Temperature and time conditions and variations used for the optimization of the PCR protocol

2.20 Agarose Gel Electrophoresis

DNA was visualised using agarose gel electrophoresis. 1.5% agarose gels were cast and run using a Bio-Rad mini-sub cell gel tank (Bio-Rad Laboratories, Hercules, California, USA). Agarose gel was made by dissolving SeaKem Le agarose powder (Cambrex bioscience, Rockland Inc. Rockland, ME, USA) in 1 x TBE buffer then adding 1µl of Gel red (Biotium, 46117 Landing Parkway, Fremont, California, USA)

DNA samples (both genomic and PCR product) were mixed with ~1 µl of loading dye (0.2% Bromophenol blue, 0.2% Xylene Cyanote) and loaded into the wells. Fragments were sized using a 1kb plus DNA ladder at 2 ng per gel (Invitrogen, Carlsbad, California, USA). The gel was run at 100V until adequate separation of the fragments was achieved; this was judged by the distance that the leading dye front, caused by bromophenol blue, had travelled in the gel. The gel was visualised using the UV light setting in a BIORAD Universal Hood and imaged using the Quantity One Gel Doc system.

2.21 Sequencing

Sequencing was carried out by the Australian Genome Research Facility (AGRF Head office, Suite 219, 55 Flemington Road, North Melbourne, VIC 3051, <http://www.agrf.org.au/>). The samples underwent Purified DNA sanger sequencing. The PCR products were 379bp for DRA exon 1, 382bp for DRA exon 2, and 672bp for DRB1 exon 2, as such 12ng of DNA per sequencing sample were set up containing 10pmol of the relevant primer in a final volume of 12µl the balance made up with H₂O. The samples were then sent to AGRF for sequencing analysis.

2.22 Pharmacology

Blood for pharmacological analysis was collected in a K₂ EDTA purple top tube and stored at -20°C until needed. The tubes were thawed and vortexed just prior to sample preparation. 50µl of whole blood was collected had 100µl of cold precipitating solution added before being vortexed for 5 seconds. This mixture was centrifuged for 10 minutes at 13200 rpm in an eppendorf tabletop microfuge. 100µl of supernatant was drawn off and added to HP autosampler vials and capped. 25µl was injected into the Applied Biosystems API2000 HPLC mass spectrometer.

2.23 ELISA

Samples were prepared and used as per the MyBioScience Sheep Kidney Injury Molecule 1 Elisa kit instructions. In brief, 100µl of sample was added to each sample well followed by 10µl of “balance solution” and 50µl of “conjugate”. A pipette was used to mix the solutions before incubating for 1 hour at 37°C. The plate was washed by removing the liquid from the wells and rinsing 5 times with wash solution. 50µl of both “substrate A” and “substrate B” were added to the wells, covered and incubated for 15 minutes at 37°C. After the incubation period 50µl of “stop solution” was added to each well and the plate read on an Epoch microplate reader at 450nm.

2.24 Banff Grading

Biopsies from allotransplanted kidneys were sectioned stained with hematoxylin and eosin (H&E). These were then blinded and graded by a 3rd party using the Banff grading schema 2013/2014 [366].

2.25 Appendix A: Pharmaceuticals

Drug	Dose Rate	Frequency	Route Administered	Volume	Possible adverse effects of administration or withdrawal of drugs
Anaesthetic Agents	Thiopental sodium (50mg/ml)	single dose	I.V	10-25 mg/kg	possibility of cardiopulmonary depression/ Hypotension (if overdosed or if administered too quickly)
	Isoflurane/O ₂ (1-2%)	administered once via inhalation	Inhalation	As needed	chance of cardiopulmonary depression/ hypotension/ heat arrest if overdosed
	Lignocane 20mg/ml (or xylocaine 2%)	given as needed (before biopsy sampling)	delivered subcutaneously (SC)	As needed	possibility of rare allergic reaction and mild irritation
	Ketamine 0.5 mg/kg	single dose	I.V	0.5 mg/kg	Chance of elevated blood pressure and larynx spasm

Post Operative Analgesia	Buprenorphine (Temgesic) 0.01 mg/kg	given as needed 6-12 hours post surgery	given SC or I.V.	As needed	respiratory depression
Tranquillisers	Xylazine (20mg/ml)	used as pre-anesthesia	delivered SC or I.V.	0.1-0.3 mg/kg	possibility of cardiopulmonary depression/hypotension if overdosed or administered too quickly.
	Diazepam IV	used as pre-anesthesia	given I.V.	0.2-0.3 mg/kg	cardiopulmonary depression/hypotension if overdosed or administered too quickly.
	Acepromazine	used as pre-anesthesia	delivered via intramuscular injection (IM)	0.02-0.04 mg/kg	Possibility of cardiopulmonary depression/hypotension if overdosed or administered too quickly.
Antibiotics	Amoxycillin (150 mg/ml)	given once at surgery and more often if required	delivered I.M or SC	~2ml/30 kg	possibility of a rare allergic reaction
	Procaine penicillin (300mg/ml) (or any antibiotic indicated for renal insufficiency)	given once at surgery and more often if required	delivered I.M or SC	~3ml/30 kg	possibility of a rare allergic reaction
Other Substances	Heparin, Mannitol (Osmitrol), Frusemide (Lasix)	To be used at the time of transplantation as indicated by the surgeons	given via I.V	used as needed	MM, CRT, and signs of bleeding will be monitored due to anticoagulation effects of heparin. Urinary output and level of

	Cyclosporine	Given every day during allotransplantation	Given in a 100ml bottle of dextrose via a central line	5mg/kg	hydration will be monitored due to diuretic effect of frusemide Dizziness and nausea, reduced food intake and a change in responsiveness and stance
	Dexamethasone	Given to control swelling	Given I.V.	2mg/mg	Muscle weakness, impaired wound healing, dizziness
Humane Killing Agents	Lethabarb	used as needed	given I.V.		used for euthanasia.

2.26 Appendix B: Reagents used

Reagents	Supplier	Cat#
α - Minimal essential Media (α -MEM)	ThermoFisher	12561056
Agarose powder	ThermoFisher	75000500
Alizarin red	Sigma Aldrich	A5533
Ascorbate	Sigma Aldrich	PHR1008
Bromophenol blue (Sigma)	Sigma Aldrich	B0126

DNA ladder, 1kb plus (invitrogen)		10787-018
Ethanol	Sigma Aldrich	E7023
Ethylenediaminetetraacetic acid (EDTA)	Sigma Aldrich	E9884
ExoSAP-IT™ PCR Product Cleanup Reagent	ThermoFisher	78200.200.UL
Hyclone Foetal Bovine Serum, MSC qualified (FBS)	GE Health Care	SH30070.03M
Gelred nucleic acid gel stain	Biotium	41001-41003-T
Glacial acetic acid (BDH)	Sigma Aldrich	A6283
Glutamate	Sigma Aldrich	G3126
Isopropanol (BDH)	Sigma Aldrich	102246L
Loading dye		
Oil Red O	Sigma Aldrich	O0625
Penicillin/ Streptomycin	ThermoFisher	15070063
Phosphate-buffered saline (PBS)	MPU	
Primers	Geneworks	N/A
Proteinase K (Invitrogen)	Sigma Aldrich	P2308
Roswell Park Memorial Institute medium (RPMI)	ThermoFisher	11875093
Sodium pyruvate	Sigma Aldrich	P2256

Toluidine blue	Sigma Aldrich	89640
Tris (Invitrogen)	ThermoFisher	15504020
Tritiated thymidine		
Xylene cyanole FF (Sigma)	Sigma Aldrich	335940
Kits		Cat #
DNeasy Blood & Tissue Kits	Qiagen	69504
QIAquick PCR Purification Kit	Qiagen	28104
LIVE/DEAD™ Fixable Aqua Dead Cell Stain Kit	ThermoFisher	L34957
StemPro Adipogenesis Differentiation kit	Gibco	A10070-01
StemPro Chondrogenesis Differentiation kit	Gibco	A1007101
StemPro Osteogenesis Differentiation kit	Gibco	A10072-01

2.27 Appendix C: Formulations and solutions

Solution	Formulation
10x TAE (2 litres)	96.8g Tris

	<p>22.8ml Glacial acetic acid</p> <p>14.90 EDTA</p> <p>dH2O to 2L</p>
1x TAE (2 litres)	<p>200ml 10x TAE</p> <p>dH2O to 2L</p>
Agarose gel (100ml)	<p>1g agarose powder</p> <p>100ml 1x TAE</p> <p>1µl Gel Red</p>
10% Neutral buffered formalin (100ml)	<p>10ml formalin</p> <p>90ml dH2O</p> <p>Sodium phosphate to pH of 7.0-7.2</p>
MSC media (100ml)	<p>10ml FBS</p> <p>1ml Ascorbic acid 100µM</p> <p>1ml Glutamate 2mM</p> <p>1m Sodium Pyruvate 1mM</p> <p>500µl Penicillin (50 iu/ml)/ Streptomycin (50µg/ml)</p> <p>87ml α-MEM</p>

Freezing media (20ml)	<p>4ml FBS</p> <p>2ml DMSO</p> <p>200µl Ascorbic Acid 100µM</p> <p>200µl Glutamate 2mM</p> <p>200µl Sodium Pyruvate 1mM</p> <p>13.4ml α-MEM</p>
SPIO media (100ml)	<p>25ml FBS</p> <p>1ml Ascorbic Acid 100µM</p> <p>1ml Glutamate 2mM</p> <p>1ml Sodium Pyruvate 1mM</p> <p>178.6µl SPIO</p> <p>50µl Protamine Sulfate 10µl/ml</p> <p>71.8ml α-MEM</p>
10% SDS solution (10ml)	<p>1g SDS powder</p> <p>9ml H2O</p>
FACs wash buffer	<p>0.1% Sodium Azide (NaN₃)</p> <p>2% FBS</p> <p>1xPBS</p>

FACs fix buffer	2% Paraformaldehyde in FACs wash buffer
Oil Red O stock solution	.5g Oil Red O powder 100ml Isopropanol
Oil Red O working solution	6ml Oil Red O stock solution 4ml H ₂ O
Toulidine Blue	1g Toulidine blue powder 100ml H ₂ O
Alizarin Red	2g Alizarin red 100ml H ₂ O

Chapter 3

MSC Characterisation

3.1 Introduction:

As discussed in chapter 1, investigations into the utility of MSCs as a candidate for clinical cell transplantation have begun and are ongoing in a range of conditions [346, 367-369]. Of critical importance to the use of MSCs clinically, is the development of quality control assays to verify the identity and genetic stability of the cells following purification and expansion. This is particularly important for MSCs given their ability to differentiate and the large number of protocols that have been used to isolate these cells. Assurance of the Quality of MSCs can be achieved through a combination of phenotypic and functional analysis.

3.1.1 MSC Characteristics

The International Society of Cellular Therapy (ISCT) [247] has stated that Human MSC must have the following characteristics;

- 1: Plastic adherence. When the MSCs are maintained in standard tissue culture conditions they must adhere to the plastic of a standard culture flask.
- 2: Specific surface antigen expression. More than 95% of the MSC must express the cell surface markers CD73, CD90, and CD105, while lacking expression (<2%) of the cell surface markers CD11b/CD14, CD19, CD34, CD45, and HLA-DR.

3: Tri lineage differentiation. MSC must be able to differentiate into Adipocytes, Chondroblasts, and Osteoblasts *in vitro*.

The purpose behind the International society for cellular therapy's statement was to try and standardise the cells that different groups were working with, thus reducing variability and potential sources of contamination, increasing the validity of results. However, they do state that as more information is obtained these criteria may change. They also note that these criteria are only valid for human MSCs [247] and for other species there is variation in the reported cell surface markers [327] so it is important that all aspects of MSC characterization are taken together. In regards to differentiation capacity, MSCs are able to differentiate into several other cell types, including myocytes [370] and neuronal like cells [371], however, the tri-lineage differentiation of adipocytes, chondroblasts, and osteoblasts is the classical assay for defining MSCs.

3.1.2 Differences Between Species

As stated earlier, there are differences between the cell surface markers of MSCs from different species [327]. The most significant marker that has differential expression is STRO-1. STRO-1 has been used as marker for enriching human MSCs [325]; cells lacking this marker do not form colonies [372], which was one of the early methods used to identify MSCs. STRO-1+ cells also have the trademark differentiation capacities of MSCs [373]. However, this marker has only been confirmed in humans, pigs [374] and rats [375], with there being no known mouse equivalent [327]. STRO-1 expression is also lacking many other animals including sheep [326, 327]. Another important surface antigen with variable expression is CD34. The ISCT says human MSCs should be negative for this marker, in contrast to this it has been found be expressed in the MSCs of some mouse strains [376]. Particular attention should be paid to the fact that the expression of these surface markers is not consistent across studies of the same species [327, 375, 377-381] meaning that, for now,

the cell surface markers still need to be taken in conjunction with the other criteria for defining MSC.

3.1.3 Ovine Mesenchymal Stem Cells

Ovine MSC have been reported as far back as 1994 when Jessop *et al* isolated bone marrow stromal cells from welsh mountain cross lambs, cultured them and differentiated them into adipocytes and Osteoblasts [382]. Although they do note that they do not have any cell surface markers to confirm that these are MSCs, based on their description of both plastic adherence and differentiation it is likely that they were correct in their assumptions. In 2004 Rhodes *et al* differentiated ovine bone marrow derived stromal cells into chondrocytes, fulfilling the tri-lineage requirement for defining MSCs [383]. Next, in 2009 McCarty *et al* had a more thorough attempt at characterizing ovine MSC [326]. Here they performed tri-lineage differentiation and examined several cell surface markers coming up with a panel of CD29, CD44, and CD166 positive and CD14, CD31, and CD45 negative [326]. Later, unpublished, work by Dr Dyane Auclair concurred with the findings of McMarty, however this work found a lack of expression of CD29 and also used C11a, CD11b, and CD106 which all produced negative results. In addition to these papers there have also been several other studies reporting a variety of flow markers for ovine MSCs. Caminal *et al* (2016) reported their cells were strongly positive for CD44 and CD90 and positive for CD105, CD140a, and CD166 though the levels of the latter there were variable from 29% to 55% [384]. Lyahyai *et al* (2012) also showed a variation in the expression of the accepted human MSC markers on their Ovine MSCs [385]. Here they used RT-qPCR to analyse transcripts for 6 cell surface markers across 6 ovine MSC isolations. They found that CD29, CD73, and CD90 were expressed at high levels in all of the isolations, CD34 was expressed in 5/6 isolations, CD45 was not expressed in any, and CD105 was only detected in low levels after 35 PCR cycles, essentially a negative result [385]. A paper from Letouzey *et al* (2015), looking at

endometrium derived ovine MSC, positively selected for CD271 and negatively for CD49f. In contrast to other papers their MSCs were negative for CD73, CD90, and CD105; although they note that this may be due to the antibodies not reacting with the ovine epitopes [386]. The main outcome of their study was that they were confident in CD271 as a marker for MSC from the endometrium [386]. CD271 as a putative marker for MSCs is beginning to accumulate positive data [387, 388]. However, this marker is lost during cell culture [389-391] thus CD271 selection can only be used as a way of isolating cells before culturing and expanding.

The most comprehensive paper to date looking at Ovine MSC cell surface markers was produced by Khan *et al* (2016) [392]. This paper examined the use of several clones of the recommended MSC markers as well as looking at the impact of different reagents to detach MSCs from flasks. They found that several of the most commonly used clones for MSC research did not cross-react with sheep; however they showed reactive clones for all the important MSC markers including CD73, CD90, and CD105 [392]. They noted that one potential source of differences in sheep MSC surface markers is the use of trypsin to detach cells from flasks. Although trypsin does result in a highly homogenous cell population it may cause disruption of cell membrane proteins. To address this they examined the scatter profile of cells detached via trypsin, accutase, EDTA, and a 3:2 mixture of accutase to EDTA and found that there was significant variability between the scatter sizes of each of the methods with trypsin and the accutase: EDTA mixture resulting in the most compact and homogenous cell sizes [392].

The cell surface markers used for this study were selected based on the above papers, in particular Khan *et al* (2016) [392] and McCarty *et al* (2009) [326] as well as markers previously established in the lab (Auclair, unpublished). The resulting panel was CD11b, CD14, CD31, CD45R, as MHC II as negative markers and CD44, CD73, CD90, CD105,

CD166, and MHC I as positive markers. These markers allowed us to check that the MSCs matched the cells used in previous studies. Aside from agreement with literature and previous work, each of the selected markers is useful in defining MSCs in their own right. CD11b, or intergrin alpha M, is known to play a role in inflammation and migration of immune cells and has been implicated in several other immune responses such as phagocytosis and cellular activation [393]. Histopathologically it is commonly used to identify macrophages and microglia, using it as a negative marker rules out these cells. CD14 is a co-receptor for the detection of bacterial lipopolysaccharide that is primarily found on monocytes, especially macrophages, and to a lesser extent on neutrophils and dendritic cells [394], given its distribution it is a suitable negative marker for MSCs which do not have a role in detection of bacteria in the innate immune system. CD31 is found on a wide variety of cells including monocytes, endothelial cells, lymphocytes, and macrophages. It is primarily involved in the formation of endothelial intercellular junctions [395]. Using CD31 as a negative marker allows for the exclusion of a wide variety of cells, in particular endothelial cells, increasing the likelihood that the isolated cells are MSCs. CD44 is involved in cell migration, homing, and adhesion and is found on a wide variety of stem cells and cancer cells [396, 397]. Given the reported abilities of MSCs to home to locations of inflammation it is unsurprising that they express CD44 and as such it makes a useful positive marker. CD45R is a protein tyrosine phosphate molecule primarily found on T and B cells [398, 399], using this as a negative marker excludes these cell types from the population. CD73, or ecto-5'-nucleotidase is involved in adenosine-monophosphate conversion to adenosine [400]. This marker has been determined to be one of the minimal criteria for defining human MSCs. CD90, or Thy-1, has a wide range of reported functions including migration, adhesion and modulating fibrosis [401]. These functions, as well as it being widely reported as a positive MSC marker, is what has made it part of the essential minimal criteria for defining human MSC. CD105, or

endoglin, acts as receptor for transforming growth factor β and as such plays roles in cell growth, proliferation, and differentiation [402] all obviously important to MSC functions. Thus, CD105 has been recognised as one of the essential positive markers for defining human MSCs. CD166 has several potential functions but primarily binds to CD6, which is a protein important in T cell activation, it also has possible roles in cell migration and adhesion [403] and is prevalent in cancers [404], given these roles it is unsurprising that MSCs express CD166 and that it a useful marker for flow cytometry. MHC I is expressed on MSCs while MHC II is not, providing a useful positive and negative marker couple [247]. There are a few notable exclusions from the panel used here these are; CD19, CD29, VCAM-1, and Stro-1. CD19, although recommended as a negative marker by the international society of cellular therapy, was not included as a working sheep specific antibody was not available. CD29 was excluded because the available clone returned negative results in both this study and previous work indicating that it may not be cross reactive. VCAM-1, although used in previous work, is not widely recognized as a useful negative marker and as such was removed to simplify the flow panel. This was also the reasoning behind the removal of Stro-1, although useful for human MSCs, Stro-1 is not expressed in sheep and as such this marker is of no use for these experiments. In addition to the flow markers plastic adherence, tri-lineage differentiation, and immune assays were used to ensure that MSCs had been isolated.

3.1.4 Chapter Aims

The aim of this study was to isolate and characterized ovine mesenchymal stem cells and then label them with superparamagnetic iron oxide (SPIO) in a reproducible manner to allow for further experimentation.

3.2 Materials and Methods:

3.2.1 MSC Isolations

Female merino sheep were anaesthetized using ketamine (0.5 mg/kg) and diazepam (0.2-0.3 mg/kg) for induction and Isoflurane (1-2%) as maintenance. The right hand side of the sheep flank was shorn over the hip with enough space to create a sterile field. A small incision was made in the skin over the superior aspect of the right hip. Using a portable image intensifier x-ray machine, an osteobell “T” needle was forced into the iliac crest until it reached the cancellous bone, being careful not to push through the other side. Next, the core of the Osteobell needle was removed and a 60ml syringe attached and drawn back to allow the collection of bone marrow aspirate. 40ml of this aspirate was then placed into a 50ml falcon tube, containing, 500IU of heparin. This bone marrow aspirate was split across 4 50ml falcon tubes, mixed with an equal amount of PBS and then under laid with 15ml of ficoll. The tubes were then centrifuged at 1000xg for 45 minutes at room temperature with the brake off. The resulting mononuclear cell layer was collected and two tubes worth was pooled into one. This was then filled with PBS to 30ml and washed to remove ficoll. The resulting pellets then underwent 2 additional washes in PBS. A cell count was performed after the second wash. Complete media was made up with 10% FBS, 1% Ascorbate, 1% Glutamate, 1% sodium pyruvate, and .5% penicillin/ streptomycin and the cells were re-suspended in it. The cells were then plated out at 30,000 cells per cm² or 5.25x10⁶ cells per T175 flask. The flasks were incubated at 37°C and 5%CO₂ for 7-10 days to allow the cells to adhere before a media change was performed.

3.2.2 MSC Expansion

After the first media change, cells were allowed to grow for 3 more days until reaching 80% confluence, at which point they were split. Flasks were washed twice with PBS to remove complete media then trypsinized for 5 minutes at 37°C to detach cells. 5ml of 5% FBS in PBS was added to quench the trypsin then the detached cells were collected in 50ml falcon tubes and filled to 20ml with PBS. The tubes were centrifuged at 250xg for 5 minutes at 4°C. The resulting pellets were then resuspended in 5ml of 5% FBS in PBS and a cell count performed. After being filled with PBS to 20ml, the tubes were centrifuged again and the supernatant discarded. The pellets were then resuspended in complete media and plated out at 10,000 cells per cm² or 1.75x10⁶ cells per T175 and cultured at 37C 5%CO₂. Once the cells reached 80% confluency in the flask they were then split again for further expansion or experimental utilization.

3.2.3 Freezing Cells

If cells were to be frozen they were centrifuged at 250xg for 5 minutes at 4°C, the supernatant was then removed and the pellet resuspended in 1ml of freezing media (complete media containing 20% FBS and 10% DMSO) per 1x10⁷ cells. 1.5 ml of the suspension was aliquoted into cryovials, placed in a “Mr Frosty” cyrobox and frozen in a -80 freezer.

3.2.4 Thawing Frozen Cells

Cryovials were placed in a water bath at 37°C until the frozen core became moveable then tipped into a 50ml tube containing 10ml of 5% FBS in PBS. This was then centrifuged at 250xg for 5minutes at 4°C. The supernatant was poured off; the pellet resuspended in 5ml of 5% FBS in PBS and a cell count performed. The suspension was filled to 20 ml with PBS and washed again then resuspended in complete media and plated at 10,000 cell/ cm². The cells were allowed to passage once before being used.

3.2.5 Flow Cytometric Analysis

Cells were trypsinised following the method described in chapter 2, section 2.10. After the cells were counted, 100,000 cells were taken per marker to be used. The cells were centrifuged at 500xg for 5 minutes. The resulting pellet was resuspended in 100µl/ 100,000 cells of FACS wash with 10% heat inactivated rabbit or donkey serum (depending on the animal the primary antibody came from) and incubated for 20minutes on ice to block the cells. While the incubation was taking place the flow tubes were set up with the primary antibody. 100µl of the cell suspension was added to each tube and incubated for 30 minutes on ice in the dark. During this incubation a 1/50 dilution of the secondary antibody was made in FACS wash, enough for 20µl per tube. The tubes were then washed with FACS wash at 500xg for 5 minutes, they were then briefly vortexed to resuspend the cells and the secondary antibody was added. The tubes were again incubated for 30minutes on ice, in the dark. Next they were washed again with FACS wash at 500xg for 5 minutes. They were then fixed by added 1ml of FACS lysing solution and incubating for 20 minutes in the dark at room temperature. The cells underwent one final wash with FACS wash solution at 500xg for 5 minutes before finally being resuspended in 200ml PBS and read on a BD FACSCantoII (BD Biosciences, San Jose, CA, <http://www.bdbiosciences.com/>) flow cytometer.

3.2.6 Adipogenic Differentiation

After cell harvesting and counting, cells were resuspended in complete media and seeded on a 12 well plate, at 4×10^4 cells per well. The plate was incubated for 2 days at 36°C, 5% CO₂ to allow the cells to adhere. On day 2 the complete media was removed and the wells washed with PBS before 2ml of complete adipogenesis differentiation media was added. The plates were incubated at 37°C with 5% CO₂ to allow differentiation to proceed. The media was changed every 4 days for a period of 20 days. After 20 days the cell were stained with Oil Red O stain to visualize lipid vacuoles.

3.2.7 Chondrogenic Differentiation

After cell harvesting and counting, cells were resuspended in complete media and seeded on a 12 well plate at 4×10^3 cells per well and incubated for 1 day at 36°C , 5% CO_2 to allow the cells to adhere. After 1 day the complete media was removed and the cell washed with PBS before 2ml of complete chondrogenesis differentiation media was added. The plates were placed back in the incubator to allow the cells to differentiate with the media being changed every 2-3 days for 20 days. After 20 days the cells were stained with Toluidine blue to stain cartilage purple.

3.2.8 Osteogenic Differentiation

After cell harvesting and counting, cells were resuspended in complete media and seeded on a 12 well plate at 2×10^4 cells per well and incubated for 2 days at 36°C , 5% CO_2 to allow the cells to adhere. After 2 days the complete media was removed and the well washed with PBS before 2 ml of Osteogenesis differentiation media was added. The plate was placed back in the incubator and to allow the cells to differentiate. The media was changed every 3 days for a period of at least 21 days. After 21 days the cells were stained with Alizarin red which labels calcified depositions red.

3.2.9 Immunosuppression Of Stimulation Assays

PMBCs were treated with Concanavalin-A (Con-A) to cause strong proliferation. The day before the PMBC were added, MSCs were seeding in the wells at .1% 1% and 10% of the PBMC number. The PMBCs were then left for 4 days to proliferate before being pulsed by the addition of tritiated thymidine. The cells were left to proliferate for an additional 24 hours before being harvested onto a filter mat. The filter was then placed in a cassette and read on a scintillation counter. The count per minute of the test wells were then normalized against the control well that received no MSC. This was used to determine the percentage of Immunosuppression caused by the various proportions of MSC.

3.2.10 Immunosuppression Of Mixed Lymphocyte Reactions (MLRs)

The MLR protocol from chapter 2 (section 2.8.1) was followed with the intent of examining the immunosuppressive abilities of autologous derived MSCs, MSCs derived from the same animal as the stimulator PMBC (the donor), or 3rd party derived MSCs was examined. To carry this out PBMC from sheep 20, 21, 22, and 25 and MSC from sheep 21 and 25 was isolated. Crosses were coordinated so that 21 and 25 acted as responders under a variety of conditions with them responding to stimulator cells from sheep 20, 22 and to each other. Stimulator cells were PBMCs that had been irradiated to cease proliferation. The day before the MLR was to be set up MSCs were irradiated to stop cell growth and added to the plate and allowed to adhere. The cells were added at 10% of the number of responder cells to be added, as this had previously been determined to be the percentage required to cause a significant Immunosuppression

The MLR was then allowed to continue as normal. During cell harvesting the wells were harvested then trypsinized and harvested again. The filter mat that the MLR was harvested onto was then placed in a scintillation cassette and read as normal. The counts per minute (CPM) from the MSC well were compared to the CPM from the control well to determine if Immunosuppression had occurred.

3.2.11 Morphology

Cells were plated in a T75cm flask and allowed to adhere for up to 7 days in complete media at 36°C, 5% CO₂. This gave the cells time to adhere fully and regain their morphology after being trypsinized or frozen. The cells were then imaged using an Olympus IX51 inverted microscope

3.2.12 Staining With SPIO

Cells were allowed to adhere and expand up to 85% confluence. 18 hours before the cell were needed the media was changed to the SPIO staining media which contains 25% FBS, 960µg/ml SPIO and 5µg/ml protamine sulphate to allow the cells to become iron labelled. Labelling was confirmed via light microscopy looking for brown depositions in the cells.

3.2.13 Viability

In the eventual large animal experiments the cells would be resuspended in saline before being given to the sheep, this solution was chosen because it is routinely given to the animals and as such the impacts are a known quantity. However, this required that the cells remain viable when suspended in saline. Additionally, it was important that labelling the cells with SPIO did not impact their survival. Viability tests were routinely performed using tryphan blue and a haemocytometer but, due to the imprecise nature of this method and the possibility of observer bias it was only used when splitting cells for growth to ensure the overall viability of the cell isolation. For experiments where a higher precision was required the thermofisher LIVE/DEAD aqua dead cell stain kit was used. 1×10^6 cells were harvested and centrifuged at 500xg for 5 minutes before being resuspended in 1ml of PBS and having 1µl of the aqua dye added. The cells were then incubated in the dark, on ice, for 30 minutes. The cells were washed with PBS once at 500xg, for 5 minutes before being resuspended in 900µl of PBS and having 100µl of 37% formaldehyde added. The mixture was incubated in the dark at room temperature for 15 minutes. Finally the cells were washed with 1% FBS in PBS at 500xg for 5 minutes before being resuspended in 1ml of 1%FBS in PBS. The cells were then read at 525nm on a flow cytometer to determine the uptake of the dye and consequently the viability of the cells.

3.2.14 Prussian Blue

The Biopal Prussian blue staining kit was used to identify cells that had taken up the SPIO label. Pursuant to the supplied instructions, a working solution of Prussian blue stain was prepared just prior to use by mixing equal amount of reagent A and reagent B. Cultured cells were first fixed by removing the complete media, washing the flask with PBS then adding 2% formalin and leaving for 10 minutes. The formalin was then removed and the cells rinsed with PBS before the Prussian blue working solution was added and the cells left to incubate for 10 minutes at room temperature in the dark. If iron was present in the cells they would stain blue in this time.

3.2.15 Iron Spectrophotometry

In order to determine the average amount of iron taken up by the MSCs, UV-Vis spectroscopy of the iron labelled cells was performed. First a standard curve was created using the superparamagnetic iron label diluted in PBS. The concentration of iron ranged from 1ng/ml to 40ng/ml. These samples had their absorbance measured over a range from 200nm to 900nm to find the wavelength with the optimal absorbance. In addition to finding the peak absorbance was, the limit of detection (LoD) and limit of quantification (LoQ) for each wavelength was calculated to allow selection of the wavelength where these would be minimized, resulting in the most accurate readings. In order to calculate the limit of detection and the limit of quantification, several blanks consisting of PBS alone were measured across the spectrum from 200nm to 900nm. The mean and the standard deviation of the blanks was calculated and, using these, the LoD and LoQ for each wavelength was determined by taking the mean absorbance at a given wavelength and adding 3 standard deviations for the LoD and 10 standard deviations for the LoQ. The results of the serial dilutions at the optimal wavelength were used to plot a standard curve.

Once the standard curve was established, SPIO labelled cell samples could be measured. To do this, 1×10^6 SPIO labelled cells were placed in a 1.5ml eppendorf tube, centrifuged at 10,000 rpm for 5 minutes then resuspended in 1ml of 10% SDS. The cell suspension was vortexed for one minute then heated for 5 minutes at 70°C to decrease turbidity. The solution was then aliquoted into 5 separate wells of a 96 well plate and the absorbance was measured at 370nm. 10% SDS in water was used as a blank and this was subtracted from the absorbance of the samples. The concentration was then calculated by putting the resulting absorbance into the equation generated by the standard curve with the addition of a correction factor to take into account any remaining turbidity in the well. This correction factor was calculated by taking the ratio of the absorbance of unlabelled cells at 370nm over 800nm. The resulting equation was expressed as follows:

$$Fe(\mu g ml^{-1}) = [A_{370} - (B * A_{800})]/S_{370}$$

Where A_{370} and A_{800} are the absorbencies at 370nm and 800nm respectively. B is the turbidity correction factor calculated using the lysed, unlabelled cells, and S_{370} is the slope of the standard curve at 370nm.

3.3 Results:

3.3.1 General Results

The iliac crest of the sheep was able to be repeatedly and accurately accessed using an X-ray image intensifier (XRII) to guide a biopsy needle and extract bone marrow aspirate. On average, 40ml of aspirate was collected and from this an average of 5×10^7 cells were isolated. This was plated onto T175cm plates at a seeding density of 30,000 cells/ cm^2 .

3.3.2 Flow Cytometry

MSCs were harvested as mentioned above and stained with the panel of flow markers, with at least 100,000 cells being used per marker. The cells were then fixed and analysed on a flow cytometer. Figure 3.1 demonstrates that the cells are positive for CD44, CD73, CD90, CD105, CD166 and MHCI while being negative for CD11b, CD14, CD31, CD45R, and MHCII. Unstained cells were used as a negative control

3.3.3 Morphology

MSC were plated out at a density of 10,000 cells/ cm^2 and allowed to adhere and grow. As the MSCs grew they began taking on their classical fibroblast-like appearance. Figure 3.2 shows a light microscope image of MSCs showing this appearance with long thin protrusions coming out of a round body.

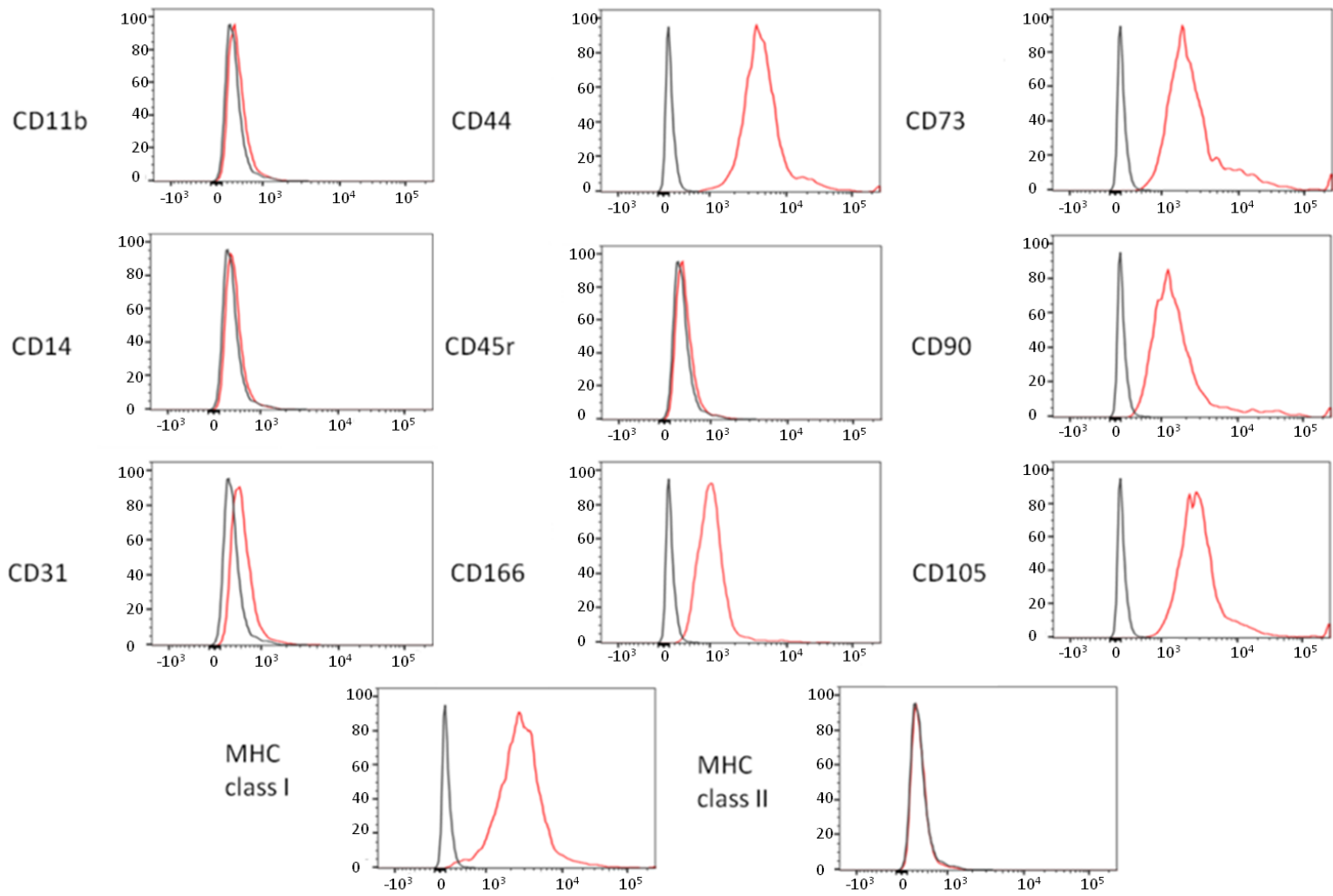


Figure 3.1 Flow cytometry analysis showing that ovine MSCs are positive for CD44 (99.9%), CD73 (98.6%), CD90 (89.1%), CD105 (99.7%) CD166 (79.4%), and MHC I (96.8%) while being negative for CD11b (5.06%), CD14 (3.74%), CD31 (8.35%), CD45r (4.43%), and MHC class II (2.84%). MSCs were cultured from bone marrow aspirate and underwent characterization. 100,000 cells were labelled per marker with a PE conjugated antibody. The cells were fixed using FACs lysing solution before being resuspended in PBS and having 5000 events read on a BD FACSCantoII. Unstained cells acted as a negative control (black line) and the counts were normalized to the mode for display.

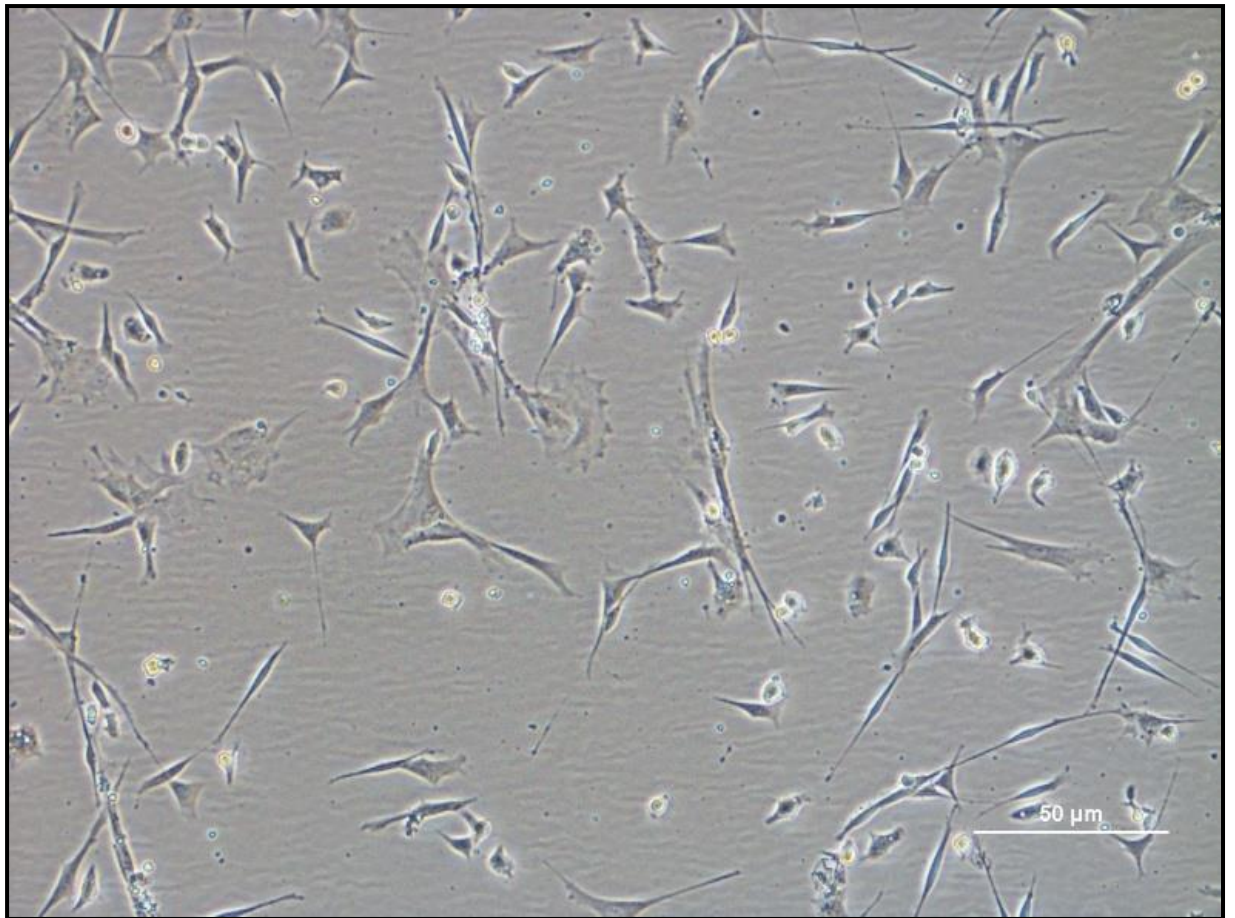


Figure 3.2 Light microscopy of ovine MSCs showing a fibroblast like morphology with small bodies and long, thin projections. Mesenchymal stem cells were isolated from the bone marrow aspirate retrieved from the iliac crest of 2 year old sheep and cultured to allow for expansion. MSCs were kept at 37C and 5% CO₂ in foetal calf serum enriched α -MEM until they reached 80% confluence at which time they were passaged. Upon adhering to the plastic flasks the MSCs would begin to display their characteristic morphology, extending elongated projections out from the main cell body. Image taken on an Olympus IX51 inverted microscope. Representative of 14 isolations.

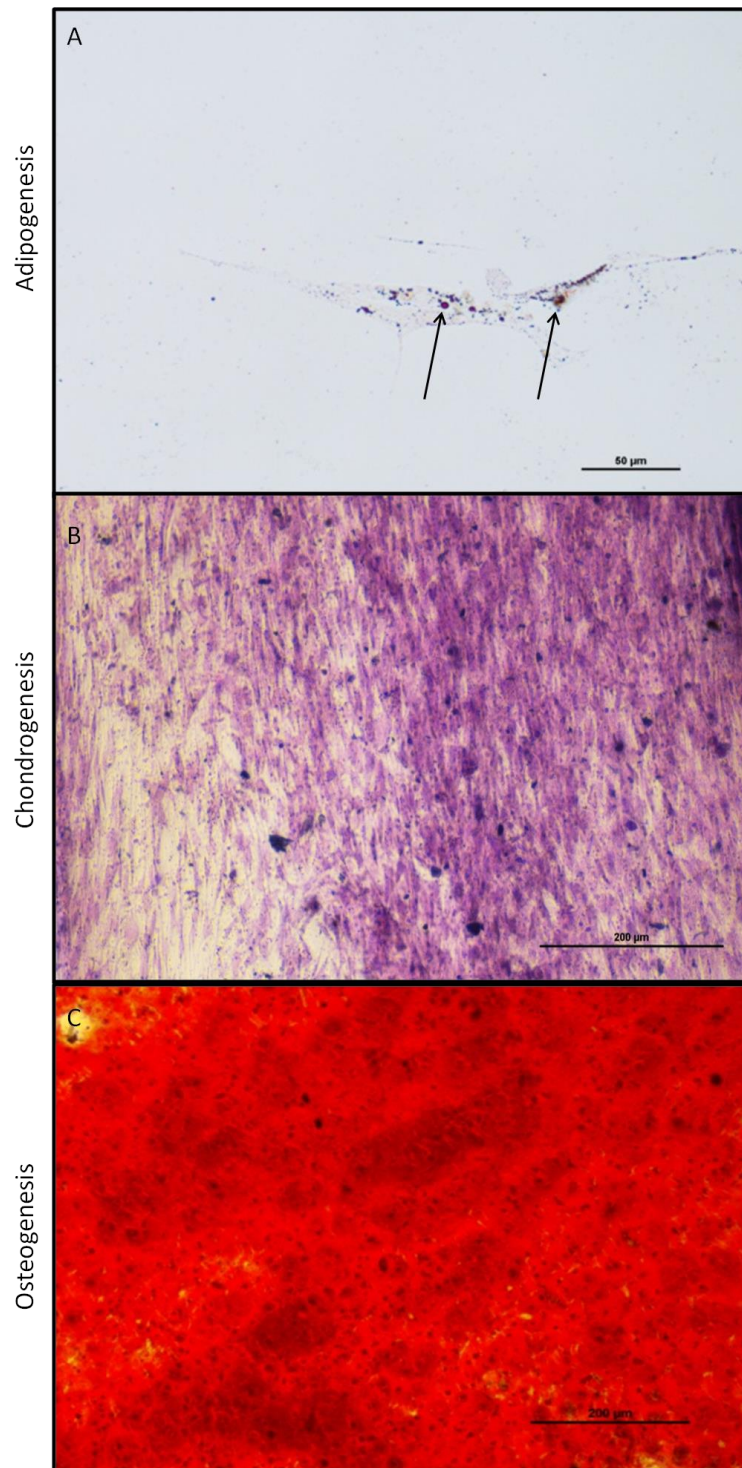


Figure 3.3 Differentiation of MSCs in to Adipocytes (A), Chondroblasts (B), and Osteoblasts (C). Adipocytes are stained with oil-Red-O which renders the fat vacuoles red (A, arrows). Chondroblasts are stained with Toulidine blue which makes the proteoglycans in cartilage turn purple. And Osteblasts are stained with Alizarin red which stains mineralization particular to bone formation. Images taken with an Olympus Ix51 inverted microscope, representative of 10 differentiation experiments.

3.3.4 Differentiation

MSC were seeded and grown according to the methods stated above using the appropriate growth media. After the required number of days the cells were fixed and stained before being analysed under light microscopy. Figure 3.3 A) shows a representative image of MSCs forced to differentiate into adipocytes. The oil-Red-O stain renders fat containing vesicles red. This image displays faint outlines of the cells with several large fat vesicles present indicating that these are adipocytes. Figure 3.3 B) shows the staining of chondroblasts with toulidine blue; this dye causes proteoglycans to turn purple. In the image a strong purple colour indicating the presence of cartilage associated proteoglycans and thus chondroblasts is seen. Lastly, figure 3.3 C) shows the staining of osteoblasts with Alizarin red which stains calcium deposits, commonly found in bone, a bright red. A wide spread red coloration indicating the presence of calcium deposit creating Osteoblasts is observed.

3.3.5 Viability

After the cells were harvested from their plates they were counted and resuspended in either complete media or saline at a concentration of 1×10^6 /ml. 1ml was then taken, stained and fixed. This was repeated at 1 hour. The samples were run on a flow cytometer to determine the viability. As the cells die they take up more dye resulting in a shift to the right on a flow histogram, as seen in figure 3.4 A. Freshly harvested cells were stained immediately to act as a negative control and to act as a positive control cells that had undergone heat induced apoptosis were used. This was achieved by placing the cells in a 70°C water bath for 1 minute before staining.

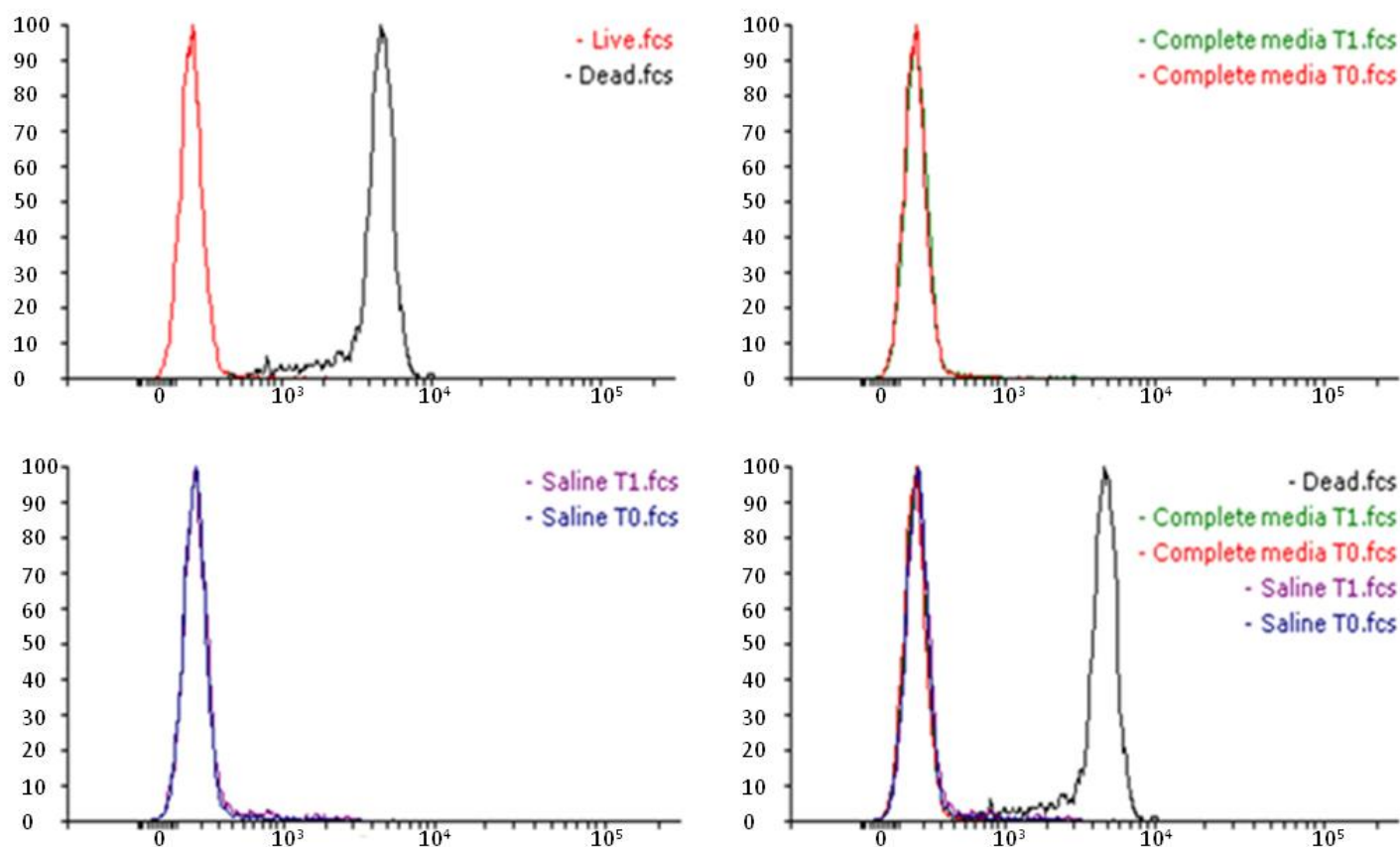


Figure 3.4 MSCs were harvested and stained with Thermofisher LIVE/DEAD aqua cell stain kit. The dye is taken up more readily by dead cells resulting in a shift to the right of the histogram when read on a flow cytometer. A) A comparison of live and dead cells using this stain. Cells were killed by heat treatment at 70°C for 1 minute before being stained. The graph shows that as cells undergo apoptosis and take up dye their resulting histogram moves to the right. B) The comparison of cells stained after being resuspended in complete media and held at room temperature measured at time 0 and 1 hour. The histograms of the two time points overlap indicating limited cell death over the one hour holding time. C) Cells resuspended in saline and measured at time 0 and after 1 hour of being held at room temperature. Again, the overlapping histograms suggest that cell death during the one hour holding time was minimal. D) Comparison of the time points from the complete media and saline cells to the dead control cells. All four of the time points overlap with each other while not overlapping with the positive control (dead). This would indicate that cell death in all test conditions was very low.

These results show that holding the cells in complete media for one hour does not impair viability (Figure 3.4 B). Additionally, resuspending the cells in saline and holding them out to 1 hour does not decrease their viability (Figure 3.4 C and D). This indicated that the cells would remain viable during the preparation for the large animal infusion experiments and surgeries and that the cells could be maintained in saline for at least an hour prior to their use.

3.3.6 Immunosuppression Of MLRs

One of the widely reported characteristics of MSCs is their ability to modulate the immune response. The mixed lymphocyte reaction and Con-A stimulation assay are robust immune proliferation assays that have been well established are suitable experiments to examine the immunosuppressive abilities of MSCs. Initially, Con-A stimulation of PMBCs was performed in the presence MSCs totalling 0.1%, 1%, or 10% of the number of PMBCs. This is further detailed under the SPIO section and resulted in a dose response curve (Figure 3.14) with 10% MSC causing a pronounced reduction in proliferation which is notable given the strong proliferative effect that Con-A has on PBMC.

Next the immunosuppressive abilities of autologous, donor, and 3rd party MSCs was examined using PBMC and MSC crosses from sheep red 20, 21, 22, and 25. Stimulator cells were PBMCs that had been irradiated to cease proliferation. The stimulator and responder pairings acted as controls showing the level of proliferation of each of the responder cells to different stimulator cells (Figure 3.5 Grey bars). MSCs were then added to the wells so that the MSCs were either autologous to the responder cells (Green bars, Autologous), from the same animal as the stimulator cells (Blue bars, Donor) or from an animal that was neither the stimulator or responder (Red bars, 3rd party)

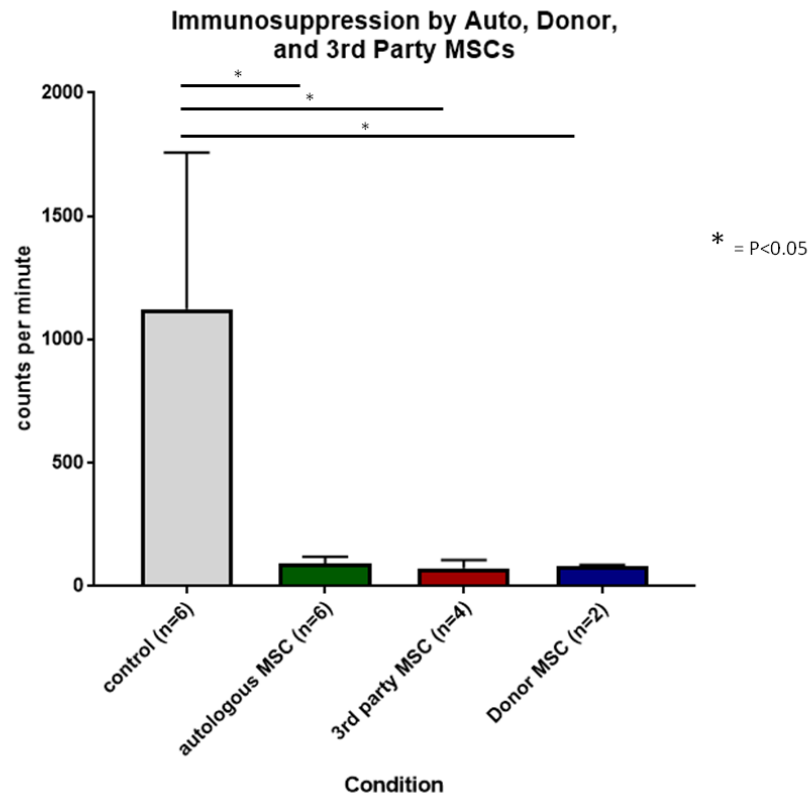


Figure 3.5 Examination of the ability of MSCs to cause Immunosuppression *in vitro*. MSCs and PBMCs were cultured at a ratio of 10:1 with the MSCs being either autologous to the responder cells (autologous), derived from the same animal as the stimulator cells (donor), or from an unrelated animal (3rd party). Stimulator cells and MSCs were irradiated before being added to prevent their proliferation. Responder cells were then added and cultured at 37°C and 5% CO₂ for 4 days at which point they were pulsed with tritiated thymidine and incubated for a further 18 hours. The cells were harvested onto a glass fibre mat which was placed into a scintillation counter cassette and the counts per minute of each well read on a Beckman LS 2800 beta counter. Auto, 3rd party, and donor MSCs all show a strong ability to suppress immune activation in a proliferation assay with their average counts per minute being significantly less than the MSC free control (Control = 1123 ± 635 cmp vs. Autologous = 89 ± 29, P = 0.0017. 3rd party = 72 ± 33, P = 0.0038. Donor = 81 ± 4, P = 0.0217). However, there were no significant differences between the MSC conditions (auto vs. 3rd party P = 0.9999, auto vs. donor P = >0.9999, 3rd party vs. Donor P = >0.9999)

The control wells had a wide range but all showed proliferation. That is, sheep 21 and 25 responded to all of the stimulator cells. When MSCs are added to the well at 10% of the total PBMC level a strong reduction in proliferation is observed. This holds true regardless of the source of the cells. This indicates that MSCs may be able to cause immunosuppression even in mismatched individuals allowing for the transplanted MSCs to be derived from alternate sources should autologous MSCs not be a viable option. As these results show that autologous MSCs are not functionally different to 3rd party or donor derived MSCs, it was decided that Autologous MSC would be used for later large animal experiments. Autologous MSCs were also easy to obtain and allowed for flexibility in the donor-recipient pairings for the surgeries that may have been complicated had donor derived MSCs been used.

3.3.7 Staining With SPIO

Tracking the cells using an MRI required that they be stained with a suitable label. To this end the cells were stained with SPIO as previously described. Various characterisation experiments were then carried to ensure that the labelling was successful and that it did not have an impact on the phenotype or function of the cells.

3.3.8 Prussian Blue Staining

MSC were cultured in T75cm flasks until they adhered and developed characteristic fibroblast-like morphology. One of the flasks then underwent SPIO labelling for 18 hours and then both the SPIO and non-SPIO flasks were fixed using formalin. Images were taken of both before Prussian blue staining was carried out. The flasks had Prussian blue added as detailed, before being washed off and topped up with PBS and imaged again

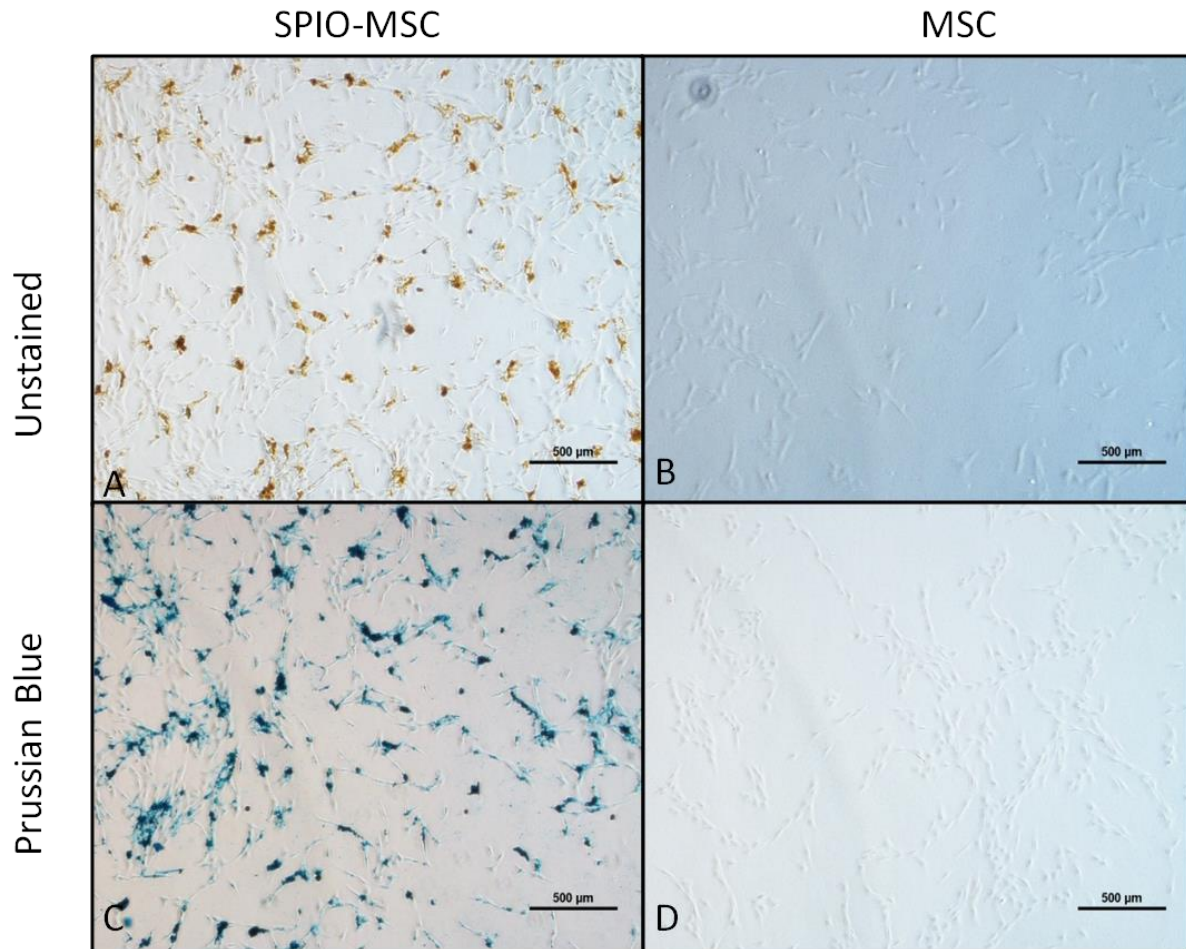


Figure 3.6 200x magnification images of Prussian blue being used to detect SPIO labelling of MSCs. MSCs were cultured until they had adhered to the flasks and had developed a fibroblast-like appearance. The MSC growth media was then changed to SPIO labelling media, in the required flasks, and the cells incubated for 18 hours at 37°C and 5% CO₂. The MSCs were then fixed using 2% formalin before having the Biopal Prussian blue stain added and being incubated at room temperature. The Prussian blue stain was washed off and images were taken using an Olympus IX51 inverted microscope. A and B show pre-Prussian blue stained cells that have either been labelled with SPIO (A) or left unlabelled (B) the iron label is evident even without the Prussian blue stain, appearing as brown deposits in the cells. C and D show the cells post Prussian blue stain with the iron labelled cells (C) now showing the blue colour that results from a positive stain while the unlabelled cells show no change (D).

Even without the Prussian blue staining the cells that have been labelled with SPIO are obvious due to the brown deposits that they display where as these are not present in the unlabelled cells. Upon application of the Prussian blue stain, a strong blue colour indicating the presence of iron is observed. Unsurprisingly, this does not happen in the unlabelled cells. This provides confidence that the labelling procedure is effective and that the Prussian blue labelling will detect iron labelled MSCs in histology.

3.3.9 Spectrophotometric Analysis

Although the Prussian blue experiments provided evidence that SPIO labelling works, it does not provide data about the consistency of the amounts of SPIO being taken up during different labelling attempts. To examine this, spectrophotometry was used. First a standard curve was created to compare test samples to. Serial dilutions were set up from 1 μ l/ml to 40 μ l/ml of iron, distributed into a plate and run on an Epoch microplate reader from 200nm to 900nm with wells of PBS acting as a blank. The results are shown in figure 3.7. A peak in absorbance is observed extending from 300nm to 400nm indicating that this is the area in which the SPIO is most strongly absorbent. In order to determine the optimal wavelength for detecting SPIO, the limit of detection and limit of quantification was calculated as described in section 3.2.15. Briefly, multiple readings of a blank (PBS) were taken and the mean and standard deviation for each of the wavelengths calculated. The mean then had 3 standard deviations added for the LoD and 10 standard deviations for the LoQ. When the LoD and LoQ are plotted alongside the peak obtained from the SPIO spectrophotometry standard curve, a spike is observed from 270nm to 310nm (Figure 3.8, red square) indicating that these wavelengths would not be the most accurate for detection of iron as the resultant LoD and LoQ would be high. By looking at the LoD and LoQ across the range of the entire peak, a minima region at 370nm is found (Figure 3.9, red square), indicating that this area will yield the highest accuracy.

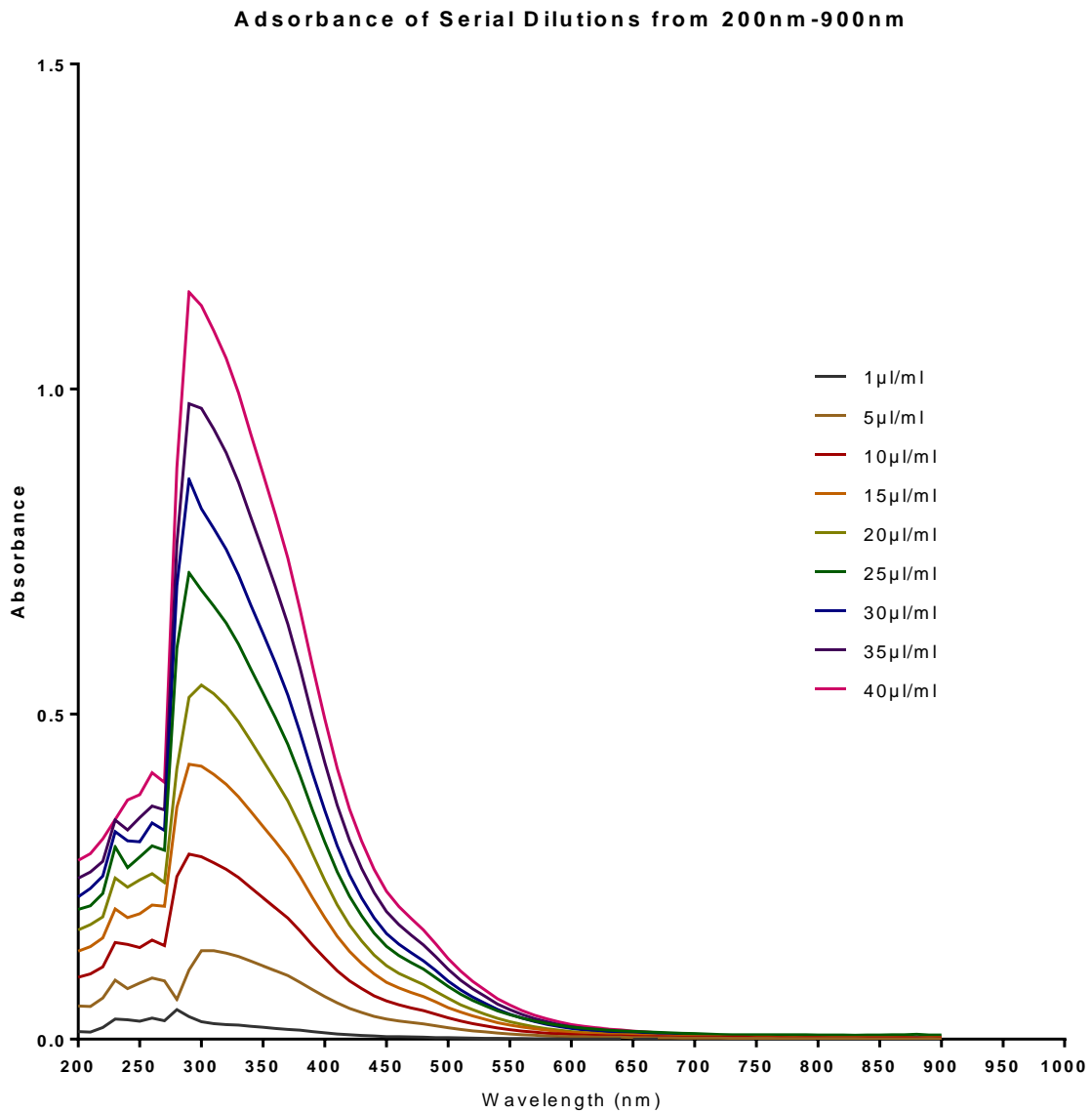


Figure 3.7 Absorbance of serial dilutions of iron contained in SPIO from 200nm to 900nm showing a peak in the 300nm to 400nm range. The SPIO solutions were made into a range of dilutions from 1µl/ml to 40µl/ml. These dilutions then had their absorbance read across a spectrum of wavelengths from 200nm to 900nm to look for areas where absorbency was high, indicating favourable wavelengths for measuring SPIO absorbance in test samples. A peak is seen across all dilutions in the 300nm to 400nm wavelength range, signalling that this range would be suitable for SPIO concentration determination.

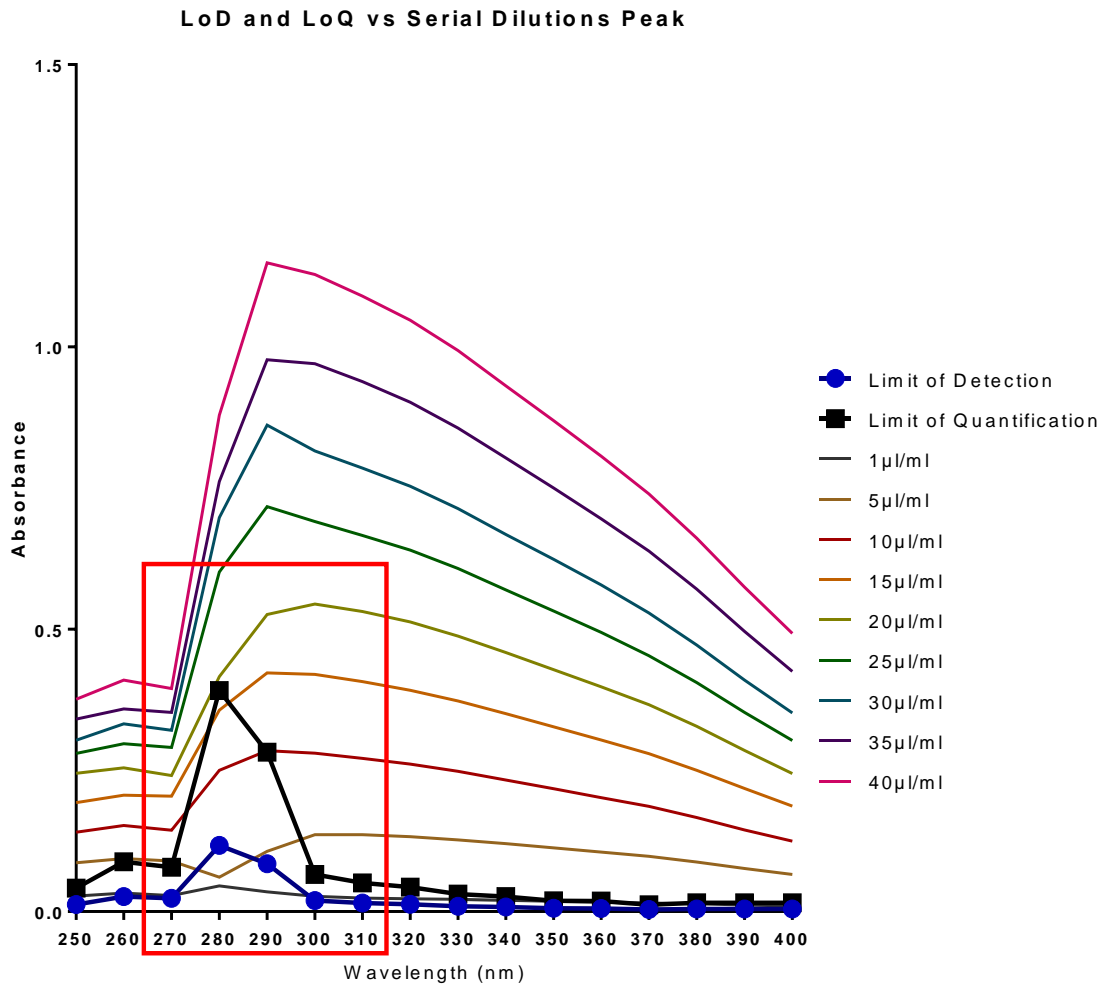


Figure 3.8 An overlay of the serial dilution peak, which extends from 270nm to 450nm, and the limits of detection and quantification for each wavelength, showing that the wavelength corresponding to the highest peak also has a high limit of quantification (Red box) making it an unsuitable choice for measuring samples as the accuracy of the machine is reduced in this region.

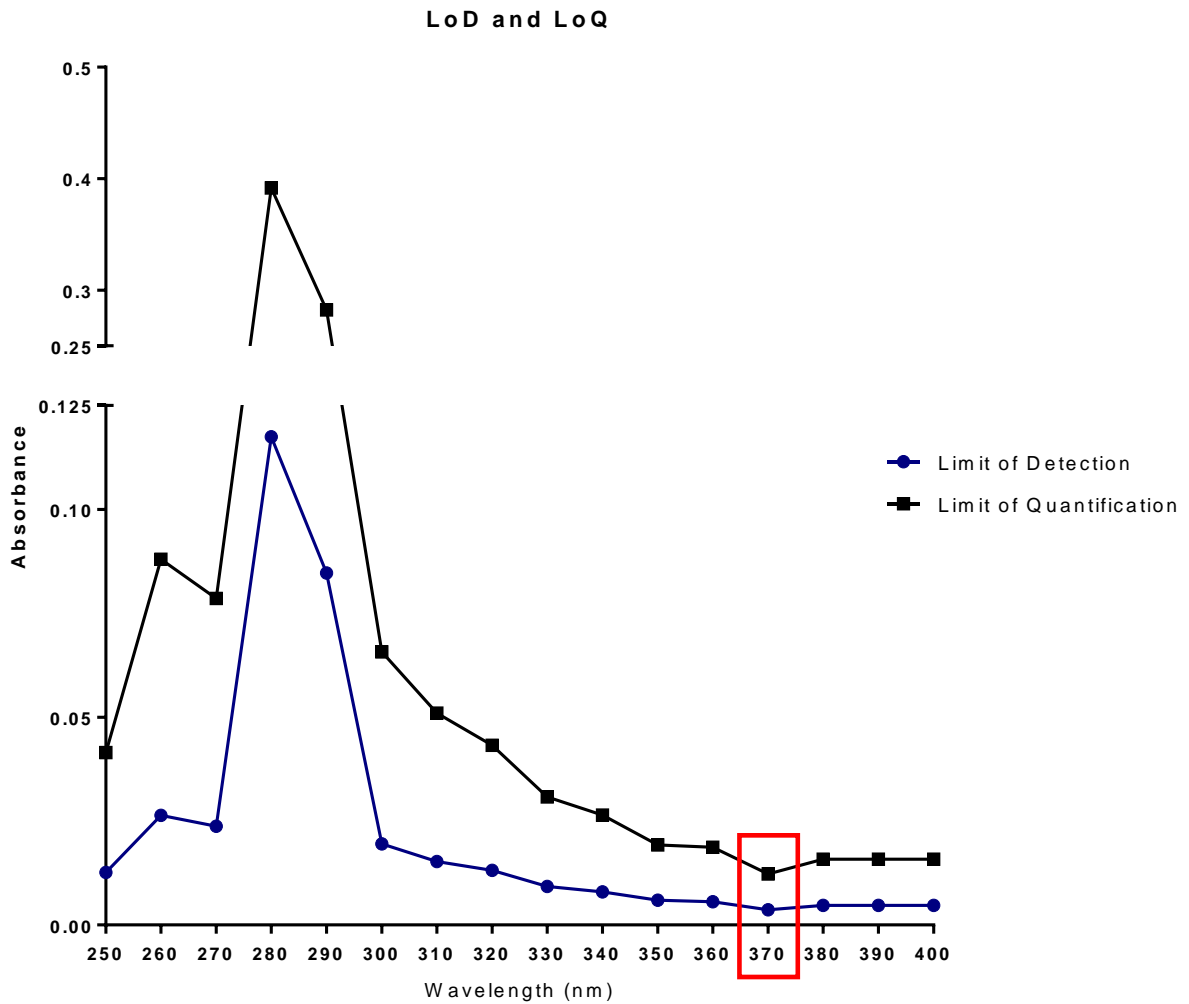


Figure 3.9 The limits of detection and quantifications across the wavelengths corresponding to the SPIO absorbance peak. The red box shows the lowest LoD and LoQ is found at 370nm, indicating that this is an appropriate wavelength to use when measuring SPIO samples as this will allow for the greatest accuracy in measurements of absorbency.

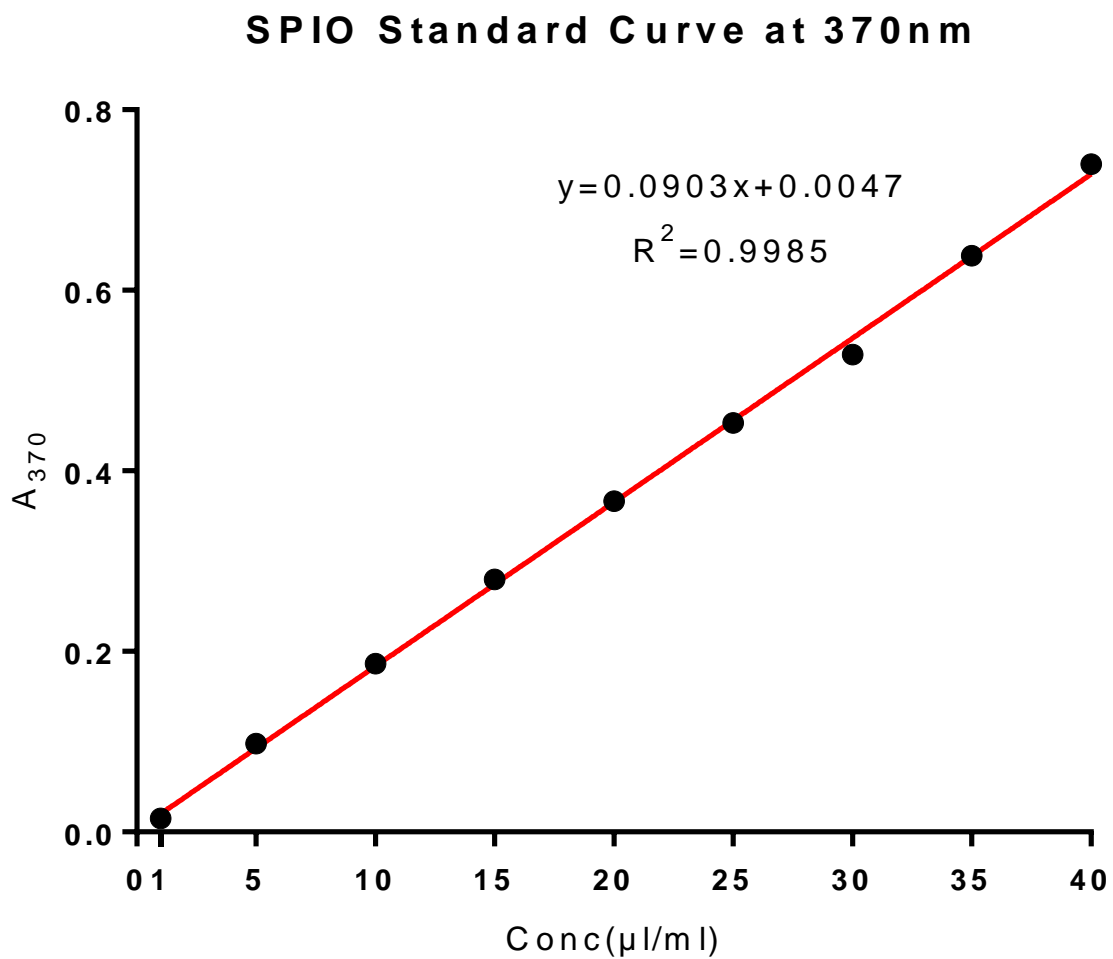


Figure 3.10 Plotting the absorbency of each serial dilution at 370nm, the wavelength with the lowest LoQ, gives a standard curve with an R^2 of 0.9985, demonstrating that measurements taken at this wavelength and in this range are accurate and are proportional to their corresponding SPIO concentrations.

Using this information, the absorbance of each of the serial dilutions was read at 370nm, a standard curve plotted and a trend line fitted. The R^2 value of which was 0.9985 indicating a very good fit and that the standard curve will provide an accurate determination of iron concentration based on absorbance.

Finally, three batches of MSCs were independently labelled using the method described in section 3.2.12. 1×10^6 cells were harvested and lysed with detergent as stated in the protocol and then the absorbance measured at 370nm and 800nm. These figures were then put into the equation above and the amount of iron was determined. This is summarized below.

	A_{370}	A_{800}	Iron concentration ($\mu\text{l/ml}$)
Sample 1	0.9544	0.0092	10.4571
Sample 2	1.0512	0.0160	11.4462
Sample 3	0.8100	0.0000	8.9701

Table 3.1 The absorbance at 370nm and 800nm of three different attempts at labelling with SPIO along with the calculated iron concentration.

From this table it is seen that three unrelated attempts at labelling MSCs with SPIO resulted in very similar iron uptake clustering around $10 \mu\text{l/ml}$ with the average being $10.2912 \mu\text{l/ml}$ of iron. The concordant nature of these results indicates that independent labelling of MSCs produces similar levels of iron uptake.

3.3.10 Impact Of SPIO On Viability

ThermoFisher Aqua LIVE/DEAD cell stain kit was used to determine if labelling the MSCs with SPIO would have an impact on cell viability. First, gating was set up by creating a comparison of live vs. dead cells as done previously. MSC were killed by heat treating them at 70°C for 5 minutes. These, along with live MSC were then stained using the aqua LIVE/DEAD cell kit according to the instructions then run on a flow cytometer. Figure 3.11 shows the overlaid histograms of SPIO labelled and unlabelled cells.

3.3.11 Flow Cytometry Analysis Of SPIO-MSCs

Once it was confirmed consistent labelling with SPIO was possible and that this labelling didn't have an impact on the viability of the cells, experiments needed to be carried out to determine if SPIO would alter the characteristics of MSCs. These experiments were the same as those used to confirm that MSCs had been isolated; the cell surface marker panel, differentiation, and Immunosuppression of stimulation assays.

Figure 3.12 shows the flow cytometry results of SPIO labelled MSCs compared to non-SPIO labelled MSCs. Across all markers examined there was no significant difference in expression. SPIO did cause some slight auto-florescence but this was addressed by using a separate SPIO labelled negative control.

3.3.12 Differentiation Of SPIO-MSCs

As already mentioned several times, the ability to differentiate into adipocytes, chondroblasts, and osteoblasts is one of the defining features of MSCs. So, having labelled the cells with SPIO it was important to ensure that they maintained this ability. The cells were labelled with SPIO for 18 hours before being harvested and being used to carry out the differentiation procedure defined previously. The results in figure 3.13 show that the SPIO labelled cells are able to differentiate just as well as the unlabelled cells.

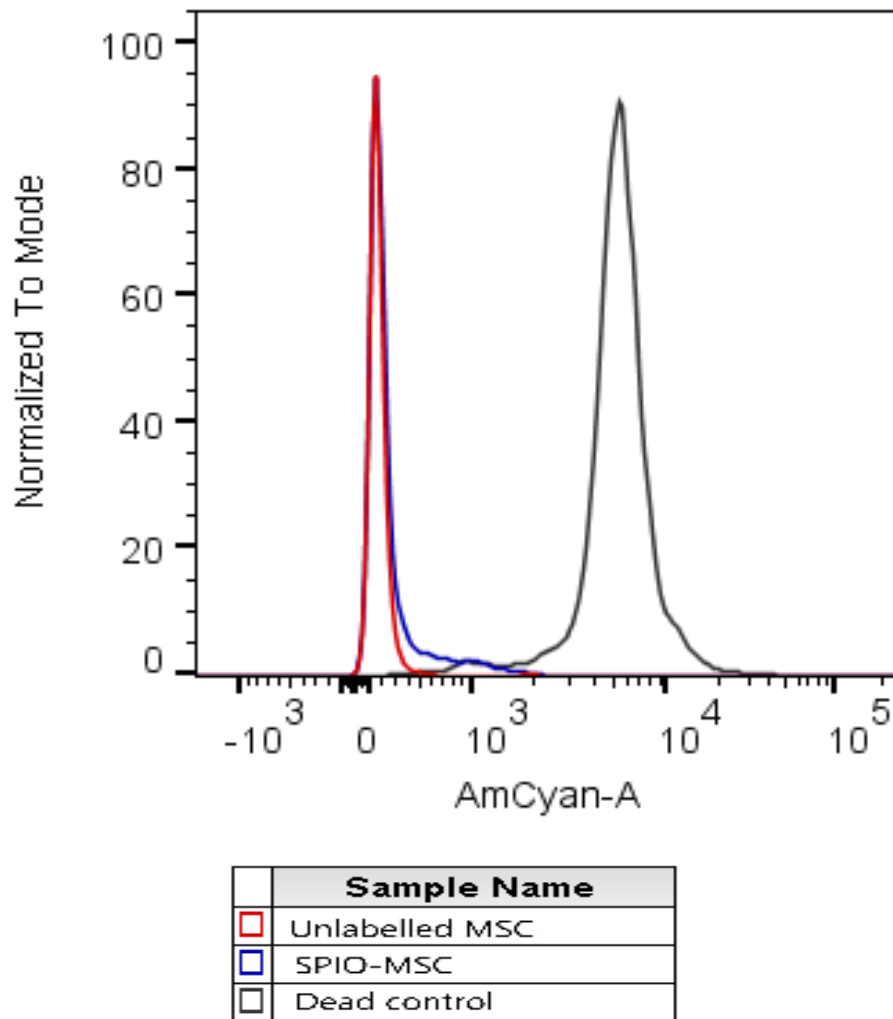


Figure 3.11 Overlaid histograms of SPIO labelled and unlabelled MSCs when stained using the thermofisher LIVE/DEAD aqua dead cell stain kit which causes dead cells to fluoresce more strongly than live cells. The histograms for both the MSCs and the SPIO-MSCs overlap indicating that there is minimal difference between their viability with 96.7% unlabelled vs. 93.3% labelled cells remaining viable. This demonstrates that labelling MSCs with SPIO does not negatively impact their viability.

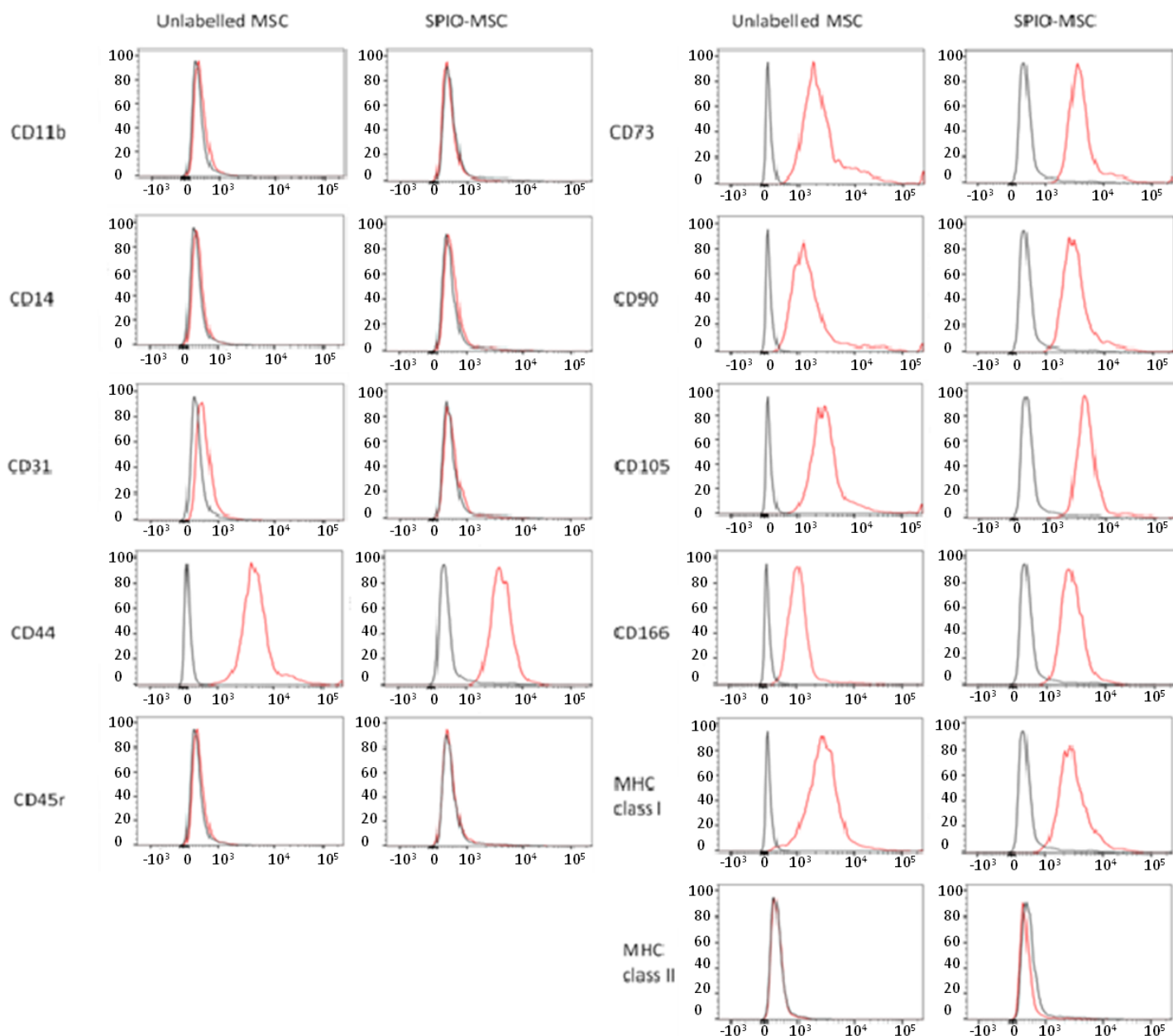


Figure 3.12 Cell surface marker panel for ovine Mesenchymal stem cells used to compare the phenotype of SPIO labelled MSCs to unlabelled MSCs. MSCs were labelled with SPIO and then run on a flow cytometer as previously described. The data demonstrates no difference between the cell surface markers of MSCs and SPIO-MSCs with both groups being positive for CD44 (99.9% vs. 99.3%), CD73 (98.6% vs. 99.7%), CD90 (89.1% vs. 97.1%), CD105 (99.7% vs. 99.5%), CD166 (79.4% vs. 92.8%) and MHC I (96.8% vs. 92.1%) while being negative for CD11b (5.06% vs. 1.78%), CD14 (3.74% vs. 5.65%), CD31 (8.35% vs. 4.89%), CD45r (4.43% vs. 4.59%), and MHCII (2.84% vs. 4.35%).

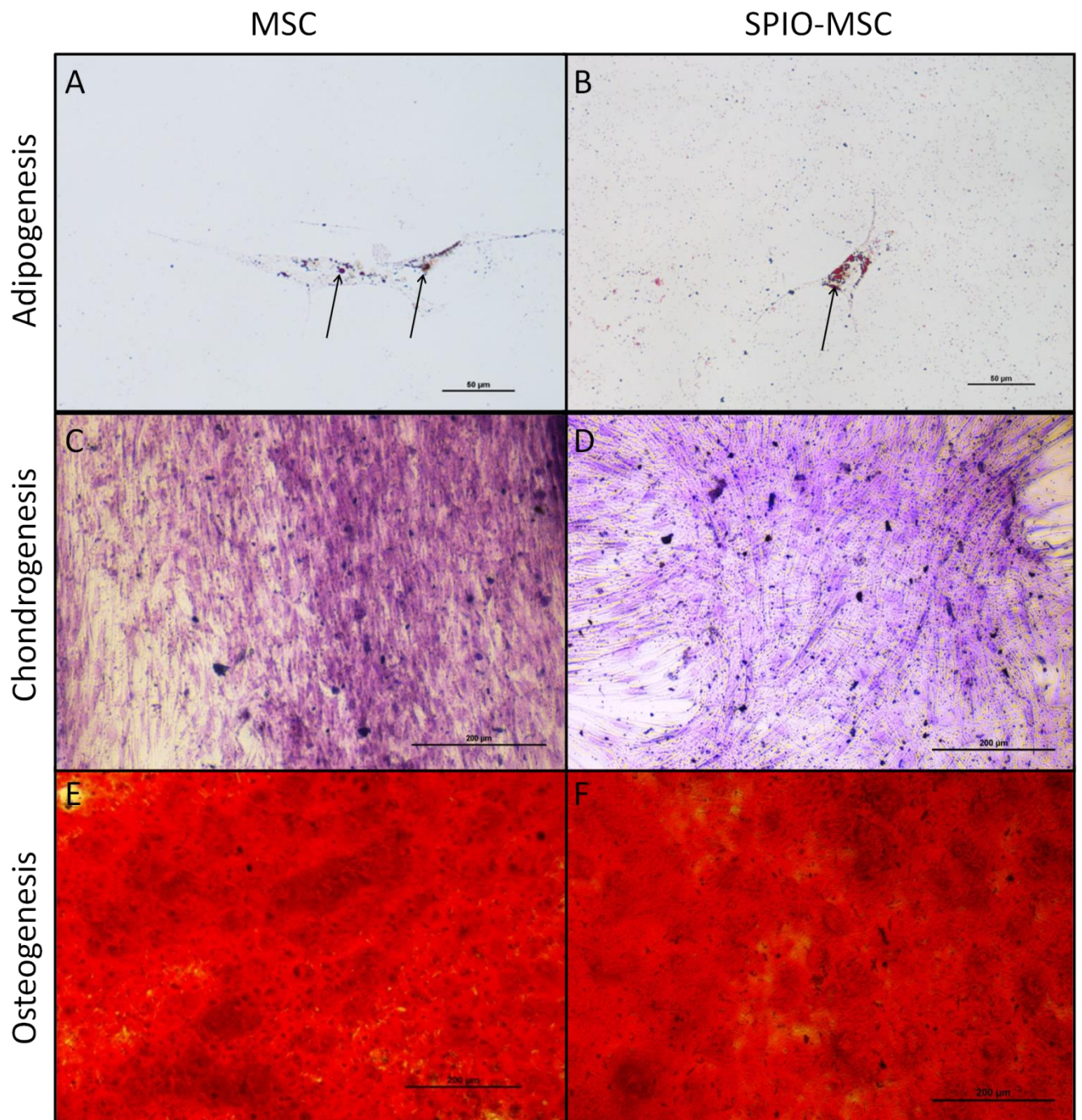


Figure 3.13 MSC tri-lineage differentiation of SPIO labelled and unlabelled MSC. Staining for adipocytes was carried out using oil-Red-O which renders the fat vacuoles red (A and B, arrows). Chondroblasts are stained with Toulidine blue which makes the proteoglycans in cartilage turn purple (C and D). And Osteoblasts are stained with Alizarin red which picks up mineralization particular to bone formation and stains it red (E and F). Both labelled and unlabelled MSCs were able to differentiate successfully indicating that SPIO does not impact tri-lineage differentiation.

3.3.13 Immunosuppression Of Con-A Stimulation Assays

Lastly, it was important to ensure that SPIO labelled cells were still able to cause immunosuppression as this was a function of MSCs that was important to future research. To assess the immunosuppressive function of SPIO-MSCs, Con-A stimulation assays supplemented with MSCs were performed.

MSCs were labelled with SPIO for 18 hours before being harvested and plated at 0.1%, 1%, or 10% of the total responder PBMCs to be added. Con-A was then used to cause stimulation and this was allowed to occur for 4 days before tritiated thymidine was added and the cells were allowed to proliferate for a further 24 hours. The cells were harvested and counted on a topcount scintillation counter. The resulting counts were normalized against the control well and inverted to get a percentage of immunosuppression.

Figure 3.14 shows the dose response curve of SPIO labelled cells vs. unlabelled cells. A two way ANOVA comparing the MSCs and SPIO-MSCs at each dose was performed with Sidak's multiple comparisons test. At 0.1% MSC the MSC group was, on average, only able to cause 1% immunosuppression with a standard deviation of 5%, while the SPIO-MSC mean immunosuppression was 0% with a SD of 2%. No statistically significant difference was found between with groups ($P=0.99$). At 1% MSC dose the MSC groups mean immunosuppression was $3\% \pm 6\%$, while the SPIO-MSCs mean immunosuppression was $10\% \pm 5\%$. Again, no statistically significant difference was observed ($P=0.06$). And at the 10% MSC dose the MSCs mean immunosuppression was $18\% \pm 3\%$ vs. $17\% \pm 1\%$ for the SPIO-MSCs. No statistically significant difference was observed ($P=0.96$)

Immunosuppression by MSCs SPIO stained vs Unstained

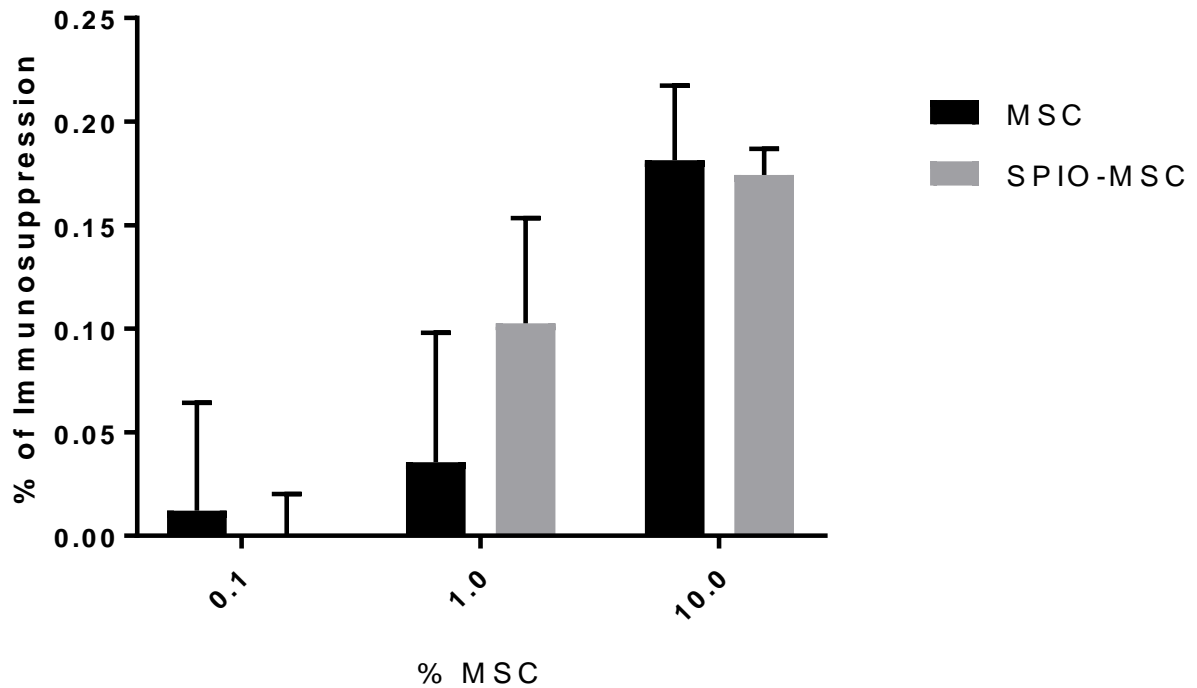


Figure 3.14 The impact of SPIO labelled MSCs and unlabelled MSCs on Con-A stimulation assays. 5×10^5 PMBCs were cultured with Con-A and either 500 (0.1%), 5000 (1%), or 50,000 (10%) MSCs or SPIO-MSCs and the percentage of immunosuppression compared to Con-A stimulated PBMCs alone calculated. No statistically significant differences were found between the MSC and SPIO-MSC groups at 0.1% MSC (MSC = $1\% \pm 5\%$ vs. SPIO-MSC = $0\% \pm 2\%$, $P=0.99$), 1% MSC (MSC = $3\% \pm 6\%$ vs. SPIO-MSC = $10\% \pm 5\%$, $P=0.06$) or 10% MSC (MSC = $18\% \pm 3\%$ vs. SPIO-MSC = $17\% \pm 1\%$, $P=0.96$)

3.4 Discussion:

From the characterization experiments that were run it can be concluded that mesenchymal stem cells have been isolated and expanded, based on their plastic adherence (Figure 3.2), tri-lineage differentiation (Figure 3.3), and cell surface marker expression (Figure 3.1). Additionally, it was observed that these MSCs have immunomodulatory capabilities with both mixed lymphocyte reactions and Con-A stimulation assays (Figure 3.5 & 3.14). In order to perform *in vivo* MSC tracking experiments it is necessary to label the cells. The label of choice for this research is SPIO, which is an iron nano-particle that can be detected by both MRI and Prussian blue staining. Whenever labelling cells it is important to ensure that the label has no impact on the functions or phenotype of the cell. To establish that SPIO had no impact on the MSCs the characterisation experiments were performed again, showing that there was no difference in the morphology of the MSCs (Figure 3.6), that they still underwent tri-lineage differentiation (Figure 3.13), and that there was no differential expression of cell surface markers (Figure 3.12). The ability of the SPIO labelled cells to cause immunosuppression of a Con-A stimulation assay (Figure 3.14) as well as the viability of the cells both labelled and unlabelled (Figure 3.11) was examined with no difference between the labelled and unlabelled cells observed. Further viability experiments were carried out looking how well the MSCs survived in saline compared to complete media out to 1 hour (Figure 3.4) and found that this had no impact on viability. Lastly, the amount of iron taken up by the cells was quantified and checked to ensure that it was concordant across several labelling experiments (Figure 3.7 to 3.9 and table 3.1). This was important for later *in vivo* cell tracking experiments as it established that results from different batches of labelled cells could be compared and combined.

The results from the characterization of SPIO-MSCs are congruent with what has been published in the literature. Farrell *et al.*, (2008) [405] labelled MSCs with SPIO for the purpose of tracking the cells after being seeded into a scaffold which was then implanted into mice for 4 weeks. Of importance to the current work was the finding that labelling MSCs with SPIO did not have an impact on tri-lineage differentiation [405]. However they did note that after 4 weeks implanted in the mice the SPIO-MSCs began to show signs of osteogenesis which was absent from the unlabelled MSCs [405].

The lack of impact of SPIO on the ability of MSCs to differentiate was backed up by both Addicott *et al.*, (2014) [406] and Hansen *et al.*, (2011) [407]. Addicott *et al* used a SPIO known as Molday ION Rhodamine-B (MIRB) which has been formulated with the intention of labelling cells for magnetic tracking, using this they labelled MSCs across a range of iron concentrations. Their findings demonstrated that MIRB-MSCs had no change in the cell surface markers they were examining (CD29, CD45, HLA class I, and CD31) nor was there a difference in the ability to differentiate into bone or fat. The results from their viability testing showed that there was no difference up to 30 μ gFe/ml. However, above this limit a decline in viability was seen with 100 μ gFe/ml resulting in only 78.8% viability [406]. For comparison the highest iron concentration found in the present study was 11.4 μ gFe/ml (table 3.1), well below the point at which impacts on viability were observed. Another of the important findings of Addicott *et al* was that MIRB-MSCs were able to disrupt PHA stimulated PBMC proliferation just as well as unlabelled MSCs with both keeping relative proliferation below 10% of the MSC-free control [406].

Hansen *et al* used ultrasmall superparamagnetic iron-oxide particles (USPIO) conjugated with the trans-activator for transcription (TAT) derived from HIV-1 to maximise iron uptake by MSCs [407]. They then set about characterizing the labelled cells by examining viability and cell surface marker expression as well as using electron microscopy to visualize USPIO

uptake. Their viability experiments support what was published in previous papers as well as the findings from the present study (figure 3.11), showing that SPIO labelling of MSCs does not have a negative impact on viability. Furthermore, Hansen *et al* showed that there was no variation in cell surface marker expression between MSCs and SPIO-MSCs with both being positive for CD105, CD90, CD70, and CD13, while being negative for CD45, CD19, CD14, and HLA-DR [407] this was a more comprehensive panel than the one used by Addicott *et al* [406]. The cell surface marker results from both Hansen *et al* and Addicott *et al* are consistent with what was observed in figure 3.12.

Although SPIO is the label used in this thesis there are other compounds that have been used as adjuncts to aid in the tracking of MSCs. A widely used label is technetium 99m (Tc-99m), a radioisotope that has found use in many medical procedures due to its short half life which allows for scanning procedures to be carried out while keeping a patients exposure to radiation low. Although it has been used in several studies to track the migration of MSCs there is very limited data from these studies on the impact of Tc-99m on MSC function and phenotype [408, 409]. There is some data showing that Tc-99m does not impact the viability of the MSCs [410]. However, this viability testing was carried out immediately after the labelling procedure so it does not provide information about the effect of MSC exposure to Tc-99m over time [410].

Another method commonly utilized to track MSCs is to transfect the cells with green fluorescent protein. The impact of GFP transfection on MSCs has been characterized by Guo *et al.*, (2012) [411] and Colosimo *et al.*, (2013) [412]. Guo *et al* isolated and expanded MSCs from rat bone marrow and then transfected the cells with GFP. They found that GFP-MSCs did not differ in their morphology, cell surface markers, or ability to differentiate when compared to non-transfected MSCs. Furthermore, GFP transfection of MSCs did not alter the expression of paracrine modulating molecules such as vascular endothelial growth factor

(VEGF) and fibroblast growth factor 2 (FGF-2), indicating that this method of cell tracking would not have an impact on the *in vivo* effects of MSCs. Colosimo *et al* used two different transfection methods. An extremely important finding was that GFP transfection of MSCs decreased viability, with recovery of cells dropping as low as 24% in some instances. Colosimo *et al* also found that GFP transfection of MSCs did not result in chromosomal instability during expansion, did not impact the expression of markers of pluripotency (SOX2, NANOG, and TERT), and did not hinder osteogenic differentiation.

The final method of tracking MSCs that has been widely used is the incorporation of fluorescent dyes. Weir *et al.*, (2008) [413] examined the application of Chloromethylbenzamido-1,1'-Dioctadecyl-3,3,3',3'-Tetramethylindocarbocyanine Perchlorate (CM-DiI) labelling of MSCs for the purpose of measuring implanted cell retention time *in vivo*. Prior to *in vivo* experimentation, Weir *et al* characterized CM-DiI labelled MSCs. They found that CM-DiI did not impact the viability or proliferation of the MSCs over two weeks. They also observed no changes in the differentiation capabilities of CM-DiI labelled MSCs. These results combined with the strong persistence of CM-DiI lead Weir *et al* to favour this dye for their later cell tracking experiments [413].

In conclusion, Ovine MSCs have been isolated, expanded, iron labelled and characterized in a reproducible way that makes them suitable for *in vivo* experimentation. The SPIO label did not impact the viability, cell surface marker expression, differentiation capacity, or immunosuppressive abilities of the MSCs. These findings are in agreement with the literature which provides further evidence that SPIO labelling preserves MSC function and characteristics. This is in contrast to the literature for other tracking modalities which is less apparent about the effects that the various labelling techniques will have on MSC phenotype and function.

Chapter 4

Optimisation of the Ovine Heterotopic Kidney Transplant Model

4.1 Introduction:

Addressing questions of medical significance in a variety of animal models is a must prior to clinical applications. Given that only 6.2% of all new molecular entities (NME) and 11.5% of biologically derived interventions make it from phase 1 trials to FDA approval [414, 415] it is imperative that the animal models underlying the pre-clinical basic science of potential interventions are well designed and developed.

4.1.1 Large Animal Models

With the current shift away from the use of primate models, a wide variety of non-primate large animals have been used in order to meet the demands of translational medical research, with some of the more common species used being pigs, sheep, goats, and cows. The anatomical and genetic similarities that these livestock share with humans make them useful for studying a wide variety of biological systems and conditions from skin conditions to the respiratory system.

One particularly complex area that benefits tremendously from large animal models is transplantation. Small animal models such as the rat model used by Spanjol *et al.*, (2011) [416] have played a significant role in advancing the understanding of transplantation science. However, due to their small size, high level of inbreeding, and short life span it is not

always possible to translate observations made in small animal models to the clinic. In addition to addressing these issues, large animal models have a variety of characteristics that make them suitable for transplantation studies such as their ease of maintenance and handling. Their size makes it possible to perform many procedures in the same manner as they would be carried out in humans, such as the cannulation of blood vessels. Additionally, they have a good tolerance for these procedures due to their docile temperament meaning they do not interfere with any medical devices placed for the duration of an experiment, and furthermore, their size and longer life spans means that a greater number of samples can be collected and monitoring can continue for extended periods of time.

Given that transplantation straddles the intersection of several different disciplines it is imperative that a wide variety of animal models be well established and characterized so that there is a thorough understanding of potential clinically applicable therapies, as well as providing controlled circumstances for more intricate and experimental forms of transplantation to be optimized. Many technically challenging forms of transplantation are currently being developed in large animals such as facial, tracheal, small bowel, and uterine transplantation. Due to the complex nature of these procedures, preclinical work in large animals is essential to explore and address many facets and possible complications before the procedures are trialled in humans. An example of this is presented by Bertolotti *et al* [417] in which they attempt address the challenges of tracheal transplantation which, to date, has not proved to be a successful technique, but would be valuable in treating patients with conditions that have resulted in tracheal damage such as tumour resection or tracheal stenosis. They performed several tracheal transplants in sheep and tested if an omental pedicle would make a difference to graft survival. Although the omental pedicle did have an impact on outcomes, it was a negative impact, resulting in more graft failures for the test group. Of interest, was the observation that the majority of their graft failures were due to infection by

Pseudomonas aeruginosa. This occurred despite prophylactic use of a broad spectrum antibiotic that should have prevented this infection. The authors postulated that the persistence of the infections could be due to poor blood circulation to the tissue immediately following transplantation, resulting in inadequate antibiotic concentrations at the transplant site [417]. This brings into focus an important issue for potential human tracheal transplants and one that may make a significant difference and this would not have been possible without the use of a sheep model.

4.1.2 Animal Models Of Ischemic Reperfusion Injury

Of primary interest in this project is solid organ transplantation, in particular, renal grafts. Being one of the most common types of transplantation as well as having a level of risk mitigation in the form of dialysis, means that kidney transplants often find themselves at the forefront of transplantation medicine. As such, it is unsurprising that there are several animal models looking at the various challenges of kidney transplantation, from mice and rats to pig and sheep models. A significant complication associated with kidney transplantation is ischemic reperfusion injury (IRI) [67] accordingly, a plethora of models have been conceived and assessed to examine this factor. Rodent models of kidney IRI are well established with their use going at least as far back as 1976, when Thureau *et al* used vascular clamping to induce IRI in rat kidneys [418], providing invaluable insights into the underlying physiology and potential therapies for kidney ischemia reperfusion injury. Oxburgh and de Caestecker developed a comprehensive methodology for inducing kidney IRI in mice [419]. They describe a protocol using either a ventral or dorsal approach in which the kidneys are externalized allowing vascular clamps to be applied before the kidneys placed back into the peritoneal cavity for the duration of the ischemic period. They also noted that historically many mouse models of kidney IRI tended to have a high morbidity rate which they attempted to address by publishing their standardized method including preferential use of the dorsal

incision approach as this resulted in faster recovery times and better survival rates [419].

Utilizing a similar method to Oxburgh and de Caestecker, Zhang *et al* published work in both 2013 [420] and 2014 [421] demonstrating the protective effects of both dexamethasone and rapamycin in kidney IRI as well as the pathways in which these drugs provided this protection. These two papers published in a relatively short time frame illustrate the speed with which valuable results can be gained using rodent models which is one of their greatest strengths. However, as previously mentioned, these studies are not easily applied to the clinic as the anatomical and physiological differences between humans and rodents are too great.

Large animal models of kidney IRI have been widely studied with pigs comprising the majority of the model animals [336, 422-436], followed by sheep [337, 437-442], and cows being a distinct minority [443].

These large animal IRI models can be generalized into two distinct groups, normothermic IRI or hypothermic IRI. Normothermic IRI refers to the clamping of the blood vessels for various periods of time while keeping the organ *in situ*, similar to the procedures performed in rodent models. Whereas hypothermic IRI often involves surgical excision of the kidney, flushing of the organ with cold preservation solution and storage on ice, a process that closely mimics human kidney transplantation. Both methods have their merits and disadvantages.

Normothermic IRI induction techniques tend to be easier to perform as the vasculature is only clamped, not severed, which can be carried out laparoscopically. This reduces the size of surgical wounds and reduces the risk of infection leading to better recovery post surgery. In contrast, hypothermic IRI induction surgeries are technically more challenging requiring a complete nephrectomy, flushing the organ with preservation solution, and finally reattaching the organ to sufficient blood flow which requires technical expertise in vascular anastomosis. Despite these challenges hypothermic IRI offers the significant advantage of more closely mimicking the process of human organ transplantation.

The differing levels of difficulty are reflected in the popularity of each method with normothermic based IRI outnumbering hypothermic methods despite hypothermic IRI being arguably the more clinically applicable approach.

4.1.3 Large Animal Models Of Kidney Allotransplantation

Although interrogation of the pathophysiology of IRI is important in improving kidney transplantation outcomes it isolates the models from the impact of immunobiology on graft function. As such, large animal models of kidney allograft transplantation are required to fully explore the many facets of kidney transplantation.

Like IRI, pigs and sheep are well represented in the literature regarding large animal kidney allograft models. Pig models are generally performed by the clamping then removal of both kidneys with the left kidney then being transferred and placed orthotopically [444-446]. Golby *et al.*, 1971 performed a large study where they performed 94 operations looking a variety of techniques and immunosuppressive agents. They made note of several complications such as death due to preoperative feeding and graft loss due to renal artery thrombosis but they did provide solutions to these issues [444]. Despite this, Terblanche *et al* in 1975 still deemed that the pig was an unsatisfactory model in which to study immunosuppressive regimes for kidney allografts due to a large number of failures unrelated to rejection [445]. Since this time, the pig allograft model has developed into a critical component of transplantation science with the model being reliable enough that re-transplantation can be carried out repeatedly and successfully [446].

The history of sheep in kidney transplantation is comparable to pigs, reaching as far back as 1959 [438, 439, 447-451]. Interestingly, much of the sheep work carried out relies on heterotopic placement of kidney grafts as opposed to the orthotopic placement favoured in pigs. One of the earliest examples of heterotopic transplantation in sheep is from 1970 by

Pedersen and Morris [449]. In this study the authors transplanted renal homografts into the neck of sheep via end-to-end anastomosis of the renal vein to the jugular vein and the renal artery to the carotid artery. They then cannulated one of the renal lymphatic ducts to allow for the collection of lymph, which was the primary focus of their study. This method of sheep renal transplantation has persisted and been used in both auto and allografts to study transplant related complications [439] and possible therapeutic strategies [451].

4.1.4 Ovine Major Histocompatibility Complex

The major histocompatibility complex (MHC) plays a significant role in organ transplantation. In sheep the DRA and DRB1 loci of the MHC class II molecule have been well studied and characterized [19, 43-46, 51]. The DRB1 loci is known to be highly polymorphic [51], when consulting the IPD-MHC database, which is a compendium of MHC genomes from various species, 106 different alleles had been published so far. This high level of polymorphism is common across all vertebrates [43]. When focussing on the DRB1 loci, the majority of studies have concentrated on exon 2 as this is the most polymorphic region [44, 51]. In contrast, the DRA region is well conserved, with sheep only having 3 currently described alleles [43]. This has resulted in the DRA loci receiving significantly less analysis. In developing the sheep heterotopic kidney transplantation model direct sequencing of these genes has been used, combined with the use of mixed lymphocyte reactions, to tissue-type sheep prior to transplantation. Thus it is possible select MHC mismatched donor and recipient animals to investigate the role of donor organ rejection in this transplant model. It also provides a platform to test therapeutic interventions aimed at ameliorating the immune rejection of transplanted organs.

4.1.5 The Ovine Heterotopic Kidney Transplant Model

For this work the sheep model of heterotopic kidney transplantation has been expanded and optimised. This model has several advantages that make it useful for transplantation studies. It can be performed as either an autograft or an allograft model with a bilateral nephrectomy should the need arise to have the animal survive on the transplanted kidney alone. The placement of the kidney in the neck allows for improved monitoring, ease of biopsy, and superior imaging quality.

Obviously, no animal model will completely reflect the human condition and so the limitations of the model need to be explored and addressed so that any results can be viewed with the correct understanding.

This chapter deals with the development and optimization of the sheep heterotopic kidney transplant model. As with any complex large animal model there were failures and unexpected results but these all lead to incremental improvements until a useful model for further experimentation had been developed.

4.1.6 Chapter Aims:

The aim of this study was to develop a reproducible and robust model of kidney transplantation that could have pharmacologically controlled graft acceptance and rejection as well as the ability to be performed in as both an allograft and an autograft to examine different aspects of transplantation science.

4.2 Materials and methods:

4.2.1 Tissue Mismatching Sheep

One of the aspects of transplantation that required investigation was organ rejection. Therefore, donor and recipient animals were mismatched based on both mixed lymphocyte reaction and direct sequencing of the DRA and DRB1 loci.

4.2.2 Blood Collection

Six animals were tissue typed and mismatched at a time. Blood samples were collected from each animal for both MLRs and sequencing. In order to collect the blood the animals were restrained by tipping them. The wool was trimmed above the left hand jugular vein, pressure was placed on the caudal region of the vein to partially occlude it causing it to protrude and become easy to identify. An 18 gauge needle attached to a 60ml syringe was then inserted into the vein and slight pressure applied, drawing out the plunger to establish blood flow. 50ml of blood was then taken into the syringe and 40ml distributed into a 50ml falcon tube containing 5ml of heparinised saline. The remaining blood was then put into an 8ml green top sodium heparin tube. All blood was collected at least a month before any further procedures were carried out to ensure that any damage to the jugular vein had healed.

4.2.3 Mixed Lymphocyte Reaction

MLRs were carried out as previously stated in chapter 2. Sheep were then assigned into mismatched donor and recipient pairs based on OLA typing and positive MLR.

4.2.4 DNA Isolation

Blood samples were collected from the sheep at least one month prior to any further procedures. DNA was then isolated from this blood as described in chapter 2 (section 2.17).

4.2.5 Design Of Primers

Primers were originally taken from two papers published by Keith Ballingal in 2005 [45] and 2010 [51]. Further Primers were designed by taking the DRA and DRB1 regions of the Ovine genome (<http://gbrowse-ext.bioinformatics.csiro.au/gb2/gbrowse/oarv3/>) and establishing areas of interest as suggested by Ballingal *et al*, this resulted in us focussing on exon 2 of the DRB1 loci and exons 2 and 3 of the DRA loci. These exons were then put into primer3 (<http://bioinfo.ut.ee/primer3-0.4.0/>) using the default parameters to determine the optimal primer pairs for each exon.

4.2.6 PCR

PCR was carried out using the Promega GoTaq Green master mix. 50µl reactions were performed using 25µl of GoTaq green master mix, 5µl of both the forward and reverse primer at 10µM concentration, 1-5µl of purified DNA depending on the isolated concentration, and then topped up to 50µl using nuclease free H₂O. PCR amplification was performed as described in chapter 2 section 2.19. Samples underwent denaturation at 94°C for 2 minutes followed by 60 cycles of 94°C for 30 seconds, 55°C for 30 seconds and 72°C for 30 seconds, then a final incubation at 72°C for 5 minutes.

PCR amplification products were analysed on a 1% agarose gel with a 100bp molecular ladder before being stained with gel red and imaged using a gel dock system.

Target	Forward Primer	Reverse Primer	Product size
DRA Exon 2	5' acacatgcatcacaggagga 3'	5' ggctaagcaggggaaggctaa 3'	379bp
DRA Exon 3	5' aggaggactggagcagaggt 3'	5' cacgtggccctctcttcta 3'	382bp
DRB1 Exon 2	5' gatcaagcacgcacaggag 3'	5' gtctcggtcgtctcacact 3'	672bp

Table 4.1 Primers were designed focussing on exon 2 and 3 of the MHC class II gene, DRA, and on exon 2 of the MHC class II gene, DRB1. The resulting primers are displayed above along with their predicted product size.

4.2.7 Sequencing

Prior to sequencing set up the PCR products were purified using a Qiaquick PCR purification kit. From the instructions, 5 volumes of buffer PB was added to 1 volume of PCR product this was then added to a Qiaquick column placed in a 2ml collection tube and spun at 13,000 rpm for 1 minute. The flow through was discarded and the column placed back in the same collection tube. The column then had 750µl of buffer PE added and was spun at 13,000 rpm for 1 minute. The flow through was discarded, the column placed back in the collection tube and spun again at 13,000 rpm for 1 minute. The column was placed in a clean 1.5ml eppendorf tube and had 50µl of buffer EB added before being spun for 1 minute at 13,000 rpm in order to elute the now purified DNA.

Sequencing of the purified DNA was performed by the Australian Genomics Research Facility. The resulting data was then analyzed using finchTV chromatogram reader. The resulting sequences were then aligned with the already published alleles using the EMBL blast algorithm to determine which allele the sheep contained or if it had a novel sequence. They were also aligned against each other to check for sequence variation.

Most importantly these were then used to check against the MLRs and make sure that the animals were mismatched at both loci to ensure that rejection would occur.

4.2.8 Pharmacokinetics

Controlling and inducing rejection was of importance to the later application of this model. Tissue typing ensured that rejection would occur, however, in order to control rejection knowledge of cyclosporine pharmacokinetics in sheep was required.

Three sheep had a central line placed into the right hand jugular to facilitate administration of the immunosuppressive drugs, they then received 5mg/kg of cyclosporine and 10mg/kg of ketoconazole once a day for a week to establish a steady state concentration before having

blood samples taken at 0, 1, 2, 4, 6, 8, 10, 12, 24, and 48 hours. The samples were then analysed by mass spectroscopy to determine drug concentration levels in the blood, as described in chapter 2 (section 2.22), from which an elimination curve can be derived.

4.2.9 Transplant Procedure

All animals were fasted for 24 hours prior to surgery and on the day of the surgery general anaesthesia was induced with diazepam (0.2-0.3 mg/kg) and ketamine (0.5mg/kg) and maintained using isoflurane (1-2%). The flanks and neck were shaved in the areas relevant to the operations and had chlorhexidine applied topically to disinfect. The animals were then moved into the operating theatre. Surgeries were carried out by Dr Christine Russell and Dr Santosh Olakengil with assistance from several volunteers.

To perform the nephrectomy of the kidney to be transplanted, the animal was placed on its right hand side so that the left hand kidney could be accessed. An incision was made 5cm caudal to the 13th rib and the underlying fat and muscle divided while cauterising any bleeds.

Once the left hand kidney was identified it was manipulated into a position to allow visualization and access to the renal vessels and ureter. These vessels were then tied off and cut before the stump was closed off. The left hand kidney was used because of the longer vessels in relation to the right kidney. As such, as much of the vessels as possible were excised with the kidney, ensuring adequate tissue for the anastomosis.

The left hand nephrectomy wound was then closed and the kidney moved to a sterile bench containing a bowl with sterile ice. Here the kidney was perfused with Custodiol KTH preservation solution and placed on ice while the neck was prepared for the placement and anastomosis of the kidney. To prepare the neck, an incision was made in the skin ventral to the jugular vein and a pocket created by separating the subcutaneous tissue. This was done to

provide access to the underlying blood vessels as well as to create a space for the kidney to be placed. The jugular vein and carotid artery were exposed and marked with elastic ties.

Both vessels were then clamped and the jugular vein was prepared for an end to side anastomosis, this involved making an incision to the side of the jugular vein. The carotid artery was prepared for an end-to-end anastomosis by cutting through it and ligating the cranial end.

The renal vein underwent end to side anastomosis with the jugular vein and the renal artery underwent end to end anastomosis with the carotid artery. The clamps were then released and the blood flow confirmed by the colour change of the kidney from a grey-brown colour to a deep purple. The ureter was externalized through the skin flap and catheterized. A surgical drain was placed through the skin to help control post operative swelling and the skin flap was closed using a continuous horizontal mattress suture with slight eversion of the skin edges to avoid growth of wool into the wound.

If a bilateral nephrectomy was to be performed the sheep was then rolled onto its left hand side (with care taken to protect the graft) to allow access to the right hand kidney. This was performed as described for the left hand kidney. At this point a central line was placed into the remaining stump of the renal vein and run into the inferior vena cava. If a bilateral nephrectomy was not required then the central line was placed into the stump of the left hand renal vein.

The animal was then taken to the MRI room while still under anaesthetic for imaging analysis as required. If not, then the isoflurane was withdrawn and the animal was allowed to regain consciousness. The animal was then monitored until it was ambulatory and had begun consuming food and water.



Figure 4.1 A) Making the incision caudal to the ribs and separating the underlying tissue to expose the kidney. B) Mobilizing the kidney to allow access to the vessels. The vessels are then tagged with elastic ties.

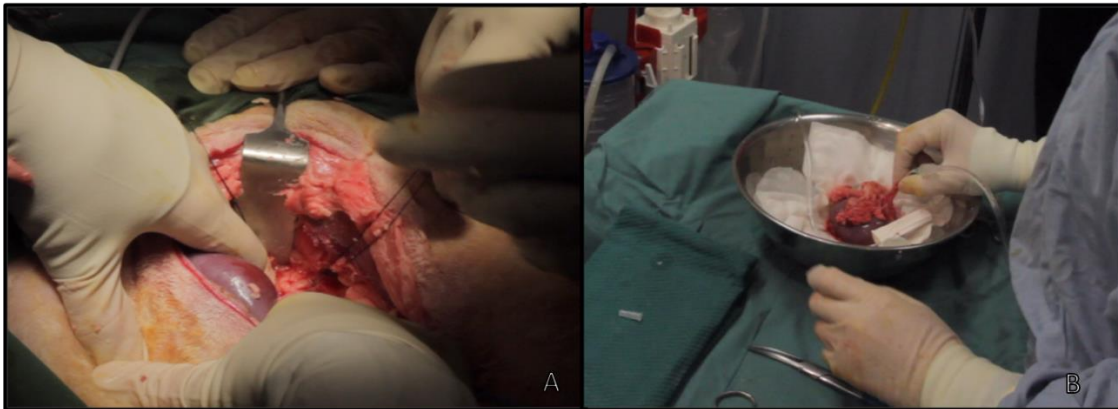


Figure 4.2 A) Once the vessels are identified they are tied off and cut. B) The kidney is removed and immediately placed on ice while being flushed with preservation solution.

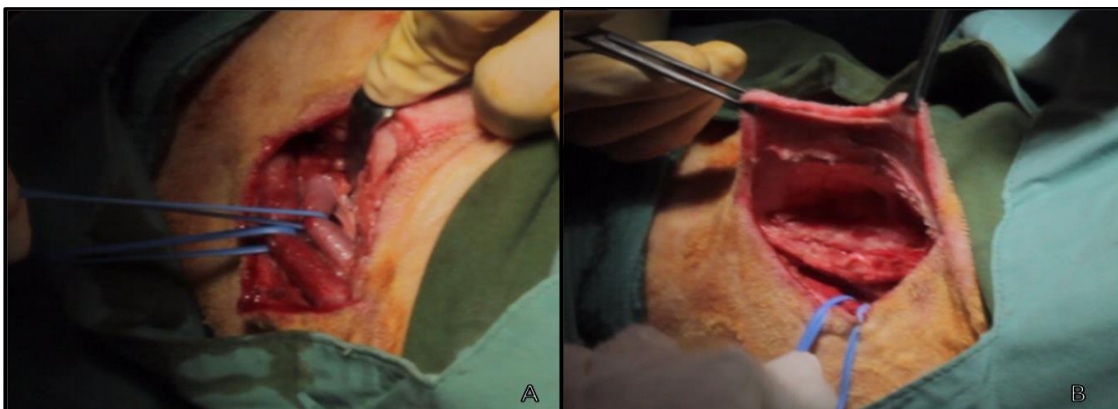


Figure 4.3 A) An incision is made in the skin above the carotid and jugular, these vessels are then identified and ties are placed around them. B) The skin directly dorsal to the exposed vessels is manipulated to create a pocket large enough for the kidney to be placed into.



Figure 4.4 A) The jugular vein is clamped to prepare for anastomosis. B) The jugular vein undergoes end-to-side anastomosis with the renal vein of the kidney graft by having an incision made in the side of the vessel, to which the end of the renal vein is sutured.

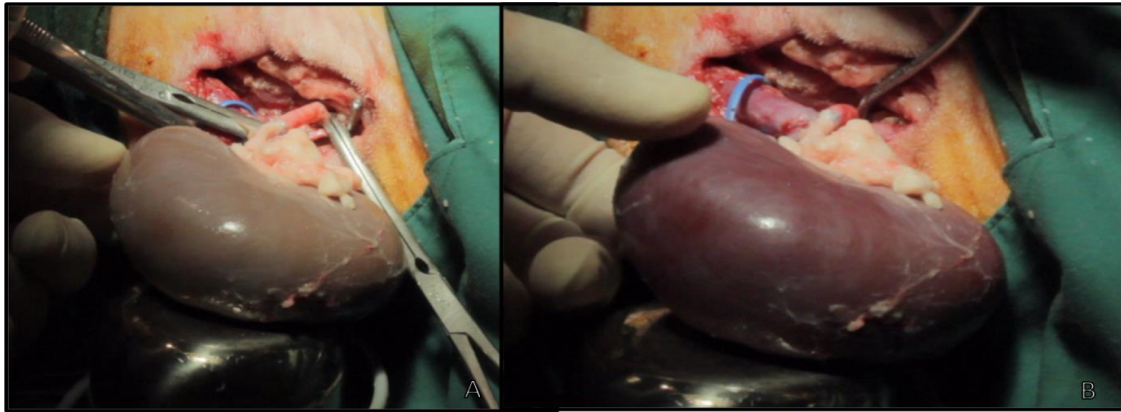


Figure 4.5 A) The carotid artery undergoes end-to-end anastomosis with the renal artery. This is illustrated in figure 4.8. B) The clamps are removed from the vessels and as blood returns to the kidney it undergoes a colour change from a dull brown to a deep purple.



Figure 4.6 A) The revascularized kidney is placed into the skin pocket and the ureter is externalized via a fistulae. B) The completed surgery with the distinct shape of the kidney graft in the closed skin pocket.

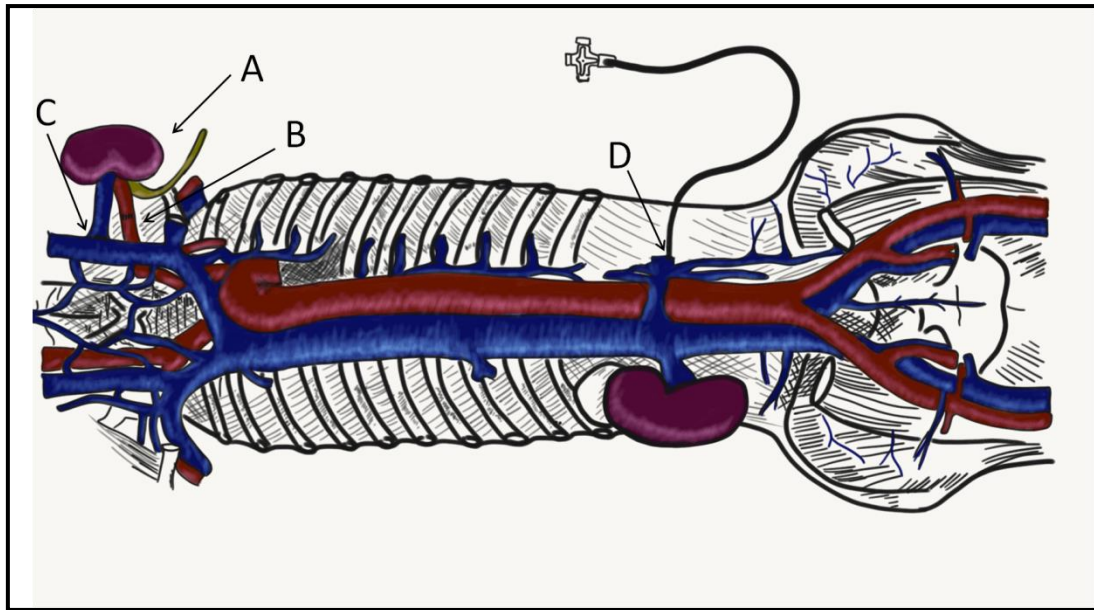


Figure 4.7 A ventral diagram through the frontal plane showing the vasculature involved in the transplant procedure. A) Shows the anastomosis of the renal vessels to the carotid artery (B) and the jugular vein (C), this is more clearly demonstrated in figure 4.8. The point at which the central venous line enters what remains of the renal vein after the nephrectomy is illustrated in D).



Figure 4.8 An illustration of the placement of the heterotopic kidney transplant graft. A) The end to side anastomosis of the renal vein and jugular vein. B) The end to end anastomosis of the renal artery to the carotid artery. C) The ureter that will be externalized through the skin to allow urine flow. D) The skin pocket that the kidney will sit in.

4.3 Results:

4.3.1 MLR

MLR's were carried out by isolating PBMCs from each of the sheep in the group and culturing them together so that each animal was a responder and a stimulator to every other animal. The plates were cultured for 5 days before being pulsed with tritiated thymidine and cultured for a further 18 hours. The cells were then harvested onto filter mats and these read using a topcount- NXT microplate scintillation counter (Perkin-Elmer). Given the variation in counts per minutes between experiments they are unable to be combined. To begin, crosses were performed between only one or two animals at a time but eventually complete crosses of six sheep at a time were carried out to ensure pairings could be selected that would have a strong immune reaction. Figure 4.9 displays the stimulation indices from all of the sheep that underwent allograft transplantation. The resulting mismatched pairs are displayed in table 4.2.

4.3.2 PCR

DNA was isolated from the whole blood of the sheep and regions of interest amplified via PCR using the primers detailed in table 4.1. The PCR products were then analysed by agarose gel electrophoresis to confirm their quality and size. Figure 4.10 below shows an example amplification of DRB1 exon2, DRA exon 2 and DRA exon 3. With the PCR product from DRB1, exon 2 running at about 650bp, the product from DRA exon 2 running just below 400bp, the same as the product for DRA exon 3. These PCR product bands are equal to the sizes predicted during primer design and displayed in table 4.1.

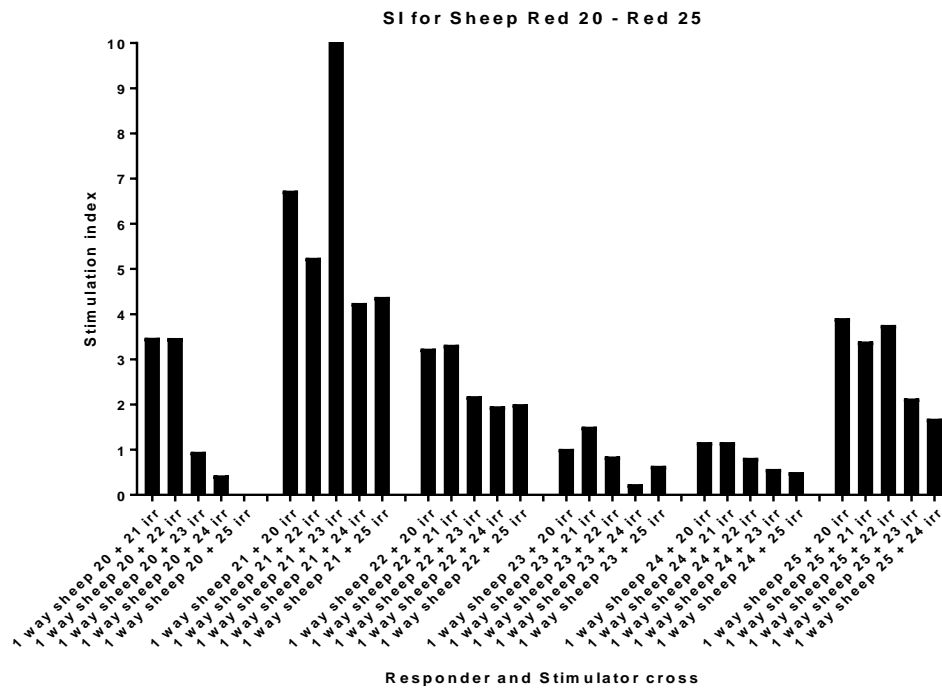
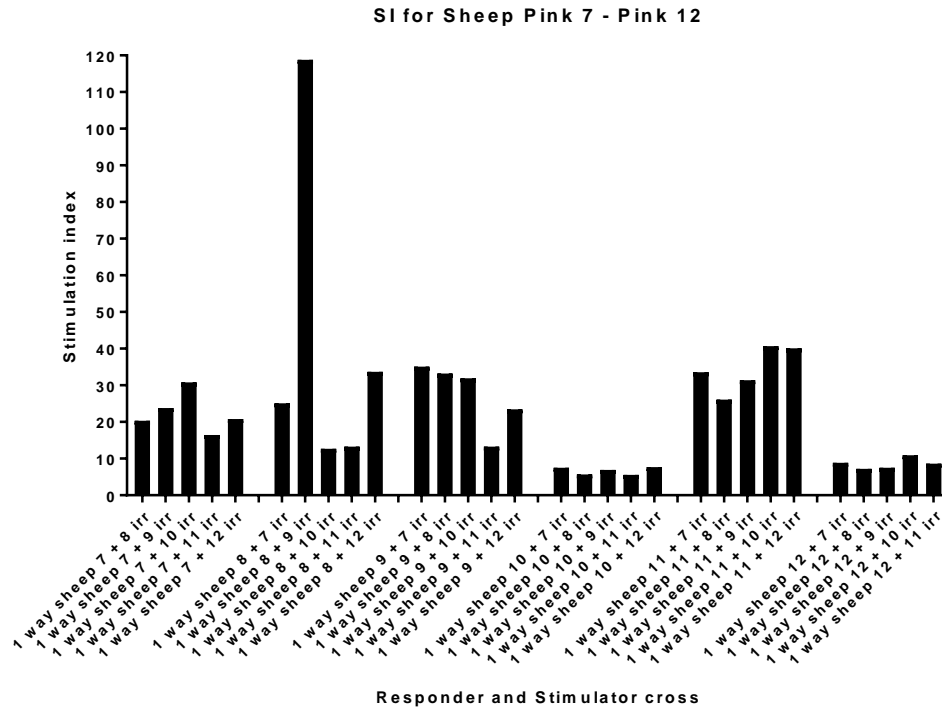


Figure 4.9 Results from the MRLs of groupings of six sheep. MLRs were performed as previously stated on groups of 6 sheep. The variation in the peak heights between experiments is significant making a direct comparison between the two groups impossible. It is also evident that some sheep have generally low levels of stimulation when they are responders even if they are strong stimulators for other sheep.

Donor	Recipient	Outcome
Red 20	Red 23	Success
Red 23	Red 20	Success
Red 21	Red 25	Success
Red 25	Red 21	Success
Pink 7	Pink 8	Early euthanasia due to kidney infection
Pink 8	Pink 7	Success
Pink 9	Pink 11	Success
Pink 2	Pink 6	Early euthanasia due to kidney infection
Pink 1	Pink 5	Completed with complications due to excess swelling of graft
Pink 4	Pink 3	Early euthanasia due to facial oedema
Grey 5	Grey 7	Early euthanasia due to lack of venous access

Table 4.2 All the pairs of sheep that underwent mismatched kidney transplantations. The pairings were decided based on the results of MLRs and direct sequencing of the OLA genes, DRA and DRB1. In some instances a sheep is listed as both a donor and a recipient, these are surgeries in which a cross-over transplant was performed.

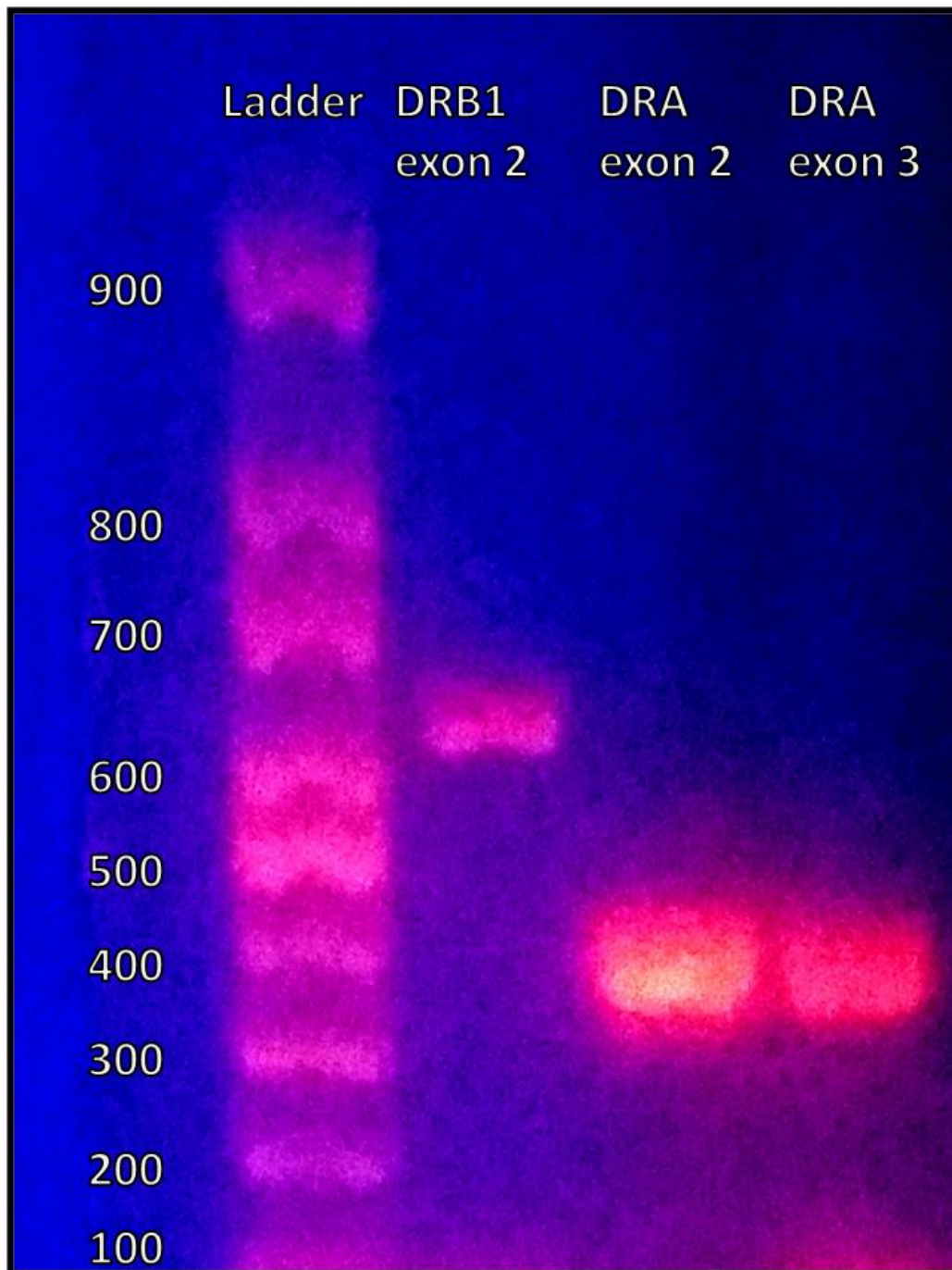


Figure 4.10 UV photography of an agarose gel. The bands are the product of the PCR amplification of sheep genomic DNA using the primers from table 4.1. The nucleotide ladder on the side makes it possible to determine the size of the PCR products to allow for positive identification. The product for DRB1 exon 2 was predicted to be 672bp in size, matching the size of the band. Similarly the bands for DRA exon 2 and DRA exon 3 match the predicted product sizes of 379 and 382, respectively

4.3.3 Sequencing

Once the PCR products were positively identified based on size they were prepared for sequencing by the AGRF. Raw data was analyzed using FinchTV and BLAST. The DRA sequences were aligned with previously identified alleles and assigned an identification number. From the sequencing, two previously described alleles, Ovar-DRA*01:01 and Ovar-DRA*01:02, and two novel alleles were identified. The majority of the sheep sequenced had the Ovar-DRA*01:02 allele variant. Figure 4.11 displays sequence alignments confirming the existence of the previously described alleles in this sheep population as well as an alignment showing the polymorphisms found in sheep Pink 5 and Red 20 that do not correspond to any known alleles.

Eight unique sequences were identified in the DRB1 gene, however none of these aligned with any previously published sequences; this is unsurprising given the highly polymorphic nature of exon 2 of the Ovar-DRB1 gene and the fact that a study of the OLA of Australian Merinos has yet to be performed. However, this meant that they could not be assigned an allele name. Instead the DRB1 genes from prospective crosses were aligned to ensure that there was a genetic mismatch. The resulting crosses and alignments are reproduced below in figure 4.12. The sequences are focused, where applicable, on the mismatches which have been highlighted. Additionally, the MRL results from the relevant crosses are reproduced below.

Although several of the crosses have mismatches at both the DRA and DRB1 loci there are some, such as Red 21 x Red 25, that only contain a mismatch at the DRB1 loci. These single mismatched crosses still reacted strongly in the MLRs showing that a single mismatch is enough to cause an immune reaction *in vivo*.

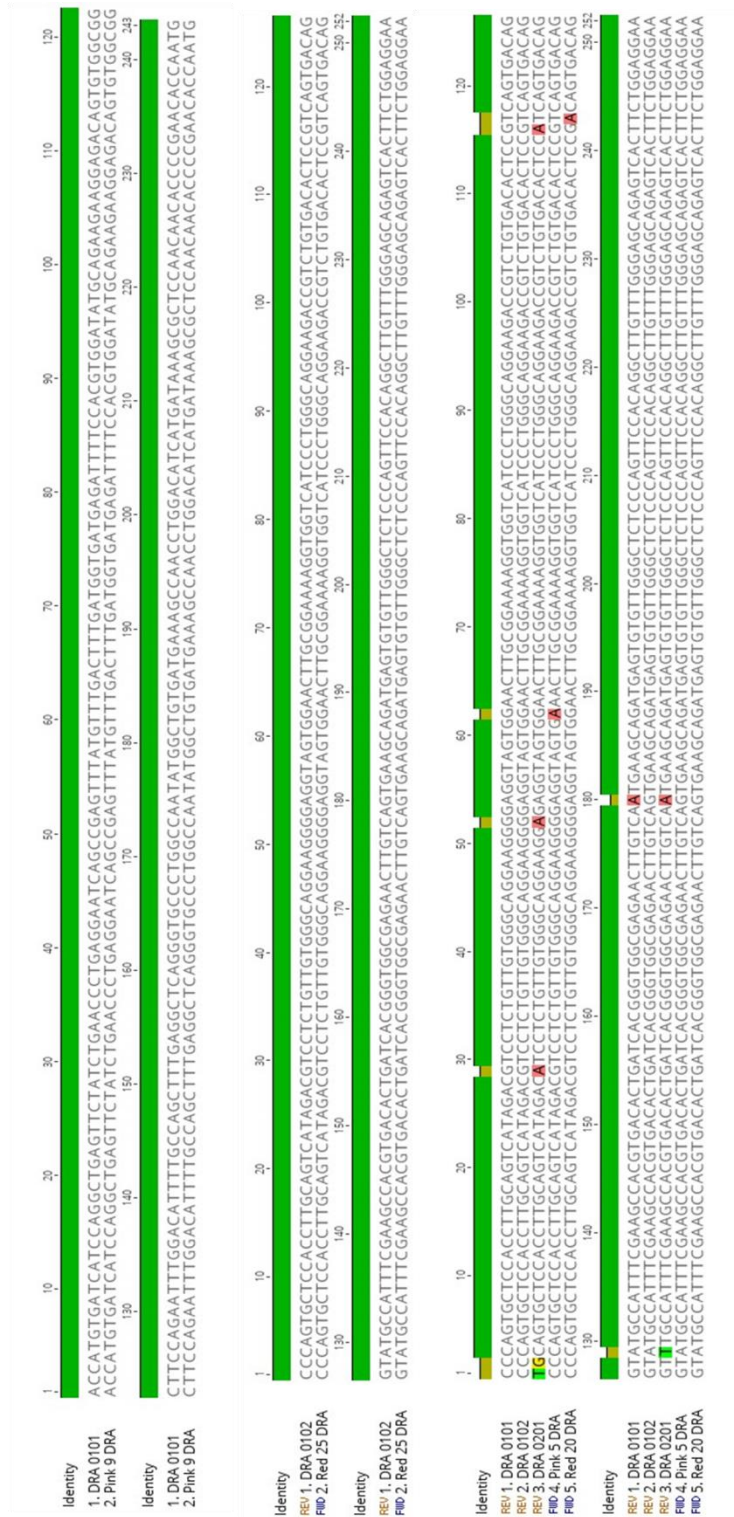


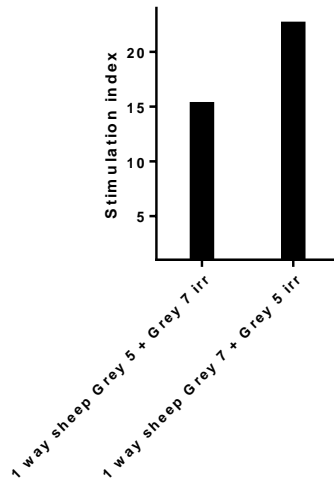
Figure 4.11 Alignments showing sequence data from the sheep in this study being homologous to the DRA 0101 sequence (left) and the DRA 0102 sequence (middle). The right hand alignment shows the sequences from the two sheep which are not homologous for any of the 3 previously described DRA alleles, as well as the positions in which they differ.

Grey 5 crossed with Grey 7

Identity	1	10	20	30	40	50	60	70	80	90	100	
1. Grey 5 DRB1	CC CAGT GCTT GAGA AGAG GCTC GTT CAGAC CCC AGT GCTC CAC CTT G CAGT CAT AGA CGT CCT CTG TTG TGG CAG GAAG GGG AGGT AGT GGA ACTT GCG GAAA AGGT											
2. Grey 7 DRB1	CC CAGT GCTT GAGA AGAG GCTC GTT CAGAC CCC AGT GCTC CAC CTT G CAGT CAT AGA CGT CCT CTG TTG TGG CAG GAAG GGG AGGT AGT GGA ACTT GCG GAAA AGGT											

Identity	140	150	160	170	180	190	200	210	220	230	240	245	
1. Grey 5 DRB1	G C G C T G G A A C C G C T G G C C C G A C G C C T G C A G C G G G C C G C G C C G T G C A G A T T T C T G C G C C A G C A A C T A C G A G T T C T T T G C A G C C T C A C G G T G C A G A G G A A G												
2. Grey 7 DRB1	G C G C T G G A A C C G C T G G C C C G A C G C C T G C A G C G G G C C G C G C C G T G C A G A T T T C T G C G C C A G C A A C T A C G A G T T C T T T G C A G C C T C A C G G T G C A G A G G A A G												

Sheep Grey 5 and Grey 7 MLR



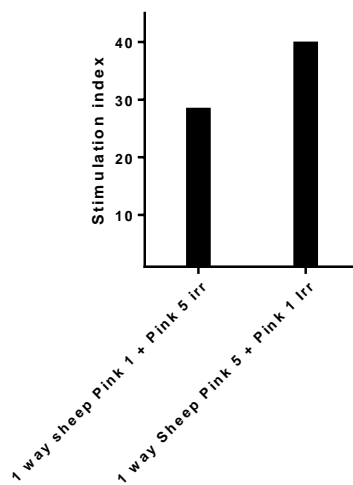
Sheep cross

Pink 1 crossed with Pink 5

Identity	40	50	60	70	80	90	100	110	120	130	
1. Pink 1 DRB1	CC CAGT GCTC CAC CTT G CAGT CAT AGA CGT CCT CTG TTG TGG CAG GAAG GGG AGGT AGT G A A C T T G C G G A A A A G G T G G T C A T C C C T G G G C A G G A A G A C C G T C T G T G										
2. Pink 5 DRB1	CC CAGT GCTC CAC CTT G CAGT CAT AGA CGT CCT CTG TTG TGG CAG GAAG GGG AGGT AGT G A A C T T G C G G A A A A G G T G G T C A T C C C T G G G C A G G A A G A C C G T C T G T G										

Identity	1	10	20	30	40	50	60	70	80	90	100	
1. Pink 1 DRB1	C G A G T G T C A C T T C C C A A C G G C A C G C A G C A G G T G C G C T T C C T G G A C A G G T A C A T C T A C A A C C G C G A G A G C A G G T G C G C T T C G A C A G C C T C G T G G G C G A G T A C C G G G C											
2. Pink 5 DRB1	C G A G T G T C A C T T C C C A A C G G C A C G C A G C A G G T G C G C T T C C T G G A C A G G T A C A T C T A C A A C C G C G A G A G C A G G T G C G C T T C G A C A G C C T C G T G G G C G A G T A C C G G G C											

Sheep Pink 1 and Pink 5 MLR



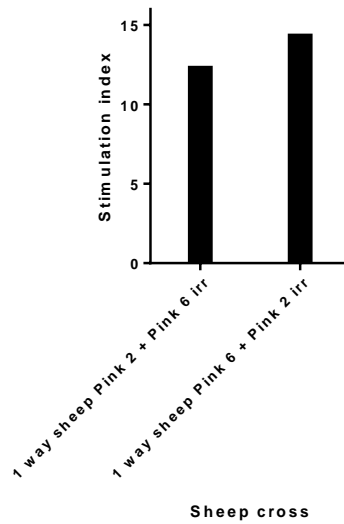
Sheep cross

Pink 2 crossed with Pink 6

Identity	1	10	20	30	40	50	60	70	80	90	100	
1. Pink 2 DRA	CC CAGT GCTT GAGAA GAGGCT CGTT CAGAC CCCAGT GCTCC ACC TTG CAGT CATAGAC GTCCT CTGTT GTGGGC AGGAA GGGGAG GTAGT GGAAC TTGCGG AAAAGGT											
2. Pink 6 DRA	CC CAGT GCTT GAGAA GAGGCT CGTT CAGAC CCCAGT GCTCC ACC TTG CAGT CATAGAC GTCCT CTGTT GTGGGC AGGAA GGGGAG GTAGT GGAAC TTGCGG AAAAGGT											

Identity	140	150	160	170	180	190	200	210	220	230	240	245	
1. Pink 2 DRB1	AGCGCTGGAACCGCTGGCCCGACGCCCTGCAGCGGGCCCGCGCCCGTGCACGATTTCTGCGCCAGCAACTACGAGTTCTTTGCAAGCCTCACGGTGCAAGGAGAG												
2. Pink 6 DRB1	AGCGCTGGAACCGCTGGCCCGACGCCCTGCAGCGGGCCCGCGCCCGTGCACGATTTCTGCGCCAGCAACTACGAGTTCTTTGCAAGCCTCACGGTGCAAGGAGAG												

Sheep Pink 2 and Pink 6 MLR

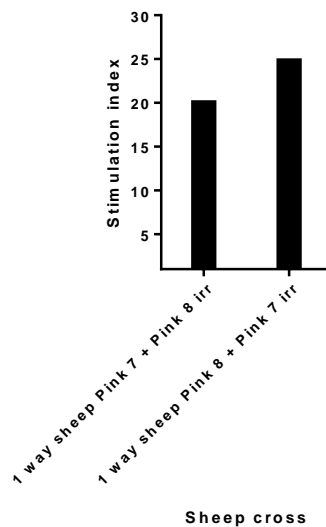


Pink 7 crossed with Pink 8

Identity	70	80	90	100	110	120	130	140	150	160	170	
1. Pink 7 DRA	TTT GATGGT GATGAGATTTTCCACGTGGATATGCAGAAGAAGGAGACAGTGTGGCGGCTTCCAGAATTTGGACATTTTGGCCAGCTTTGAGGCTCAGGGTGCCCTGGCC/											
2. Pink 8 DRA	TTT GATGGT GATGAGATTTTCCACGTGGATATGCAGAAGAAGGAGACAGTGTGGCGGCTTCCAGAATTTGGACATTTTGGCCAGCTTTGAGGCTCAGGGTGCCCTGGCC/											

Identity	1	10	20	30	40	50	60	70	80	90	100	
1. Pink 7 DRB1	CGAGTGTCACTTCTCCAACGGCACGCAGCAGGTGCGTTCCTGGACAGGTACATCTACAACCGGAGAGCAGGTGCGCTTCGACAGCCTCGTGGGCGAGTACCGGGC											
2. Pink 8 DRB1	CGAGTGTCACTTCTCCAACGGCACGCAGCAGGTGCGTTCCTGGACAGGTACATCTACAACCGGAGAGCAGGTGCGCTTCGACAGCCTCGTGGGCGAGTACCGGGC											

Sheep Pink 7 and Pink 8 MLR

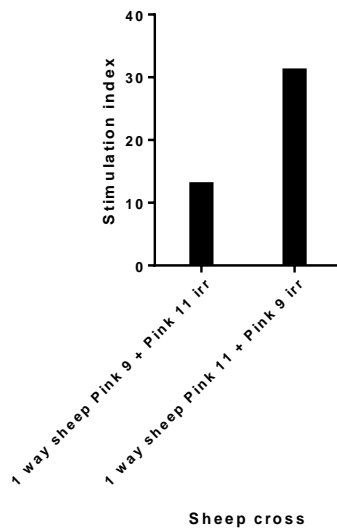


Pink 9 crossed with Pink 11

Identity	60	70	80	90	100	110	120	130	140	150	160	
1. Pink 9 DRA	ATGTTTGACTTTGATGGTGATGAGATTTCCACGTGGATATGCAGAAGAAGGAGACAGTGTGGCGGCTTCCAGAATTTGGACATTTTGCAGCTTTGAGGCTCAGGGT											
2. Pink 11 DRA	ATGTTTGACTTTGATGGTGATGAGATTTCCACGTGGATATGCAGAAGAAGGAGACAGTGTGGCGGCTTCCAGAATTTGGACGTTTTTGCAGCTTTGAGGCTCAGGGT											

Identity	1	10	20	30	40	50	60	70	80	90	100	
1. Pink 9 DRB1	CGAGTGTCACTTCTCCAACGGCACGCAGCAGGTGGCGTTCCTGACAGGTACATACAAACCGCAGGAGCAGGTGCGCTTCGACAGCCTCGTGGGCGAGTACCGGG											
2. Pink 11 DRB1	CGAGTGTCACTTCTCCAACGGCACGCAGCAGGTGGCGTTCCTGACAGGTACATACAAACCGCAGGAGCAGGTGCGCTTCGACAGCCTCGTGGGCGAGTACCGGG											

Sheep Pink 9 and Pink 11 MLR

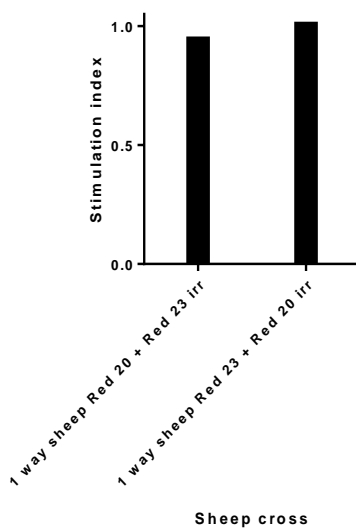


Red 20 crossed with Red 23

Identity	80	90	100	110	120	130	140	150	160	170	18	
1. Red 20 DRA	GCAGGAAGGGAGGTAGTGGAACTTGCAGAAAAGTGGTGCATCCCTGGGCAGGAAGACCGTCTGTGACACTCCGACAGTGACAGGTATGCCATTTTGAAGCCACGTGA											
2. Red 23 DRA	GCAGGAAGGGAGGTAGTGGAACTTGCAGAAAAGTGGTGCATCCCTGGGCAGGAAGACCGTCTGTGACACTCCGACAGTGACAGGTATGCCATTTTGAAGCCACGTGA											

Identity	140	150	160	170	180	190	200	210	220	230	240	245
1. Red 20 DRB1	GCGCTGGAACCGCTGGCCCGACGCCCTGCAGCGGGCCCGCCCGCGTGCACGATTTTCTGGCCAGCAACTACGAGTTCTTTGCAAGCCTCGGGTGCAGAGGAGAG											
2. Red 23 DRB1	GCGCTGGAACCGCTGGCCCGACGCCCTGCAGCGGGCCCGCCCGCGTGCACGATTTTCTGGCCAGCAACTACGAGTTCTTTGCAAGCCTCGGGTGCAGAGGAGAG											

Sheep Red 20 and Red 23 MLR



Red 21 crossed with Red 25

Identity

1. Red 21 DRA
2. Red 25 DRA

140 150 160 170 180 190 200 210 220 230 240 245

1. Red 21 DRB1
2. Red 25 DRB1

Sheep Red 21 and Red 25 MLR

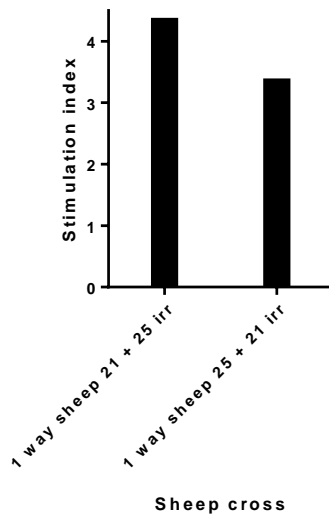


Figure 4.12 OLA genotype sequence alignments of the sheep transplant crosses with the allogeneic base pairs highlighted and the corresponding MLR stimulation indices. The sheep underwent both mixed lymphocyte reaction analysis as well as direct sequence analysis of the ovine DRA and DRB1 genes. Based on the results of these two techniques the animals were assigned tissue mismatched pairs to undergo kidney transplantation.

4.3.4 Pharmacology

Three sheep had a central line inserted into their right hand jugular vein to enable dosing with 5mg/kg cyclosporine and 10mg/kg ketoconazole for 5 days to establish a steady state concentration. Blood was taken over the course of 48 hours starting the 5th day in order to establish an elimination curve for the cyclosporine.

In figure 4.13, blood CyA levels are seen reaching C_{max} at 2 hours, before following 1st order elimination kinetics being quickly cleared giving a half life of 4 hours. Plotting the log of the elimination curve gives an elimination constant of 0.36 h^{-1} . This elimination rate is consistent with what has previously been reported for the pharmacokinetics of cyclosporine and ketoconazole in sheep [452]. Importantly, therapeutic blood levels are maintained out to at least 24 hours. This allowed the sheep to be dosed once a day and maintain the immunosuppression level required to avoid rejection. Although ketoconazole is an antifungal agent it plays an important role in this immunosuppressive regime by acting to inhibit CYP3A4, the enzyme that is primarily responsible for the elimination of cyclosporine. By combining cyclosporine and ketoconazole the level of immunosuppressive drug required to maintain the allograft can be reduced, and by doing so reduce the possibility of adverse events occurring.

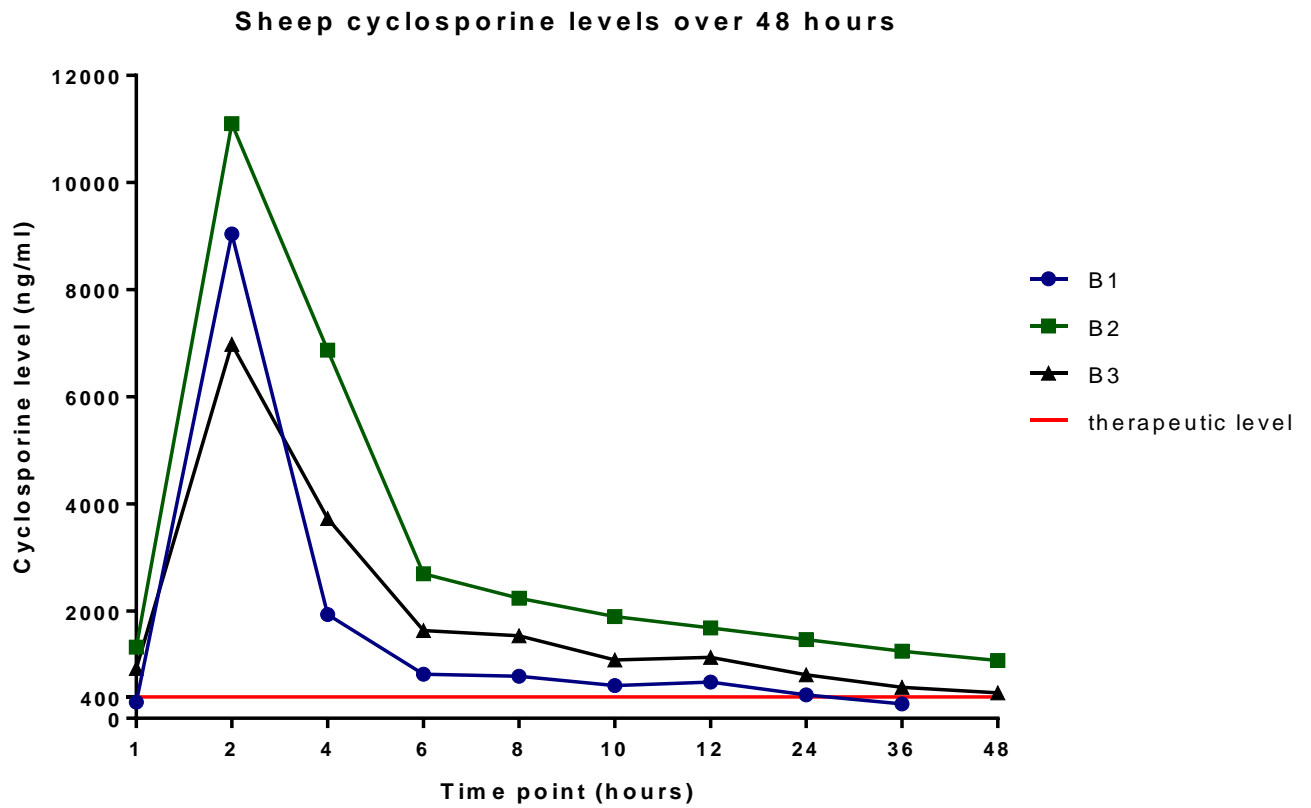


Figure 4.13 Elimination curve of cyclosporine over 48 hours from three sheep. The sheep were given cyclosporine at a dose of 5mg/kg and ketoconazole at 10mg/kg daily for 5days to establish a steady state concentration before having blood samples taken at 1, 2, 4, 6, 8, 10, 12, 24, 36, and 48 hours after the final administration. This blood was then analyzed for cyclosporine levels using a mass spectrophotometer to allow for an elimination curve to be created. Therapeutic levels of cyclosporine are maintained out to 24 hours in all 3 sheep.

4.3.5 Development Of Surgical Protocol

Several refinements were made to the surgical and experimental protocol over the course of the study. These were often due to complications causing the experiment to fail. Below is a detailed list of the changes that were implemented and the complication that necessitated the change.

4.3.5.1 Sheep Grey 7, Occluded Right Hand Jugular Subsequent To Venepuncture

Sheep Grey 7 received a kidney from Grey 5 and underwent a bilateral nephrectomy. Although the transplant itself went well, issues began immediately after. At this point, a central line was being placed into the right hand jugular after the transplant had concluded. The idea behind this was to spare the right hand jugular if there was an issue with the left hand side. However, in this instance a line was unable to be placed into the right hand jugular due to occlusion from a hematoma that had formed when blood was taken not long before hand. An attempted was made to place a line into a vein on the ear and although this allowed some ability to give drugs it seemed to be too late and ineffective resulting in kidney dysfunction and requiring euthanasia. Following this transplant, two changes were made. 1) A month waiting period between any blood procurement and the surgery was instituted. 2) A central line was placed into the right hand jugular before the transplant began. This allowed administration of drugs and fluid as well as sampling blood. The risk of an unusable left hand jugular was deemed to be lower than the possibility of post operative complications associated with placing the CVC.

4.3.5.2 Sheep Pink 3, Occlusion Of The Right Hand Jugular Around The CVC

Resulting In Facial Oedema

Sheep Pink 3 received a left hand kidney from sheep Pink 4; it then underwent a bilateral nephrectomy. The surgery for Pink 3 went well and drugs were given and blood taken successfully through the CVC. However, complications began to arise when the animal developed facial oedema resulting in breathing and eating difficulties (figure 4.14, A).

Additionally, the CVC became difficult to give drugs or fluid through and to collect blood from.

Attempts to treat these complications were made using dexamethasone to control inflammation and mannitol to increase urine output thus decreasing fluid retention. These strategies were unsuccessful. Due to welfare concerns the animal was humanely killed and an autopsy performed to ascertain what had occurred. Upon dissection of the right hand jugular, which the CVC was placed into, it was noted that the vessel had become completely occluded by a clot that had formed around the catheter (Figure 4.14, B, arrow). This, combined with the pressure placed on the left hand jugular by the transplanted kidney resulted in decreased cranial venous return causing the facial oedema and the associated complications. After this transplant the idea of placing a central line through the stump of the renal vein and into the inferior vena cava was developed (figure 4.15). Because of the greater size and blood flow of the vena cava there is an almost non-existent risk of a clot capable of occluding the vessel forming. Although this procedure is more technically challenging than placing a CVC into the jugular the benefits are vast. A CVC is still placed in the right hand jugular during the surgery to allow venous access; however, this is removed once the vena cava line is established. Additionally, if the vena cava line should become unusable it is still possible to place a line in the right hand jugular giving an important level of redundancy.



Figure 4.14 Sheep Pink 3 developed facial oedema (A) resulting in difficulty breathing and eating. After attempts at treatment were unsuccessful, Pink 3 was humanely killed. During the necropsy a clot was discovered around the CVC in the right side jugular vein (B, arrow). This occlusion combined with the pressure on the left hand jugular from the transplanted kidney resulted in decreased venous return, precipitating the facial oedema.

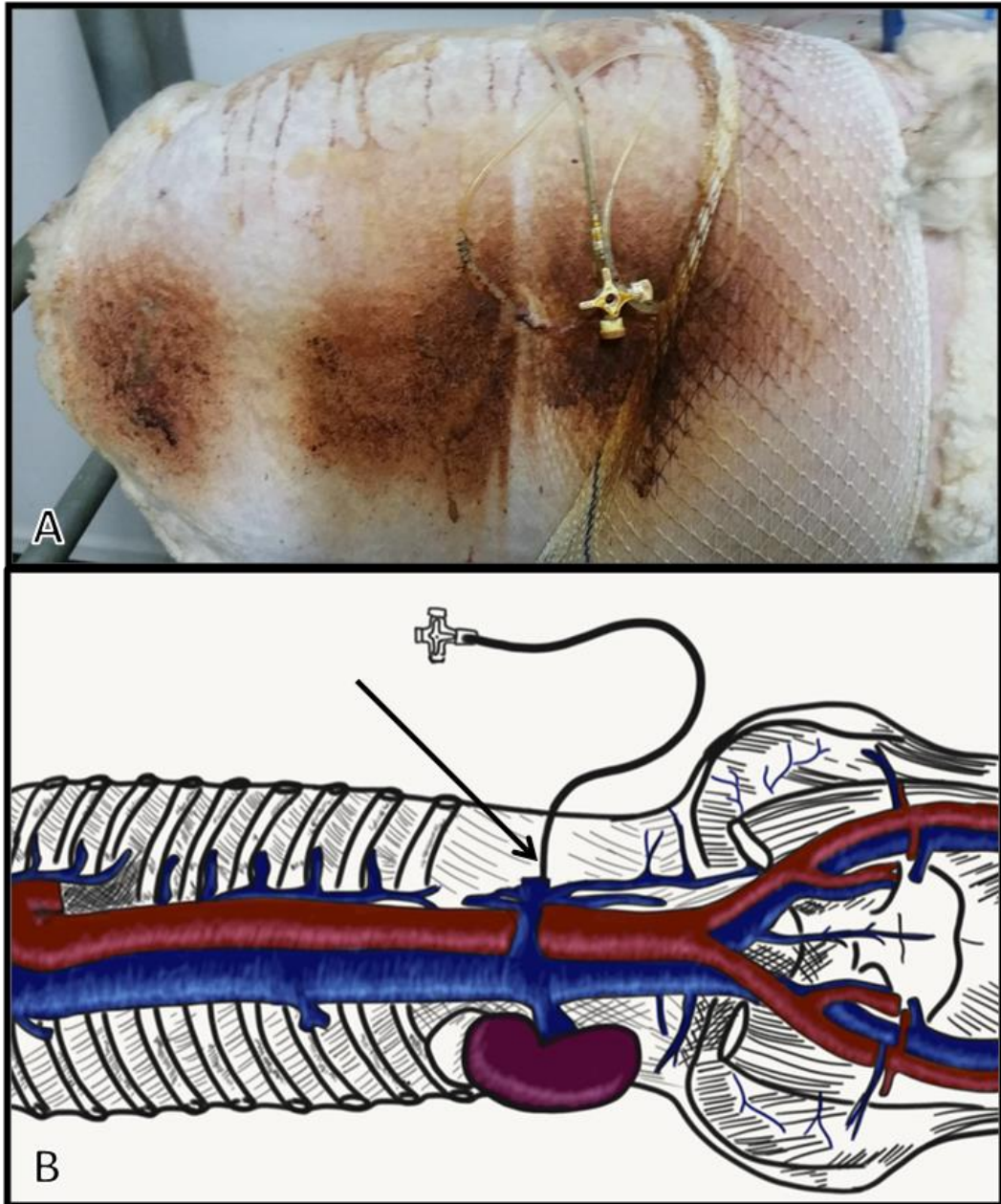


Figure 4.15 Following the events of sheep Pink 3 the idea of placing a central line into the stump of the renal vein that remains post nephrectomy was put into place. A) Shows an in place central line going into the closed nephrectomy wound. B) is an illustration of the central line entering the vasculature through the renal vein stump (arrow) and into the inferior vena cava.

4.3.5.3 Sheep Pink 5, Excessive Swelling Of The Transplant Site, Reopening The Wound

Sheep Pink 5 received a left hand kidney from sheep Pink 1. The surgery itself was successful and no issues arose. However, on day 2, the site of the kidney graft became very swollen. Attempts to control this using dexamethasone had some success in halting and reducing the swelling and so treatment was discontinued. The swelling then returned on day 7 to the point that a high amount of pressure was placed on the wound sutures and the skin flap covering the transplanted kidney. Treatment with dexamethasone was commenced again. However, this was less successful and the continued swelling resulted in a rupture of the wound. The rupture was cleaned and covered with sterile gauze and compression bandages and the dexamethasone was continued with an aim to reduce the swelling to the point that the wound could be sutured again. Although the wound was not able to be closed, the animal suffered no ill effects out to the 14 day time point. Given the continued use of dexamethasone to address the animal's welfare, rejection did not occur in the experimental time frame.

As a result of the complications experienced with Pink 5 all future surgeries were completed by placing a surgical drain into the skin flap to reduce the swelling and prevent rupture of the wound. This additionally allowed us to restrict the use of dexamethasone so as to avoid impacting the rejection of the graft. A reduction in the swelling also resulted in less discomfort for the animals, a significant goal of animal model development.



Figure 4.16 A) The swelling around the graft site in sheep Pink 5 that eventually resulted in the wound rupturing. Attempts to treat the swelling pharmacologically were unsuccessful. B, arrow) demonstrates a surgical drain that has been placed into the skin pocket containing the kidney graft. This drain helps in controlling the swelling surrounding the graft.



Figure 4.17 The kidney graft of sheep Pink 6. The kidney was placed incorrectly meaning that the ureter had to be externalized at the cranial end of the transplant site (arrow). This resulted in the urine flowing over and into the wound causing infection. The infected kidney began to fail, causing the serum creatinine and urea to spike above the humane end point guide lines and as such the animal was euthanized.

4.3.5.4 Sheep Pink 6, Incorrect Kidney Placement

Sheep Pink 6 received a kidney from Pink 2 and it underwent a bilateral nephrectomy. There was a surgical complication in that the kidney was placed in backwards which resulted in the ureter being at the cranial end of the wound (figure 4.17). This caused urine to continually flow back onto the wound and into the skin flap creating an infection of the kidney and stopping its function. The serum creatinine and urea then quickly rose to 600 at which point the animal was humanely killed as per the animal ethics protocol.

Following this surgery, additional care was taken during the preparation of the kidney to be transplanted, additionally, the direction of the urine flow was monitored and the skin flap examined for pooling of fluid.

4.3.5.5 Sheep Pink 8, Infection Of The Kidney Post Biopsy

Sheep Pink 8 underwent a cross over transplant with sheep Pink 7 and both had a bilateral nephrectomy. The surgery was successful for both animals however only Pink 7 made it out to the full term of the experiment. Sheep Pink 8 had an issue with the skin pocket not fully adhering to the kidney capsule. This allowed for the accumulation of microorganisms under the skin flap and once the kidney capsule was pierced by a biopsy needle the kidney became infected, resulting in its failure. This then caused a rapid rise of creatinine and urea and necessitated euthanasia. This surgery changed if biopsies would be performed, if the skin flap had not adhered to the kidney capsule then biopsies would not be carried out and although this meant that some data would be missed it was balanced out by having the animals complete the experiment and the other measurements that were able to be collected.

4.2.5.6 Sheep Pink 14, Post Transplant Wedge Biopsy Causing Haemorrhage

Sheep Pink 14 underwent an autotransplant before being given 2×10^6 cells/ kg of SPIO labelled MSCs. With this animal it was decided that being able to have a biopsy from day one would be a useful time point, hopefully showing the impact of ischemia reperfusion injury on the kidney and the resulting recovery. However, once the wedge biopsy was performed the kidney had difficulty clotting. Eventually this came under control and the surgeon was able to close. But as the animal was being moved the wedge biopsy site opened again causing unseen haemorrhaging. The animal never fully recovered and eventually died from exsanguination. This surgery concluded attempts at performing a wedge biopsy.

4.4 Discussion:

The purpose of this chapter is to show the difficulties associated with large animal work and the changes that were made to the model to address these challenges. After the adjustments detailed in this chapter were carried out, there was a greater success rate of animals making it to the end point of experiments (40% pre-modifications vs. 71% post modifications). One of the end points used in the allotransplant model was the examination of rejection, which was monitored by serum creatinine and urea. In these experiments the sheep would receive a tissue mismatched kidney and undergo a bilateral nephrectomy. They would then received CyA and Ketoconazole for the first 7 days before having this withdrawn to allow rejection to occur, the maximum time period for these experiments was 14 days. However, if the animal's creatinine levels reached 600 and stayed there for 2 days, it would be euthanized; this was still deemed a completed experiment as long as the reduction in kidney function was due to rejection. This experiment was able to be performed repeatedly while controlling rejection with the immunosuppressant drugs and having rejection occur, when required, by the withdrawal of the immunosuppression. This was achieved by first

performing pharmacokinetics to determine the elimination rate of CyA from sheep, allowing a dose rate that maintained therapeutic immunosuppression levels while minimizing potential adverse effects. In addition to this, the sheep were tissue typed using both mixed lymphocyte reactions and direct sequencing of the DRA and DRB1 regions of the ovine major histocompatibility complex. Using these techniques allowed for tissue mismatching, ensuring that the sheep would reject the transplanted kidney upon withdrawal of the immunosuppressive regime. By withdrawing immunosuppression it was possible to examine acute rejection episodes, providing a baseline for possible future interventions. Sequencing at the DRA and DRB1 regions was useful for predicting rejection but, because only two of the many OLA genes were viable targets for sequencing, this method was not able to predict tolerance.

In addition to the allograft model, the autograft variant was also utilized, wherein a sheep would receive its own kidney. This protocol is ideal for examining the ischemic reperfusion injury associated with transplantation without the confounding influences of immunoreactions and immunosuppressive drugs. As this protocol requires the kidney to be removed, placed on ice, then transplanted it more closely mimics the IRI found in human kidney transplantation than what would be created in a warm ischemic model such as that used by Yoon *et al* (2015) [436] where they leave the kidney *in situ* and clamp the blood vessels. The autograft model was used when examining the migration of MSCs in response to IRI, as detailed in chapter 5.

Several changes were made to the standard operating procedures for the transplantation model, of particular importance were the alterations made in order to ensure the well being of the animals. Post operative swelling around the transplantation site caused serious discomfort in some animals and in sheep Pink 5 resulted in the wound rupturing. To address this, a surgical drain was placed into the transplant skin flap, this was very effective at controlling

the postoperative swelling, resulting in less discomfort for the sheep as signified by a reduction in teeth grinding and drooping ears. Another significant animal welfare issue was caused by the placement of a CVC line into the right hand jugular vein. In sheep Pink 3 the CVC line placement allowed a clot to obstruct the jugular vein, causing decreased venous return, resulting in facial oedema that impacted the animals breathing and eating. To avoid this, a central line was placed into the inferior vena cava via the stump of the renal vein that resulted from the nephrectomy. Although both of these alterations were technically difficult and added complexity to an already complicated surgery, they were necessary as the welfare of the animals is always a priority in animal experimentation. Finding ways to minimized harm through refinement, reduce the number of animals used, and creating alternatives to replace animal models is crucial to the ethical use of large animals for scientific research.

The ovine heterotopic kidney transplant model occupies a niche in translational medicine that other animal models do not. Although there are large animal models of IRI the vast majority use a normothermic, *in situ*, vascular clamping method [336, 337, 425, 427, 429, 431-433, 435-437, 440-442]. This technique is excellent for studying warm ischemia and the subsequent reperfusion as it is able to be performed laparoscopically and is less technically challenging than performing a nephrectomy and transplantation. However, vascular clamping models lack the ability to replicate the conditions of a human kidney transplant and so are not directly translatable to the clinic. Hypothermic IRI models do exist that involve a nephrectomy, cold preservation, and autotransplantation. Many of these models transplant the kidney back into the abdomen [335, 422, 424, 430]. This closely replicates the procedure of a human kidney transplant, in which the donated kidney is often placed in the iliac fossa and connected to the external iliac artery and vein. This procedure can be complicated when performed in a quadruped due to the physical hindrance caused by the hind legs.

Additionally, the abdominal placement of the kidney makes imaging and biopsies difficult

due to the obstructing tissue. The heterotopic kidney transplant model described in this thesis addresses these impairments by placing the kidney in the neck and using the carotid artery and jugular vein for blood flow. This provides greater resolution when imaging and access when performing biopsies as the only obstruction is the skin flap. Furthermore, the collection of urine is simplified by the ureter being externalised through the skin and catheterized.

The advantages of the heterotopic placement of the transplanted kidney also apply to the allotransplant variation of the model, as other large animal kidney allotransplant models utilize the iliac fossa, orthotopic placement favoured in hypothermic IRI models [444-446]. This is in addition to the ability to control rejection that is afforded by the tissue mismatching and the CyA pharmacokinetics developed for this model.

In conclusion, through encountering complications and creating refinements to address them, a model of kidney transplantation that is robust, reproducible, able to undergo controlled rejection, and can be tailored to examine several aspects of transplantation has been designed. Furthermore, several redundancies have been introduced to the transplant procedure and aftercare to address common problems. Given the size of the sheep, it is possible to continually take samples of both blood and kidney biopsies without impacting the well-being of the animal. The size of the animals also allows for clinically relevant monitoring such as MRI to be used. These factors combined with the docile nature of sheep makes this model very well suited for studying transplantation.

Chapter 5:

MSC Tracking in Autotransplantation

5.1 Introduction:

The application of MSCs for solid organ transplantation is still in its infancy as a potential therapeutic and as such there are many questions that are yet to be answered. One of the important questions is where do the MSCs go when they are administered? Given their role in repair and immunosuppression it is possible that they may track to areas of inflammation and immune response, however any conjecture about this would be speculation. Additionally is it unclear if the route of administration of the MSCs will have an impact on how the MSCs migrate and what their ultimate fate is.

5.1.1 Tracking MSCs

There have been several studies looking at the tracking and migration of MSCs in a variety of animals and conditions. Studies looking at the tracking of MSCs in rodents are numerous and of particular interest to this work are the studies that look at their migration in renal injury models. Sun *et al.*, (2008) [453], injected iron labelled MSCs into control rats and rats with acute renal failure (ARF) and then scanned them using an MRI out to 8 days. In both control and ARF rats they found a decrease in signal intensity in the renal cortex and upon histology and Prussian blue staining found the cells that had localized to the kidney were largely bound in the glomerular capillaries, corresponding with what was observed in the MRI scans [453]. Rats that had unlabelled MSCs injected did not see a similar decrease in signal intensity demonstrating that MRI and iron labelling is a viable method for tracking MSCs. This finding was backed up by Jung *et al.*, (2009) [454], who induced ischemia in the

left kidney and then injected iron labelled MSCs into both kidneys. They then performed T2* scans at 2, 15, 30, and 72 hours post injection and compared these to pre-injection scans. They found there was significant signal variation in both kidneys up until 2 hours post administration and that this signal intensity correlated highly with the number of iron labelled cells detected via Prussian blue histology staining [454]. Although they noticed a difference in signal intensity between the normal and ischemic cortex early on this was resolved by the 15 hour mark which is the time point at which most of the signal had been lost. Due to the rapid decrease in signal and the small number of retained cells they hypothesised that the increased signal was due to mechanical trapping of the cells and not local trophic effects, with the damaged glomerular tufts having a greater ability to trap MSCs.

Other methods of tracking MSCs have also been used. Assis *et al.*, (2010) [408] used technetium-99m (Tc-99m) to radio label cells and track their migration in a model of myocardial infarction. Because Tc-99m has a short half life they also used 4'-6'-diamidino-2-phenylindole (DAPI) staining of cells to examine migration ex-vivo. Tc-99m labelled cells were injected systemically through the tail vein 7 days after myocardial infarction was induced. Using a gamma camera they observed a wide distribution of MSCs with a majority of them accumulating in the lungs with a small amount moving to the heart, kidneys, spleen, and bladder [408]. Of note was that infarcted hearts had a significantly increased recruitment of MSCs compared to control, and after 7 days DAPI labelled cells were only detected in the infarcted areas of the heart.

Hindle *et al.*, (2016) [455] used MSCs transfected with green fluorescent protein expressing lentivirus to examine the retention of MSCs in an ovine model of cartilage defects. The transfected MSCs were implanted into femoral condyle defects with hydrogel and collagen membranes and left for 4 weeks before the condyle was removed and examined under laser scanning microscopy. They demonstrated that the MSCs implanted using hydrogel were still

present at 4 weeks and that the condyle defect had been repaired showing promise for the use of MSCs in orthopaedics [455].

The Hindle study also raised the important question of how long MSCs remain in a certain location or how long are they able to be detected. In looking to address this question, Weir *et al.*, (2008) [413] looked at retention of MSCs labelled with either CFSE or CM-DIL after either direct subcutaneous injection or after being bound to a silicon matrix which was then implanted subcutaneously. The results from this study identified CM-DIL as a superior dye to track MSCs than CFSE as CFSE showed rapid signal loss over 8 days *in vitro*, whereas CM-DIL was able to be detected out to five weeks [413]. *In vivo* they were able to detect fluorescent labelled MSC out to six weeks with both the direct injection and the biomaterial scaffold. Although this showed that dyes were able to stain MSCs without having a negative impact and that CM-DIL could allow for MSCs to be tracked for extended periods of time, the locations in which they were tracking the cells were easily accessible and relatively shallow. These dyes would be unlikely to be useful for *in vivo* tracking of MSCs in large animal models of deep tissue or internal organ disorders.

Each of these approaches to labelling and tracking MSCs has its positives and its negatives and selecting the best way to track MSCs for a particular study is an important consideration. For the purposes of this study, SPIOs presented the best possibility for tracking of MSCs. As shown by Burk *et al.*, (2016) [456], iron labelled MSCs are able to be tracked by both MRI and histology long term. In their study they injected iron labelled MSCs into horse tendon lesions and followed the distribution for up to 24 weeks, being able to identify the MSCs by both MRI and histology [456]. Iron labels have also been shown to be useful when looking at the distribution of MSCs in the internal organs. Of particular relevance was the study carried out by Yoo *et al.*, (2011) [457] in which they injected iron labelled MSCs into one of the kidneys of two healthy dogs. They reported a strong MRI hypointensity of the renal cortex of

the injected kidney one day post administration [457]. Although they only used two dogs and the signal was lost by day 8 this experiment still showed the ability of SPIO to be detected via MRI in deep tissues and internal organs. For this study the a SPIO nanoparticle was chosen to label the MSCs. SPIO, as demonstrated in chapter 3, is able to be taken up into MSCs without having any impact on their function or phenotype. Additionally, SPIOs are a clinically safe compound having originally found use as an MRI contrast agent for liver lesions [458]. And finally, being able to use both an MRI and histology to detect the presence of SPIO labelled cells greatly increased the likelihood that MSCs would be detected.

5.1.2 The Ovine Model Of Kidney Heterotopic Autotransplantation

As mentioned above, studies of MSC tracking in small animals such as mice, has provided valuable information on the migration of MSCs. However, given their small size it is difficult to translate these results directly to what could be expected in humans [459].

This size disparity is one of the primary reasons that sheep are a more suitable pre-clinical animal model than many rodents. Other advantages to using sheep as an animal model are that they are easy to handle and docile when housed with an accompanying sheep, the cannulation of blood vessels is uncomplicated and easy to maintain with minimal chance of adverse effects, and dosage of pharmaceutical agents is likewise relatively simple. As a surgical model, and in particular as a model of kidney transplantation, techniques that are performed on humans are able to be utilized [438, 451]. The size of the blood vessels allows anastomosis to be performed without microsurgical techniques, and also allows for straightforward nephrectomy and kidney retrieval [438]. The animals are able to tolerate general anaesthesia well when adequate precautions are taken such as fasting [460, 461], this is important for the present study as it requires repeated anaesthesia of the animals over a period of five days. Additionally, the size and structure of the kidneys are such that changes are able to be identified using an MRI. This study made use of the autotransplant variation of

the model, allowing for the interaction between ischemia reperfusion injury and MSC homing to be studied in the absence of the immunological considerations of the allotransplant variant.

5.1.3 Detecting The Presence Of Iron Label Using Pixel Intensity

The purpose of labelling MSCs with SPIO is so that they become visible on MRI images. To understand this application, an understanding of how MRIs work and what SPIO is, is required. Nuclear magnetic resonance is concerned with the behaviour of atoms subjected to a magnetic field. In particular it refers to the ability of nuclei to absorb and emit electro-magnetic radiation [462, 463]. Nuclei can either have a zero or non-zero magnetic moment, this depends on the composition and spin of the nucleus, with even numbered nuclei having zero spin and odd numbered nuclei having non-zero spin and thus a non-zero magnetic moment [464]. When a nucleus with a non-zero magnetic moment is placed into a magnetic field it will either align parallel or anti-parallel to the direction of the magnetic field. For example, hydrogen has a spin of $\frac{1}{2}$, when this is measured in a magnetic field two spin states are observed, $\frac{1}{2}$ and $-\frac{1}{2}$ with one of these corresponding to the parallel state and one to the anti-parallel state [465]. Importantly, one of these states will have a lower energy and the nuclei will favour this. However, this can be disturbed by changes in thermal energy. In practice, this means that when an object consisting of many of these nuclei is placed into a magnetic field the proportion of nuclei that fall parallel and anti-parallel is roughly even with only a small number of nuclei not being cancelled out by a corresponding nuclei in the opposite state [466]. Even though only a fraction of total nuclei are not cancelled out it is enough to generate an image on the macro scale. Next, a radio frequency pulse is applied to the object which results in the unmatched protons spinning in a different direction. When this radio frequency is removed the protons begin to relax back to their initial states in the magnetic field. It is this relaxation that is measured [467].

In MRIs it is the relaxation of hydrogen that is measured as hydrogen is abundant in water and fat, which comprise a large percent of mammalian bodies [465]. The relaxation of the hydrogen nuclei can be influenced by the compounds and the makeup of the surrounding tissue and these differences allow for the creation of detailed images of soft tissue structures [463]. SPIOs are compounds that have a superparamagnetic iron oxide core surrounded by a carboxydextran coating [468]. SPIOs are able to impact the relaxation time of nuclei by creating microscopic magnetic field in-homogeneity [469]. This has a particular impact on the relaxation of nuclei in the transverse plane; this decay is referred to as the transverse relaxation time or T2 [469]. By this mechanism, SPIOs are able to shorten the relaxation time of nuclei and, when measured with a T2 specific program, this results in a darkening of the images in the areas that the iron label has accumulated.

5.1.4 Analysis Of MRI Images With ImageJ

By using SPIO to label the cells it is then possible to identify areas of darkening which correspond with the presence of the iron label. However, given that the cells are being labelled before administration the iron label will not necessarily accumulate in great enough amounts to be detected by the naked eye as it normally would if injected alone. In order to address this, the images need to be analyzed by other means. As the darkening of the MRI images by the SPIO is actually a reduction in pixel intensity, image analysis software can be used to give accurate numbers that will represent the presence or absence of SPIO. Using Image J, it is possible to select areas of interest and calculate the average pixel intensity which can then be compared to other images, with a reduction in the pixel intensity corresponding to a positive detection of SPIO.

5.1.5 Chapter Aims:

The aims of this study were to elucidate the migration and distribution pattern of MSCs in a sheep model of kidney autotransplantation. This study administered the MSCs in a systemic fashion and the results were compared to unpublished data from previous work carried out by Dr Dyan Auclair in which she administered the cells directly into the transplanted kidney.

5.2 Materials and methods:

5.2.1 Preparation Of MSCs

Ovine MSCs were isolated and expanded as detail in chapter 2 sections 2.19 (MSC isolation) and 2.11 (MSC expansion). Briefly, sheep were anaesthetised and had the wool above their iliac crest shaven. An osteobell “T” needle was then inserted into the iliac crest, guided by a portable x-ray, until it reached the cancellous bone. The centre of the needle was removed, a syringe attached and 40mls worth of bone marrow aspirate collected into a heparinized tube. This bone marrow aspirate underwent PBS dilution and a ficoll density gradient was used to separate the mononuclear cells. The mononuclear cell layer was collected and washed with PBS before being resuspended in complete cell growth media, placed into T175 cell culture flasks, and incubated for 10 days so the MSCs would adhere to the plastic.

Once the cells had adhered the media was changed to wash off non-adherent cells and they were allowed to grow for 2-3 days before being split. The flasks were treated with trypsin for 5 minutes at 37°C then 5ml of 5%FBS in PBS was added to stop the reaction. The detached cells were collected in a 50ml tube, topped up with PBS, and then spun at 250xg for 5 minutes at 4°C. The supernatant was poured off, the pellet was resuspended 5%FBS in PBS,

and cell count was performed. The tubes were topped up with PBS and spun once more at 250xg for 5 minutes at 4°C. The supernatant was poured off and the pellets resuspended in complete media. Expansion involved plating the cells at 10,000 cells/cm² in α MEM with 10% FBS. Once the cells reached 80% confluence they were split again. The cells were maintained like this up until the day before the surgery.

5.2.2 Labelling MSCs With SPIO

18 hours before the surgery was to commence the media was changed to the SPIO staining media which contains 25% FBS, 960µg/ml SPIO and 5µg/ml protamine sulphate to allow the cells to become iron labelled. Labelling was confirmed via light microscopy looking for brown depositions in the cells.

5.2.3 Surgery

The surgery was carried out as previously described in chapter 4. The left hand kidney was removed and flushed with cold preservation solution and placed on ice. The left hand side of the neck was then prepared, exposing the carotid artery and jugular vein and creating a pocket under the skin.

The kidney then underwent end to end anastomosis with the renal artery and the carotid artery and end to side anastomosis with the renal vein and jugular vein. The ureter was externalized through the skin and catheterized with Silastic tubing.

The right hand kidney remained in place to ensure the health of the sheep should the transplanted kidney fail and a central line was placed into the inferior vena cava via the stub of the left renal vein. Following MRI scans the animals were recovered and received pain relief in the form of I.M. Buprenorphine (0.01mg./kg) for the first three days and antibiotics in the form of I.V. cefazolin (500mg) for the duration of the experiment.

5.2.4 Administration Of MSCs

On the day of the surgery the cells were harvested as the surgery was being carried out and re-suspended in saline. This was timed to try and reduce the time the cells spent in saline.

Once the transplant was complete the sheep were moved to the MRI room and ventilated to maintain anaesthesia using isoflurane. The sheep were then scanned in a left lateral decubitus position in a 1.5T Siemens Sonata (Siemens AG, Munich, Germany) Magnetic Resonance Image (MRI) machine for pre-administration and anatomical scans. The cells were then administered systemically via a central line placed into the inferior vena cava via the stump of the renal vein.

5.2.5 MRI Tracking

The scan sequences were designed and interpreted by a dedicated MRI technician. The transplanted kidney scans (3 mm slice thickness) were carried out before the administration of MSCs, immediately post administration, 15 minutes post, and 30 minutes post. In addition to the kidney scans, the lungs and liver (5 mm slice thickness) were scanned pre and post injection. Repeated anatomical scans were taken of structures of interest to establish the scan areas followed by a T2* sequence protocol. Upon euthanasia of the sheep, the organs of interest were removed, placed in water, and underwent *ex vivo* scanning. The images generated from the scans were then exported to imageJ (<https://imagej.net>) and the average pixel intensity of the area of the transplanted kidney calculated across the z stack. The results from the immediate, 15 minute, and 30 minutes post-administration time points were then expressed as a percentage of the pre-administration average

5.2.6 Kidney Biopsies

Where possible, biopsies were taken of the transplanted kidney. First the sheep was restrained and the skin over the kidney was numbed by injecting 1ml of 2% lignocaine (Pfizer, cat no. EK04). A small incision was made with a 15 blade and then, using a punch biopsy gun, a core sample was collected and placed into 10% buffered formalin. Pressure was placed on the biopsy site with sterile gauze and urine flow observed to ensure kidney function was not negatively impacted. The area was sprayed with betadine and a dressing placed over it. The preserved biopsy cores were then embedded in paraffin wax prior to sectioning and staining with hematoxylin and eosin (H&E) and Prussian blue by the SA pathology histology service.

Biopsies were not taken if the skin had not fully adhered to the kidney capsule as this presented too great a risk of both undetected bleeding and the possibility of the kidney becoming infected.

5.2.7 Histology

On day 5 the animal was humanely euthanized using 20 of 325mg/ml pentobarbitone. Tissue samples were then taken from organs of interest: The transplanted kidney, the native right hand kidney, lungs, liver, and spleen. These samples were collected into 10% formalin until they were processed. The samples were mounted and embedded in paraffin wax by the Royal Adelaide hospital histology service. Sections were then cut, with one being stained with H&E, while the rest were set aside for Prussian blue staining.

5.2.8 Prussian Blue Staining

Unstained sections of each of the organs underwent Prussian blue staining using the Biopal Prussian blue staining kit.

The sections were deparaffinised using sequential ethanol and xylene baths in the following order. Xylene, 5 minutes repeated 3 times. 100% ethanol for 5 minutes repeated 3 times. 90% ethanol for 5 minutes. 70% ethanol for 5 minutes. 50% ethanol for 5 minutes and finally washed in PBS for 5 minutes.

Once the slides were deparaffinised, Solution A and Solution B from the Biopal Prussian Blue staining kit were mixed in equal volumes just prior to use. The working solution was then placed on the slides and left for 10 minutes in the dark at room temperature. The solution was gently rinsed off with PBS and a cover slide placed on top of the section.

The slides were examined under a confocal microscope to look for areas of blue, indicating the presence of iron, and thus the iron labelled MSCs. Once a section was confirmed to contain iron labelled MSCs, the tissue block was sent to the SA pathology histology lab to have an adjacent section cut and stained with Pearl's Prussian blue and counterstained with nuclear red to allow for better visualization of the tissue structures and location of the MSCs.

In order to identify and image MSCs in the sections a Nanozoomer S210 digital slide scanner (Hamamatsu photonics, 325-6, Sunayama-cho, [Naka-ku](#), [Hamamatsu City](#), [Shizuoka](#), 430-8587, Japan) was used and the resulting images analyzed in NDPview.

5.2.9 Quantification Of MSCs

Comparisons of the number of MSCs located in the transplanted kidney and native kidney were enumerated using NDPview. As the size and shape of the tissue slides is not regular, direct counts are not possible. To overcome this, three randomly placed 20mm² quadrants were selected on each slide and the number of MSCs within these counted. The Number of MSCs was average across all three sheep and expressed as cm².

5.3 Results:

Four sheep underwent heterotopic kidney autografts with the right kidney remaining in place. MRI scans of relevant areas were taken, followed by systemic injection of iron labelled cells, then another round of MRI scans. The average cold perfusion time of the kidneys was 67 minutes and the average time that the sheep were under general anaesthesia was 7 hours. One sheep was removed from the study on day 2 due to surgical complications. The rest of the sheep were maintained until day 5.

The images taken of the transplanted kidney did not show any notable changes upon visual inspection and so underwent Image J analysis. For comparison, several images of MRIs from work performed by Dr Dyan Auclair were used. Her sheep had SPIO labelled cells injected directly into the kidney graft just prior to completion of the anastomosis. In these images the deposition of the labelled cells is clearly visible and was subsequently confirmed by Prussian blue staining.

5.3.1 Sheep Pink B14

Sheep Pink 14 underwent a bone marrow biopsy and had MSCs isolated and expanded a month prior to surgery. It underwent an autotransplantation and received 2x10⁶ cells/kg of iron labelled MSCs into the inferior vena cava via a central line.

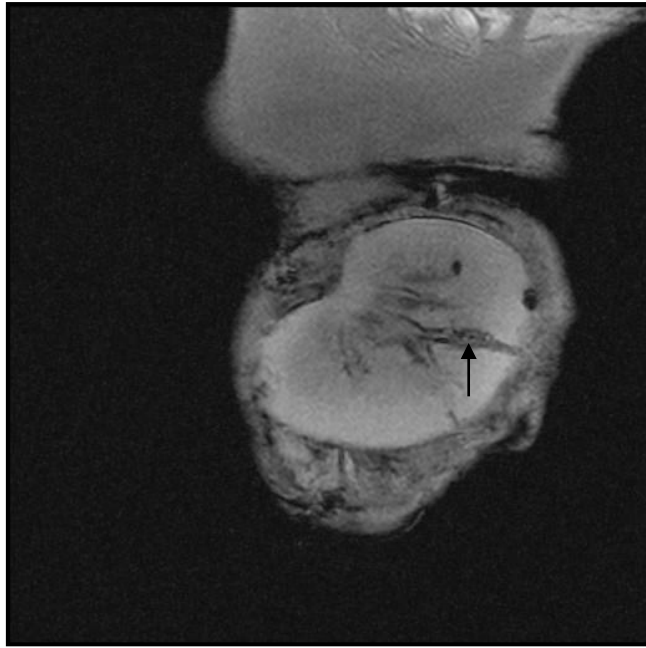


Figure 5.1 T2* MRI section of the heterotopic kidney allograft of sheep Pink 14 on day 2. A bleed resulting from a wedge biopsy is evident (arrow).

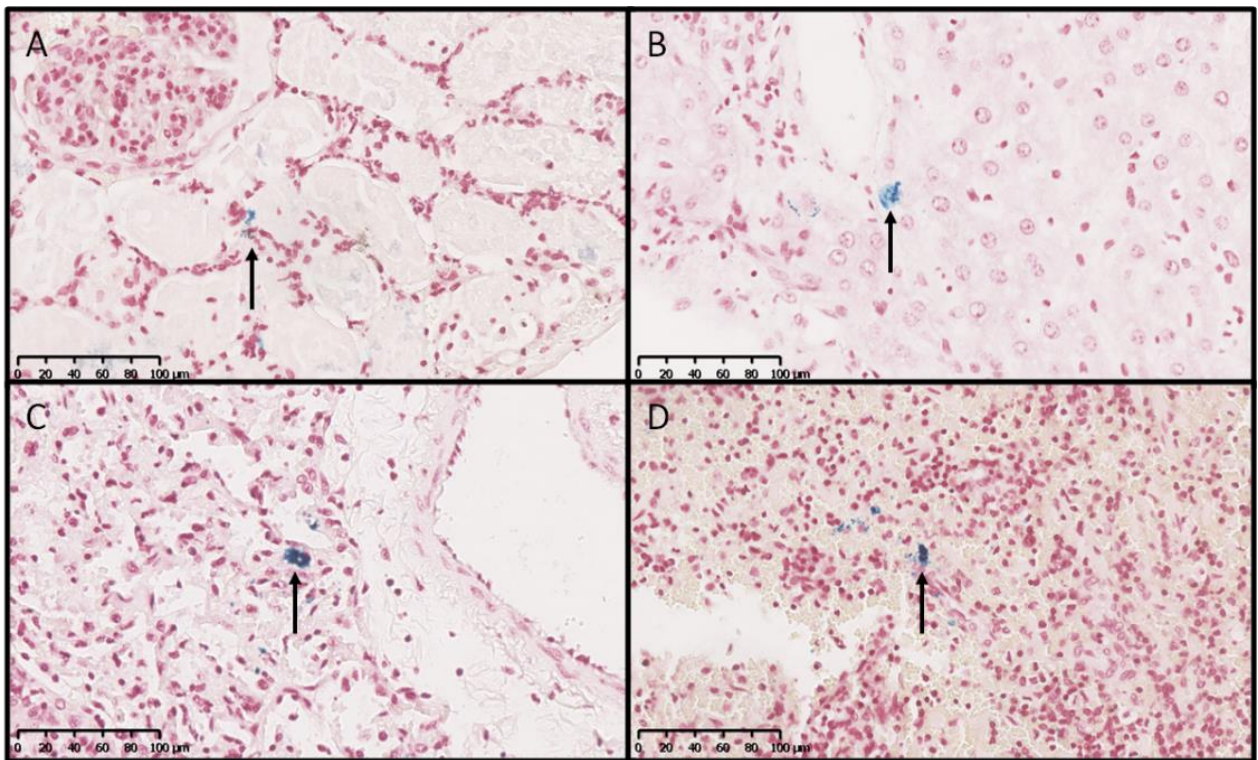


Figure 5.2 Sections from the transplanted kidney (A), liver (B), lung (C), and spleen (D) from sheep Pink 14 were stained with Perl's Prussian blue and counter stained with nuclear red to identify the iron labelled MSCs. All tissues of interest were positive for MSCs (Arrows).

Prior to closing the transplantation wound and administration of the MSCs, a wedge biopsy was performed to act as a control for histological analysis. However, this wedge biopsy did not clot correctly and resulted in an internal bleed after the skin flap had been closed. The bleed can be seen in figure 5.1.

Despite several attempts the bleeding could not be controlled and the animal was euthanized on day two as per ethical requirements. Due to the bleed, Pink 14's results are not used in the pixel intensity analysis as it is unknown what impact the haemorrhaging would have on the average pixel intensity.

Histological analysis of Pink 14 using Prussian blue is still included as it provides a look at the migration pattern of the MSCs one day after administration.

From this histology a wide distribution of cells throughout the animal's organs is seen to have occurred as early as day 2. However, there is no obvious pattern or preferential localization.

5.3.2 Sheep Red 15

Sheep Red 15 had an autotransplant and systemic administration of MSCs. It underwent MRI scans on day 1, 4, and 5. It was euthanized on day 5 and *ex vivo* images were taken of various organs of interest before the tissue was processed for histological analysis.

During the course of this experiment several minor clinical issues were encountered including, a urinary flow obstruction that was overcome by flushing the urinary catheter, and the skin flap covering the transplanted kidney did not fully adhere to the kidney capsule. This prevented planned punch biopsies from being collected due to the high risk of bleeding and infection.

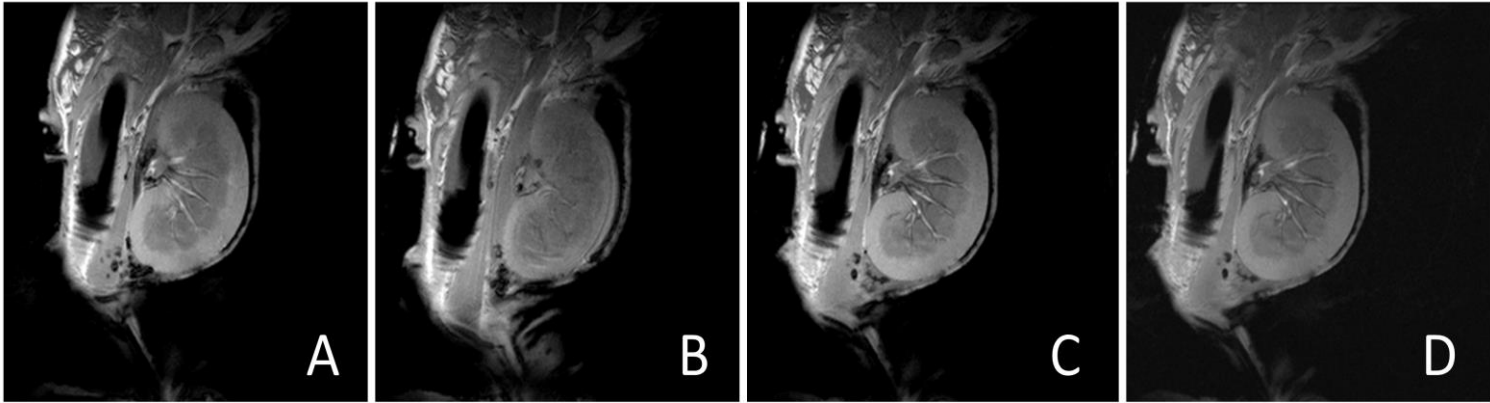


Figure 5.3 T2* MRI sections of the heterotopic kidney allograft of sheep Red 15. A) Pre-MSC administration. B) Immediately Post MSC Administration. C) 15 minutes post MSC administration. D) 30 minutes post MSC Administration.

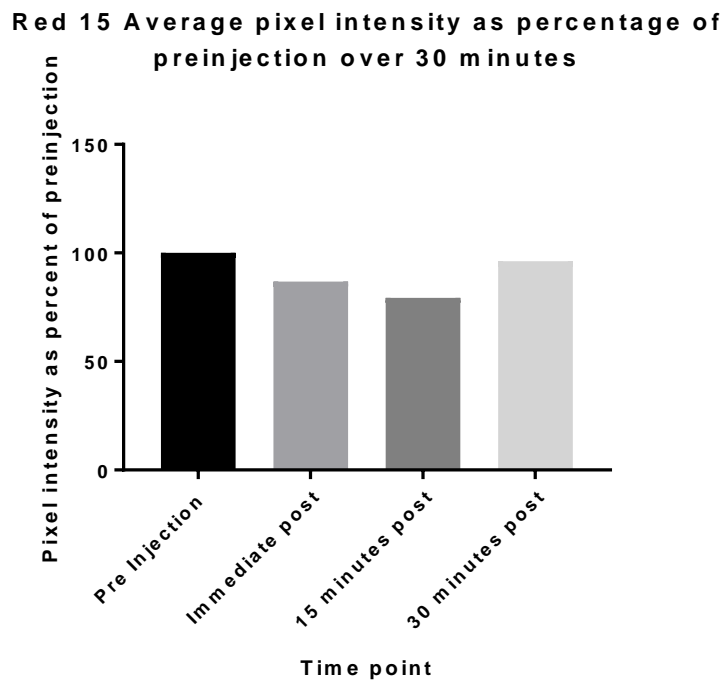


Figure 5.4 Average pixel intensity of the MRI cross sections of the transplanted kidney of Red 15 over 30 minutes. The pixel intensity was determined by analysing each section of the MRI Z stack at each time point in imageJ. A reduction in signal intensity is seen immediately post administration and 15 minutes post administration of SPIO-MS.

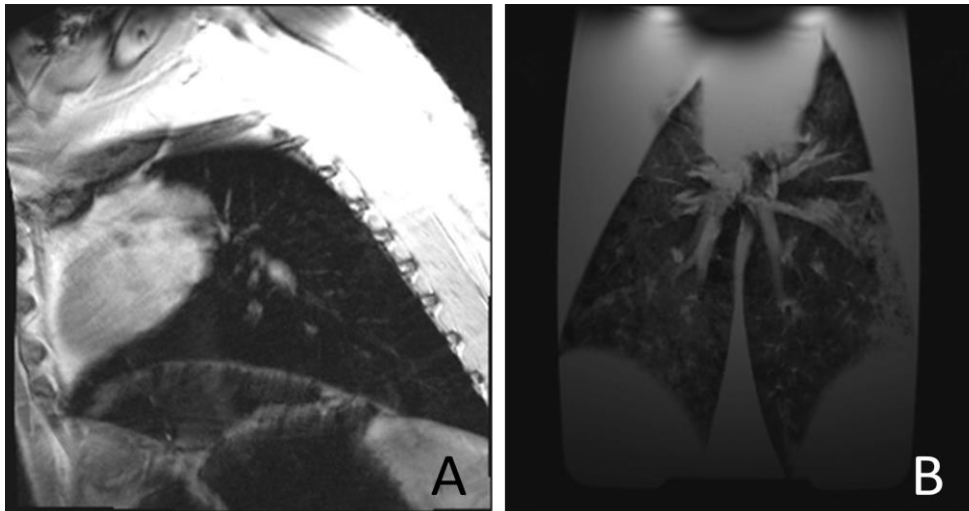


Figure 5.5 T2* MRI images of the lungs of Sheep Red 15. A) Shows the *in vivo* scan pre administration of MSCs. The MRI is unable to provide detailed images of most of the *in vivo* lungs due to air being a poor refractive medium for imaging. B) A section of Red 15s lungs after being necropsied and filled with water. The water provides sufficient density for the MRI to image the surrounding tissue providing improved imaging compared to *in vivo*.

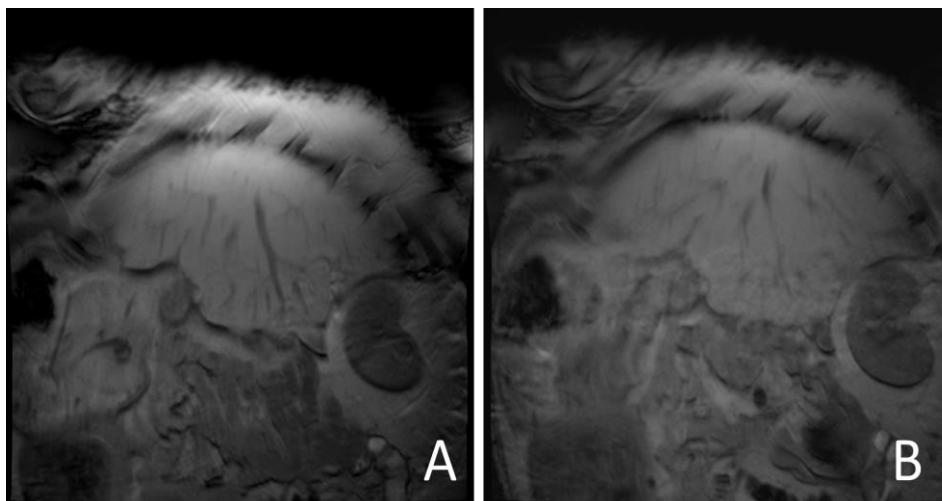


Figure 5.6 T2* MRI images of the liver and right hand kidney of sheep Red 15. A) A section of liver from Red 15 pre-administration of MSCs. B) A section of the liver of Red 15 post-administration of MSCs. No difference is observed between the two time points.

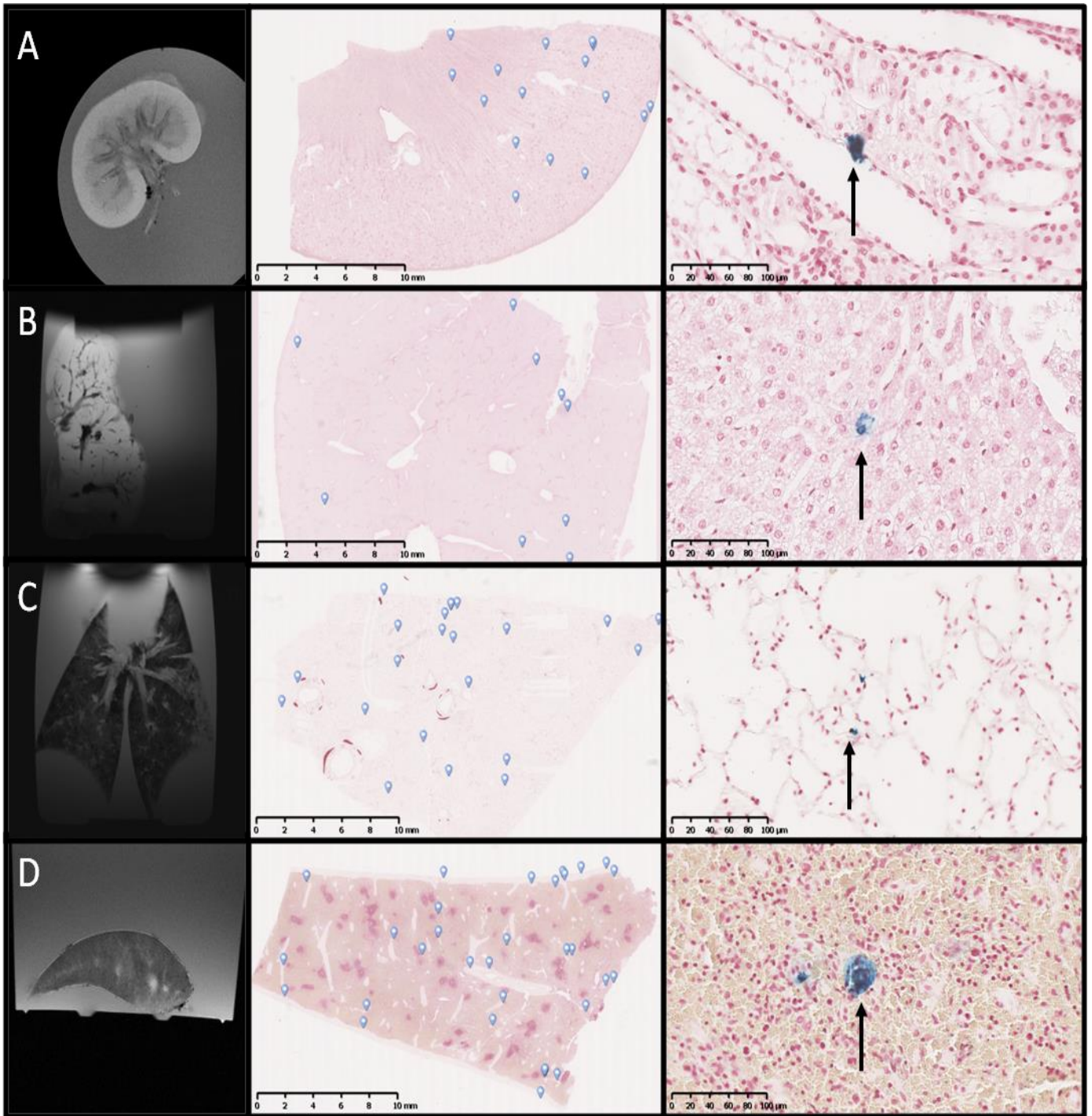


Figure 5.7 Imaging of the organs of interest of sheep Red 15, 5 days after administration of SPIO-MSCs
 A) Transplanted kidney B) Liver C) Lungs and D) Spleen. The left side images are of *ex vivo*, water submerged organs. The middle images are of whole Prussian blue stained histology sections with the locations of SPIO-MSCs indicated by the blue tags. The right side images are 400x magnification of the Prussian Blue stained sections showing representative images of the SPIO-MSCs.

Immediately after the surgery was complete, Sheep red 15 was placed in the MRI and had control images taken of the transplanted kidney, liver, lungs, spleen, and right hand kidney. It then received 2×10^6 Cells/kg of iron labelled MSCs and had scans of the transplanted kidney taken over the course of 30 minutes. Upon analysing these images in imageJ there was a reduction in average pixel intensity immediately post injection and 15 minutes post injection (Figure 5.4). This was deemed to be due to the presence of the MSCs. However the average pixel intensity recovers by the 30 minutes mark.

From the histology and Prussian blue staining the presence of MSCs in all the organs of interest is observed (Figure 5.7). There was a greater abundance of MSCs in the lungs and spleen. There is no obvious pattern to the distribution of the MSCs in the kidney, liver, and lungs, however, the MSCs in the spleen are mainly found around the blood vessels and in the red pulp. One significant difference is that the number of MSCs in the transplanted kidney is higher than that seen in the native kidney (figure 5.18).

5.3.3 Sheep Red 16

Sheep Red 16 had an autotransplant and systemic administration of MSCs and underwent MRI scans on day 1, 4, and 5. It was euthanized on day 5 and *ex vivo* images were taken of various organs of interest before having sections taken for histology.

The only issue of note was that the skin flap did not adhere to the kidney capsule making punch biopsies an infection and bleeding risk, as such they were not carried out.

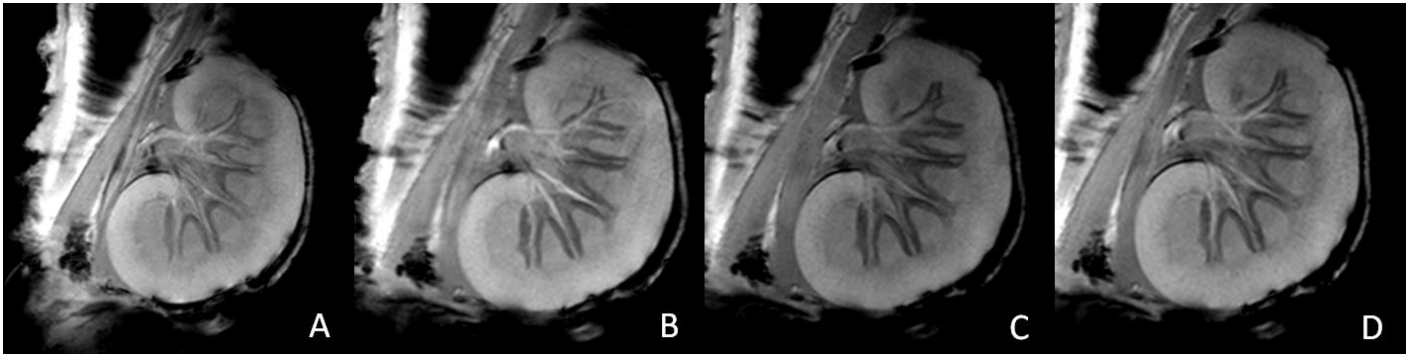


Figure 5.8 MRI images of the heterotopically transplanted kidney of sheep Red 16. The sheep received 2×10^6 cells/kg of iron labelled MSCs systemically immediately post transplantation. A) Is a representative MRI section of the transplanted kidney pre MSC administration. B) Is the transplanted kidney immediately post injection. C) Is the kidney 15 minutes post administration, and D) is 30 minutes post administration. A definitive change in signal intensity cannot be detected upon visual examination of these images.

Red 16 Average pixel intensity as percentage of preinjection over 30 minutes

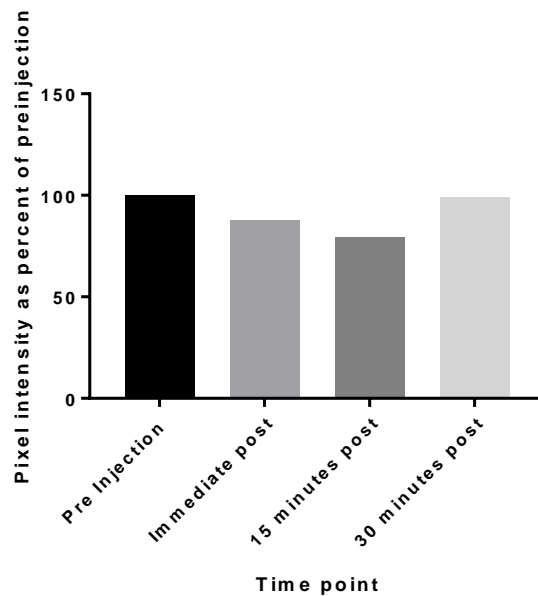


Figure 5.9 Average pixel intensity of the transplanted kidney of sheep Red 16 over 30 minutes post administration of iron labelled MSCs. The pixel intensity was determined by analysing each section of the MRI Z stack at each time point in imageJ. A reduction in signal intensity is seen immediately post administration and 15 minutes post administration of SPIO-MSC.

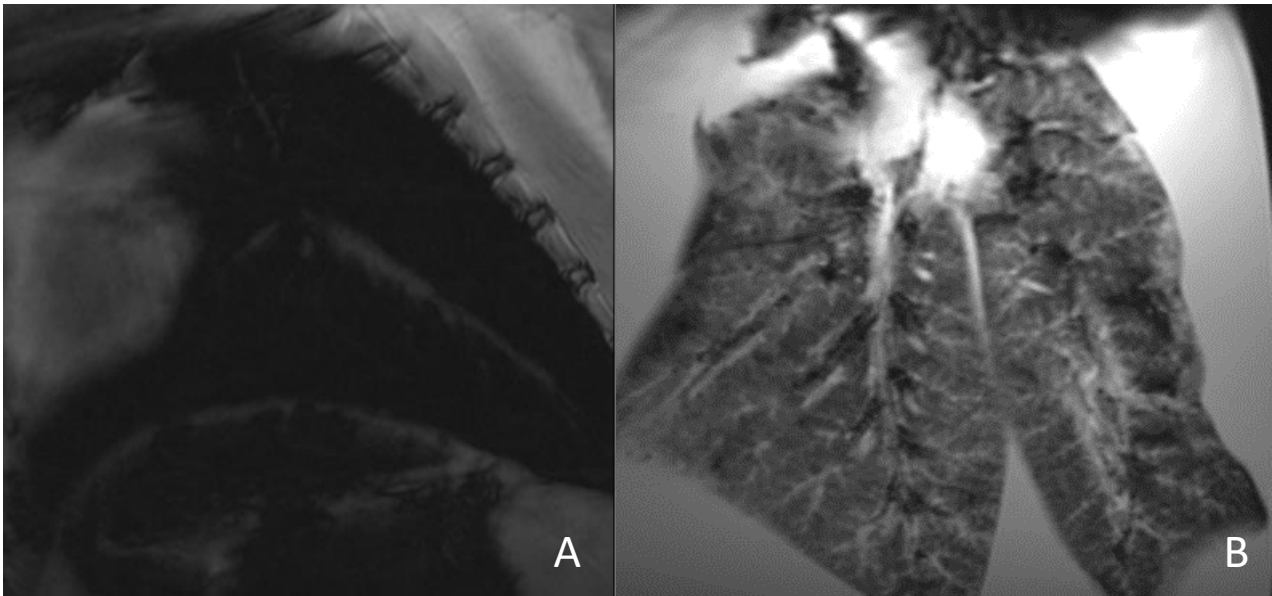


Figure 5.10 T2* MRI images of the lungs of sheep Red 16. A) shows the attempt at imaging the lungs *in vivo* on day 1. Due to the lungs being filled with air they do not image well as air is a poor MRI medium. B) On day 5 the lungs were removed post necropsy and filled with water and imaged again. The addition of water acts to increase the density of the lungs making imaging possible. No depositions of SPIO-MSCs are identifiable in either image.

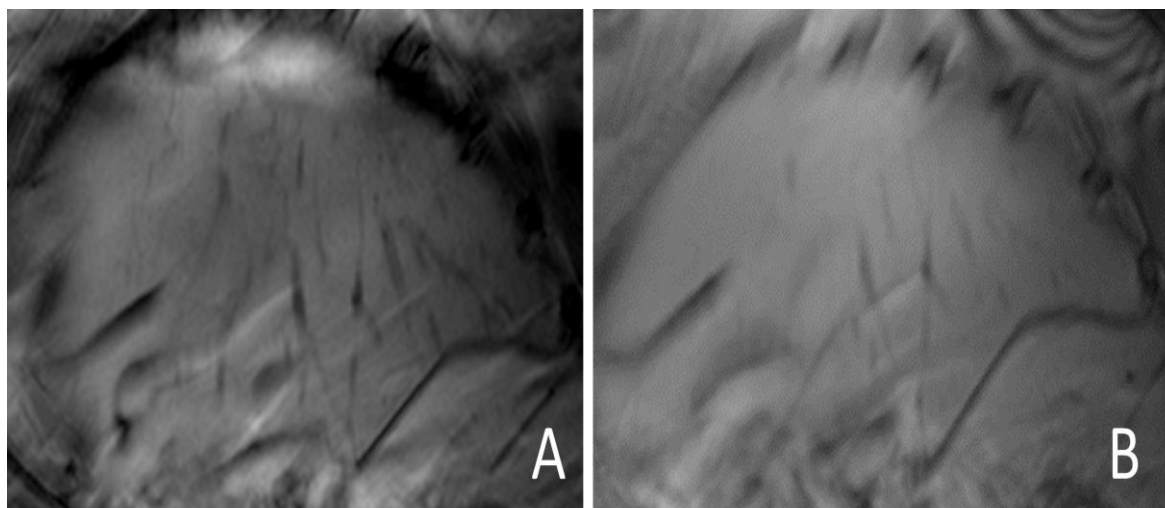


Figure 5.11 T2* MRI images of the liver of sheep Red 16. A) shows the scans taken pre administration of SPIO- MSCs while B) shows the liver post injection on day 1. No difference that can be attributed to SPIO-MSCs can be seen.

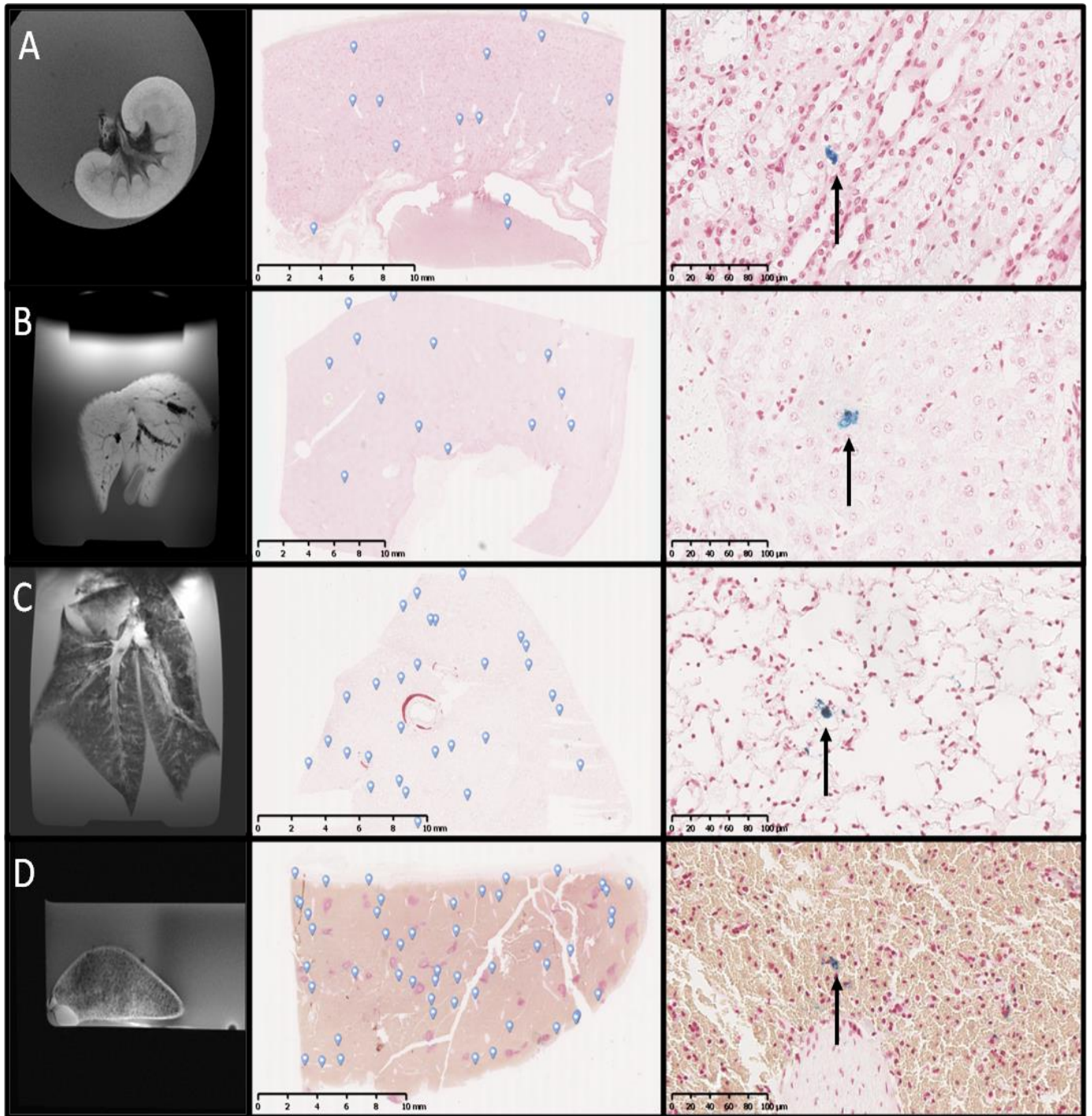


Figure 5.12 Imaging of the organs of interest of sheep Red 16, 5 days after administration of SPIO-MSCs
 A) Transplanted kidney B) Liver C) Lungs and D) Spleen. The left column images are of *ex vivo*, water submerged organs. The middle column images are of whole, Prussian blue stained, histology sections with the locations of SPIO-MSCs indicated by the blue tags. The right column images are 400x magnification of the Prussian blue stained sections showing representative examples of tissue situated SPIO-MSCs.

Red 16 was also taken to the MRI once the surgery was complete and had 2×10^6 MSC/kg administered into the inferior vena cava. It had scans taken of the organs of interest prior to administration and then the transplanted kidney was followed up out to 30 minutes. Similar to Red 15 a reduction in average pixel intensity is observed immediately post administration and 15 minutes post administration, this is seen to recover by the 30 minute mark (figure 5.9). Again this was deemed to be due to the MSCs passing through the kidney.

From the histology and Prussian blue staining, MSCs are detected in all of the organs examined (Figure 5.12). The MSCs show the same distribution as that seen in Red 15, being located in the transplanted kidney, the liver, the lungs, and the spleen. Again a greater aggregation in the transplanted kidney is seen than that in the native kidney (figure 5.18)

5.3.4 Sheep Red 19

Red 19 underwent the same procedures as Red 15 and Red 16. It had control MRI scans taken immediately after surgery was complete and then had 2×10^6 MSC/kg administered systemically. Follow up scans were taken out to 30 minutes for the transplanted kidney and then again on days 4 and 5.

Similar to Red 15 and Red 16 a decrease in average pixel intensity is seen at the immediate and 15 minute post administration time points, which is then removed at the 30 minute time point (figure 5.14). The difference seen here is less than that previously observed, but is still present. The distribution of the MSCs is also similar to what is observed in the other animals with SPIO labelled cells being detected in all organs of interest but no obvious localization in the tissues themselves (figure 5.16). As previously noticed in Red 15 and Red 16, there was also a greater accumulation of MSCs in the transplanted kidney in comparison to the native kidney (5.18)

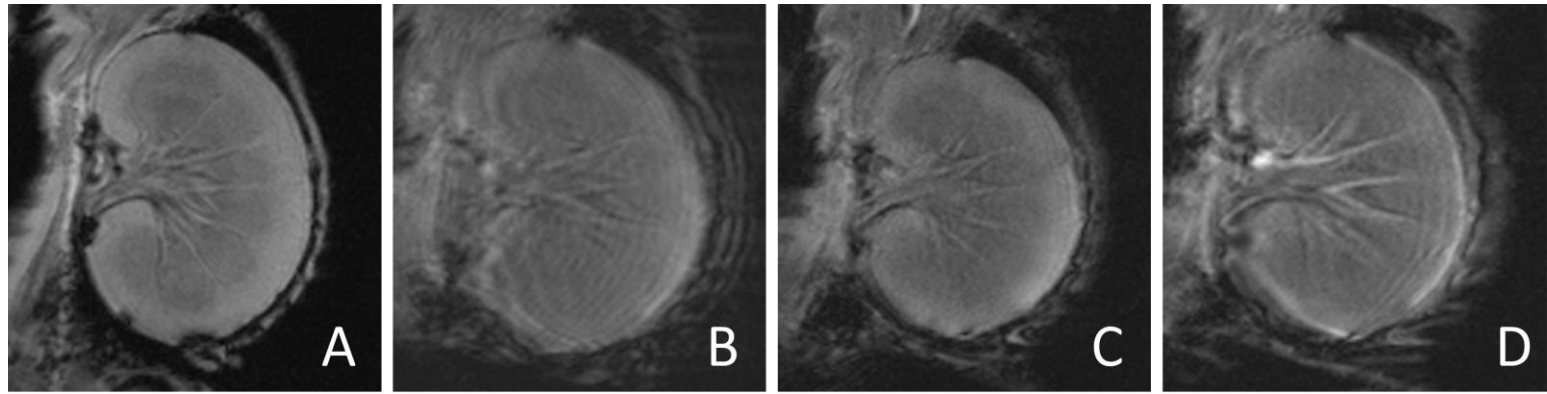


Figure 5.13 T2* MRI images of the heterotopically transplanted kidney of sheep Red 19. The sheep received 2×10^6 cells/kg of iron labelled MSCs systemically immediately post transplantation. A) Is a representative MRI section of the transplanted kidney pre MSC administration. B) Is the transplanted kidney immediately post injection. C) Is the kidney 15 minutes post administration, and D) is 30 minutes post administration. A definitive change in signal intensity cannot be detected upon visual examination of these images.

Red 19 Average pixel intensity as percentage of preinjection over 30 minutes

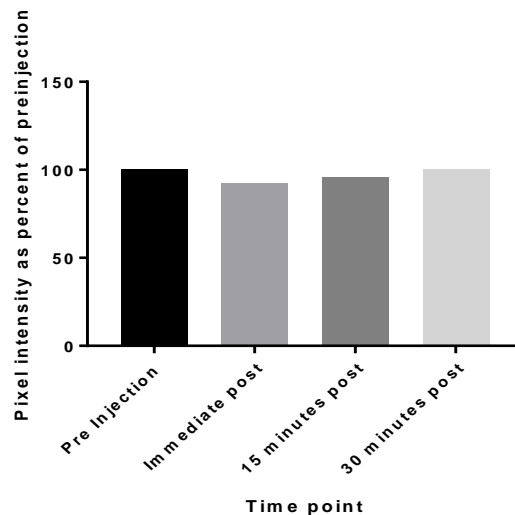


Figure 5.14 Average pixel intensity of the transplanted kidney of sheep Red 19 as a percentage of pre MSC injection pixel intensity. The pixel intensity was determined by analysing each section of the MRI Z stack at each time point in imageJ. A reduction in signal intensity is seen immediately post administration and 15 minutes post administration of SPIO-MSC.

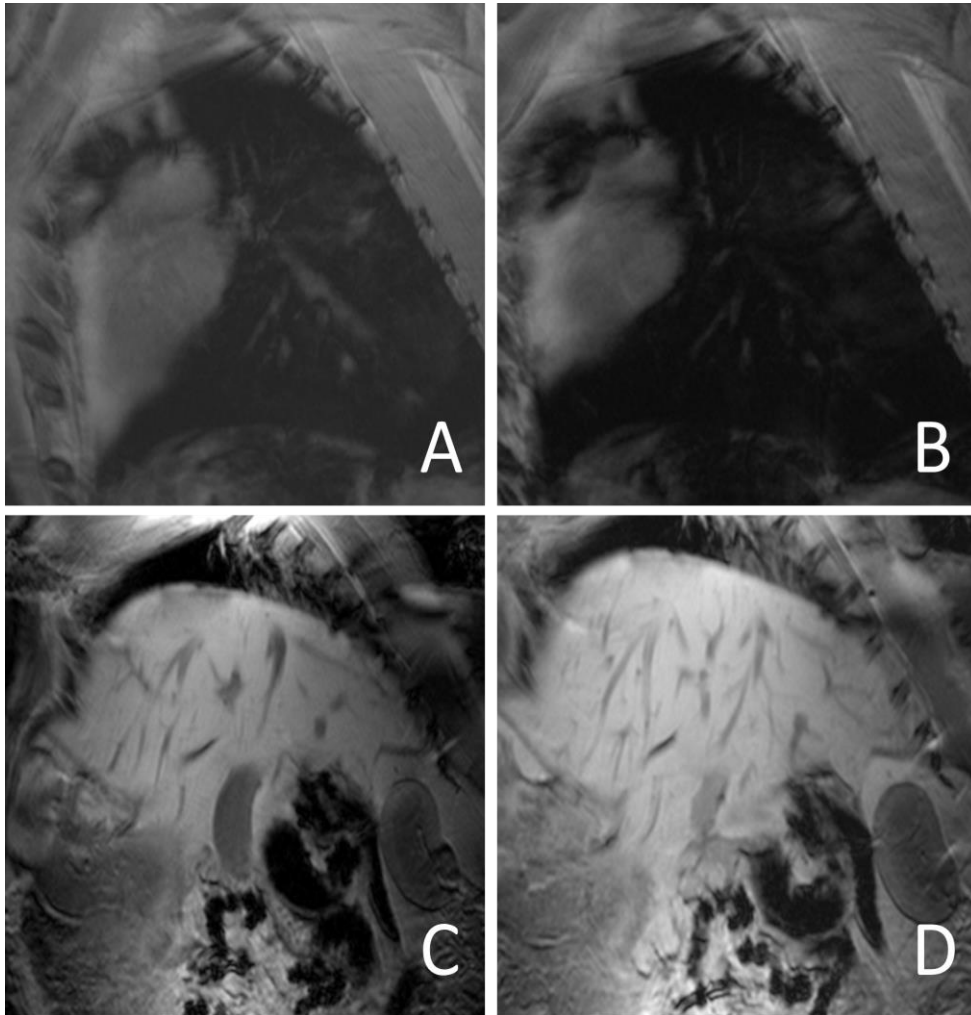


Figure 5.15 T2* MRI sections of sheep Red 19 showing the lungs pre (A) and post (B) administration of SPIO labelled MSCs. As well as the liver and native kidney pre (C) and post (D) SPIO-MSC administration. Due to the low density of air in the lungs the MRI is unable to effectively image the lung tissue preventing any detection of SPIO-MSC *in vivo*. The images of the liver and native kidney shows no difference that can be attributed to SPIO-MSC.

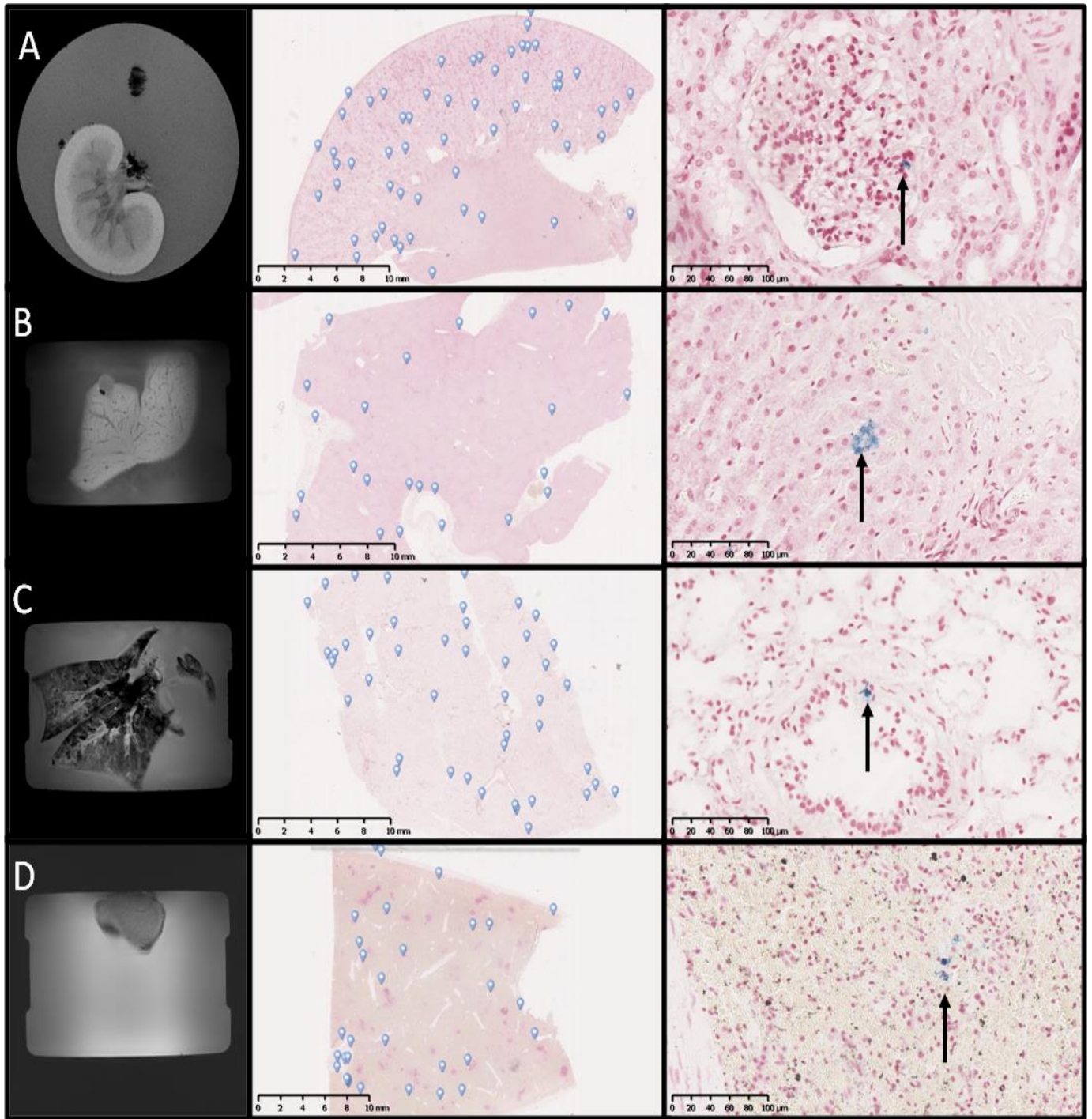


Figure 5.16 Imaging of the organs of interest of sheep Red 19, 5 days after administration of SPIO-MSCs. A) Transplanted kidney B) Liver C) Lungs and D) Spleen. The left column images are of *ex vivo*, water submerged organs. The middle column images are of whole Prussian blue stained histology sections with the locations of SPIO-MSCs indicated by the blue tags. The right column images are 400x magnification of the Prussian Blue stained sections showing representative examples tissue situated SPIO-MSCs.

5.3.5 General Results

When the normalized average pixel intensities are combined and analyzed using an one way ANOVA with multiple comparisons, a significant decrease in pixel intensity is noted at the 15 minutes mark ($p=0.0175$), however this has dissipated by the 30 minute time point. A decrease in pixel intensity is also seen immediately after administration of MSCs, but this is not significant ($p=0.0758$). The presumed cause of this decrease, and subsequent recovery, in pixel intensity is the passage of the iron labelled MSCs through the kidney.

From histology and Prussian blue staining, a wide distribution of MSCs in all of the organs studied is observed with no obvious preferential migration. However, upon visual inspection a difference in the amount of MSCs in the transplanted kidney and the native kidney is apparent (Figure 5.18). Performing a statistical analysis of the distribution of MSCs in the transplanted kidney and the native kidney a significant difference is found with 22 MSCs per CM^2 in the transplanted kidney while the native kidney only had 6 MSCs per CM^2 ($p<0.0001$, Figure 5.19) This multi organ distribution is present in all of the animals studied. Looking at the results from sheep Pink 14, which was euthanized on day 2, it is apparent that the MSCs have already distributed themselves around the body by this time point and, from the histology of sheep Red 15, Red 16, and Red 19, the MSCs are seen to persist in this distribution out to at least day 5. In addition to the main tissues of interest, the venous anastomosis site of sheep Red 19 was collected and histology was performed. Figure 5.20 shows that MSCs are also able to be located in the areas of anastomosis.

Previous, unpublished, work by Dr Dyan Auclair looking at the direct injection of MSCs into the renal artery of the transplanted kidney were used as a comparison to these current results to determine the kinds of distribution that are able to be identified using the two different methods of delivery. This work showed a much greater accumulation of MSCs in the graft.

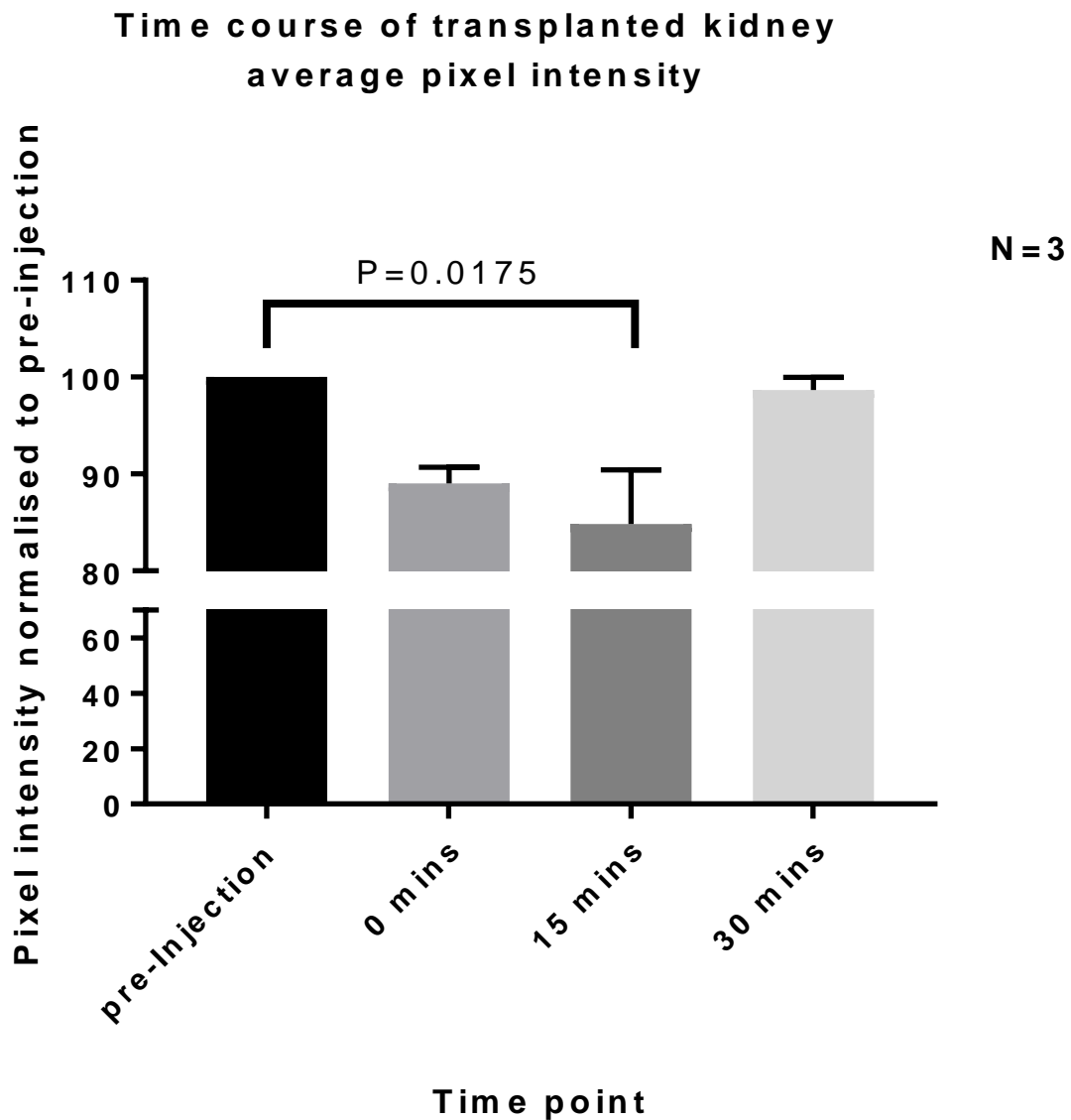


Figure 5.17 Combined pixel intensities of sheep Red 15, Red 16, and Red 19. The pixel intensities of the MRI images from the transplanted kidney were calculated using ImageJ. These were then normalized against the pre SPIO-MSA administration scans. Combining the data from all three eligible sheep, a decrease in pixel intensity is observed at 0 minutes and 15 minutes post administration, however, only the decrease at 15 minutes post SPIO-MSA administration is statistically significant ($p=0.0175$). This reduction in signal intensity is lost by the 30 minute time point.

Transplanted Kidney

Native Kidney

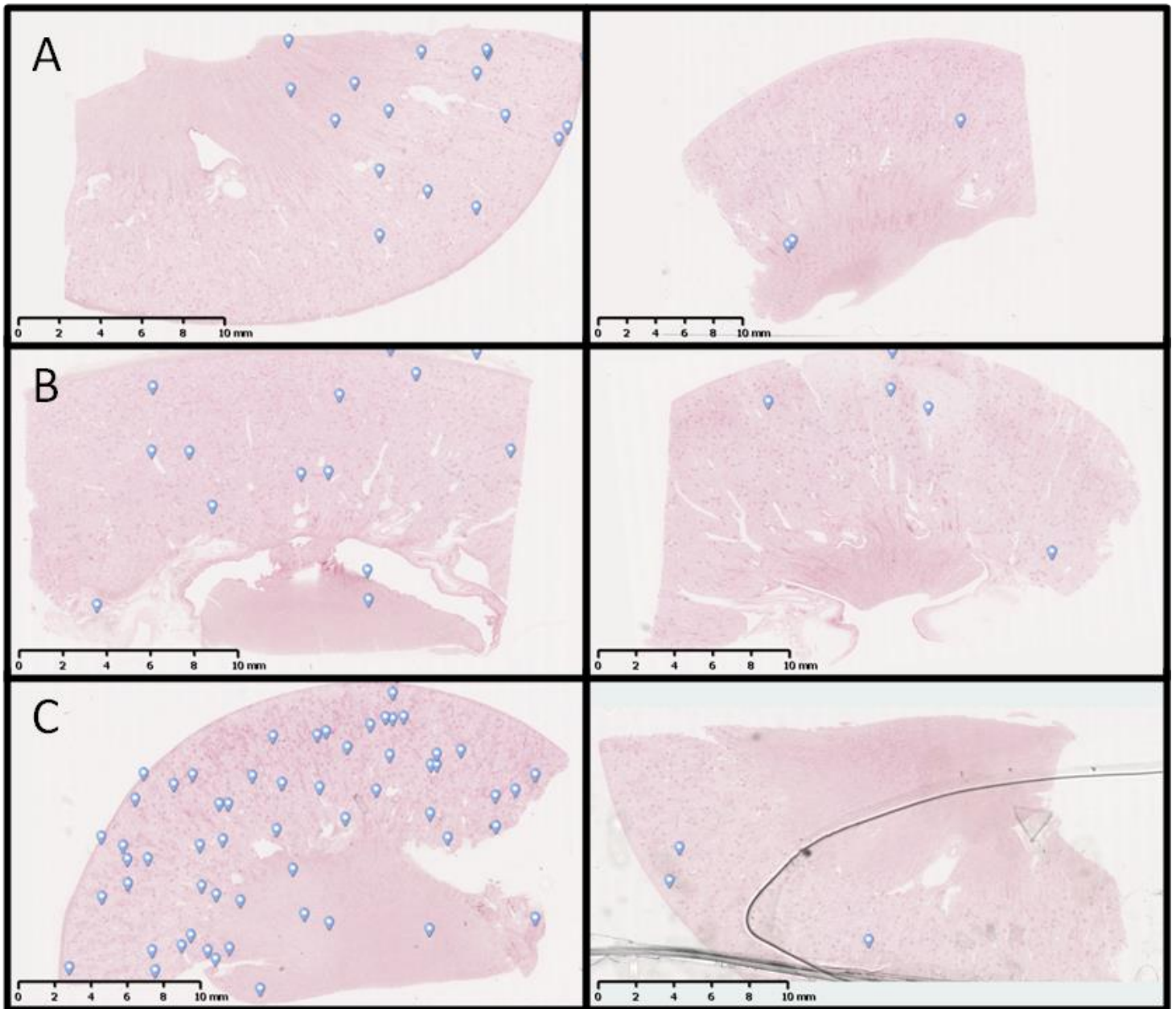


Figure 5.18 Macro-scale images of the transplanted and native kidneys of sheep Red 15 (A), Red 16 (B), and Red 19 (C) show the variation in distribution of MSCs (blue markers). The sections are all taken from kidneys that were removed 5 days after the administration of SPIO-MSCs. Sections were then stained with Prussian blue and counter stained with nuclear red to highlight deposits of SPIO. A larger proportion of SPIO-MSCs is seen in the transplanted kidney compared to the native kidney.

MSC distribution in Native vs Transplanted kidneys

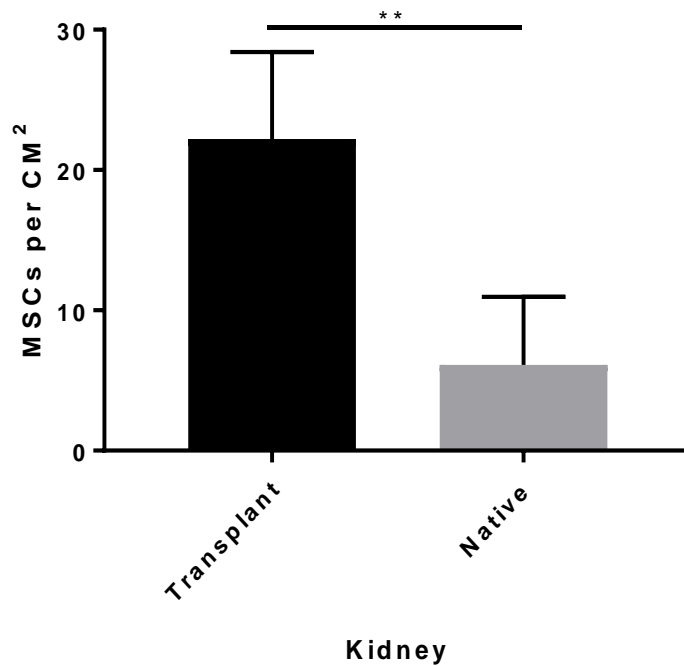


Figure 5.19 The average number of MSCs per CM² across all three sheep in both the transplanted kidney and the native kidney. A higher localization is noted in the transplanted kidneys (22 MSCs/CM² vs. 6 MSCs/CM². **=P<0.0001)

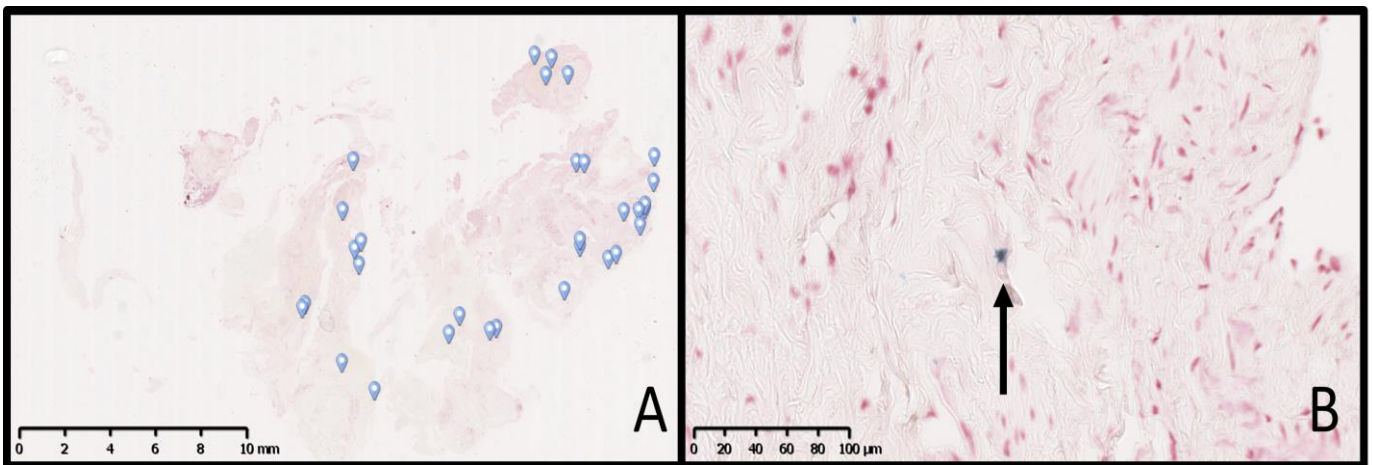


Figure 5.20 Prussian blue staining of the venous anastomosis of sheep Red 19's kidney autograft. A) Shows the location of the MSCs in the tissue indicated by the blue markers. B) 400x magnification shows a representative image of a tissue resident SPIO-MSC (Arrow).

5.4 Discussion:

Iron labelling of MSCs and imaging using an MRI has previously been used to determine their location in this model. In the previous studies, carried out by Dr Dyan Auclair, MSCs were administered directly into the transplanted kidney just prior to completion of the anastomosis. The results of that study showed a very obvious conglomeration of MSCs in the transplanted kidney at various time points using MRI. In comparison, any of the large groupings of MSCs have been unable to be identified in the kidney graft or any of the other organs of interest, indicating that the migration of the MSCs to the area of ischemic reperfusion injury created by the graft is not great enough for detection.

By using image analysis software it is possible to detect the cells passing through the kidney at 15 minutes post administration. However this is transient and cannot be detected at the 30 minute time point indicating that homing of MSCs to the kidney at that early time point is limited. A possible explanation for this is that the MSCs are being mechanically trapped in the glomerulai as hypothesized by Jung *et al.*, 2009 [454], when they made a similar observation with their rat model of renal ischemic injury when treated with iron labelled MSCs. A significant difference between the findings of Jung *et al* and those of the present study is the time over which the MRI hypointensity persisted. In Jung's work they detected a difference out to 15 hours [454] while signal had been lost by 30 minutes in the current study. A possible explanation for this is that the larger size of the sheep results in a more subtle change which is harder to detect and thus lost sooner or that the larger glomerular size of the sheep allows the MSC to pass through faster than in rats.

The presence of MSCs in the lungs, liver, and spleen are in line with what has been observed in other animal models by various groups including rats [408, 470, 471] and mice [472]. By

looking at histology and Prussian blue staining of the transplanted kidney, native kidney, liver, lungs, and spleen the only obvious distribution difference is the lack of MSCs in the native kidney.

The observation of MSCs in the transplanted kidney, but not the native kidney, at day five in all of the animals would suggest that the MSCs have migrated there or are there through trophic effects as opposed to mechanical trapping as could be the possible explanation for the observed hypointensity at 15 minutes after injection. The proposition that the MSCs have not been physically trapped is further bolstered by the locations of the MSCs in the kidney, given that they have a wide distribution in all areas of the kidney, where as if they were simply trapped by the glomerular tufts, it would be expected that the majority of the MSCs would be detected in these structures. However, it cannot be discounted that the trophic effects of the MSCs to the transplanted kidney may have been aided by the use of the carotid artery as the blood supply. The heterotopic placement of the kidney may have contributed to the significant difference in distribution between the transplant and native kidneys, although this difference in MSC distribution is also observed in other models of kidney IRI [454].

Both the liver and the spleen are known to naturally accumulate iron through the breakdown of blood cells; as such it is important that care is taken to avoid false positives. Even when being stringent in identifying MSCs in these organs a large number of the iron labelled cells are still observed. This aligns with previous studies and suggests that these are the organs in which MSCs are eventually eliminated [408, 470-472]. This raises the question of whether the observed iron label is still bound in the MSCs or if it has been taken up by a macrophage, both scenarios result in MSCs ending up in these organs in large numbers. If the MSCs have been taken up by phagocytosis it has been proposed that doing so allows the MSC secretome to affect a tolerogenic phenotype in the immune cells that have ingested them and this could account for part of their *in vivo* impact [473, 474].

Finally, the finding of the MSCs in the lungs is supported widely and seems to be a primary deposition location in many studies [408, 470-472, 475]. This has been hypothesized to be due to the small capillaries in the lungs which results in the MSCs becoming trapped [475]. When injecting the cells intravenously, the lungs are the first organ that they will encounter with such small capillaries, potentially explaining the observed accumulation of the cells.

Using this data, and that of previous studies carried out by Dyan Auclair which showed much greater MSC accumulation when DAA is used, it would seem that the best way to target MSCs to areas of interest is to apply them directly. This is perhaps of most significance in cases where the anti-inflammatory and regenerative aspects of Mesenchymal stem cells are of interest. Alternatively, there have been several attempts to modify MSCs *ex vivo* to induce greater migration or organ specific migration such as what has been demonstrated by Ma *et al.*, 2016 [476], when they unregulated the expression of CCR7 in xenogeneic MSC (and previously syngeneic MSC) in order to increase their migration to secondary lymphoid organs and were successful in this without having any negative impact on the phenotype of the MSC. It is has also been established that treating MSC with pro-inflammatory markers increases their efficacy as shown by Fan *et al* in 2012 [477].

However, untreated MSCs were used for the studies described in this thesis. So, as detailed in chapter 6, a direct arterial injection into the graft just prior to the completion of the anastomosis was used, as the data and literature suggested that this was the most efficient way to ensure localization of the MSC to the transplanted kidney.

Chapter 6

Impact of MSCs on Kidney Allografts

6.1 Introduction:

There have been several pilot studies and clinical trials looking at the application of MSCs for kidney transplantation [339-348]. However, these studies have thus far been inconclusive about the effectiveness of MSCs in this setting and have also left, unanswered, many other questions relating to the best method of utilization.

6.1.1 Benefits Of Direct Arterial Administration Of MSCs

Questions still persist around the optimal method of administration of MSCs. Most groups prefer the use of systemic venous administration due to the ability of MSCs to home to areas of injury [478, 479] and the perceived risk of damaging the graft via blockage of small vessels using other methods [249]. Additionally, venous administration allows for the MSCs to be delivered post surgery without disturbing the graft.

Although the benefits of systemic administration are significant, the findings detailed in chapter five combined with previous work from Dyan Auclair, indicate that direct arterial administration provides much greater accumulation of MSCs and that the same number of cells can be administered arterially without deleterious effects. Furthermore, when considering the mechanisms through which MSCs exert their beneficial effects it is possible that many of them would be aided by localization to an allograft.

In particular, MSCs are able to prevent the maturation of dendritic cells, one of the most important APCs in transplantation [264, 265]. By preventing the usual maturation that occurs when DCs are stimulated, MSCs may inhibit their migration and presentation to effector immune cells, thus inhibiting both the direct and indirect cellular response to an allograft [57]. In a transplant setting DCs have a higher chance of interacting with stimulating antigens if they are in or near the allograft, as such MSCs that are localized to the graft have a higher chance of preventing this stimulation and the subsequent maturation. By being located in the graft, MSCs are also able to attract Tregs and induce their proliferation, resulting in a suppression of the immune system [260]. Perhaps most significantly, MSCs are able to have a direct impact on CD8 T cells, reducing their cytotoxicity upon their recruitment to an allograft [245, 261].

Although this is not an exhaustive list of MSC based immunosuppression, these mechanisms show that localized MSCs are able to act on multiple pathways to reduce the deleterious effects of the immune system on a kidney transplant. Moreover, the reparative effects of MSCs are dependent upon reacting to local inflammatory stimuli and excreting pro-regenerative cytokines [313, 480, 481]. This is likely to benefit from the MSCs being situated in a kidney graft, as transplantation related damage creates an inflammatory environment with increases in various cytokines that have been shown to up regulate MSC functions [199, 200].

6.1.2 Direct Arterial Administration In Small Animal Models Of Kidney

Transplantation

Evidence measuring the effectiveness of DAA of MSCs in kidney allograft transplantation is limited, due to the relatively few experiments in which it has been investigated. The majority of the work has been performed by a single group from the University of Pavia, Italy.

The first paper by Zonta et al, in 2010, was one of the earliest papers to describe favourable outcomes associated with administration of MSCs in kidney transplantation. They used a rat model of kidney allograft transplantation and tested whether administration via the tail vein or the renal artery gave better results across histological measures of rejection and biochemical measures of kidney function [334]. They found that both groups performed better than control but that the DAA group had superior results compared to the intravenous group with better functional recovery as measured by creatinine levels, less inflammatory infiltrate, and greater preservation of tubules arteries and glomeruli [334].

In more recent studies investigating the direct arterial injection method they examine in detail the key aspects of MSC treatment for kidney transplantation. In their followup publication in 2010 they observed that direct injection of MSCs gave better outcomes in both syngeneic and allogeneic kidney transplants by reducing the cellular infiltration of the grafts [328].

Further work by this group in 2014 examined the mechanisms behind the observed positive outcomes of DAA [482]. In this paper they identified that MSCs have the ability to move cytokine profiles to a tolerogenic environment. In doing this they act to suppress Th1 cells, inactivate monocytes/ macrophages, and recruit Tregs fitting well with the known mechanisms of MSC immunoregulation [482]. In addition to the immune system effects it was discovered that MSCs were able to bolster the systems used to aid in the survival of tubular cells as well stimulating their regeneration, demonstrating that MSCs may be able to combat transplant related graft dysfunction through multiple, non-redundant, pathways [482].

They expanded their work on the protective and regenerative abilities of MSCs in 2017 by looking at the effects of perfusing MSCs vs MSC derived extracellular vesicles (EV) on ischemic damage to machine perfused rat kidneys [330]. To do this they first induced warm ischemia in rat kidneys by clamping the renal artery. After 20 minutes of warm ischemia they

performed a nephrectomy, removing the kidney with the hilum intact to allow continuous perfusion for 4 hours at 4°C. The kidneys were perfused with either UW solution, UW solution supplemented with 3×10^6 MSCs, or UW solution supplemented with EV isolated from 3×10^6 MSCs.

Both the MSC and EV groups demonstrated superior results in several measurements of ischemic damage when compared to UW solution alone [330]. The MSC and EV groups had an up regulation of genes involved in cell energy metabolism and in ion membrane transport. The effluent from the MSC/EV kidneys also had metabolites that suggested a larger use of energy substrates [330]. Interestingly, the EV group showed better histopathological preservation of kidney structures in comparison to the MSC group. This may have been related to a group of genes associated with protection against intracellular acidosis that were only up regulated in the EV group. The authors hypothesized that these improved outcomes may be due to the prompt availability of MSC derived mediators in the EV group, allowing for earlier opposition to the damaging reactions of ischemia.

These results suggest that MSC/EV may be able to protect against reperfusion injury by halting the changes in metabolism associated with ischemia, which are the precursors to reperfusion injury [183, 193, 194]. To exploit these beneficial effects however, it is necessary to utilize the direct arterial administration method of MSC delivery to kidneys.

6.1.3 Direct Arterial Administration In Large Animal Models Of Solid Organ Transplantation

Although the evidence for the use of DAA in kidney transplantation is promising in rodent models, it is lacking in large animals. The use of direct injection of MSCs into any form of large animal solid organ allograft model is currently limited to experiments carried

out by Wittwer *et al* in 2014 [483] and Schnapper *et al* in 2018 [484] both of which examined the pre-treatment with MSCs of deceased heart, lung transplantation in pigs.

Wittwer *et al* developed a porcine model of lung transplantation from non-beating-heart-donors (NBHD) with the aim to facilitate the study of novel approaches to improving outcomes of extended criteria lung donation [483]. The 2014 work involved the induction of cardiac arrest and subsequent ventilation of the cadaveric lungs *in situ* for 3 hours. During which 50×10^6 MSCs were administered either via the pulmonary artery or nebulised and delivered endo-bronchially.

The lungs were then perfused with cold preservation solution, removed, and stored at 4°C for 3 hours. After the cold ischemic period the left lung was transplanted into a size matched recipient and reperfusion carried out for 4 hours, after which point the animal was euthanized. Pulmonary vascular resistance (PVR), dynamic lung compliance (DLC), oxygenation, and sterology were used to assess the effectiveness of the treatment [483].

Their results suggest that direct arterial injection of MSCs may result in dysfunction of transplanted lungs. They noted a decrease in oxygenation, and a significant increase in PVR compared to control transplanted lungs, indicating that the small vessels of the lung may be blocked. This is in line with some complications that have been seen in other MSCs experiments [249]. The endo-bronchial nebulisation administration, however, gave good oxygenation and PVR results, similar to non-transplanted lungs. With this group they also found a greatly increased DLC which they claim as a positive [483]. However, high DLCs are associated with a loss of elasticity as seen in emphysema [485].

Schnapper *et al* repeated the experiments of Wittwer but focused their attention to the structural composition of the lungs, with a particular respect to histological and ultrastructural signs of IR injury and changes in the lungs surfactant system [484]. They found that 3 hours

of warm ischemia caused few, if any, histological signs of IR injury, but, did have a negative impact on the surfactant system of the lungs by causing a decrease in the volume of lamellar bodies, the organelles responsible for production of surfactant molecules.

The application of MSCs, either arterially or endo-bronchially, was unable to negate the impact on the surfactant system [484]. Overall, the evidence suggests that arterial injection of MSC may be inferior to endo-bronchial administration for lung transplantation. Although these results are instructive with respect to regenerative medicine, the fact that the transplanted lungs were only *in situ* and reperfused for 4 hours means that it is unknown what affect on the immune system the various methods of administration would have had.

The deleterious effects of MSCs when delivered arterially to lung transplants may not be an issue in kidney transplantation. This is backed up by the work of Behr *et al* who examined the impact of arterial MSC injection in a sheep model of IRI [337, 437]. In their model they used a balloon catheter to occlude the right renal artery and induce ischemia for 45 minutes. The balloon was then removed to allow reperfusion injury to occur. The test groups then had 80×10^6 MSCs injected either 1 hour after injury or 2 weeks after injury.

They found significant engraftment of MSCs in the tubules and glomeruli in the early administration group [337]. However, in their subsequent experiments their results conflicted with this. In the later work, they performed bilateral occlusion of the renal arteries resulting in ischemia reperfusion injury in both kidneys, before infusing 50×10^6 MSCs simultaneously into each renal artery. Their results showed an engraftment of MSCs in the glomeruli but not tubules. They also found that MSCs did not repair kidney parenchyma and that no beneficial effect was observed with MSC infusion [437].

Although the results in terms of engraftment are mixed, an important observation is that they did not note any negative effects associated with DAA, supporting the safety of local MSC

administration. They also note that they attempted to inject MSCs directly into the kidney tissue but abandoned this due to bleeding and tissue destruction leading to kidney damage [337], further supporting DAA as an optimal administration route for MSCs.

6.1.4 Chapter Aims:

The aim of this chapter is to examine the effects of direct arterial administration of MSCs on the outcomes of an ovine model of kidney allotransplantation and rejection. This is the first time that MSCs have been used in a large animal model of kidney allotransplantation, as such the outcomes may be impacted by several factors such as IRI, immune reaction, and the effect of the immunosuppressive drug, cyclosporine. Importantly, clinically relevant doses of MSCs were used and the protective effects of MSCs on both early graft function and rejection were examined.

6.2 Materials and Methods:

6.2.1 MLRs

Pre-operatively, one way mixed lymphocyte reactions were performed on animals in groups of 6 as described in chapter 2 (see section 2.8.1). This was performed to determine alloreactivity and for comparison to immune sequencing allowing for optimal transplant pairings to be selected.

6.2.2 Sequencing

In tandem to the MLRs, sequencing of the ovine DRA and DRB1 genes was carried out on all candidate animals as described in chapter 2. DNA was first isolated from whole blood (section 2.17), followed by PCR to amplify regions of interest (Section 2.19), which was confirmed by gel electrophoresis (Section 2.20), before sequencing was carried out by sending samples to the Australian Genome Research Facility (Section 2.21)

6.2.3 Preparation Of MSCs

One month prior to surgery the donor animals underwent bone marrow biopsies to isolate and expand MSCs (Sections 2.9 and 2.11). The MSCs were then characterized via flow cytometry (Section 2.14) and their ability to differentiate into chondrocytes, adipocytes and osteocytes (2.15)

6.2.4 Heterotopic Kidney Allograft Surgery

Heterotopic kidney allograft transplantations were carried out as described in chapter 4. Briefly, the animals were anesthetized and prepared for surgery by having their wool trimmed and a central line placed into the right jugular vein to allow fluid and drugs to be given, before being transported to the operating theatre. Once on the operating table an incision made on the left flank. The left side kidney had its blood vessels and ureter tied off and cut while the stumps and the wound were closed. The kidney was then moved to a sterile bench and perfused with cold custodial solution and placed on ice. While the kidney was being preserved, the neck of the recipient sheep had an incision made in the skin above the left hand jugular vein and carotid artery, the skin was manipulated to create a pocket in which the kidney would sit. The vessels were clamped and cut to allow for the jugular vein to undergo end to side anastomosis with the renal vein and the carotid artery to undergo end to end anastomosis with the renal artery. The clamps on the blood vessels were released and blood flow confirmed via colour change in the kidney. The ureter was externalized through the skin flap and the incision closed. A surgical drain was placed in into the pocket to control the subsequent swelling. At this point the animal was given 5mg/kg cyclosporine I.V. The animal was then rolled onto its left hand side with care being taken to avoid damaging the transplanted kidney. A complete nephrectomy was performed on the right hand kidney and a central line placed into the inferior vena cava via the right renal vein stump. The wound was

then closed and the animal allowed to recover, upon which time they were given 10mg/kg ketoconazole orally.

The animals were then given 5mg/kg cyclosporine and 10mg/kg ketoconazole daily for the first 7 days. This was then withdrawn to allow rejection to occur. The animals were sacrificed on day 14 or when their serum creatinine reached 600ng/ml. The protocol for these experiments is summarised in figure 6.1

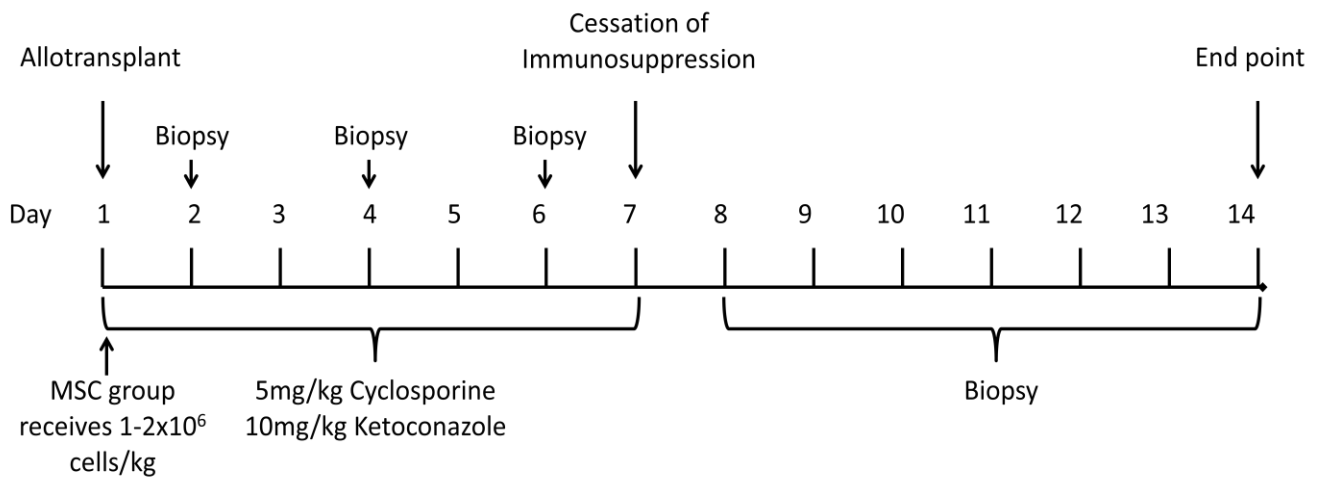


Figure 6.1 Summary protocol for the duration of the allotransplantation experiments. A heterotopic kidney allotransplant was performed from a tissue mismatched donor and a bilateral nephrectomy carried out. The animal was then given immunosuppression in the form of cyclosporine for the first 7 days before having this withdrawn to allow rejection to occur. The sheep assigned to the MSC groups received 1-2x10⁶ cells/kg of autologous MSCs that had been isolated and expanded a month prior.

6.2.5 Administration Of MSCs

In the MSC group $1-2 \times 10^6$ cell/kg of autologous MSCs were harvested from their flasks just prior to surgery and placed in 10ml of saline supplemented with 500 units of heparin. At the time of the arterial anastomosis the MSCs were slowly injected into the renal artery, the anastomosis was then completed, and the clamps released.

6.2.6 Punch Biopsies Of The Transplanted Kidney

Every second day for the first week a punch biopsy was performed on the transplanted kidney. The sheep was restrained, the area numbed using 1ml of lignocaine, and a small incision made to allow access to the kidney. The core sample was then taken using a Bard Max-core 18 gauge punch biopsy needle and pressure placed on the biopsy site using gauze to minimize bleeding. The biopsy sample was placed in 10% neutral buffered formalin for later processing. The frequency of biopsies was increased to once per day during the second week of the experiment. The exception to this is if the skin failed to adhere to the kidney capsule, in which case biopsies were not performed as the risk of infection was too great.

On the day that the animal was euthanized tissue samples were collected from the transplanted kidney, liver, lungs, and spleen. These were placed into 10% NBF for processing.

6.2.7 Histology

Tissue samples and biopsies were embedded in parafin before being sectioned and stained using hematoxylin and eosin (H&E) stain as well as Alcian blue and Periodic acid–Schiff (ABPAS) stain. These were then visualized under an Olympus IX51 inverted microscope and scored according to the Banff classification of acute renal allograft rejection [366].

6.2.8 Blood Sampling

Blood samples were collected each day, prior to dosing with cyclosporine, from the inferior vena cava central line. 2 x 8ml z serum clot activator “red top” tubes and 2 x 4ml K₂ EDTA “purple top” tubes were collected each day. The red tops tubes were used for measuring serum creatinine and urea, and the purple tops were used for pharmacology.

6.2.9 Pharmacology

50ul of whole blood was taken from the purple topped EDTA tubes and processed to determine cyclosporine levels on a ABI2000 liquid chromatography mass spectrometer as described in chapter 2, section 2.22.

6.2.10 Urine Samples

5ml of urine was collected from the catheter placed into the transplanted kidney ureter. These were frozen at -80°C for later use in ELISA analysis of urinary markers of kidney dysfunction.

6.2.11 ELISA

Urine samples were thawed and used in the MyBioScience Sheep Kidney Injury Molecule 1 Elisa kit in accordance with the provided instructions. In brief, 100µl of urine was added to each sample well followed by 10µl of “balance solution” and 50µl of “conjugate” before mixing and incubating for 1 hour at 37°C. The plate was then washed by removal of liquid from the wells and rinsing 5 times with wash solution. 50µl of both “substrate A” and “substrate B” were added to the wells, covered and incubated for 15 minutes at 37°C. After the incubation period 50µl of “stop solution” was added to each well and the plate read on an Epoch microplate reader at 450nm.

6.3 Results:

6.3.1 Mixed Lymphocyte Reactions

The full mixed lymphocyte reaction results are included in chapter 4, in this chapter only the results from the successfully allotransplanted sheep are included.

The sheep used for the control group were selected from Pink series sheep, numbers 7-12.

Sheep Pink 10 and Pink 12 are absent from the above graph because their base immune stimulation was very high. This has the result of forcing the stimulation index down, masking any actual immune response, which can be seen in figure 4.9. With the results from sheep Pink 10 and Pink 12 being exceedingly low. Additionally, this high base immune stimulation can indicate an underlying issue with the animal that may impact the experiment, for this reason sheep Pink 10 and Pink 12 were excluded from consideration for the experiment.

With 4 sheep left it was decided to attempt a cross over transplant using Pink 7 and Pink 8 as they had similar stimulation responses to each other. Although sheep Pink 8 had a very strong reaction to sheep Pink 9 this match was not used because no other pairing had a similarly strong reaction. Unfortunately Pink 8 suffered complications and had to be euthanized early (as detailed in chapter 4). In response to this a non-crossover transplant was performed using Sheep Pink 11 as the recipient and Pink 9 as the donor. This allowed greater resources to be focused on a single animal to ensure survival to the experimental end point.

Control group MLR results

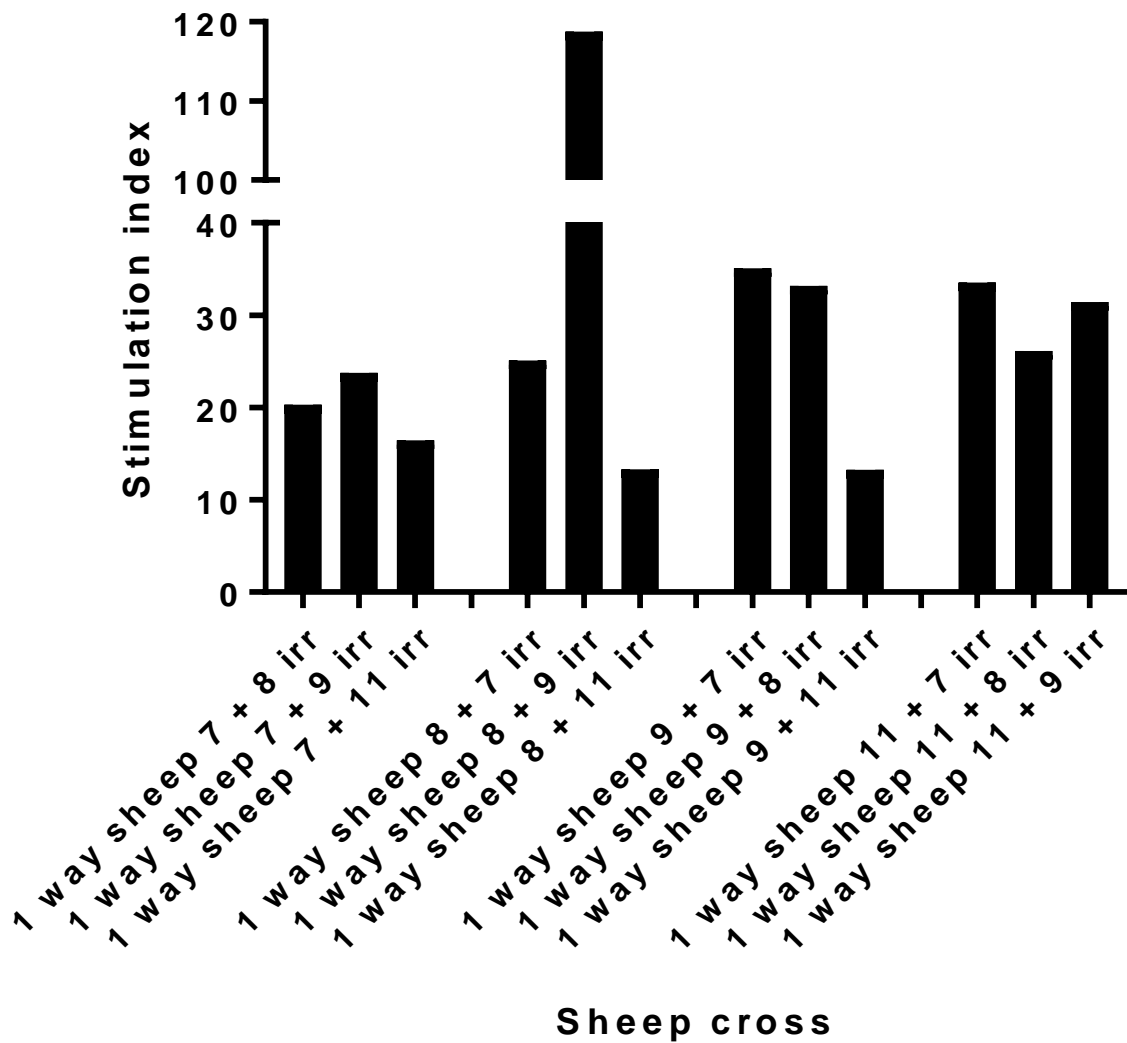


Figure 6.2 One way mixed lymphocyte reactions from the pool of sheep designated for the control experiments. PBMCs were collected from each of the sheep and the cells split into stimulators and responders, with the stimulators being irradiated to halt cellular division, the MLRs were then carried out as detailed in chapter 2, section 2.8. The reactions were then set up so that each sheep would respond to every other sheep. Transplantation pairs were selected based on mutually high stimulation indices of two sheep.

MSC group MLR results

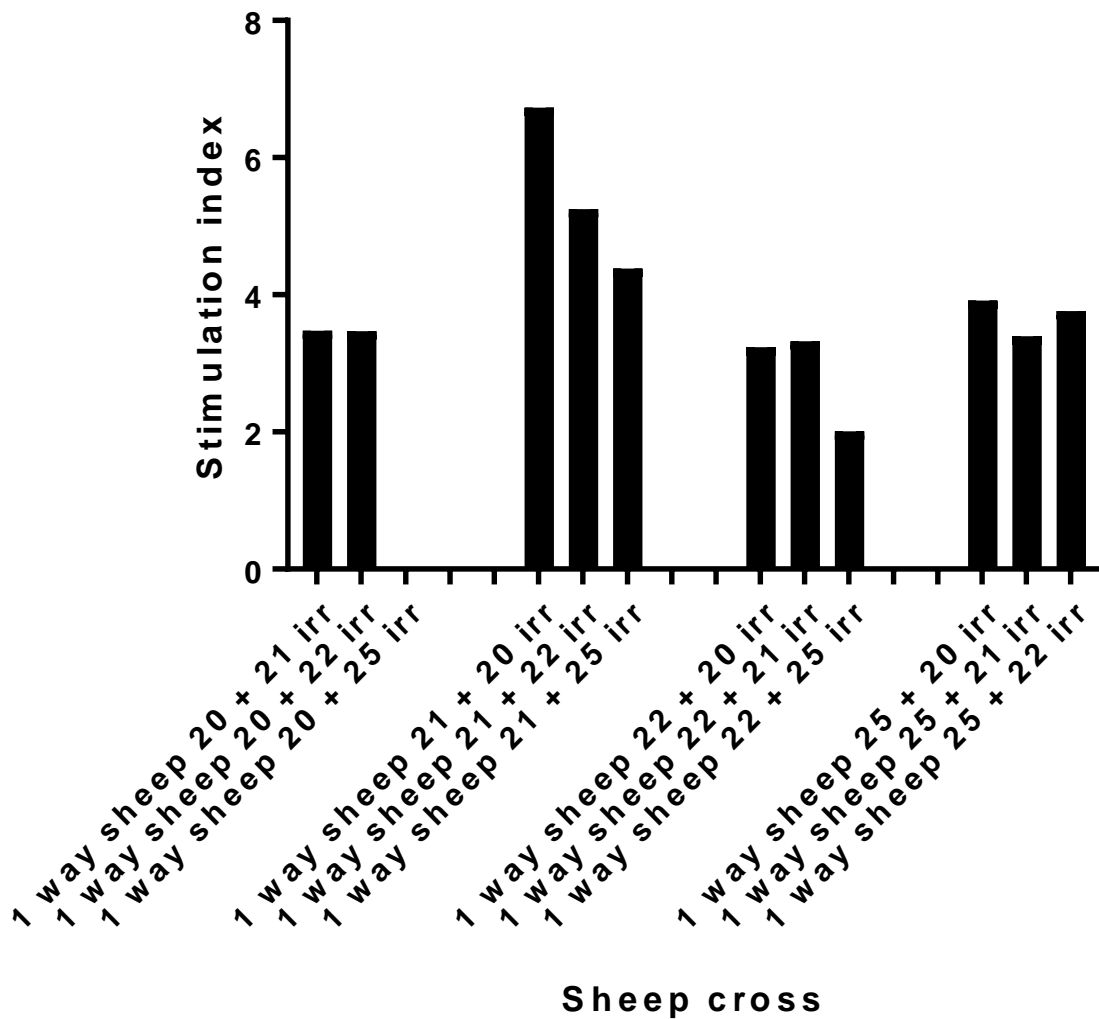


Figure 6.3 One way mixed lymphocyte reactions from the pool of sheep designated for the MSC recipient experiments. PBMCs were collected from each of the sheep and the cells split into stimulators and responders, with the stimulators being irradiated to halt cellular division. The reactions were then set up so that each sheep would respond to every other sheep. The MLRs were carried out as detailed in chapter 2, section 2.8 Transplantation pairs were selected based on mutually high stimulation indices of two sheep.

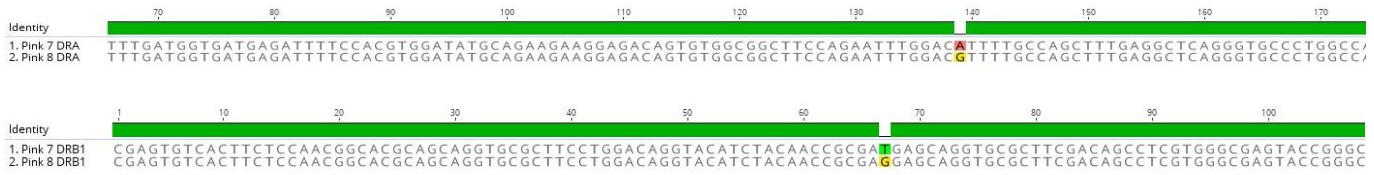
Similar to the control group pool, the MSC group had issues with high base immune reactions resulting in sheep Red 23 and Red 24 being excluded from consideration. Additionally, it was discovered that sheep Red 24 had been exposed to and possibly consumed, the hepatotoxic plant *Heliotropium europaeum*, sometimes referred to as potato weed. Given that cyclosporine metabolism is dependent on the liver associated enzyme cytochrome P450 3A, it was uncertain how *Heliotropium europaeum* induced hepatotoxicity would impact cyclosporine elimination. Thus sheep Red 24 was removed from possible use for any further experiments.

6.3.2 Tissue Typing

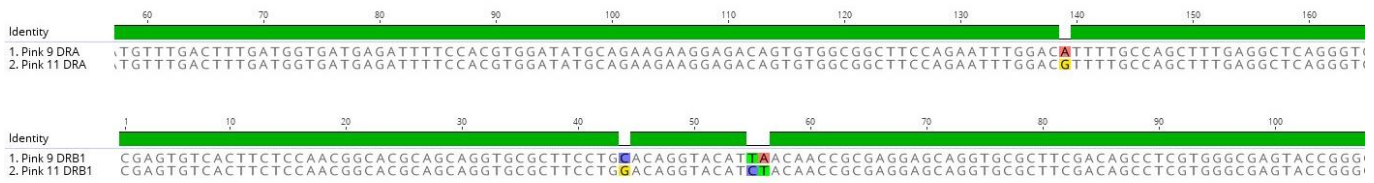
Direct sequencing of the Ovar DRA and DRB1 genes was performed to confirm that the sheep donor-recipient pairs would be tissue mismatched as detailed in chapter 4.

The haplotype sequences show that each sheep pairing had at least one mismatched allele, ensuring that the host immune system would react in response to the allograft. As it was not feasible to sequence further ovine leukocyte antigen genes it is possible that there are further mismatches that remain to be investigated, but for the purposes of the experiment a single mismatch was sufficient to indicate that rejection would occur.

Pink 7 crossed with Pink 8



Pink 9 crossed with Pink 11



Red 21 crossed with Red 25

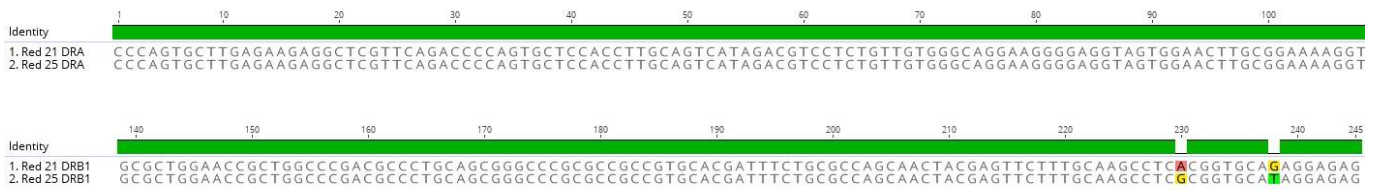


Figure 6.4 Sequence alignments of the DRA and DRB1 genes from the eventual transplantation pairings. Sequencing was carried out at the same time as MLRs and both results used to inform animal selection. Mismatches in these genes ensure a vigorous immune response once cyclosporine is withdrawn. The mismatched base pairs are highlighted. Although not all animals have the same number of mismatches they all produced strong MLR reactions.

6.3.3 Control Sheep

After excluding animals that had complications preventing a completion of the experimental terms, this left 2 control animals, Pink 7 and Pink 11.

6.3.3.1 Sheep Pink 7

Pink 7 underwent a crossover transplant with Pink 8, unfortunately the kidney function of Pink 8 rapidly declined after a biopsy was performed and had to be euthanized early. The transplant for Pink 7 went well lasting four hours and thirty minutes with an ischemia time of 93 minutes. Recovery was uncomplicated with the animal becoming ambulatory and consuming food and water less than 2 hours after surgery. Pink 7 persistent until day 13 before rejection induced graft failure caused a creatinine level above 600 μ mol/L, the experimental cut off, requiring euthanasia.

The only notable complications were when the sheep pulled the urinary catheter out on day 8 requiring that the animal be anesthetised so a replacement catheter could be inserted, this was then pulled out again on day 9 but was able to be replaced without the need for anaesthesia and was anchored with several sutures. Additionally, there was blockage of the urinary catheter day 11 but this was able to be cleared using saline. Aside from these issues no other problems arose and, based on the creatinine and urea levels, Pink 7 had good renal function almost immediately after surgery. A sharp and steady increase in both creatinine and urea beginning on day 9 was preceded by the withdrawal of cyclosporine on day 7.

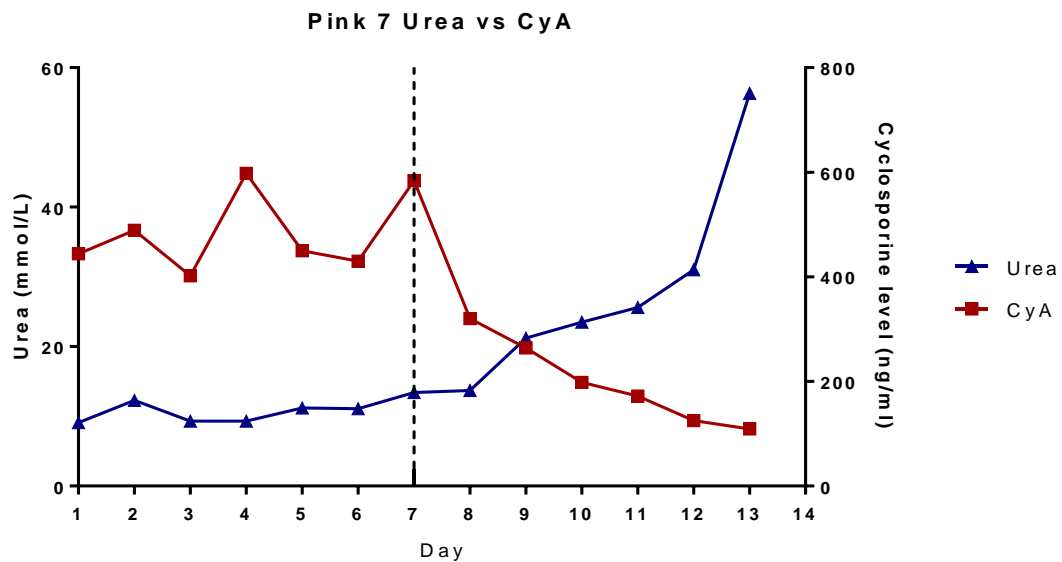
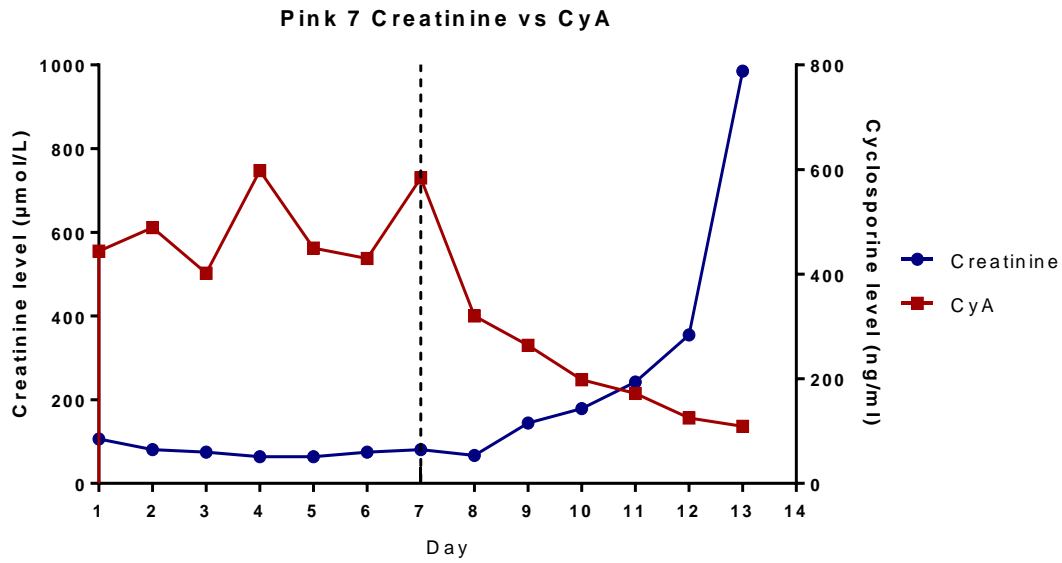


Figure 6.5 Creatinine and urea levels of sheep Pink 7 over the course of the transplant experiment vs cyclosporine levels. The transplant was carried out on day 1 and for each day during the first week the animal received 5mg/kg of cyclosporine and 10mg/kg of ketoconazole. This was withdrawn on day 7 (dashed line). From here, a steady decrease in the cyclosporine level is seen as well as a concurrent increase in both creatinine and urea.

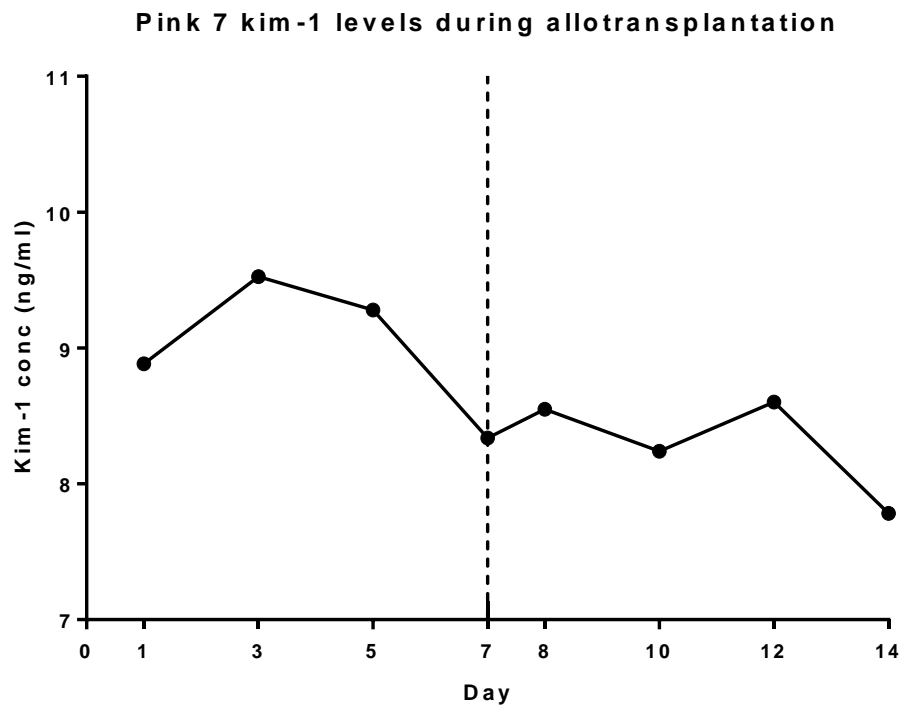


Figure 6.6 Kim-1 levels of sheep Pink 7 over the course of the experiment. The dashed line represents the withdrawal of immunosuppression on day 7 and also acts to divide the experiment into the early graft function phase and the rejection phase. An increase in urinary kim-1 is observed during the early graft phase in response to the IRI experienced by the kidney during the transplant procedure.

The Kim-1 urine level in Pink 7 peaked on day 3 after the ischemic injury caused by the transplant procedure. This is to be expected as cells undergo de-differentiation and shed the extracellular domain of kim-1 as they attempt to repair the damage. This is then followed by a decrease in kim-1 levels from days 3 to 7 as the cells regenerate. Unexpectedly, the kim-1 levels remained low as the immunosuppressant was withdrawn and rejection began. Given the wide ranging damage that occurs during rejection it was predicted that this would result in increased kim-1 levels, however this reduction during rejection is not isolated to Pink 7 and is consistent amongst all animals tested (n=4).

6.3.3.2 Sheep Pink 11

Sheep Pink 11 underwent a heterotopic kidney transplant, receiving a left hand kidney from sheep Pink 9, followed by a bilateral nephrectomy. The animal received 5mg/kg cyclosporine and 10mg/kg ketoconazole for the first 7 days of the transplant. This was then withdrawn and the graft allowed to reject. Pink 11 persisted until day 14, the end time point, before its serum creatinine made it over 600 μ mol/L. The surgery lasted three hours and eleven minutes with an ischemic time of 35 minutes, which was the shortest ischemic time of any allotransplant. The sheep was standing and eating an hour and 46 minutes after the completion of the surgery with good urine flow from the transplanted kidney. The complications were similar to those observed in Pink 7 with the urinary catheter being pulled out on day 4, requiring anaesthesia for it to be put back in and anchored using sutures. Following this there was an obstruction in the catheter on day 5 which impeded urine flow. This was able to be fixed with only minor adjustments of the catheter.

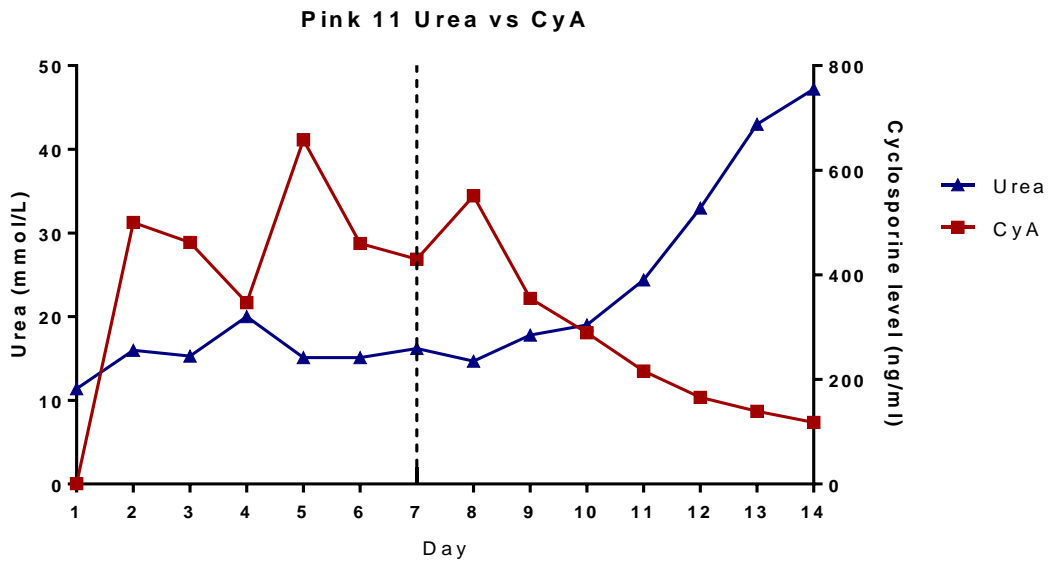
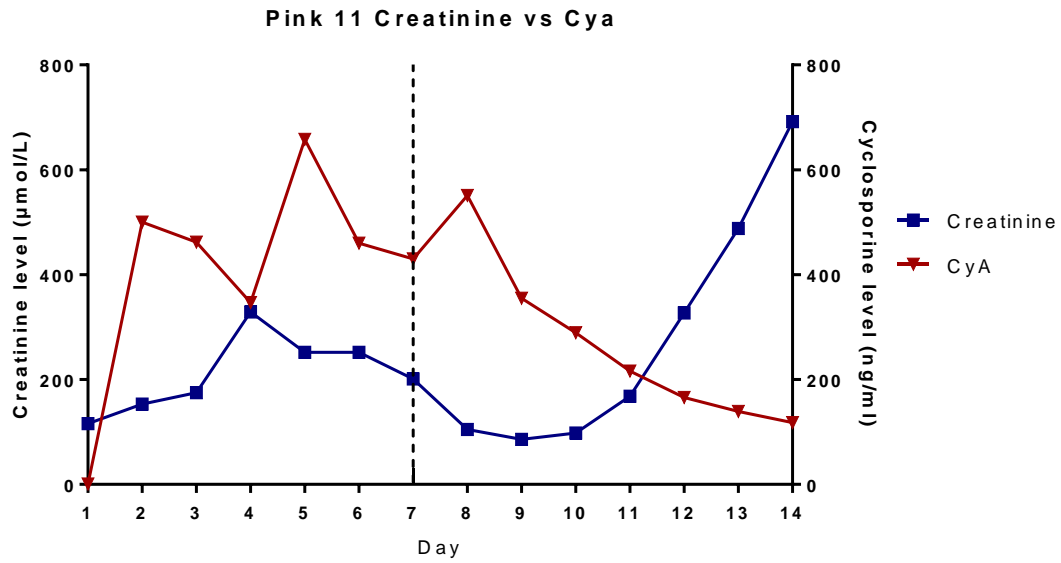


Figure 6.7 Sheep Pink 11 serum creatinine and urea levels vs blood cyclosporine levels over the course of 14 days from transplantation (day 1) to withdrawal of immunosuppressive (day 7) to euthanasia (day 14). Both creatinine and urea remain at adequate levels for the first 7 days until the cessation of cyclosporine, upon which time rejection begins to occur and an increase in both creatinine and urea is seen as cyclosporine levels fall.

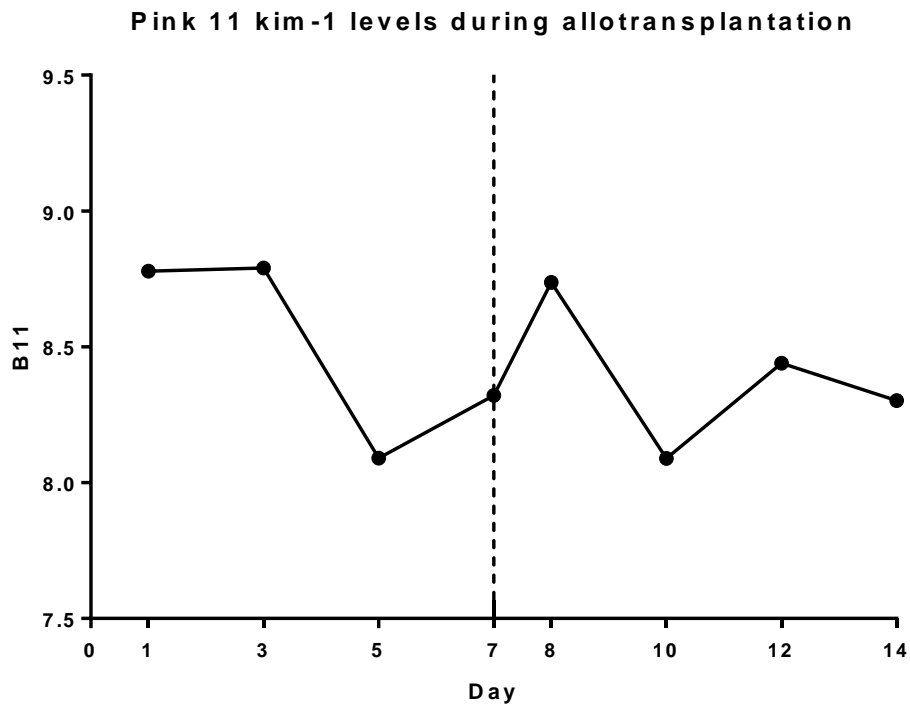


Figure 6.8 Urinary kim-1 levels of sheep Pink 11 during the transplant experiment. Like Pink 7, kim-1 was elevated for the first 3 days after the completion of the transplant with the peak kim-1 level being reached on day 3. This is in response to the IRI damage experienced by the kidney followed by the beginning of the cellular repair process. The withdrawal of cyclosporine on day 7 was followed by another peak, something not seen in the other allotransplants, but this soon decreases and falls to its lowest point on day 11 before finishing the experiment slightly elevated.

Based on figure 6.7, there was sufficient kidney function to keep the blood creatinine and urea levels within normal range for the first 3 days. However, on day 4 there was a peak in creatinine and urea, this corresponds with Pink 11 pulling the urinary catheter out, stopping the flow of urine and decreasing kidney function. The withdrawal of immunosuppressant on day 7 was, again, quickly followed by an increase in serum creatinine and urea indicating a progression to rejection.

The urinary kim-1 levels of Pink 11, like Pink 7 peaked at day 3 and then began to decrease. There was another peak on day 8 before the decrease during rejection similar to what was seen in Pink 7, the underlying cause of this decrease is unknown.

6.3.4 MSC Sheep

6.3.4.1 Sheep Red 21

Red 21 underwent a crossover transplantation with Red 25. The surgery time was 5 hours and the ischemic time was 1 hour and 20 minutes. The animal was given 5mg/kg cyclosporine and 10mg/kg ketoconazole for the first 7 days. During the course of the experiment the animal encountered several issues. On day 3 swelling of the area around the transplanted kidney was noted, although not unexpected it justified closer monitoring after what occurred with sheep Pink 5. Red 21 also developed diarrhoea on day 3 which improved by day 5, however on day 5 there were indications that the animal was dehydrated, namely, the darkened colour and decreased flow of the urine. This was addressed by giving 1 litre of I.V fluids for the next two days. On day 7 there was clotting of the urinary stent, this was fixed by adjusting its position in the ureter. The adjustment then had the unintended consequence of making it possible for the stent to be pulled out by the sheep. A replacement catheter was inserted and urine flow re-established, although this catheter also had a tendency to come out of its position, however, the swelling around the kidney made it difficult to

suture the catheter in place without the risk of creating an infection in the graft, so vetbond super glue was used as a temporary solution. Sheep Red 21 made it to the experimental end point of 14 days before being euthanized.

4 weeks prior to the transplant surgery, Red 21 underwent a bone marrow biopsy to allow for the isolation and expansion of MSCs. The surgery itself was uneventful and the sheep recovered well with no lasting effects. The MSCs were isolated using a ficoll density gradient then selected using plastic adherence as detailed in chapter 2 (Section 2.9). On the day of the transplant the MSCs were harvested from their flasks under sterile conditions, they were then resuspended in 10ml of saline supplemented with 500 units of heparin; in total 55.6×10^6 cells were successfully harvested. Just prior to the completion of the arterial anastomosis the cells were injected into the renal artery using a 16 gauge catheter.

The serum creatinine and urea levels of Red 21 follow the pattern seen in the control animals, steady for the first 7 days, then quickly increasing after the withdrawal of immunosuppressant. The one anomaly is a peak in both creatinine and urea on or around days 2 and 3, this is unlikely to be explained by the observed dehydration as this did not occur until day 5 and may have been a result of diarrhoea precipitated by decreased graft function.

Unfortunately, the skin pocket used to contain the transplanted kidney did not fully adhere to the kidney capsule. Due to this it was decided that biopsies would not be taken during the course of the experiment as the risk of losing the kidney due to infection was too great.

Instead it was decided that the data gained from the other metrics outweighed the potential gain from the time course biopsies. The urinary kim-1 levels of Red 21 have a different progression to those seen in control group. The kim-1 levels of Red 21 doesn't reach its peak on day 3 like the control animals; this is instead delayed until day 7 but is, again, followed by a decrease in kim-1 levels during the rejection phase of the experiment.

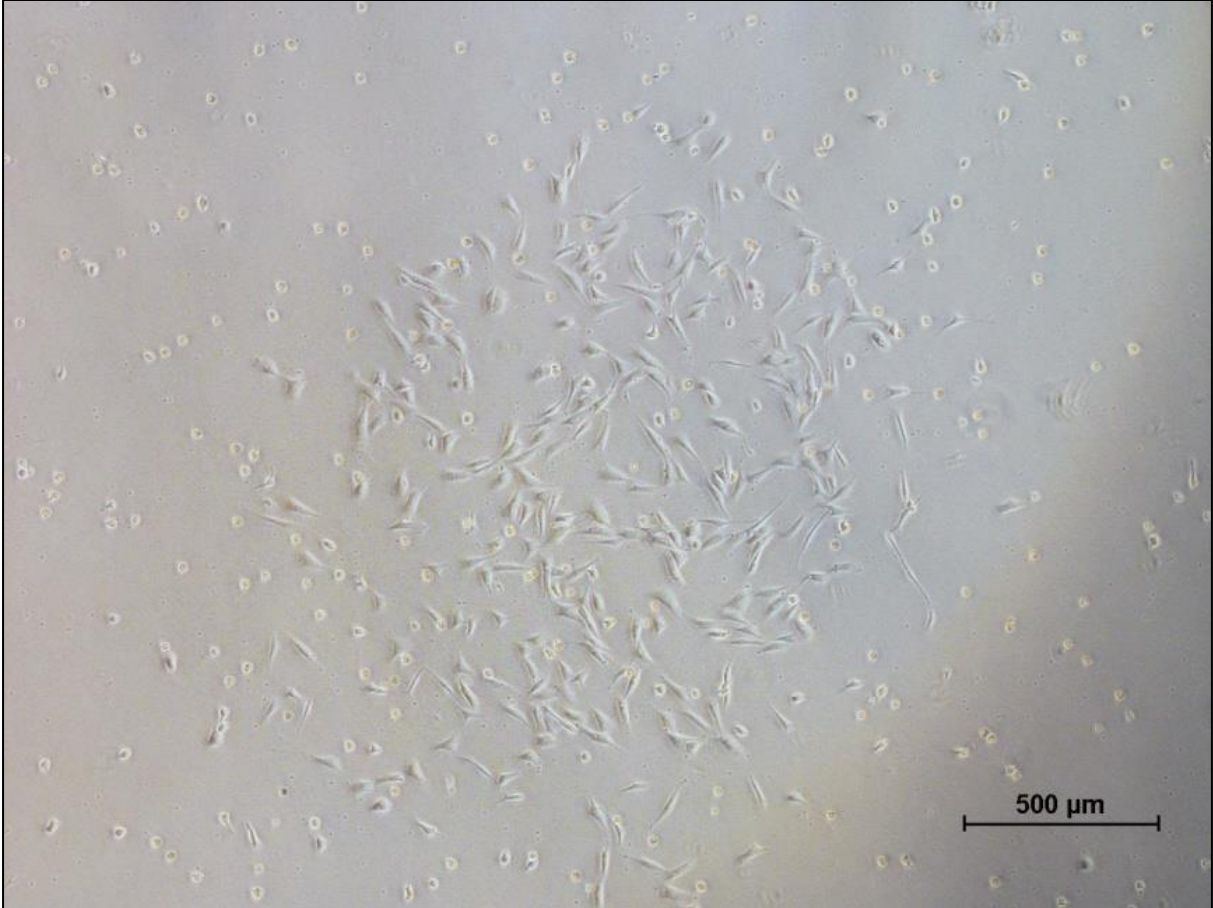


Figure 6.9

200x light microscope image of MSCs 10 days after being isolated from sheep Red 21. After being initially isolated using a ficoll density gradient the cells are then selected for using plastic adherence by being cultured in plastic flasks for 10 days. Here the seeded MSCs are beginning to take on their characteristic “fibroblast like” morphology.

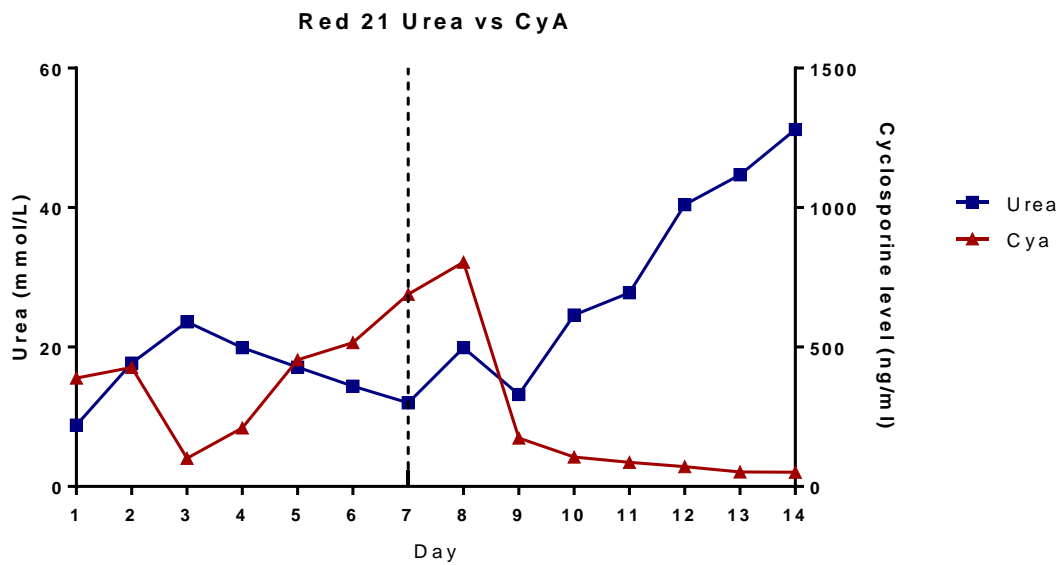
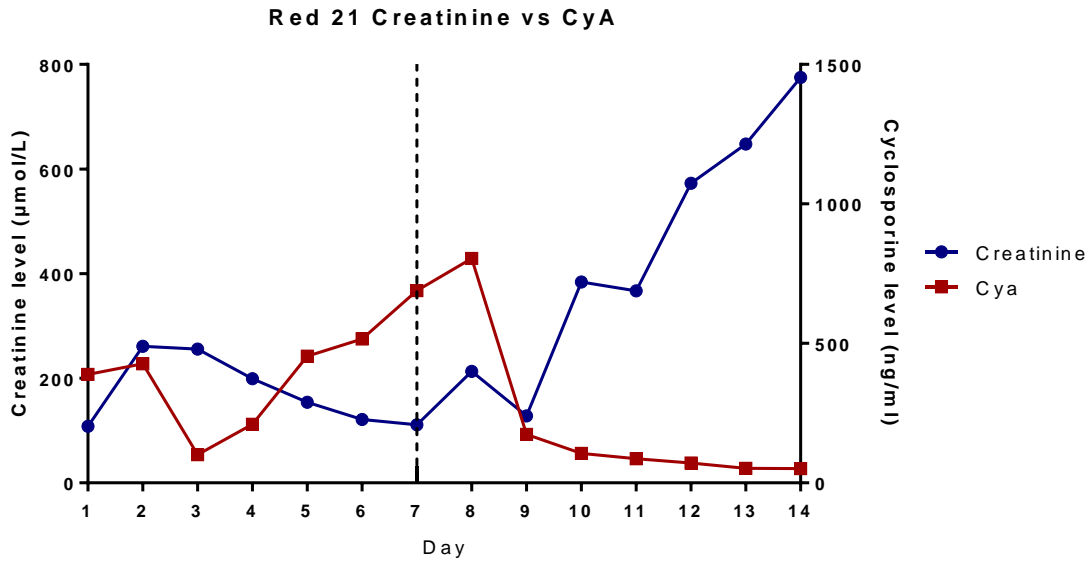


Figure 6.10 Serum creatinine and urea vs. blood cyclosporine levels for sheep Red 21. Both creatinine and urea levels of Red 21 were elevated during the early phase of the experiment but started to normalize in the days following. The cessation of immunosuppressant on day 7 (dashed line) resulted in rejection and a steep increase in both creatinine and urea until euthanasia of the sheep on day 14.

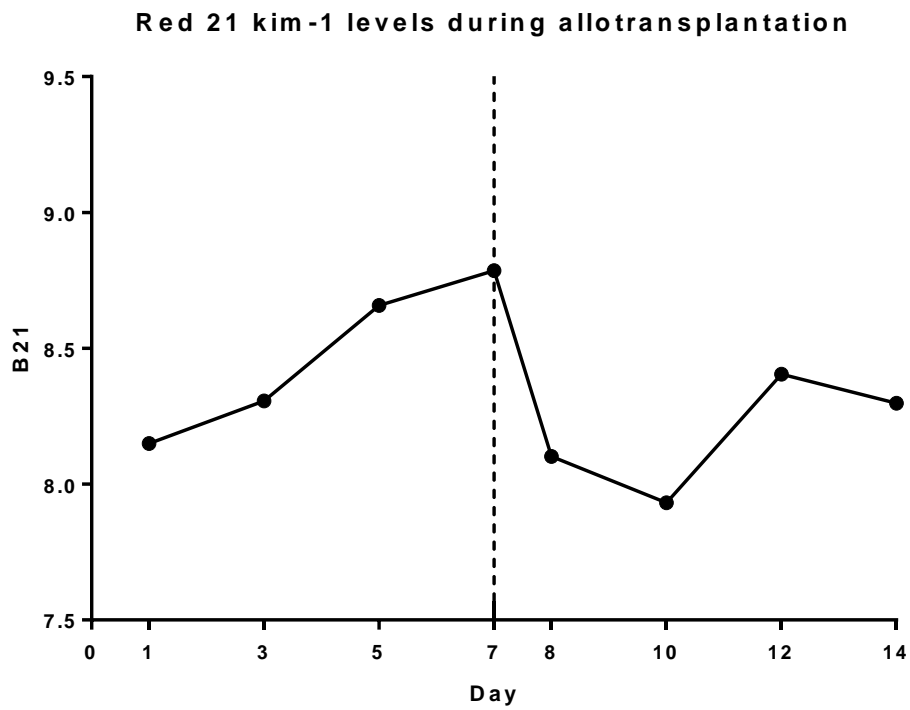


Figure 6.11 Urinary kim-1 levels of Red 21 over the course of the transplant experiment. The kim-1 levels remain at a relatively low level for the days immediately after the surgery only peaking on day 7 before falling during the rejection period of the experiment. In the final few days the kim-1 levels begin to rise again as the graft endures catastrophic damage from rejection.

6.3.4.2 Sheep Red 25

Red 25 underwent a crossover surgery with Red 21 and a bilateral nephrectomy. The surgery lasted 4 and a half hours and the kidney had an ischemic time of 81 minutes. As per the experimental protocol, Red 25 received 5mg/kg of cyclosporine and 10mg/kg of ketoconazole for the first 7 days of the experiment. This was then withdrawn to allow the graft to be rejected. There were several complications throughout the experiment but these were overcome and the animal was able to make it to the 14 day end point. Post surgery, Red 25 was slower to recover than Red 21 and once it did it experienced swelling around the transplanted kidney almost immediately. There were problems with the flow of the urine for the first 2 days but this was resolved by day 3 after some adjustments to its position in the ureter. There was a further issue on day 5 with the stent becoming blocked by a small blood clot; this was able to be rinsed out with saline, this occurred again on days 7, 8, and 12. An increase in temperature was noted on day 6; additional antibiotics were given to attempt to address this however the temperature persisted out to day 14. No other signs or symptoms of infection manifested. On day 10 a significant swelling developed around the neck and jaw of Red 25 causing some discomfort, this was likely caused by rejection associated immune functions. As rejection proceeded the sheep began to display further signs of pain and discomfort such as teeth grinding, and a prostrate body position. Pain relief was given to help with this until euthanasia on day 14.

Like Red 21, Red 25 also underwent a bone marrow biopsy 4 weeks prior to the transplant surgery. The animals recovered from this well with no lasting impact. The bone marrow was processed and MSCs expanded as previously detailed (chapter 2 sections 2.9 and 2.11). On the day of the surgery the MSCs isolated and expanded from Red 25 were harvested yielding 68.8×10^6 cells which were then injected into the renal artery of the kidney graft just prior to the completion of the arterial anastomosis.

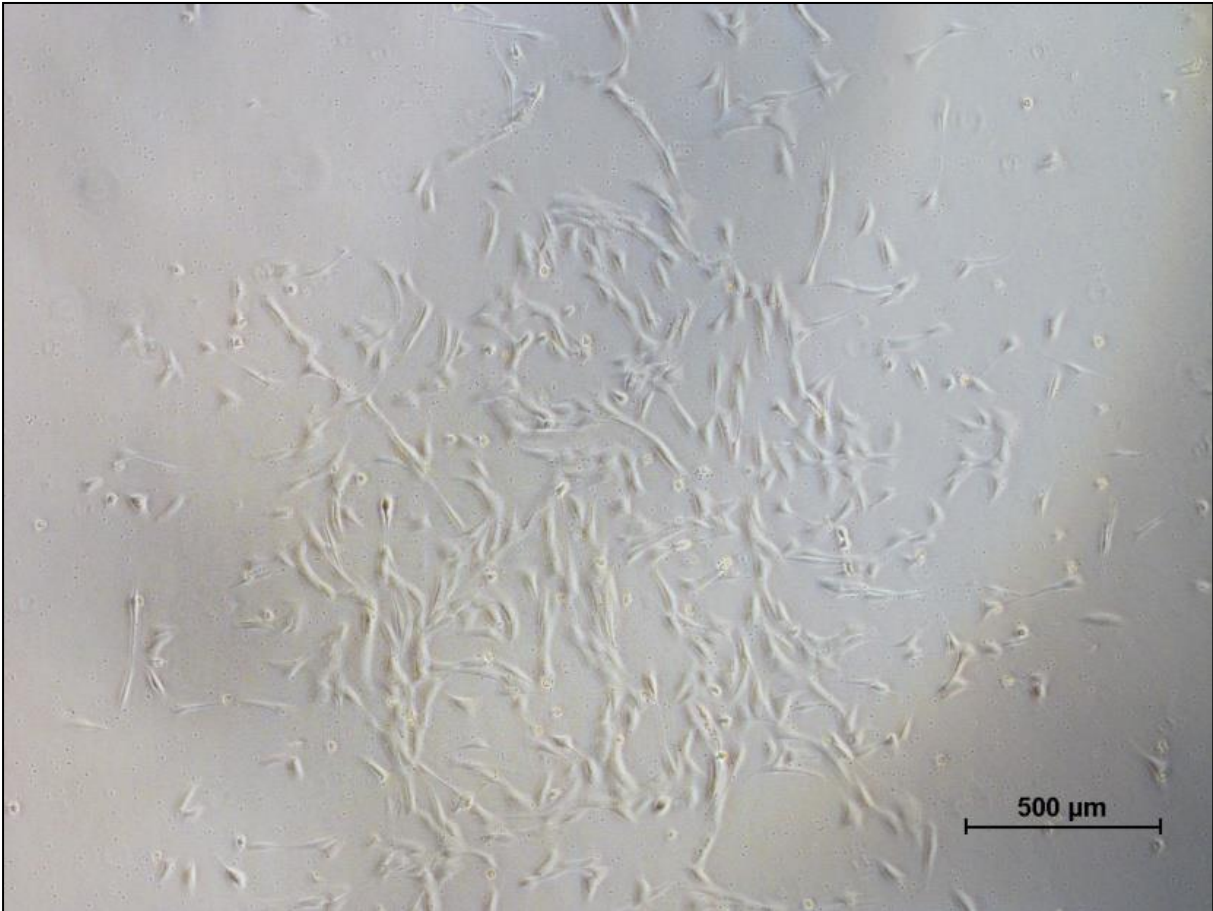


Figure 6.12 200x light microscope image of MSCs 10 days after being isolated from sheep Red 25. As previously detailed, bone marrow aspirate was isolated from the iliac crest of Red 25 4 weeks prior to the transplant surgery to allow for MSCs to be expanded. This image shows the MSCs after undergoing plastic adherence selection.

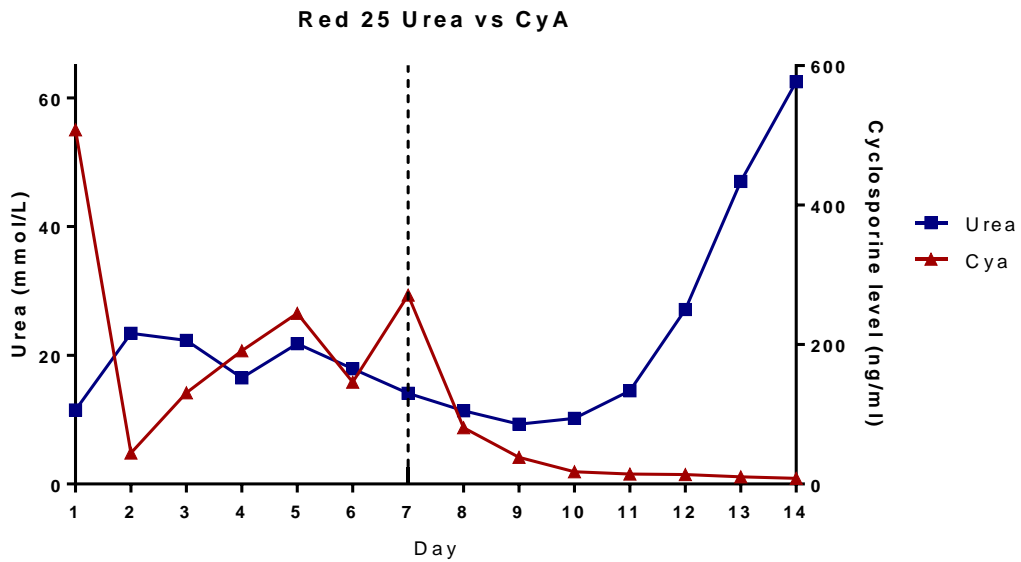
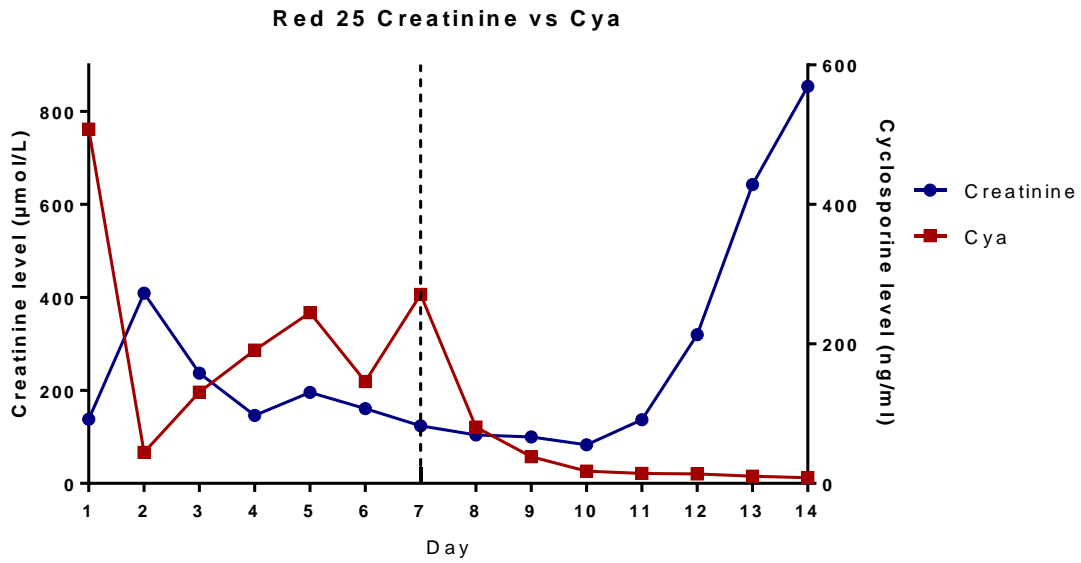


Figure 6.13 Serum creatinine and urea vs. Cyclosporine from sheep Red 25 during the 14 days of the transplantation experiment. Day 2 saw a spike in both creatinine and urea before reducing to a normal range out to day 10 when rejection induced graft function caused both creatinine and urea to rapidly increase over the following days out to the day 14 end point.

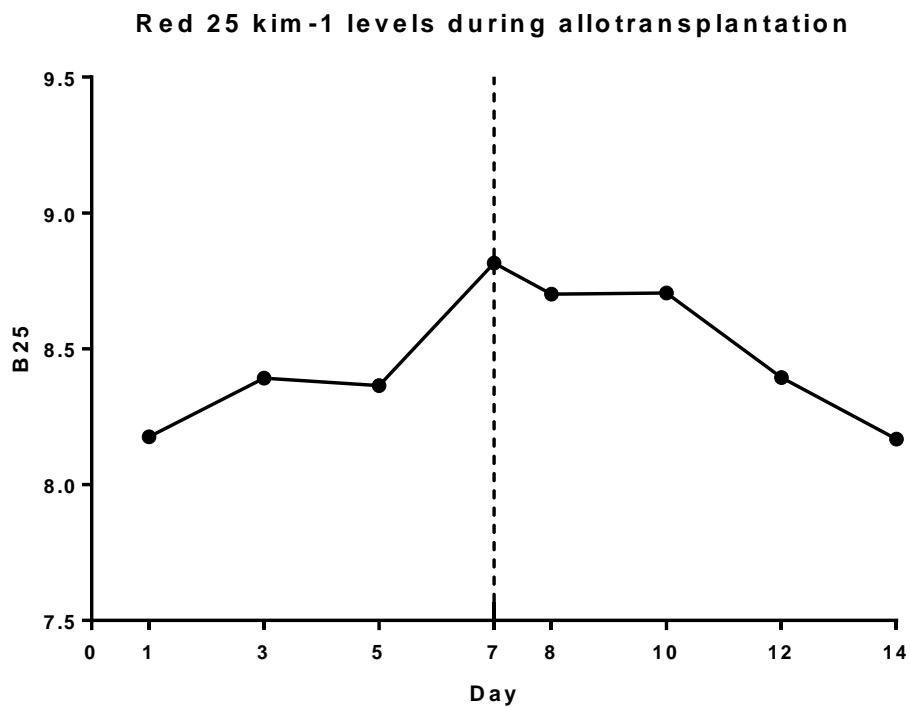


Figure 6.14 Sheep Red 25 kim-1 levels over the course of the 14 day transplant experiment. Kim-1 levels don't peak until day 7, later than what is seen in the control animals and more concordant with Red 21. The Kim-1 levels then decline over the following 7 days until the animal is euthanized. The insults to the kidney that should cause damage occurred on day 1 (transplantation) and days 7-14 (rejection) yet these are not reflected in the resulting kim-1 levels.

The serum creatinine and urea levels of Red 25 followed a pattern similar to that seen in Red 21. A peak on day 2 preceded a general downward projection in both serum and creatinine before the rejection associated increases after the cessation of immunosuppressant on day 7 and terminating in a final creatinine of 854 μ mol/L and a serum urea of 62.5 mmol/L indicating kidney graft failure.

Red 25 also had issues with the skin pocket not adhering to the kidney capsule, as such the time course biopsies were not able to be taken.

The urinary kim-1 levels of Red 25 are analogous to those seen in Red 21, with the peak level occurring on day 7. This peak was then followed by a decrease in kim-1 during the rejection phase of the experiment.

6.3.5 Results Comparison

Combining and comparing the creatinine and urea results from the control and MSC groups gives time course graphs that follow very similar patterns. As each group only contains 2 animals the errors bars are very large and the significance of the results cannot be determined. However, the MSC group has higher creatinine and urea in the early graft phase but that this tends towards the control group levels as the experiment continues.

The other difference between the two is the urea of the MSC group is lower on day 9. However, after day 9 the urea levels increase until they are in line with what is seen in the control group. As this is a single time point and the group's N numbers are small, it cannot be ruled out that this difference was due to chance.

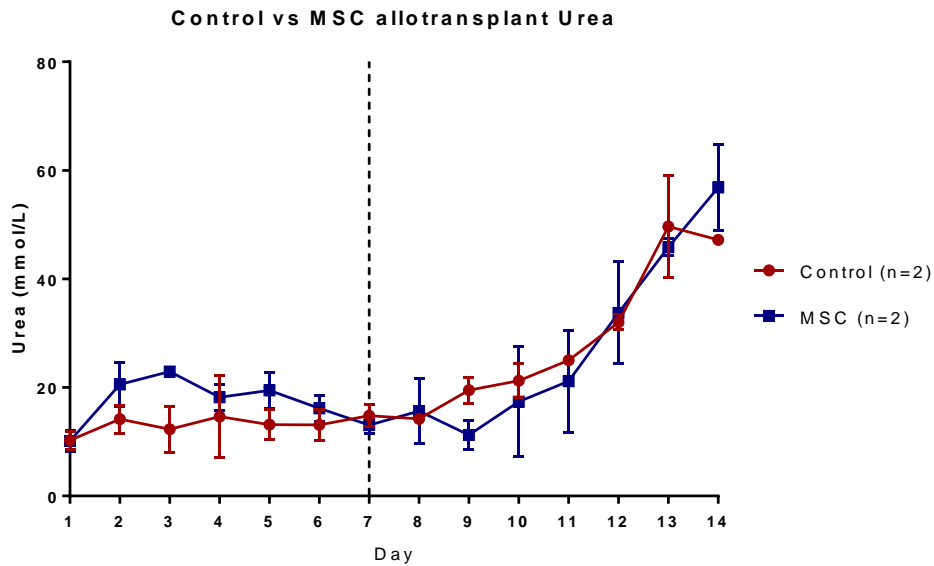
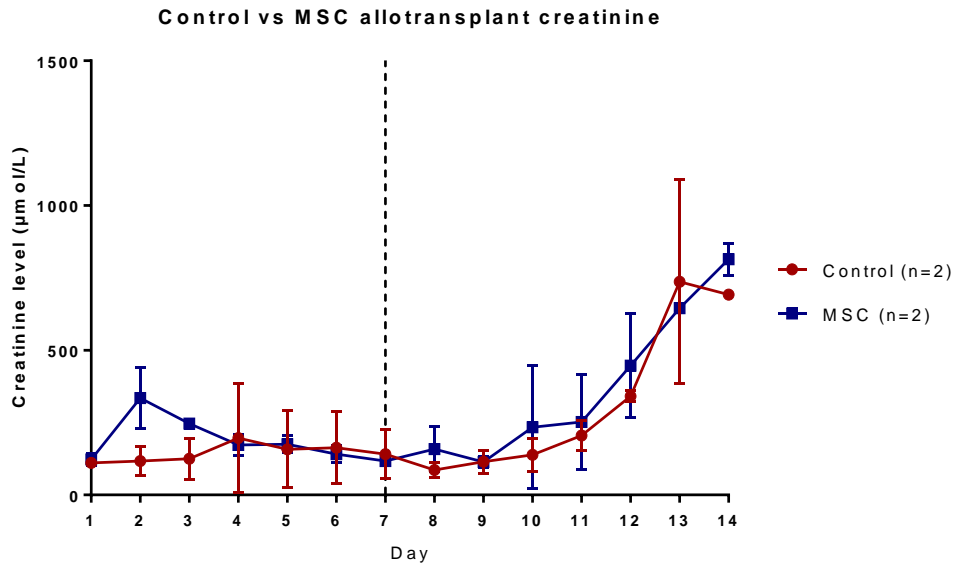


Figure 6.15 Plotting the average serum and creatinine and urea of the control group and the MSC groups it is observed that they follow a similar progression over the course of the 14 day experiment. In the first week both groups maintain creatinine and urea within a normal range. Withdrawal of cyclosporine on day 7 precipitates a rapid increase indicating graft failure due to rejection. Notable deviations are creatinine being higher in the MSC group on day 2 (117 $\mu\text{mol/l}$ vs. 335 $\mu\text{mol/l}$) and urea being higher in the control group on day 3 (12.30 mmol/l vs. 22.95 mmol/l)

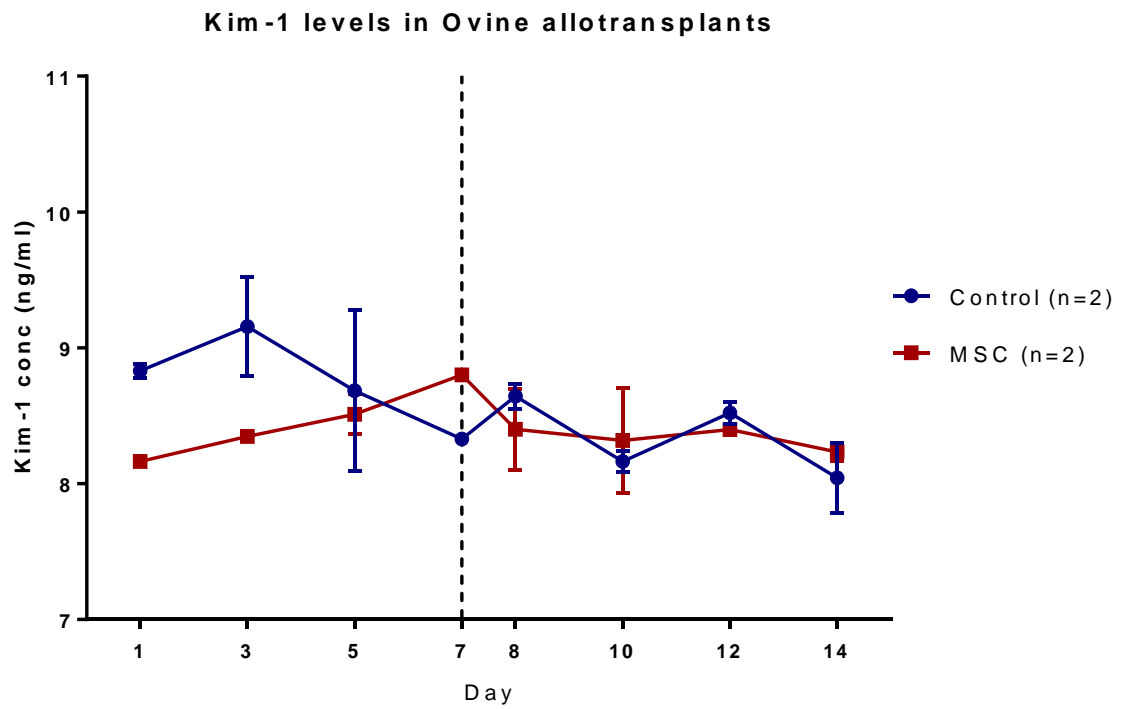


Figure 6.16 Graph showing the average urinary kim-1 levels of the control and MSC groups over the course of the 14 days post transplant. The control group experienced a peak on day 3 while the MSC groups peaked on day 7. This resulted in a difference on day 3 with the control group excreting 9.158 ng/ml of kim-1 and the MSC group excreting 8.349 ng/ml of kim-1

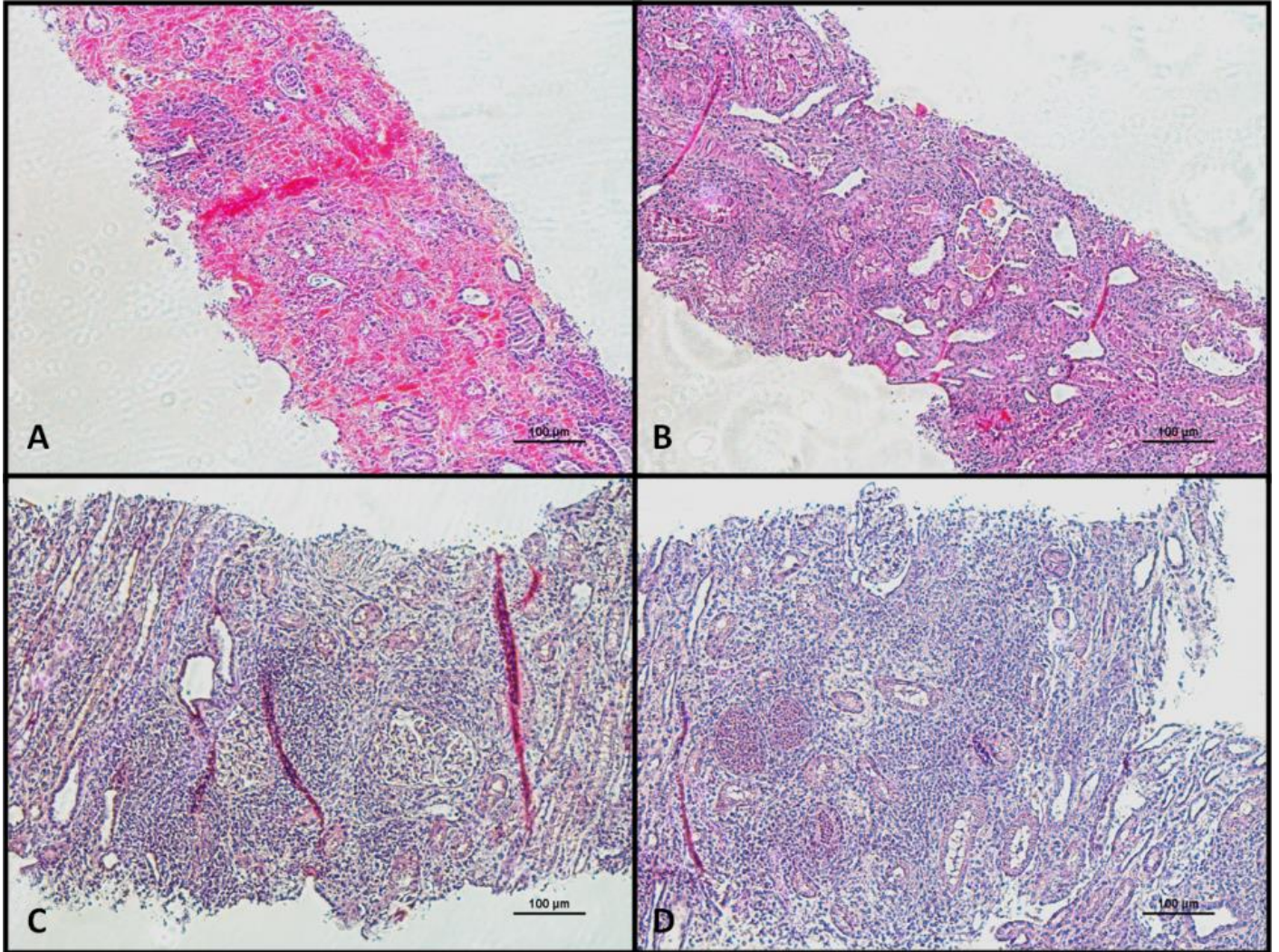


Figure 6.17 100x histological images from the terminal time point of sheep Pink 7 (A), Pink 11 (B), Red 21 (C) and Red 25 (D). Punch biopsies were collected on the final day of the experiment and stained with H&E to allow for visualization of rejection associated markers. All sections show extensive signs of rejection, most prominently, interstitial cellular infiltrate (dark purple dots). The section from Pink 7 shows signs of haemorrhaging (bright pink staining).

Banff scores of control allografts vs. MSC treated allografts

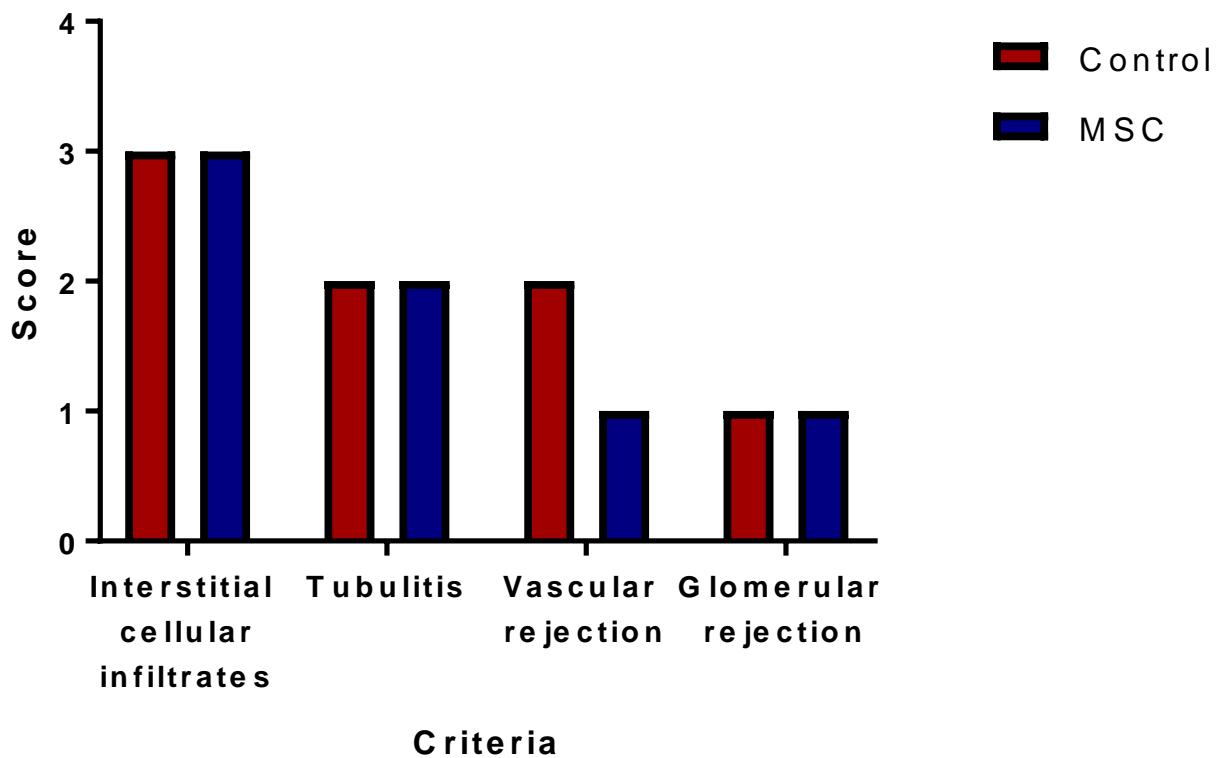


Figure 6.18 Banff grading scores of terminal punch biopsies of both control and MSC treated sheep. Tissue from transplanted kidneys was collected during the necropsy and placed in formalin. The tissue was then embedded in paraffin, cut, and stained with H&E to allow histological analysis. The sections were blinded and scored by two 3rd party individuals according to the Banff grading schema 2013/2014. The rejection score is the same for all categories except vascular rejection in which the MSC group is lower.

The analysis of the kim-1 results from the control and MSC groups shows that the MSC group has a lower urinary kim-1 level during the early phase of the experiment with the difference reaching its greatest level on day 3. After this the kim-1 levels of both groups trend slightly downwards during the rejection phase.

Because biopsies were unable to be performed through the experiment on some sheep it was not possible to carry out a time course histological analysis of rejection. The only comparison that can be made is using the biopsy samples collected at the time of death which are displayed in figure 6.17. From these images, it is apparent that all four sheep had high levels of cellular infiltrate and disruption to the kidney structures. The section from Pink 7 is seen to have a large amount of blood throughout the tissue (bright pink stain) due to haemorrhaging caused by rejection disrupting the vasculature, this resulted in the sections from Pink 7 being unable to be scored for rejection. The slides were scored by two 3rd party experts according to the 2013/2014 Banff grading schema, this is presented in figure 6.18. The resulting data indicates that across the categories of interstitial cellular infiltration, tubulitis, and glomerular rejection the two groups scored the same. However, vascular rejection was lower in MSC group.

6.4 Discussion:

The early evidence supporting the use of MSCs in kidney transplantation provided positive outcomes across several measures [328, 329, 331, 334]. However, this evidence was largely gained using small animal models, and, as MSCs moved to the clinic, positive results became less obvious [341-343, 345]. The majority of pilot studies hedge these unconvincing results in terms of safety profiles, which is certainly one of the important aspects of pilot studies. Of some concern however, is that these inconclusive results have continued in larger clinical trials [346-348]. As discussed in chapter 1 many of the findings of the clinical trials

are not definitive and have several confounding factors that have the potential to obscure the actual impact that MSCs have in these cohorts. This is not to say that MSCs are not a worthwhile candidate for cellular therapy, rather, it may be an indication that their clinical application was rushed and that there is a need to return to basic science to gain a greater understanding of the best practice for the use of MSCs in kidney transplantation.

The present study has used a large animal model of kidney allograft transplantation and rejection to examine the impact of direct arterial administration of MSCs into the renal artery on graft function and immunomodulation. This is the first such experiment to be carried out in a large animal model. Based on the work presented in chapter 5, previous work carried out by Dr Dyan Auclair (unpublished), the mechanisms through which MSCs exert their beneficial effects [245, 260, 261, 264, 313, 480, 481], and the results of the relevant literature [328, 330, 334, 482] it was decided that a direct arterial injection of MSCs would be used to try and achieve the highest possible accumulation of MSCs to the kidney allograft, while avoiding deleterious effects. This was done in an effort to create an environment suited to fostering the beneficial influence of MSCs on the progress of the graft.

No deleterious effects were observed by the direct arterial administration of MSCs during the experiments, demonstrating that this method of administration is safe. From these results however, it seems that the positive impact of the MSCs was minimal on early graft function and negligible on conferring resistance to rejection in the absence of mainline immunosuppressive drugs. Looking at the creatinine and urea results, the MSC group seemingly performed worse during the early phase of the experiment with higher serum levels for the first 3 days indicating a lessened graft function. This could potentially be explained by the presence of the MSCs in the kidney blocking small vessels as has been described in other models [249]. The high creatinine and urea would seemingly be at odds with the decreased kim-1 levels in the MSC group. However, if the MSCs were resident in

the graft during the early phase of the experiment it is possible that as they were reducing the impact of ischemia reperfusion injury [330] they were also causing blockages in the small vessels of the kidney. Thus, a consequence of MSCs reducing transplant related damage may be early graft dysfunction, but this would appear to abate in a relatively short time frame.

During the rejection phase of the experiment there were no observed differences between the control and MSC group. There are several possibilities that could explain this outcome. First, there could be an issue regarding the size of kidneys of a larger animal and the variability of nephron number between both species and individuals in a species. The larger size of the sheep kidney [486] in relation to rodent kidneys [487] results in greater distances that MSCs would need to travel in order to reach all damaged areas in a transplanted kidney, this may result in an unequal distribution of MSC throughout the kidney and thus some areas may not benefit from their administration. Additionally, there is significant variation in the number of nephrons both between species and within a species. However, given the inbred nature of experimental rodent models this variation will be minimized whereas this ovine model makes use of out bred sheep [486, 487]. This gives a further variable that is exceedingly difficult to correct for but is also more representative of a human population [488]. If the issue comes down to variation in nephron number then it may require increasing the dosage to ensure adequate cell number to have a positive effect. If the issue is a lack of distribution due to size and a macro scale form of steric hindrance, then this could possibly be overcome via the use of machine perfusion of MSCs with increased flow pressure, forcing the cells into areas with constricted vasculature.

Another possibility to explain the lack of positive result is that the MSCs weren't activated in this model. It is known that inflammatory markers are able to drive MSCs to produce immunosuppressive and anti-inflammatory cytokines [313, 480, 489]. As the cold ischemia time was relatively short, on average 72 minutes, it is possible that there was not enough

damage to the kidney for the MSCs to have a significant effect or to be activated. This could also explain the lack of resistance to rejection. MSCs migrate and engraft in areas of high damage [478, 479], if the damage in this model wasn't enough to enable this engraftment then it is possible that the MSCs weren't present when the immunosuppressant was withdrawn, thus they could not act in an immunoprotective role.

An unexpected result was the low levels of urinary kim-1 during rejection in all animals examined. Given the extensive damage that occurred leading to graft dysfunction and failure it was expected that kim-1, as a marker of kidney damage, would become elevated. A possible explanation for this result may be that the time between IRI and rejection induced injury is so short in this model that cellular kim-1 levels hadn't had time to be replenished.

Although the results from these experiments are mixed they offer several possibilities for the future exploration of MSCs in transplantation. The low N number of the groups makes it so that definitive conclusions cannot be drawn. But, even with this limitation, the observed early difference in kim-1 levels between the two groups suggests that MSCs given at this early time point and given intra arterially may help protect against IRI induced damage but could also contribute to delayed graft function due to the occlusion of blood vessels.

Chapter 7

Concluding discussion

The ability of MSCs to cause immunosuppression [253, 264, 310], regenerate damage tissues [251, 455, 490], and home to sites of injury [478, 491, 492] have been noted and demonstrated repeatedly in many different settings. These characteristics have ensured that MSCs remain a popular candidate for clinical cellular transplantation and they have been found to provide improved outcomes in several conditions [493-497].

Theoretically, the beneficial effects of MSCs would seem to be uniquely suited to addressing the challenges associated with solid organ transplantation. However, the application of MSCs in human kidney transplant patients has produced underwhelming results thus far [341, 346, 348]. Although disappointing, this should not be especially surprising given the complexity of both solid organ transplantation and cellular therapy. A move back to basic science will allow a better understanding of the plethora of variables that can impact such an ambitious idea. With these factors acting as an impetus, this thesis examined the application of MSCs in a large animal model of heterotopic kidney transplantation.

7.1 Ovine Mesenchymal Stem Cells

MSCs were first isolated and characterized in sheep in 1994 [382], since then they have been further characterized and compared to MSCs from other species [326, 327, 384, 392, 498]. The work presented in this thesis is in agreement with the description of ovine MSCs from the literature and shows the cells isolated in sheep are analogous to those isolated in humans [242, 247].

Given the size of sheep, is it possible to isolate and expand MSCs without sacrificing the animal in a simple procedure lasting less than an hour, allowing for research on autologous MSCs to be conducted.

Of major concern to this work was the ability to label MSCs without any deleterious effects or changes in function. As shown in chapter 3, this was able to be achieved with no changes to differentiation, cell surface marker expression, and immunosuppressive ability. It was also demonstrated that the amount of iron label taken up in each labelling experiment was comparable, allowing for the MRI and SPIO based analysis carried out in chapter 5.

Unfortunately, the iron label used herein, Resovist®, is no longer produced. This hampered the ability to label the cells during the later allotransplantation experiments, stopping additional tracking from being carried out under those conditions. Although other superparamagnetic iron oxide nano particles are available they have not been validated to show their impact on MSCs in this research, although this would be possible for future experiments.

7.2 Ovine Heterotopic Kidney Transplant Model

Large animal research has been ensconced in transplant medicine since its inception and has been vital in developing many of the techniques and methods that allow such radical operations to be successful [447, 448, 499, 500].

The research presented here has built upon that long history of work by the use of a sheep model of both auto and allotransplantation [438, 439, 447-451]. Refinements to this model required a significant undertaking, as detailed in chapter 4. Several surgical modifications such as placing a central line into the inferior vena cava, and the use of a wound drain have acted to address a number of the complications associated with this model, benefitting future work. In addition to the surgical aspects of the model, the pharmacological and

immunological features of transplantation were addressed allowing for the control of rejection.

This model fills a gap in transplantation research as the number of large animal kidney transplant models is limited [446, 501, 502] but profoundly required, as shown by the lack of large animal work preceding the application of MSCs to human kidney transplant patients [335].

Although there are several large animal models of IRI [336, 422-424, 432, 433, 442], these are unable to study the intricate interactions that occur between the immune system, IRI, and immunosuppressant drugs in solid organ transplantation. Furthermore, many of the IRI models use a warm ischemia, vessel constriction, style of ischemia induction [336, 427, 432, 434, 442]. Although easier to perform it does not fully mimic the cold ischemia that human transplant organs undergo [503]. Vessel obstruction induced IRI also avoids the damage associated with the procurement and transplantation of an organ [66, 182]. This model is able to replicate these events both by themselves, as with the autotransplant variant, or in conjunction with the immune reaction, as with the allotransplant variant. Additionally, the placement of the kidney in the neck allows for superior visualisation and monitoring of the graft post transplant.

Even with the refinements made there are still several limitations to this model. The ovine leukocyte antigen system still remains poorly described and much of the genetic information is yet to be mapped. This restricted the number of OLA genes that could be sequenced, confining the picture that this technique could give about possible immune interactions between donor and recipient pairs to the DRA and DRB1 genes. Another disadvantage faced when using sheep is a relative lack of species specific reagents available, this was most

apparent when trying to create a sheep specific flow panel for MSCs and in the search for useful ELISA kits.

7.3 *In Vivo* Tracking Of Mesenchymal Stem Cells

A dearth of knowledge persists around the optimal method for the application of MSCs in kidney transplantation. The experiments presented in chapter 5 have attempted to further develop the information relating to the question of the best route of administration.

Venous administration is currently favoured by many groups [329, 331, 333] and has been used in all of the clinical trials so far performed [346-348] and all but one of the pilot studies carried out [339-345]. The use of venous administration has valuable benefits, including the ability to dose at anytime, independent of when the transplant was carried out, without requiring surgical intervention. Additionally it is seen as a safer way to give MSCs, avoiding any possibility of clotting or blocking fine blood vessels [249] and it is thought that, given MSCs ability to home to sites of injury [456, 504, 505], intravenously administered MSCs would be able to move to the areas where they are required.

Using the iron nano particle labelling technique from chapter 3, it was possible to track the movement of MSCs in sheep that had undergone autotransplantation using a 1.5T MRI machine and Prussian blue histological staining. Administering the MSCs though a central line placed in the inferior vena cava gave a reading that indicated the MSCs passed though the transplanted kidney at 15 minutes post administration, but that by 30 minutes there were not enough cells present to be detectable.

Upon histological examination of tissue collected 5 days post administration, it was found that the MSCs were dispersed throughout all of the organs sampled, those being the lungs, liver, spleen, transplanted kidney, and native kidney. This finding was in agreement with what had been previously found in the literature [408, 470-472]. It has been speculated that a

majority of intravenously administered MSCs becoming trapped in the lungs, as the lungs are the first major organ I.V. MSCs encounter and are replete with small vessels able to trap the cells [506]. The localization of the MSCs to the spleen and liver is proposed to be associated with the elimination of the cells due to the high density of resident macrophages [475, 507]. Ways and means to avoid this loss of MSCs is a potential avenue to increase the efficacy of a given dose of cells. Finding the cells in the native kidney was somewhat unexpected as it was not damaged or occluded during the transplant procedure. A possible explanation is that the cells simply became trapped in the fine vasculature of the kidney, similar to what is seen in the lungs. However, the number of cells found in the native kidney was significantly less than what was observed in the transplanted kidney. This difference could be due to the homing ability of the MSCs tracking to the damaged kidney which could also have been aided by the superior blood flow provided to the transplanted MSCs from the carotid artery.

The accumulation in the transplanted kidney is considerably less than what was observed in previous experiments where the cells were administered into the renal artery. This difference in accumulation could explain the superior outcomes of direct arterial administration of MSCs into transplanted kidneys relative to intravenously administered MSCs observed in the literature [334].

This experiment had several limitations. One of the most significant was the inability to image the lungs *in vivo*. As it has been shown repeatedly that MSCs accumulate in the lungs, it would have been useful to know how soon this occurs and how long they persist. However, imaging the lungs at a resolution congruent with the detection requirements of SPIO labelled MSCs would have necessitated the use of hyperpolarized gases [508] and special ventilation equipment that was not available. Another shortcoming was a lack of resolution of *in situ* organs. Although the placement of the transplanted kidney allowed for exceptional imaging, the rest of the organs had issues with interference from surrounding tissues. These

experiments were carried out using a 1.5T MRI, since their completion however, a 3T MRI has been installed at the large animal research and imaging facility. Any further research using this machine should have a much greater resolution and sensitivity.

7.4 Mesenchymal Stem Cells In Kidney Transplantation

The specific properties of MSCs have generated considerable excitement about their possible application to solid organ transplantation and in particular their application to kidney transplantation. The anticipated outcomes of this interest have yet to be borne out in a clinical setting, but given the results from small animal [328, 329, 331-334] and *in vitro* work it is evident that MSCs do hold potential, it is the matter of scaling this potential to humans that presents a problem. Using large animal translational models can help answer many of the unresolved questions. The work presented here has attempted to refine the use of MSCs in kidney transplantation by providing evidence in support of the use of direct arterial administration. The accumulated information from the cell tracking experiments in chapter 5 and the literature [328, 330, 334, 482] suggest that DAA may provide better outcomes in kidney transplantation. To test this, a tissue mismatched sheep model of kidney allotransplantation was treated with MSCs given directly into the renal artery just prior to the completion of the anastomosis. When compared to the control group, the MSC group failed to have any statistically significant improved outcomes. There were some changes between the groups that suggest the MSCs may have had an impact, namely the reduced kim-1 levels in the MSC groups (figure 6.16) suggesting a reduction in kidney damage, and a spike in serum and creatinine during the first 3 days in the MSC group (figure 6.15) perhaps explained by the transplanted cells obstructing vasculature. However, due to the small sample size of the groups neither of these observations reached statistical significance, this is also the greatest limitation of this study. In order for a more conclusive result to be achieved, further work needs to be carried out. Another limitation was the inability to biopsy the kidney

regularly in several of the sheep due to the skin pocket not adhering to the kidney capsule. When biopsies had previously been carried out under such a circumstance it resulted in the kidney becoming infected causing graft failure. So, although it resulted in a lack of longitudinal histological information, this was judged to be an acceptable compromise to ensure the completion of the experiment and the attainment of the other forms of data.

7.5 Future Directions

There are several avenues that exist for possible future exploration of MSCs in kidney transplantation. One that has been touched on in other literature [482, 509, 510] is the use of machine perfusion with MSC supplemented preservation solution to give a greater accumulation of MSCs in the graft. If this was also paired with an increased pressure, as seen in attempts to regenerate kidneys [511], it could result in an even greater distribution of cells, overcoming any issues caused by the entrapment in small vessels.

The topic of regenerating organs is also a possible area of interest. As noted in chapter 6 the transplanted kidneys did not undergo any particularly harsh conditions and so their damage would have been minimal and this may have resulted in less MSC recruitment to the organ. The relationship between MSCs and organ damage could therefore be of greatest use in extended criteria donors or organs that have been damaged in ways that would usually prevent them from being used for transplantation. This has been examined to some extent by Baulier *et al.*, (2014) looking at prolonged ischemia [335] where they found that MSC infusion resulted in improved renal function in their model. Given these positive results and the other characteristic of MSCs, looking at the treatment of other forms of transplant related damage could be an area that these cells find an application in. One particularly intriguing possibility is the use of machine perfusion to pre-treat damaged organs in an attempt to repair and regain function. This has already been applied in both liver [512] and kidney [513] with

normothermic machine perfusion and shown positive results, so supplementing the perfusate with MSCs could potentially aid this technique.

Lastly, and perhaps most promising, is the modification of MSCs to achieve greater results. This has already been attempted by several groups using various methods. The preconditioning of MSCs with inflammatory markers has already been previously mentioned in chapter 5. This has shown very positive results in up-regulating several of the beneficial functions of MSCs [313, 477, 480, 481, 489]. A more potent way to achieve increased MSC efficacy is the use of genetic engineering. This has been shown to work by several groups working to increase the homing potential of MSCs by the up regulation of chemokine receptors, in particular CXCR4 [514-518]. With the vast and varied research being conducted on MSCs, as demonstrated by the above examples, it is just a matter of time before their potential is unlocked and they gain a wider use in modern medicine.

7.6 Concluding Statement:

Mesenchymal stem cells are a promising candidate for treating several issues in kidney transplantation. The work presented in this thesis has demonstrated a large animal model of heterotopic kidney transplantation that can be used to tease out further translational information regarding the best practice for applying MSCs to the clinic. Additionally, it has offered further evidence that injecting the MSCs directly into the renal artery is a feasible and safe delivery method that resulted in no short term deleterious effects. However, no immediate benefit was observed and no long term data was collected due to limitations of the study design.

Bibliography

1. Rana, A., et al., *Survival benefit of solid-organ transplant in the United States*. JAMA Surg, 2015. **150**(3): p. 252-9.
2. ANZDATA, *ANZDATA Registry. 40th Report, Chapter 6: Australian transplant waiting list. Australia and New Zealand Dialysis and Transplant Registry, Adelaide, Australia. 2018. 2017.*
3. Huang, E., D.L. Segev, and H. Rabb, *Kidney transplantation in the elderly*. Semin Nephrol, 2009. **29**(6): p. 621-35.
4. Stallone, G., B. Infante, and L. Gesualdo, *Older donors and older recipients in kidney transplantation*. J Nephrol, 2010. **23 Suppl 15**: p. S98-103.
5. Morris, P.J., et al., *Analysis of factors that affect outcome of primary cadaveric renal transplantation in the UK. HLA Task Force of the Kidney Advisory Group of the United Kingdom Transplant Support Service Authority (UKTSSA)*. Lancet, 1999. **354**(9185): p. 1147-52.
6. Harrison, J.H., J.P. Merrill, and J.E. Murray, *Renal homotransplantation in identical twins*. Surg Forum, 1956. **6**: p. 432-6.
7. Merrill, J.P., et al., *Successful homotransplantation of the human kidney between identical twins*. J Am Med Assoc, 1956. **160**(4): p. 277-82.
8. Murray, J.E., J.P. Merrill, and J.H. Harrison, *Renal homotransplantation in identical twins. 1955*. J Am Soc Nephrol, 2001. **12**(1): p. 201-4.
9. Hardy, J.D., et al., *LUNG HOMOTRANSPLANTATION IN MAN*. Jama, 1963. **186**: p. 1065-74.
10. Marino, I.R. and C. Cirillo, *An abridged photographic history of organ transplantation*. Exp Clin Transplant, 2014. **12 Suppl 1**: p. 11-6.
11. Starzl, T.E., *History of Clinical Transplantation*. World J Surg, 2000. **24**(7): p. 759-82.
12. Rydberg, L., *ABO-incompatibility in solid organ transplantation*. Transfus Med, 2001. **11**(4): p. 325-42.
13. Hosoi, E., *Biological and clinical aspects of ABO blood group system*. J Med Invest, 2008. **55**(3-4): p. 174-82.
14. Morath, C., et al., *ABO-Incompatible Kidney Transplantation*. Front Immunol, 2017. **8**: p. 234.
15. Goldberg, A.C. and L.V. Rizzo, *MHC structure and function - antigen presentation. Part 1*. Einstein (Sao Paulo), 2015. **13**(1): p. 153-6.
16. Gruen, J.R. and S.M. Weissman, *Human MHC class III and IV genes and disease associations*. Front Biosci, 2001. **6**: p. D960-72.
17. Giles, C.M., et al., *Expression of MHC class I determinants on erythrocytes of SLE patients*. Clin Exp Immunol, 1987. **69**(2): p. 368-74.
18. Goldberg, A.C. and L.V. Rizzo, *MHC structure and function – antigen presentation. Part 2*. Einstein (Sao Paulo), 2015. **13**(1): p. 157-62.
19. Dukkupati, V.S., et al., *'Ovar-Mhc' - ovine major histocompatibility complex: structure and gene polymorphisms*. Genet Mol Res, 2006. **5**(4): p. 581-608.
20. Marino, J., J. Paster, and G. Benichou, *Allorecognition by T Lymphocytes and Allograft Rejection*. Front Immunol, 2016. **7**: p. 582.
21. Hewitt, E.W., *The MHC class I antigen presentation pathway: strategies for viral immune evasion*. Immunology, 2003. **110**(2): p. 163-9.
22. Fruci, D., et al., *Major histocompatibility complex class I and tumour immuno-evasion: how to fool T cells and natural killer cells at one time*. Curr Oncol, 2012. **19**(1): p. 39-41.

23. Bevan, M.J., *Cross-priming*. Nature Immunology, 2006. **7**: p. 363.
24. Delgoffe, G.M., et al., *The mammalian Target of Rapamycin (mTOR) regulates T helper cell differentiation through the selective activation of mTORC1 and mTORC2 signaling*. Nat Immunol, 2011. **12**(4): p. 295-303.
25. Bretscher, P.A., *On the Mechanism Determining the Th1/Th2 Phenotype of an Immune Response, and its Pertinence to Strategies for the Prevention, and Treatment, of Certain Infectious Diseases*. Scand J Immunol, 2014. **79**(6): p. 361-76.
26. Sallusto, F., et al., *Two subsets of memory T lymphocytes with distinct homing potentials and effector functions*. Nature, 1999. **401**(6754): p. 708-12.
27. Grifka-Walk, H.M., D.A. Giles, and B.M. Segal, *IL-12-polarized Th1 cells produce GM-CSF and induce EAE independent of IL-23*. Eur J Immunol, 2015. **45**(10): p. 2780-6.
28. Fujimura, K., et al., *CD4 T cell-intrinsic IL-2 signaling differentially affects Th1 and Th17 development*. J Leukoc Biol, 2013. **94**(2): p. 271-9.
29. Halim T, Y.F., et al., *Group 2 Innate Lymphoid Cells Are Critical for the Initiation of Adaptive T Helper 2 Cell-Mediated Allergic Lung Inflammation*. Immunity, 2014. **40**(3): p. 425-35.
30. Bodmer, W.F., *The HLA system: structure and function*. J Clin Pathol, 1987. **40**(9): p. 948-58.
31. Mellins, E.D. and L.J. Stern, *HLA-DM and HLA-DO, key regulators of MHC-II processing and presentation*. Curr Opin Immunol, 2014. **0**: p. 115-22.
32. Schinstock, C.A., M.J. Gandhi, and M.D. Stegall, *Interpreting Anti-HLA Antibody Testing Data: A Practical Guide for Physicians*. Transplantation, 2016. **100**(8): p. 1619-28.
33. Lee, S.J., et al., *High-resolution donor-recipient HLA matching contributes to the success of unrelated donor marrow transplantation*. Blood, 2007. **110**(13): p. 4576-83.
34. Pena, J.R., D. Fitzpatrick, and S.L. Saidman, *Complement-dependent cytotoxicity crossmatch*. Methods Mol Biol, 2013. **1034**: p. 257-83.
35. Dunn, P.P., *Novel Approaches and Technologies in Molecular HLA Typing*. Methods Mol Biol, 2015. **1310**: p. 213-30.
36. Dunckley, H., *HLA typing by SSO and SSP methods*. Methods Mol Biol, 2012. **882**: p. 9-25.
37. Smith, L.K., *HLA typing by direct DNA sequencing*. Methods Mol Biol, 2012. **882**: p. 67-86.
38. Piazza, A., et al., *Virtual Crossmatch in Kidney Transplantation*. Transplantation Proceedings, 2014. **46**(7): p. 2195-2198.
39. Bray, R.A., *Lymphocyte Crossmatching by Flow Cytometry*, in *Transplantation Immunology: Methods and Protocols*, A.A. Zachary and M.S. Leffell, Editors. 2013, Humana Press: Totowa, NJ. p. 285-296.
40. Dierselhuis, M. and E. Goulmy, *The relevance of minor histocompatibility antigens in solid organ transplantation*. Curr Opin Organ Transplant, 2009. **14**(4): p. 419-25.
41. Lee, C.Y., et al., *Conserved haplotype blocks within the sheep MHC and low SNP heterozygosity in the Class IIa subregion*. Animal Genetics, 2012. **43**(4): p. 429-437.
42. Siva Subramaniam, N., et al., *A comprehensive mapping of the structure and gene organisation in the sheep MHC class I region*. BMC Genomics, 2015. **16**: p. 810.
43. Ballingall, K.T., et al., *Trans-species polymorphism and selection in the MHC class II DRA genes of domestic sheep*. PLoS One, 2010. **5**(6): p. e11402.
44. Ballingall, K.T., K. Fardoe, and D.J. McKeever, *Genomic organisation and allelic diversity within coding and non-coding regions of the Ovar-DRB1 locus*. Immunogenetics, 2008. **60**(2): p. 95-103.
45. Miltiadou, D., et al., *Haplotype characterization of transcribed ovine major histocompatibility complex (MHC) class I genes*. Immunogenetics, 2005. **57**(7): p. 499-509.
46. Ballingall, K.T., et al., *Expression and characterization of ovine major histocompatibility complex class II (OLA-DR) genes*. Anim Genet, 1992. **23**(4): p. 347-59.
47. Puri, N.K., et al., *Biochemical and molecular analysis of sheep MHC class II molecules*. Vet Immunol Immunopathol, 1987. **17**(1-4): p. 231-41.

48. Fabb, S.A., et al., *Isolation, characterization and evolution of ovine major histocompatibility complex class II DRA and DQA genes*. Anim Genet, 1993. **24**(4): p. 249-55.
49. Gao, J., et al., *A complete DNA sequence map of the ovine major histocompatibility complex*. BMC Genomics, 2010. **11**: p. 466.
50. Subramaniam, R., et al., *MHC class II DR allelic diversity in bighorn sheep*. Gene, 2012. **506**(1): p. 217-22.
51. Ballingall, K.T. and R. Tassi, *Sequence-based genotyping of the sheep MHC class II DRB1 locus*. Immunogenetics, 2010. **62**(1): p. 31-9.
52. Deverson, E.V., et al., *Class II major histocompatibility complex genes of the sheep*. Anim Genet, 1991. **22**(3): p. 211-25.
53. Jugo, B.M. and A. Vicario, *Lymphocyte antigens in sheep: linkage to the MHC class II DRB1 gene*. Eur J Immunogenet, 2001. **28**(4): p. 451-8.
54. Ali, A.O., et al., *The genetic architecture of the MHC class II region in British Texel sheep*. Immunogenetics, 2017. **69**(3): p. 157-163.
55. Lin, C.M. and R.G. Gill, *Direct and indirect allograft recognition: pathways dictating graft rejection mechanisms*. Curr Opin Organ Transplant, 2016. **21**(1): p. 40-4.
56. Brennan, T.V., et al., *Preferential Priming of Alloreactive T Cells with Indirect Reactivity*. American Journal of Transplantation, 2009. **9**(4): p. 709-718.
57. Herrera, O.B., et al., *A novel pathway of alloantigen presentation by dendritic cells*. J Immunol, 2004. **173**(8): p. 4828-37.
58. Grazia, T.J., et al., *A two-step model of acute CD4 T-cell mediated cardiac allograft rejection*. J Immunol, 2004. **172**(12): p. 7451-8.
59. Ali, J., et al., *Targeting indirect pathway CD4 T-cell alloresponses in the prevention of chronic transplant rejection*. Lancet, 2015. **385** Suppl 1: p. S17.
60. Nadazdin, O., et al., *Contributions of direct and indirect alloresponses to chronic rejection of kidney allografts in nonhuman primates*. J Immunol, 2011. **187**(9): p. 4589-97.
61. Stone, J.P., et al., *Altered Immunogenicity of Donor Lungs via Removal of Passenger Leukocytes Using Ex Vivo Lung Perfusion*. Am J Transplant, 2016. **16**(1): p. 33-43.
62. Qiu, C.H., et al., *Novel subset of CD8{alpha}+ dendritic cells localized in the marginal zone is responsible for tolerance to cell-associated antigens*. J Immunol, 2009. **182**(7): p. 4127-36.
63. Harper, S.J., et al., *CD8 T-cell recognition of acquired alloantigen promotes acute allograft rejection*. Proc Natl Acad Sci U S A, 2015. **112**(41): p. 12788-93.
64. Ruedl, C., et al., *Anatomical origin of dendritic cells determines their life span in peripheral lymph nodes*. J Immunol, 2000. **165**(9): p. 4910-6.
65. Bruce Alberts, A.J., Julian Lewis, Martin Raff, Keith Roberts, and Peter Walter, *Molecular Biology of the Cell. 4th edition*. 2002.
66. Wigmore, S.J., et al., *Kidney damage during organ retrieval: data from UK National Transplant Database. Kidney Advisory Group*. Lancet, 1999. **354**(9185): p. 1143-6.
67. Chen, C.C., W.C. Chapman, and D.W. Hanto, *Ischemia-reperfusion injury in kidney transplantation*. Front Biosci (Elite Ed), 2015. **7**: p. 117-34.
68. !!! INVALID CITATION !!! {}.
69. Vegrn, F., L. Apetoh, and F. Ghiringhelli, *Th9 cells: a novel CD4 T-cell subset in the immune war against cancer*. Cancer Res, 2015. **75**(3): p. 475-9.
70. Veldhoen, M., et al., *TGFbeta in the context of an inflammatory cytokine milieu supports de novo differentiation of IL-17-producing T cells*. Immunity, 2006. **24**(2): p. 179-89.
71. Yang, J., et al., *Targeting Th17 cells in autoimmune diseases*. Trends Pharmacol Sci, 2014. **35**(10): p. 493-500.
72. Duhon, T., et al., *Production of interleukin 22 but not interleukin 17 by a subset of human skin-homing memory T cells*. Nat Immunol, 2009. **10**(8): p. 857-63.
73. Qin, S., et al., *Th22 cells are associated with hepatocellular carcinoma development and progression*. Chin J Cancer Res, 2014. **26**(2): p. 135-41.

74. Nurieva, R.I., et al., *Bcl6 mediates the development of T follicular helper cells*. Science, 2009. **325**(5943): p. 1001-5.
75. Allam, A., et al., *TFH cells accumulate in mucosal tissues of humanized-DRAG mice and are highly permissive to HIV-1*. Sci Rep, 2015. **5**: p. 10443.
76. Xie, X., et al., *Th17 promotes acute rejection following liver transplantation in rats*. J Zhejiang Univ Sci B, 2010. **11**(11): p. 819-27.
77. Wang, Y., et al., *The Ratio of Circulating Regulatory T Cells (Tregs)/Th17 Cells Is Associated with Acute Allograft Rejection in Liver Transplantation*. PLoS One, 2014. **9**(11).
78. Yuan, X., et al., *A novel role of CD4 Th17 cells in mediating cardiac allograft rejection and vasculopathy*. J Exp Med, 2008. **205**(13): p. 3133-44.
79. Vanaudenaerde, B.M., et al., *The role of interleukin-17 during acute rejection after lung transplantation*. Eur Respir J, 2006. **27**(4): p. 779-87.
80. Pourgholaminejad, A., et al., *Is TGFbeta as an anti-inflammatory cytokine required for differentiation of inflammatory TH17 cells?* J Immunotoxicol, 2016. **13**(6): p. 775-783.
81. Lei, L., et al., *IL-21 induction of CD4+ T cell differentiation into Th17 cells contributes to bleomycin-induced fibrosis in mice*. Cell Biology International, 2015. **39**(4): p. 388-399.
82. Edwards, J.P., et al., *Regulation of the expression of GARP/latent TGF-beta1 complexes on mouse T cells and their role in regulatory T cell and Th17 differentiation*. J Immunol, 2013. **190**(11): p. 5506-15.
83. Park, H., et al., *A distinct lineage of CD4 T cells regulates tissue inflammation by producing interleukin 17*. Nat Immunol, 2005. **6**(11): p. 1133-41.
84. Zhang, J., et al., *TH17-Induced Neutrophils Enhance the Pulmonary Allergic Response Following BALB/c Exposure to House Dust Mite Allergen and Fine Particulate Matter From California and China*. Toxicological Sciences, 2018. **164**(2): p. 627-643.
85. Syrjälä, S.O., et al., *Increased Th17 rather than Th1 alloimmune response is associated with cardiac allograft vasculopathy after hypothermic preservation in the rat*. The Journal of Heart and Lung Transplantation, 2010. **29**(9): p. 1047-1057.
86. Banuelos, J., et al., *BCL-2 protects human and mouse Th17 cells from glucocorticoid-induced apoptosis*. Allergy, 2016. **71**(5): p. 640-50.
87. Chung, B.H., et al., *Increase of Th17 Cell Phenotype in Kidney Transplant Recipients with Chronic Allograft Dysfunction*. PLoS One, 2015. **10**(12).
88. Deppong, C.M., et al., *CTLA4Ig inhibits effector T cells through regulatory T cells and TGF-beta*. J Immunol, 2013. **191**(6): p. 3082-9.
89. Saida, Y., et al., *Critical Roles of Chemoresistant Effector and Regulatory T Cells in Antitumor Immunity after Lymphodepleting Chemotherapy*. J Immunol, 2015. **195**(2): p. 726-35.
90. Grossman, W.J., et al., *Human T regulatory cells can use the perforin pathway to cause autologous target cell death*. Immunity, 2004. **21**(4): p. 589-601.
91. Arce-Sillas, A., et al., *Interleukin 10 and dendritic cells are the main suppression mediators of regulatory T cells in human neurocysticercosis*. Clin Exp Immunol, 2016. **183**(2): p. 271-9.
92. Krustrup, D., et al., *Time elapsed after transplantation influences the relationship between the number of regulatory T cells in lung allograft biopsies and subsequent acute rejection episodes*. Transplant Immunology, 2014. **31**(1): p. 42-47.
93. Moore, C., et al., *Retinoic Acid Generates Regulatory T Cells in Experimental Transplantation*. Transplantation Proceedings, 2011. **43**(6): p. 2334-2337.
94. He, W., et al., *Prolonged survival effects induced by immature dendritic cells and regulatory T cells in a rat liver transplantation model*. Molecular Immunology, 2016. **79**(Supplement C): p. 92-97.
95. Sanchez, A.M., *The Development and Function of Memory Regulatory T Cells After Acute Viral Infections*. 2012. **189**(6): p. 2805-14.
96. Brincks, E.L., et al., *Antigen-specific memory T(reg) control memory responses to influenza virus infection*. J Immunol, 2013. **190**(7): p. 3438-46.

97. Rosenblum, M.D., S.S. Way, and A.K. Abbas, *Regulatory T cell memory*. Nat Rev Immunol, 2016. **16**(2): p. 90-101.
98. Rosenblum, M.D., *Response to self antigen imprints regulatory memory in tissues*. **480**(7378): p. 538-42.
99. Gratz, I.K., et al., *Cutting edge: Self-antigen controls the balance between effector and regulatory T cells in peripheral tissues*. J Immunol, 2014. **192**(4): p. 1351-5.
100. Nutt, S.L., et al., *The generation of antibody-secreting plasma cells*. Nature Reviews Immunology, 2015. **15**: p. 160.
101. Humpert, M.-L., et al., *CXCR7 influences the migration of B cells during maturation*. European Journal of Immunology, 2014. **44**(3): p. 694-705.
102. Luque, S., M. Lúcia, and O. Bestard, *Refinement of humoral immune monitoring in kidney transplantation: the role of "hidden" alloreactive memory B cells*. Transplant International, 2017. **30**(10): p. 955-968.
103. Agematsu, K., et al., *Generation of plasma cells from peripheral blood memory B cells: synergistic effect of interleukin-10 and CD27/CD70 interaction*. Blood, 1998. **91**(1): p. 173-80.
104. Roche, A.M., et al., *Antibody blocks acquisition of bacterial colonization through agglutination*. Mucosal Immunol, 2015. **8**(1): p. 176-85.
105. Splith, K., et al., *Antibody-Mediated Rejection of Arterialised Venous Allografts Is Inhibited by Immunosuppression in Rats*. PLoS One, 2014. **9**(3).
106. Sonnen, A.F.-P. and P. Henneke, *Structural Biology of the Membrane Attack Complex*, in *MACPF/CDC Proteins - Agents of Defence, Attack and Invasion*, G. Anderlueh and R. Gilbert, Editors. 2014, Springer Netherlands: Dordrecht. p. 83-116.
107. Nauta, A.J., et al., *The membrane attack complex of complement induces caspase activation and apoptosis*. Eur J Immunol, 2002. **32**(3): p. 783-92.
108. Kochi, S.K., R.C. Johnson, and A.P. Dalmasso, *Complement-mediated killing of the Lyme disease spirochete Borrelia burgdorferi. Role of antibody in formation of an effective membrane attack complex*. The Journal of Immunology, 1991. **146**(11): p. 3964-3970.
109. Rauterberg, E.W., et al., *Complement membrane attack (MAC) in idiopathic IgA-glomerulonephritis*. Kidney International, 1987. **31**(3): p. 820-829.
110. Rodriguez, E., et al., *Value of plasmatic membrane attack complex as a marker of severity in acute kidney injury*. Biomed Res Int, 2014. **2014**: p. 361065.
111. Hidalgo, L.G., et al., *NK Cell Transcripts and NK Cells in Kidney Biopsies from Patients with Donor-Specific Antibodies: Evidence for NK Cell Involvement in Antibody-Mediated Rejection*. American Journal of Transplantation, 2010. **10**(8): p. 1812-1822.
112. Abe, T., et al., *Graft-Derived CCL2 Increases Graft Injury During Antibody-Mediated Rejection of Cardiac Allografts*. Am J Transplant, 2014. **14**(8): p. 1753-64.
113. Streilein, J.W., C. Arancibia-Caracamo, and H. Osawa, *The role of minor histocompatibility alloantigens in penetrating keratoplasty*. Dev Ophthalmol, 2003. **36**: p. 74-88.
114. Fuquay, R., et al., *Renal ischemia-reperfusion injury amplifies the humoral immune response*. J Am Soc Nephrol, 2013. **24**(7): p. 1063-72.
115. Sellarés, J., et al., *Understanding the Causes of Kidney Transplant Failure: The Dominant Role of Antibody-Mediated Rejection and Nonadherence*. American Journal of Transplantation, 2012. **12**(2): p. 388-399.
116. Oberbarnscheidt, M.H., et al., *Non-self recognition by monocytes initiates allograft rejection*. J Clin Invest, 2014. **124**(8): p. 3579-89.
117. Wu, C., *Graft-Infiltrating Macrophages Adopt an M2 Phenotype and Are Inhibited by Purinergic Receptor P2X7 Antagonist in Chronic Rejection*. 2016. **16**(9): p. 2563-73.
118. Miura, M., T. El-Sawy, and R.L. Fairchild, *Neutrophils Mediate Parenchymal Tissue Necrosis and Accelerate the Rejection of Complete Major Histocompatibility Complex-Disparate Cardiac Allografts in the Absence of Interferon- γ* . Am J Pathol, 2003. **162**(2): p. 509-19.

119. Vinther, A.M.L., et al., *Characterization and differentiation of equine experimental local and early systemic inflammation by expression responses of inflammation-related genes in peripheral blood leukocytes*. BMC Vet Res, 2016. **12**.
120. Barker, C.E., et al., *Transplantation and inflammation: implications for the modification of chemokine function*. Immunology, 2014. **143**(2): p. 138-45.
121. el Sayed, S.O. and M. Dyson, *Responses of dermal mast cells to injury*. J Anat, 1993. **182**(Pt 3): p. 369-76.
122. Walsh, L.J., *Ultraviolet B irradiation of skin induces mast cell degranulation and release of tumour necrosis factor-alpha*. Immunol Cell Biol, 1995. **73**(3): p. 226-33.
123. Theoharides, T.C., et al., *Mast cells and inflammation*. Biochimica et Biophysica Acta (BBA) - Molecular Basis of Disease, 2012. **1822**(1): p. 21-33.
124. De Filippo, K., et al., *Mast cell and macrophage chemokines CXCL1/CXCL2 control the early stage of neutrophil recruitment during tissue inflammation*. Blood, 2013. **121**(24): p. 4930-7.
125. Nourshargh, S. and R. Alon, *Leukocyte Migration into Inflamed Tissues*. Immunity, 2014. **41**(5): p. 694-707.
126. Goldszmid, R.S., et al., *NK cell-derived interferon- γ orchestrates the cellular dynamics and differentiation of monocytes into inflammatory dendritic cells at the site of infection*. Immunity, 2012. **36**(6): p. 1047-59.
127. Hettinger, J., et al., *Origin of monocytes and macrophages in a committed progenitor*. Nat Immunol, 2013. **14**(8): p. 821-30.
128. Bergler, T., et al., *Infiltration of Macrophages Correlates with Severity of Allograft Rejection and Outcome in Human Kidney Transplantation*. PLoS One, 2016. **11**(6).
129. Raffetseder, U.t.e., et al., *Differential regulation of chemokine CCL5 expression in monocytes/macrophages and renal cells by Y-box protein-1*. Kidney International, 2009. **75**(2): p. 185-196.
130. Murooka, T.T., et al., *CCL5-mediated T-cell chemotaxis involves the initiation of mRNA translation through mTOR/4E-BP1*. Blood, 2008. **111**(10): p. 4892-901.
131. Mishima, T., et al., *Allograft inflammatory factor-1 augments macrophage phagocytotic activity and accelerates the progression of atherosclerosis in ApoE^{-/-} mice*. Int J Mol Med, 2008. **21**(2): p. 181-7.
132. Gouwy, M., et al., *Chemokines and other GPCR ligands synergize in receptor-mediated migration of monocyte-derived immature and mature dendritic cells*. Immunobiology, 2014. **219**(3): p. 218-229.
133. Inaba, K., et al., *Efficient Presentation of Phagocytosed Cellular Fragments on the Major Histocompatibility Complex Class II Products of Dendritic Cells*. The Journal of Experimental Medicine, 1998. **188**(11): p. 2163-2173.
134. Benichou, G., Takizawa, P., Olson, Clifford., McMillan, M., Saercarz, E., *Donor major histocompatibility complex (MHC) peptides are presented by recipient MHC molecules during graft rejection*. J Exp Med, 1992. **175**(1): p. 305-8.
135. Cummings, J.-S., et al., *Natural killer cell responses to dendritic cells infected by the ANRS HIV-1 vaccine candidate, MVAHIV*. Vaccine, 2014. **32**(43): p. 5577-5584.
136. Perier, A., et al., *Mutations of the von Hippel-Lindau gene confer increased susceptibility to natural killer cells of clear-cell renal cell carcinoma*. Oncogene, 2011. **30**: p. 2622.
137. Ali, J., et al., *Recipient natural killer cell allorecognition of passenger donor lymphocytes and its effect on adaptive alloimmunity after transplantation*. The Lancet, 2015. **385**(Supplement 1): p. S18.
138. Lubben, N.B., et al., *HIV-1 Nef-induced Down-Regulation of MHC Class I Requires AP-1 and Clathrin but Not PACS-1 and Is Impeded by AP-2*. Mol Biol Cell, 2007. **18**(9): p. 3351-65.
139. Huard, B. and K. Fruh, *A role for MHC class I down-regulation in NK cell lysis of herpes virus-infected cells*. Eur J Immunol, 2000. **30**(2): p. 509-15.

140. Rabinovich, B.A., et al., *Activated, but not resting, T cells can be recognized and killed by syngeneic NK cells*. J Immunol, 2003. **170**(7): p. 3572-6.
141. Yu, G., et al., *NK cells promote transplant tolerance by killing donor antigen-presenting cells*. J Exp Med, 2006. **203**(8): p. 1851-8.
142. Kreisel, D., et al., *In vivo two-photon imaging reveals monocyte-dependent neutrophil extravasation during pulmonary inflammation*. Proc Natl Acad Sci U S A, 2010. **107**(42): p. 18073-8.
143. Beland, S., et al., *Innate immunity in solid organ transplantation: an update and therapeutic opportunities*. Expert Rev Clin Immunol, 2015. **11**(3): p. 377-89.
144. Bennouna, S. and E.Y. Denkers, *Microbial Antigen Triggers Rapid Mobilization of TNF- α to the Surface of Mouse Neutrophils Transforming Them into Inducers of High-Level Dendritic Cell TNF- α Production*. The Journal of Immunology, 2005. **174**(8): p. 4845-4851.
145. Enderby, C. and C.A. Keller, *An overview of immunosuppression in solid organ transplantation*. Am J Manag Care, 2015. **21**(1 Suppl): p. s12-23.
146. Panther, F., et al., *Inhibition of nuclear translocation of calcineurin suppresses T-cell activation and prevents acute rejection of donor hearts*. Transplantation, 2011. **91**(6): p. 597-604.
147. Chow, C.W. and R.J. Davis, *Integration of Calcium and Cyclic AMP Signaling Pathways by 14-3-3*. Mol Cell Biol, 2000. **20**(2): p. 702-12.
148. Matsuda, S. and S. Koyasu, *Mechanisms of action of cyclosporine*. Immunopharmacology, 2000. **47**(2): p. 119-125.
149. Barbarino, J.M., et al., *PharmGKB summary: cyclosporine and tacrolimus pathways*. Pharmacogenet Genomics, 2013. **23**(10): p. 563-85.
150. Scalea, J.R., et al., *Tacrolimus for the prevention and treatment of rejection of solid organ transplants*. Expert Rev Clin Immunol, 2016. **12**(3): p. 333-42.
151. Akar, Y., et al., *Systemic toxicity of tacrolimus given by various routes and the response to dose reduction*. Clinical & Experimental Ophthalmology, 2005. **33**(1): p. 53-59.
152. Lancia, P., E. Jacqz-Aigrain, and W. Zhao, *Choosing the right dose of tacrolimus*. Arch Dis Child, 2015. **100**(4): p. 406-13.
153. Zheng, S., et al., *Pharmacokinetics of Tacrolimus during Pregnancy*. Ther Drug Monit, 2012. **34**(6): p. 660-70.
154. Stienstra, N.A., et al., *Development of a Simple and Rapid Method to Measure the Free Fraction of Tacrolimus in Plasma Using Ultrafiltration and LC-MS/MS*. Ther Drug Monit, 2016. **38**(6): p. 722-727.
155. Stocco, G., et al., *Pharmacogenetics of azathioprine in inflammatory bowel disease: A role for glutathione-S-transferase?* World J Gastroenterol, 2014. **20**(13): p. 3534-41.
156. Salser, J.S., D.J. Hutchison, and M.E. Balis, *Studies on the mechanism of action of 6-mercaptopurine in cell-free preparations*. J Biol Chem, 1960. **235**: p. 429-32.
157. Gearry, R.B. and M.L. Barclay, *Azathioprine and 6-mercaptopurine pharmacogenetics and metabolite monitoring in inflammatory bowel disease*. Journal of Gastroenterology and Hepatology, 2005. **20**(8): p. 1149-1157.
158. Chen, S., P.L. Nagy, and H. Zalkin, *Role of NRF-1 in bidirectional transcription of the human GPAT-AIRC purine biosynthesis locus*. Nucleic Acids Res, 1997. **25**(9): p. 1809-16.
159. Ransom, J.T., *Mechanism of action of mycophenolate mofetil*. Ther Drug Monit, 1995. **17**(6): p. 681-4.
160. Hudson, W.H., C. Youn, and E.A. Ortlund, *The structural basis of direct glucocorticoid-mediated transrepression*. Nat Struct Mol Biol, 2013. **20**(1): p. 53-8.
161. van der Laan, S. and O.C. Meijer, *Pharmacology of glucocorticoids: Beyond receptors*. European Journal of Pharmacology, 2008. **585**(2): p. 483-491.

162. Vandevyver, S., et al., *New insights into the anti-inflammatory mechanisms of glucocorticoids: an emerging role for glucocorticoid-receptor-mediated transactivation*. *Endocrinology*, 2013. **154**(3): p. 993-1007.
163. Rettenmeier, R., et al., *Isolation and characterization of the human tyrosine aminotransferase gene*. *Nucleic Acids Res*, 1990. **18**(13): p. 3853-61.
164. McGrane, M.M., et al., *Metabolic control of gene expression: in vivo studies with transgenic mice*. *Trends in Biochemical Sciences*, 1992. **17**(1): p. 40-44.
165. Langlais, D., et al., *The Stat3/GR Interaction Code: Predictive Value of Direct/Indirect DNA Recruitment for Transcription Outcome*. *Molecular Cell*, 2012. **47**(1): p. 38-49.
166. Newton, R. and N.S. Holden, *Separating Transrepression and Transactivation: A Distressing Divorce for the Glucocorticoid Receptor?* *Molecular Pharmacology*, 2007. **72**(4): p. 799-809.
167. Ashwell, J.D., F.W.M. Lu, and M.S. Vacchio, *Glucocorticoids in T Cell Development and Function*. *Annual Review of Immunology*, 2000. **18**(1): p. 309-345.
168. Jonat, C., et al., *Antitumor promotion and antiinflammation: down-modulation of AP-1 (Fos/Jun) activity by glucocorticoid hormone*. *Cell*, 1990. **62**(6): p. 1189-204.
169. Auphan, N., et al., *Immunosuppression by glucocorticoids: inhibition of NF-kappa B activity through induction of I kappa B synthesis*. *Science*, 1995. **270**(5234): p. 286-90.
170. Schacke, H., W.D. Docke, and K. Asadullah, *Mechanisms involved in the side effects of glucocorticoids*. *Pharmacol Ther*, 2002. **96**(1): p. 23-43.
171. Diekmann, F. and J.M. Campistol, *Practical considerations for the use of mTOR inhibitors*. *Transplant Res*, 2015. **4**(Suppl 1).
172. Shihab, F., et al., *Focus on mTOR inhibitors and tacrolimus in renal transplantation: Pharmacokinetics, exposure–response relationships, and clinical outcomes*. *Transplant Immunology*, 2014. **31**(1): p. 22-32.
173. Stallone, G., et al., *mTOR inhibitors effects on regulatory T cells and on dendritic cells*. *J Transl Med*, 2016. **14**(1): p. 152.
174. Sabers, C.J., et al., *Isolation of a protein target of the FKBP12-rapamycin complex in mammalian cells*. *J Biol Chem*, 1995. **270**(2): p. 815-22.
175. Ersahin, T., N. Tuncbag, and R. Cetin-Atalay, *The PI3K/AKT/mTOR interactive pathway*. *Mol Biosyst*, 2015. **11**(7): p. 1946-54.
176. Magnuson, B., B. Ekim, and D.C. Fingar, *Regulation and function of ribosomal protein S6 kinase (S6K) within mTOR signalling networks*. *Biochem J*, 2012. **441**(1): p. 1-21.
177. Beretta, L., et al., *Rapamycin blocks the phosphorylation of 4E-BP1 and inhibits cap-dependent initiation of translation*. *Embo j*, 1996. **15**(3): p. 658-64.
178. Karaki, S., et al., *Chapter One - The Eukaryotic Translation Initiation Factor 4E (eIF4E) as a Therapeutic Target for Cancer*, in *Advances in Protein Chemistry and Structural Biology*, R. Donev, Editor. 2015, Academic Press. p. 1-26.
179. Hurez, V., et al., *Chronic mTOR inhibition in mice with rapamycin alters T, B, myeloid, and innate lymphoid cells and gut flora and prolongs life of immune-deficient mice*. *Aging Cell*, 2015. **14**(6): p. 945-56.
180. Pallet, N. and C. Legendre, *Adverse events associated with mTOR inhibitors*. *Expert Opin Drug Saf*, 2013. **12**(2): p. 177-86.
181. Oray, M., et al., *Long-term side effects of glucocorticoids*. *Expert Opinion on Drug Safety*, 2016. **15**(4): p. 457-465.
182. Taber, T.E., et al., *Deceased donor organ procurement injuries in the United States*. *World J Transplant*, 2016. **6**(2): p. 423-8.
183. Widgerow, A.D., *Ischemia-reperfusion injury: influencing the microcirculatory and cellular environment*. *Ann Plast Surg*, 2014. **72**(2): p. 253-60.
184. He, C., et al., *Temperature Increase Exacerbates Apoptotic Neuronal Death in Chemically-Induced Ischemia*. *PLoS One*, 2013. **8**(7).

185. Chandler, M.P., et al., *Increased nonoxidative glycolysis despite continued fatty acid uptake during demand-induced myocardial ischemia*. Am J Physiol Heart Circ Physiol, 2002. **282**(5): p. H1871-8.
186. Fliegel, L., *Functional and cellular regulation of the myocardial Na⁺/H⁺ exchanger*. J Thromb Thrombolysis, 1999. **8**(1): p. 9-14.
187. Kiedrowski, L., *NCX and NCKX Operation in Ischemic Neurons*. Annals of the New York Academy of Sciences, 2007. **1099**(1): p. 383-395.
188. Wu, D., et al., *Ischemia/reperfusion induce renal tubule apoptosis by inositol 1,4,5-trisphosphate receptor and L-type Ca²⁺ channel opening*. Am J Nephrol, 2008. **28**(3): p. 487-99.
189. Orrenius, S., M.J. McCabe, Jr., and P. Nicotera, *Ca(2+)-dependent mechanisms of cytotoxicity and programmed cell death*. Toxicol Lett, 1992. **64-65 Spec No**: p. 357-64.
190. Orrenius, S., B. Zhivotovsky, and P. Nicotera, *Regulation of cell death: the calcium-apoptosis link*. Nat Rev Mol Cell Biol, 2003. **4**(7): p. 552-65.
191. Zhivotovsky, B. and S. Orrenius, *Calcium and cell death mechanisms: A perspective from the cell death community*. Cell Calcium, 2011. **50**(3): p. 211-221.
192. Trump, B.F. and I.K. Berezsky, *Calcium-mediated cell injury and cell death*. Faseb j, 1995. **9**(2): p. 219-28.
193. Zweier, J.L. and M.A.H. Talukder, *The role of oxidants and free radicals in reperfusion injury*. Cardiovascular Research, 2006. **70**(2): p. 181-190.
194. Saksela, M., R. Lapatto, and K.O. Raivio, *Irreversible conversion of xanthine dehydrogenase into xanthine oxidase by a mitochondrial protease*. FEBS Letters, 1999. **443**(2): p. 117-120.
195. Chung, H.Y., et al., *Xanthine dehydrogenase/xanthine oxidase and oxidative stress*. Age (Omaha), 1997. **20**(3): p. 127-40.
196. Cantu-Medellin, N. and E.E. Kelley, *Xanthine oxidoreductase-catalyzed reactive species generation: A process in critical need of reevaluation*. Redox Biology, 2013. **1**(1): p. 353-358.
197. Ritov, V.B., et al., *Direct oxidation of polyunsaturated cis-parinaric fatty acid by phenoxyl radicals generated by peroxidase/H₂O₂ in model systems and in HL-60 cells*. Toxicol Lett, 1996. **87**(2-3): p. 121-9.
198. Cheng, T.M., et al., *Haemoglobin-induced oxidative stress is associated with both endogenous peroxidase activity and H₂O₂ generation from polyunsaturated fatty acids*. Free Radic Res, 2011. **45**(3): p. 303-16.
199. Qi, X.-F., et al., *Reactive oxygen species are involved in the IFN- γ -stimulated production of Th2 chemokines in HaCaT keratinocytes*. Journal of Cellular Physiology, 2011. **226**(1): p. 58-65.
200. Al-Amran, F.G., et al., *Blockade of the Monocyte Chemoattractant Protein-1 Receptor Pathway Ameliorates Myocardial Injury in Animal Models of Ischemia and Reperfusion*. Pharmacology, 2014. **93**(5-6): p. 296-302.
201. Belzer, F.O. and J.H. Southard, *Principles of solid-organ preservation by cold storage*. Transplantation, 1988. **45**(4): p. 673-6.
202. Rosenbaum, D.H., et al., *Perfusion Preservation versus Static Preservation for Cardiac Transplantation: Effects on Myocardial Function and Metabolism*. The Journal of Heart and Lung Transplantation, 2008. **27**(1): p. 93-99.
203. Collins, G.M., M. Bravo-Shugarman, and P.I. Terasaki, *Kidney preservation for transportation. Initial perfusion and 30 hours' ice storage*. Lancet, 1969. **2**(7632): p. 1219-22.
204. Andrews, P.M. and S.B. Bates, *Improving Euro-Collins flushing solution's ability to protect kidneys from normothermic ischemia*. Miner Electrolyte Metab, 1985. **11**(5): p. 309-13.
205. Guibert, E.E., et al., *Organ Preservation: Current Concepts and New Strategies for the Next Decade*. Transfus Med Hemother, 2011. **38**(2): p. 125-42.
206. Pruijm, J., et al., *Cellular damage and early metabolic function of transplanted livers stored in Eurocollins or University of Wisconsin solution*. Eur Surg Res, 1991. **23**(5-6): p. 285-91.

207. Belzer, F.O., et al., *A new perfusate for kidney preservation*. Transplantation, 1982. **33**(3): p. 322-3.
208. Belzer, F.O., et al., *Beneficial effects of adenosine and phosphate in kidney preservation*. Transplantation, 1983. **36**(6): p. 633-5.
209. Southard, J.H., M.J. Rice, and F.O. Belzer, *Preservation of renal function by adenosine-stimulated ATP synthesis in hypothermically perfused dog kidneys*. Cryobiology, 1985. **22**(3): p. 237-42.
210. Wahlberg, J.A., J.H. Southard, and F.O. Belzer, *Development of a cold storage solution for pancreas preservation*. Cryobiology, 1986. **23**(6): p. 477-82.
211. Martinez, J., et al., *[Outcomes using two preservation solutions (UW/HTK) in liver transplantation from brain death donors]*. Rev Med Chil, 2014. **142**(10): p. 1229-37.
212. Liu, Q., et al., *Preservation of canine composite facial flaps using uw solution*. Archives of Facial Plastic Surgery, 2010. **12**(4): p. 263-268.
213. van der Plaats, A., et al., *Effect of University of Wisconsin organ-preservation solution on haemorheology*. Transpl Int, 2004. **17**(5): p. 227-33.
214. Gao, S., et al., *Hyperbranched Polyglycerol as a Colloid in Cold Organ Preservation Solutions*. PLoS One, 2015. **10**(2).
215. Cittanova, M.L., et al., *Effect of hydroxyethylstarch in brain-dead kidney donors on renal function in kidney-transplant recipients*. The Lancet, 1996. **348**(9042): p. 1620-1622.
216. Parsons, R.F. and J.V. Guarrera, *Preservation solutions for static cold storage of abdominal allografts: which is best?* Curr Opin Organ Transplant, 2014. **19**(2): p. 100-7.
217. Bretschneider, H.J., et al., *Myocardial resistance and tolerance to ischemia: physiological and biochemical basis*. J Cardiovasc Surg (Torino), 1975. **16**(3): p. 241-60.
218. Bretschneider, H.J., *Myocardial Protection*. Thorac cardiovasc Surg, 1980. **28**(05): p. 295-302.
219. Erhard, J., et al., *Comparison of histidine-tryptophan-ketoglutarate (HTK) solution versus University of Wisconsin (UW) solution for organ preservation in human liver transplantation. A prospective, randomized study*. Transpl Int, 1994. **7**(3): p. 177-81.
220. Braathen, B., et al., *One single dose of histidine-tryptophan-ketoglutarate solution gives equally good myocardial protection in elective mitral valve surgery as repetitive cold blood cardioplegia: A prospective randomized study*. The Journal of Thoracic and Cardiovascular Surgery, 2011. **141**(4): p. 995-1001.
221. Rao, P.S. and A. Ojo, *The alphabet soup of kidney transplantation: SCD, DCD, ECD-- fundamentals for the practicing nephrologist*. Clin J Am Soc Nephrol, 2009. **4**(11): p. 1827-31.
222. Saidi, R.F., et al., *Outcomes in partial liver transplantation: deceased donor split-liver vs. live donor liver transplantation*. HPB (Oxford), 2011. **13**(11): p. 797-801.
223. Matas, A.J., et al., *OPTN/SRTR 2012 Annual Data Report: kidney*. Am J Transplant, 2014. **14 Suppl 1**: p. 11-44.
224. Israni, A.K., et al., *OPTN/SRTR 2012 Annual Data Report: deceased organ donation*. Am J Transplant, 2014. **14 Suppl 1**: p. 167-83.
225. Siedlecki, A., W. Irish, and D.C. Brennan, *Delayed Graft Function in the Kidney Transplant*. Am J Transplant, 2011. **11**(11): p. 2279-96.
226. Hwang, J.K., et al., *Long-term outcomes of kidney transplantation from expanded criteria deceased donors at a single center: comparison with standard criteria deceased donors*. Transplant Proc, 2014. **46**(2): p. 431-6.
227. Pierobon, E.S., et al., *Optimizing utilization of kidneys from deceased donors over 60 years: five-year outcomes after implementation of a combined clinical and histological allocation algorithm*. Transpl Int, 2013. **26**(8): p. 833-41.
228. Lee, C.M., et al., *The kidneys that nobody wanted: support for the utilization of expanded criteria donors*. Transplantation, 1996. **62**(12): p. 1832-41.
229. Jansen, J., *The First Successful Allogeneic Bone-Marrow Transplant: Georges Mathé*. Transfusion Medicine Reviews, 2005. **19**(3): p. 246-248.

230. Afzali, B., et al., *Comparison of Regulatory T Cells in Hemodialysis Patients and Healthy Controls: Implications for Cell Therapy in Transplantation*. Clin J Am Soc Nephrol, 2013. **8**(8): p. 1396-405.
231. Yang, J., et al., *Third-party Tolerogenic Dendritic Cells Reduce Allo-reactivity In vitro and Ameliorate the Severity of Acute graft-Versus-host Disease in Allo-bone Marrow Transplantation*. Scandinavian Journal of Immunology, 2013. **78**(6): p. 486-496.
232. Crop, M.J., et al., *Donor-derived mesenchymal stem cells suppress alloreactivity of kidney transplant patients*. Transplantation, 2009. **87**(6): p. 896-906.
233. Tavassoli, M. and W.H. Crosby, *Transplantation of marrow to extramedullary sites*. Science, 1968. **161**(3836): p. 54-6.
234. Friedenstein, A.J., R.K. Chailakhjan, and K.S. Lalykina, *The development of fibroblast colonies in monolayer cultures of guinea-pig bone marrow and spleen cells*. Cell Tissue Kinet, 1970. **3**(4): p. 393-403.
235. Friedenstein, A.J., et al., *Stromal cells responsible for transferring the microenvironment of the hemopoietic tissues. Cloning in vitro and retransplantation in vivo*. Transplantation, 1974. **17**(4): p. 331-40.
236. Friedenstein, A.J., *Precursor cells of mechanocytes*. Int Rev Cytol, 1976. **47**: p. 327-59.
237. Bianco, P., P.G. Robey, and P.J. Simmons, *Mesenchymal Stem Cells: Revisiting History, Concepts, and Assays*. Cell Stem Cell, 2008. **2**(4): p. 313-9.
238. Caplan, A.I., *Mesenchymal stem cells*. J Orthop Res, 1991. **9**(5): p. 641-50.
239. Lindner, U., et al., *Mesenchymal Stem or Stromal Cells: Toward a Better Understanding of Their Biology?* Transfus Med Hemother, 2010. **37**(2): p. 75-83.
240. Caplan, A.I., *Mesenchymal Stem Cells: Time to Change the Name!* STEM CELLS Translational Medicine, 2017. **6**(6): p. 1445-1451.
241. Simmons, P.J., et al., *Isolation, characterization and functional activity of human marrow stromal progenitors in hemopoiesis*. Prog Clin Biol Res, 1994. **389**: p. 271-80.
242. Collins, E., et al., *Differential efficacy of human mesenchymal stem cells based on source of origin*. J Immunol, 2014. **193**(9): p. 4381-90.
243. Bartholomew, A., et al., *Mesenchymal stem cells suppress lymphocyte proliferation in vitro and prolong skin graft survival in vivo*. Exp Hematol, 2002. **30**(1): p. 42-8.
244. Nauta, A.J. and W.E. Fibbe, *Immunomodulatory properties of mesenchymal stromal cells*. Blood, 2007. **110**(10): p. 3499-506.
245. Engela, A.U., et al., *Mesenchymal stem cells control alloreactive CD8(+) CD28(-) T cells*. Clin Exp Immunol, 2013. **174**(3): p. 449-58.
246. Usha Shalini, P., et al., *In vitro allogeneic immune cell response to mesenchymal stromal cells derived from human adipose in patients with rheumatoid arthritis*. Cell Immunol, 2017.
247. Dominici, M., et al., *Minimal criteria for defining multipotent mesenchymal stromal cells. The International Society for Cellular Therapy position statement*. Cytotherapy, 2006. **8**(4): p. 315-7.
248. Gronthos, S., et al., *Molecular and cellular characterisation of highly purified stromal stem cells derived from human bone marrow*. J Cell Sci, 2003. **116**(Pt 9): p. 1827-35.
249. Ge, J., et al., *The Size of Mesenchymal Stem Cells is a Significant Cause of Vascular Obstructions and Stroke*. Stem Cell Reviews and Reports, 2014. **10**(2): p. 295-303.
250. Yao, W., et al., *Reversing bone loss by directing mesenchymal stem cells to bone*. Stem Cells, 2013. **31**(9): p. 2003-14.
251. Deng, K., et al., *Mesenchymal stem cells and their secretome partially restore nerve and urethral function in a dual muscle and nerve injury stress urinary incontinence model*. Am J Physiol Renal Physiol, 2015. **308**(2): p. F92-f100.
252. Hoogduijn, M.J., et al., *Mesenchymal stem cells induce an inflammatory response after intravenous infusion*. Stem Cells Dev, 2013. **22**(21): p. 2825-35.

253. Amarnath, S., et al., *Bone marrow-derived mesenchymal stromal cells harness purinergic signaling to tolerize human Th1 cells in vivo*. *Stem Cells*, 2015. **33**(4): p. 1200-12.
254. Tang, J., et al., *Transforming growth factor- β -Expressing Mesenchymal Stem Cells Induce Local Tolerance in a Rat Liver Transplantation Model of Acute Rejection*. *STEM CELLS*, 2016. **34**(11): p. 2681-2692.
255. He, Y., et al., *Indoleamine 2, 3-Dioxygenase Transfected Mesenchymal Stem Cells Induce Kidney Allograft Tolerance by Increasing the Production and Function of Regulatory T Cells*. *Transplantation*, 2015. **99**(9): p. 1829-38.
256. van Kooten, C., et al., *Mesenchymal stromal cells in clinical kidney transplantation: how tolerant can it be?* *Curr Opin Organ Transplant*, 2016. **21**(6): p. 550-558.
257. Ahmadi, M., et al., *Contributory Anti-Inflammatory Effects of Mesenchymal Stem Cells, Not Conditioned Media, On Ovalbumin-Induced Asthmatic Changes in Male Rats*. *Inflammation*, 2016. **39**(6): p. 1960-1971.
258. Pers, Y.M., et al., *Mesenchymal stem cells for the management of inflammation in osteoarthritis: state of the art and perspectives*. *Osteoarthritis and Cartilage*, 2015. **23**(11): p. 2027-2035.
259. Gu, N., et al., *Anti-inflammatory and Antiapoptotic Effects of Mesenchymal Stem Cells Transplantation in Rat Brain with Cerebral Ischemia*. *Journal of Stroke and Cerebrovascular Diseases*, 2014. **23**(10): p. 2598-2606.
260. Hu, J., et al., *Mesenchymal stem cells attenuate ischemic acute kidney injury by inducing regulatory T cells through splenocyte interactions*. *Kidney Int*, 2013. **84**(3): p. 521-31.
261. Li, M., et al., *Mesenchymal stem cells suppress CD8(+) T cell-mediated activation by suppressing natural killer group 2, member D protein receptor expression and secretion of prostaglandin E(2), indoleamine 2, 3-dioxygenase and transforming growth factor- β* . *Clin Exp Immunol*, 2014. **178**(3): p. 516-24.
262. Zafranskaya, M., et al., *PGE2 contributes to in vitro MSC-mediated inhibition of non-specific and antigen-specific T cell proliferation in MS patients*. *Scand J Immunol*, 2013. **78**(5): p. 455-62.
263. Wise, A.F., et al., *Human mesenchymal stem cells alter macrophage phenotype and promote regeneration via homing to the kidney following ischemia-reperfusion injury*. *Am J Physiol Renal Physiol*, 2014. **306**(10): p. F1222-35.
264. Wheat, W.H., et al., *Suppression of Canine Dendritic Cell Activation/Maturation and Inflammatory Cytokine Release by Mesenchymal Stem Cells Occurs Through Multiple Distinct Biochemical Pathways*. *Stem Cells Dev*, 2017. **26**(4): p. 249-262.
265. Liu, W.H., et al., *Novel mechanism of inhibition of dendritic cells maturation by mesenchymal stem cells via interleukin-10 and the JAK1/STAT3 signaling pathway*. *PLoS One*, 2013. **8**(1): p. e55487.
266. Feng, X., et al., *Restored Immunosuppressive Effect of Mesenchymal Stem Cells on B Cells After Olfactory 1/Early B Cell Factor–Associated Zinc-Finger Protein Down-Regulation in Patients With Systemic Lupus Erythematosus*. *Arthritis & Rheumatology*, 2014. **66**(12): p. 3413-3423.
267. Consentius, C., et al., *Mesenchymal Stromal Cells Prevent Allostimulation In Vivo and Control Checkpoints of Th1 Priming: Migration of Human DC to Lymph Nodes and NK Cell Activation*. *STEM CELLS*, 2015. **33**(10): p. 3087-3099.
268. Spaggiari, G.M., et al., *Mesenchymal stem cells inhibit natural killer–cell proliferation, cytotoxicity, and cytokine production: role of indoleamine 2,3-dioxygenase and prostaglandin E2*. *Blood*, 2008. **111**(3): p. 1327-1333.
269. Chae, H.K., et al., *Immunomodulatory effects of soluble factors secreted by feline adipose tissue-derived mesenchymal stem cells*. *Vet Immunol Immunopathol*, 2017. **191**: p. 22-29.

270. English, K., et al., *Cell contact, prostaglandin E(2) and transforming growth factor beta 1 play non-redundant roles in human mesenchymal stem cell induction of CD4+CD25(High) forkhead box P3+ regulatory T cells*. Clin Exp Immunol, 2009. **156**(1): p. 149-60.
271. de Oliveira Bravo, M., J.L. Carvalho, and F. Saldanha-Araujo, *Adenosine production: a common path for mesenchymal stem-cell and regulatory T-cell-mediated immunosuppression*. Purinergic Signal, 2016. **12**(4): p. 595-609.
272. Davies, L.C., et al., *Mesenchymal Stromal Cell Secretion of Programmed Death-1 Ligands Regulates T Cell Mediated Immunosuppression*. Stem Cells, 2017. **35**(3): p. 766-776.
273. Su, J., et al., *Phylogenetic distinction of iNOS and IDO function in mesenchymal stem cell-mediated immunosuppression in mammalian species*. Cell Death Differ, 2014. **21**(3): p. 388-96.
274. Sato, K., et al., *Nitric oxide plays a critical role in suppression of T-cell proliferation by mesenchymal stem cells*. Blood, 2007. **109**(1): p. 228-234.
275. Ren, G., et al., *Mesenchymal Stem Cell-Mediated Immunosuppression Occurs via Concerted Action of Chemokines and Nitric Oxide*. Cell Stem Cell, 2008. **2**(2): p. 141-150.
276. DelaRosa, O., et al., *Requirement of IFN-gamma-mediated indoleamine 2,3-dioxygenase expression in the modulation of lymphocyte proliferation by human adipose-derived stem cells*. Tissue Eng Part A, 2009. **15**(10): p. 2795-806.
277. Zhang, B., *CD73: A novel target for cancer immunotherapy*. Cancer Res, 2010. **70**(16): p. 6407-11.
278. Milne, G.R. and T.M. Palmer, *Anti-inflammatory and immunosuppressive effects of the A2A adenosine receptor*. ScientificWorldJournal, 2011. **11**: p. 320-39.
279. Lawrence, T., *The Nuclear Factor NF- κ B Pathway in Inflammation*. Cold Spring Harb Perspect Biol, 2009. **1**(6).
280. Karwacz, K., et al., *PD-L1 co-stimulation contributes to ligand-induced T cell receptor down-modulation on CD8(+) T cells*. EMBO Mol Med, 2011. **3**(10): p. 581-92.
281. Kythreotou, A., et al., *PD-L1*. J Clin Pathol, 2017.
282. Yokosuka, T., et al., *Programmed cell death 1 forms negative costimulatory microclusters that directly inhibit T cell receptor signaling by recruiting phosphatase SHP2*. The Journal of Experimental Medicine, 2012. **209**(6): p. 1201-1217.
283. Korbecki, J., et al., *Cyclooxygenase pathways*. Acta Biochim Pol, 2014. **61**(4): p. 639-49.
284. Zhou, W., et al., *Cyclooxygenase inhibition abrogates aeroallergen-induced immune tolerance by suppressing prostaglandin I2 receptor signaling*. J Allergy Clin Immunol, 2014. **134**(3): p. 698-705.e5.
285. Li, D., et al., *Overexpression of COX-2 but not indoleamine 2,3-dioxygenase-1 enhances the immunosuppressive ability of human umbilical cord-derived mesenchymal stem cells*. Int J Mol Med, 2015. **35**(5): p. 1309-16.
286. Brown, J.M., et al., *Bone Marrow Stromal Cells Inhibit Mast Cell Function Via a COX2 Dependent Mechanism*. Clin Exp Allergy, 2011. **41**(4): p. 526-34.
287. Hata, A.N. and R.M. Breyer, *Pharmacology and signaling of prostaglandin receptors: multiple roles in inflammation and immune modulation*. Pharmacol Ther, 2004. **103**(2): p. 147-66.
288. Tang, E.H., et al., *Activation of prostaglandin E2-EP4 signaling reduces chemokine production in adipose tissue*. J Lipid Res, 2015. **56**(2): p. 358-68.
289. Chen, K., et al., *Human umbilical cord mesenchymal stem cells hUC-MSCs exert immunosuppressive activities through a PGE2-dependent mechanism*. Clinical Immunology, 2010. **135**(3): p. 448-458.
290. Yanez, R., et al., *Prostaglandin E2 plays a key role in the immunosuppressive properties of adipose and bone marrow tissue-derived mesenchymal stromal cells*. Exp Cell Res, 2010. **316**(19): p. 3109-23.
291. Xu, C., et al., *TGF- β Promotes Immune Responses in the Presence of Mesenchymal Stem Cells*. The Journal of Immunology, 2014. **192**(1): p. 103-109.

292. Ueno, T., et al., *Mesenchymal stem cells ameliorate experimental peritoneal fibrosis by suppressing inflammation and inhibiting TGF-beta1 signaling*. *Kidney Int*, 2013. **84**(2): p. 297-307.
293. Yoshimura, A. and G. Muto, *TGF-β Function in Immune Suppression*, in *Negative Co-Receptors and Ligands*, R. Ahmed and T. Honjo, Editors. 2011, Springer Berlin Heidelberg: Berlin, Heidelberg. p. 127-147.
294. Lu, L., et al., *Role of SMAD and Non-SMAD Signals in the Development of Th17 and Regulatory T Cells*. *J Immunol*, 2010. **184**(8): p. 4295-306.
295. Schlenner, S.M., et al., *Smad3 binding to the foxp3 enhancer is dispensable for the development of regulatory T cells with the exception of the gut*. *J Exp Med*, 2012. **209**(9): p. 1529-35.
296. Lv, K., et al., *Galectin-9 promotes TGF-beta1-dependent induction of regulatory T cells via the TGF-beta/Smad signaling pathway*. *Mol Med Rep*, 2013. **7**(1): p. 205-10.
297. Bingisser, R.M., et al., *Macrophage-derived nitric oxide regulates T cell activation via reversible disruption of the Jak3/STAT5 signaling pathway*. *J Immunol*, 1998. **160**(12): p. 5729-34.
298. Eriksson, U., et al., *Human Bronchial Epithelium Controls TH2 Responses by TH1-Induced, Nitric Oxide-Mediated STAT5 Dephosphorylation: Implications for the Pathogenesis of Asthma*. *The Journal of Immunology*, 2005. **175**(4): p. 2715-2720.
299. Rawlings, J.S., K.M. Rosler, and D.A. Harrison, *The JAK/STAT signaling pathway*. *Journal of Cell Science*, 2004. **117**(8): p. 1281-1283.
300. Kiu, H. and S.E. Nicholson, *Biology and significance of the JAK/STAT signalling pathways*. *Growth Factors*, 2012. **30**(2): p. 88-106.
301. Seif, F., et al., *The role of JAK-STAT signaling pathway and its regulators in the fate of T helper cells*. *Cell Commun Signal*, 2017. **15**(1): p. 23.
302. Murphy, K.M., *Permission to Proceed: Jak3 and STAT5 Signaling Molecules Give the Green Light for T Helper 1 Cell Differentiation*. *Immunity*, 2008. **28**(6): p. 725-7.
303. Huang, J.S., et al., *Effect of nitric oxide-cGMP-dependent protein kinase activation on advanced glycation end-product-induced proliferation in renal fibroblasts*. *J Am Soc Nephrol*, 2005. **16**(8): p. 2318-29.
304. Klein, M. and T. Bopp, *Cyclic AMP Represents a Crucial Component of Treg Cell-Mediated Immune Regulation*. *Front Immunol*, 2016. **7**: p. 315.
305. Taylor, M.W. and G.S. Feng, *Relationship between interferon-gamma, indoleamine 2,3-dioxygenase, and tryptophan catabolism*. *Faseb j*, 1991. **5**(11): p. 2516-22.
306. Ye, Q.X., et al., *Indoleamine 2,3-dioxygenase and inducible nitric oxide synthase mediate immune tolerance induced by CTLA4Ig and anti-CD154 hematopoietic stem cell transplantation in a sensitized mouse model*. *Exp Ther Med*, 2017. **14**(3): p. 1884-1891.
307. Mándi, Y. and L. Vécsei, *The kynurenine system and immunoregulation*. *Journal of Neural Transmission*, 2012. **119**(2): p. 197-209.
308. Ren, G., et al., *Species variation in the mechanisms of mesenchymal stem cell-mediated immunosuppression*. *Stem Cells*, 2009. **27**(8): p. 1954-62.
309. Gao, F., et al., *Mesenchymal stem cells and immunomodulation: current status and future prospects*. *Cell Death & Disease*, 2016. **7**: p. e2062.
310. Chow, L., et al., *Mechanisms of Immune Suppression Utilized by Canine Adipose and Bone Marrow-Derived Mesenchymal Stem Cells*. *Stem Cells Dev*, 2017. **26**(5): p. 374-389.
311. Cagliani, J., et al., *Immunomodulation by Mesenchymal Stromal Cells and Their Clinical Applications*. *J Stem Cell Regen Biol*, 2017. **3**(2).
312. Rubtsov, Y., et al., *Molecular Mechanisms of Immunomodulation Properties of Mesenchymal Stromal Cells: A New Insight into the Role of ICAM-1*. *Stem Cells International*, 2017. **2017**: p. 6516854.

313. Sivanathan, K.N., et al., *Interferon-gamma modification of mesenchymal stem cells: implications of autologous and allogeneic mesenchymal stem cell therapy in allotransplantation*. *Stem Cell Rev*, 2014. **10**(3): p. 351-75.
314. Chen, K., et al., *Human umbilical cord mesenchymal stem cells hUC-MSCs exert immunosuppressive activities through a PGE2-dependent mechanism*. *Clin Immunol*, 2010. **135**(3): p. 448-58.
315. Yuan, X., G. Cheng, and T.R. Malek, *The importance of regulatory T-cell heterogeneity in maintaining self-tolerance*. *Immunol Rev*, 2014. **259**(1): p. 103-14.
316. Xu, H., et al., *IDO: a double-edged sword for T(H)1/T(H)2 regulation*. *Immunol Lett*, 2008. **121**(1): p. 1-6.
317. Bai, L., et al., *Human bone marrow-derived mesenchymal stem cells induce Th2-polarized immune response and promote endogenous repair in animal models of multiple sclerosis*. *Glia*, 2009. **57**(11): p. 1192-203.
318. Umeshappa, C.S., et al., *Differential requirements of CD4(+) T-cell signals for effector cytotoxic T-lymphocyte (CTL) priming and functional memory CTL development at higher CD8(+) T-cell precursor frequency*. *Immunology*, 2013. **138**(4): p. 298-306.
319. Asari, S., et al., *Mesenchymal stem cells suppress B cell terminal differentiation*. *Exp Hematol*, 2009. **37**(5): p. 604-15.
320. Corcione, A., et al., *Human mesenchymal stem cells modulate B-cell functions*. *Blood*, 2006. **107**(1): p. 367-372.
321. Blanco, B., et al., *Immunomodulatory effects of bone marrow versus adipose tissue-derived mesenchymal stromal cells on NK cells: implications in the transplantation setting*. *European Journal of Haematology*, 2016. **97**(6): p. 528-537.
322. Qu, M., et al., *Bone marrow-derived mesenchymal stem cells suppress NK cell recruitment and activation in Polyl:C-induced liver injury*. *Biochemical and Biophysical Research Communications*, 2015. **466**(2): p. 173-179.
323. Ribeiro, A., et al., *Mesenchymal stem cells from umbilical cord matrix, adipose tissue and bone marrow exhibit different capability to suppress peripheral blood B, natural killer and T cells*. *Stem Cell Res Ther*, 2013. **4**(5): p. 125.
324. Crop, M.J., et al., *Human mesenchymal stem cells are susceptible to lysis by CD8(+) T cells and NK cells*. *Cell Transplant*, 2011. **20**(10): p. 1547-59.
325. Williams, E.L., K. White, and R.O.C. Oreffo, *Isolation and Enrichment of Stro-1 Immunoselected Mesenchymal Stem Cells from Adult Human Bone Marrow*, in *Stem Cell Niche: Methods and Protocols*, K. Turksen, Editor. 2013, Humana Press: Totowa, NJ. p. 67-73.
326. McCarty, R.C., et al., *Characterisation and developmental potential of ovine bone marrow derived mesenchymal stem cells*. *J Cell Physiol*, 2009. **219**(2): p. 324-33.
327. Boxall, S.A. and E. Jones, *Markers for characterization of bone marrow multipotential stromal cells*. *Stem Cells Int*, 2012. **2012**: p. 975871.
328. De Martino, M., et al., *Mesenchymal stem cells infusion prevents acute cellular rejection in rat kidney transplantation*. *Transplant Proc*, 2010. **42**(4): p. 1331-5.
329. Franquesa, M., et al., *Mesenchymal stem cell therapy prevents interstitial fibrosis and tubular atrophy in a rat kidney allograft model*. *Stem Cells Dev*, 2012. **21**(17): p. 3125-35.
330. Gregorini, M., et al., *Perfusion of isolated rat kidney with Mesenchymal Stromal Cells/Extracellular Vesicles prevents ischaemic injury*. *J Cell Mol Med*, 2017.
331. Hara, Y., et al., *In vivo effect of bone marrow-derived mesenchymal stem cells in a rat kidney transplantation model with prolonged cold ischemia*. *Transpl Int*, 2011. **24**(11): p. 1112-23.
332. Wu, X., et al., *Micro-vesicles derived from human Wharton's Jelly mesenchymal stromal cells mitigate renal ischemia-reperfusion injury in rats after cardiac death renal transplantation*. *J Cell Biochem*, 2017.
333. Yu, P., et al., *Marrow Mesenchymal Stem Cells Effectively Reduce Histologic Changes in a Rat Model of Chronic Renal Allograft Rejection*. *Transplant Proc*, 2017. **49**(9): p. 2194-2203.

334. Zonta, S., et al., *Which is the most suitable and effective route of administration for mesenchymal stem cell-based immunomodulation therapy in experimental kidney transplantation: endovenous or arterial?* *Transplant Proc*, 2010. **42**(4): p. 1336-40.
335. Baulier, E., et al., *Amniotic fluid-derived mesenchymal stem cells prevent fibrosis and preserve renal function in a preclinical porcine model of kidney transplantation.* *Stem Cells Transl Med*, 2014. **3**(7): p. 809-20.
336. Athanasiadis, D., et al., *Remote Ischemic Preconditioning May Attenuate Renal Ischemia-Reperfusion Injury in a Porcine Model of Supraceliac Aortic Cross-Clamping.* *J Vasc Res*, 2015. **52**(3): p. 161-71.
337. Behr, L., et al., *Intra renal arterial injection of autologous mesenchymal stem cells in an ovine model in the postischemic kidney.* *Nephron Physiol*, 2007. **107**(3): p. p65-76.
338. Hesketh, E.E., et al., *Renal ischaemia reperfusion injury: a mouse model of injury and regeneration.* *J Vis Exp*, 2014(88).
339. Perico, N., et al., *Autologous mesenchymal stromal cells and kidney transplantation: a pilot study of safety and clinical feasibility.* *Clin J Am Soc Nephrol*, 2011. **6**(2): p. 412-22.
340. Perico, N., et al., *Mesenchymal stromal cells and kidney transplantation: pretransplant infusion protects from graft dysfunction while fostering immunoregulation.* *Transpl Int*, 2013. **26**(9): p. 867-78.
341. Peng, Y., et al., *Donor-derived mesenchymal stem cells combined with low-dose tacrolimus prevent acute rejection after renal transplantation: a clinical pilot study.* *Transplantation*, 2013. **95**(1): p. 161-8.
342. Lee, H., et al., *Intra-osseous injection of donor mesenchymal stem cell (MSC) into the bone marrow in living donor kidney transplantation; a pilot study.* *J Transl Med*, 2013. **11**: p. 96.
343. Reinders, M.E., et al., *Autologous bone marrow-derived mesenchymal stromal cells for the treatment of allograft rejection after renal transplantation: results of a phase I study.* *Stem Cells Transl Med*, 2013. **2**(2): p. 107-11.
344. Saadi, G., et al., *Mesenchymal stem cell transfusion for desensitization of positive lymphocyte cross-match before kidney transplantation: outcome of 3 cases.* *Cell Prolif*, 2013. **46**(2): p. 121-6.
345. Mudrabettu, C., et al., *Safety and efficacy of autologous mesenchymal stromal cells transplantation in patients undergoing living donor kidney transplantation: a pilot study.* *Nephrology (Carlton)*, 2015. **20**(1): p. 25-33.
346. Tan, J., et al., *Induction therapy with autologous mesenchymal stem cells in living-related kidney transplants: a randomized controlled trial.* *Jama*, 2012. **307**(11): p. 1169-77.
347. Vanikar, A.V., et al., *Co-infusion of donor adipose tissue-derived mesenchymal and hematopoietic stem cells helps safe minimization of immunosuppression in renal transplantation - single center experience.* *Ren Fail*, 2014. **36**(9): p. 1376-84.
348. Pan, G.H., et al., *Low-dose tacrolimus combined with donor-derived mesenchymal stem cells after renal transplantation: a prospective, non-randomized study.* *Oncotarget*, 2016. **7**(11): p. 12089-101.
349. Shih, C.J., et al., *Immunosuppressant dose reduction and long-term rejection risk in renal transplant recipients with severe bacterial pneumonia.* *Singapore Med J*, 2014. **55**(7): p. 372-7.
350. Sawinski, D., et al., *Calcineurin Inhibitor Minimization, Conversion, Withdrawal, and Avoidance Strategies in Renal Transplantation: A Systematic Review and Meta-Analysis.* *Am J Transplant*, 2016. **16**(7): p. 2117-38.
351. Han, S.S., et al., *Pharmacokinetics of tacrolimus according to body composition in recipients of kidney transplants.* *Kidney Research and Clinical Practice*, 2012. **31**(3): p. 157-162.
352. Robles-Piedras, A.L. and E.H. Gonzalez-Lopez, *Tacrolimus levels in adult patients with renal transplant.* *Proc West Pharmacol Soc*, 2009. **52**: p. 33-4.

353. Patel, S.A., et al., *Mesenchymal stem cells protect breast cancer cells through regulatory T cells: role of mesenchymal stem cell-derived TGF-beta*. J Immunol, 2010. **184**(10): p. 5885-94.
354. Ljujic, B., et al., *Human mesenchymal stem cells creating an immunosuppressive environment and promote breast cancer in mice*. Sci Rep, 2013. **3**: p. 2298.
355. Kuriyan, A.E., et al., *Vision Loss after Intravitreal Injection of Autologous "Stem Cells" for AMD*. N Engl J Med, 2017. **376**(11): p. 1047-1053.
356. Le Blanc, K., et al., *HLA expression and immunologic properties of differentiated and undifferentiated mesenchymal stem cells*. Exp Hematol, 2003. **31**(10): p. 890-6.
357. Lett B, S.K., Coates PT., *Mesenchymal stem cells for kidney transplantation*. World J Clin Urol, 2014. **3**(2): p. 87-95.
358. Eggenhofer, E., et al., *Mesenchymal stem cells together with mycophenolate mofetil inhibit antigen presenting cell and T cell infiltration into allogeneic heart grafts*. Transpl Immunol, 2011. **24**(3): p. 157-63.
359. Inoue, S., et al., *Immunomodulatory effects of mesenchymal stem cells in a rat organ transplant model*. Transplantation, 2006. **81**(11): p. 1589-95.
360. Casiraghi, F., et al., *Pretransplant infusion of mesenchymal stem cells prolongs the survival of a semiallogeneic heart transplant through the generation of regulatory T cells*. J Immunol, 2008. **181**(6): p. 3933-46.
361. Nauta, A.J., et al., *Donor-derived mesenchymal stem cells are immunogenic in an allogeneic host and stimulate donor graft rejection in a nonmyeloablative setting*. Blood, 2006. **108**(6): p. 2114-20.
362. Seifert, M., et al., *Detrimental effects of rat mesenchymal stromal cell pre-treatment in a model of acute kidney rejection*. Front Immunol, 2012. **3**: p. 202.
363. Sbano, P., et al., *Use of donor bone marrow mesenchymal stem cells for treatment of skin allograft rejection in a preclinical rat model*. Arch Dermatol Res, 2008. **300**(3): p. 115-24.
364. Ge, W., et al., *Infusion of mesenchymal stem cells and rapamycin synergize to attenuate alloimmune responses and promote cardiac allograft tolerance*. Am J Transplant, 2009. **9**(8): p. 1760-72.
365. Solari, M.G., et al., *Marginal mass islet transplantation with autologous mesenchymal stem cells promotes long-term islet allograft survival and sustained normoglycemia*. J Autoimmun, 2009. **32**(2): p. 116-24.
366. Haas, M., et al., *Banff 2013 meeting report: inclusion of c4d-negative antibody-mediated rejection and antibody-associated arterial lesions*. Am J Transplant, 2014. **14**(2): p. 272-83.
367. Squillaro, T., G. Peluso, and U. Galderisi, *Clinical Trials with Mesenchymal Stem Cells: An Update*. Cell Transplantation, 2016. **25**(5): p. 829-848.
368. Le Blanc, K., et al., *Mesenchymal stem cells for treatment of steroid-resistant, severe, acute graft-versus-host disease: a phase II study*. Lancet, 2008. **371**(9624): p. 1579-86.
369. Liang, J., et al., *Allogeneic mesenchymal stem cells transplantation in refractory systemic lupus erythematosus: a pilot clinical study*. Annals of the Rheumatic Diseases, 2010. **69**(8): p. 1423-1429.
370. Liu, J., et al., *Sodium Butyrate Promotes the Differentiation of Rat Bone Marrow Mesenchymal Stem Cells to Smooth Muscle Cells through Histone Acetylation*. PLoS ONE, 2014. **9**(12): p. e116183.
371. Li, J.-F., et al., *Differentiation of hUC-MSC into dopaminergic-like cells after transduction with hepatocyte growth factor*. Molecular and Cellular Biochemistry, 2013. **381**(1): p. 183-190.
372. Simmons, P. and B. Torok-Storb, *Identification of stromal cell precursors in human bone marrow by a novel monoclonal antibody, STRO-1*. Blood, 1991. **78**(1): p. 55-62.
373. Dennis, J.E., et al., *The STRO-1+ Marrow Cell Population Is Multipotential*. Cells Tissues Organs, 2002. **170**(2-3): p. 73-82.

374. Noort, W.A., et al., *Human versus porcine mesenchymal stromal cells: phenotype, differentiation potential, immunomodulation and cardiac improvement after transplantation*. Journal of Cellular and Molecular Medicine, 2012. **16**(8): p. 1827-1839.
375. Harting, M., et al., *Immunophenotype characterization of rat mesenchymal stromal cells*. Cytotherapy, 2008. **10**(3): p. 243-53.
376. Peister, A., et al., *Adult stem cells from bone marrow (MSCs) isolated from different strains of inbred mice vary in surface epitopes, rates of proliferation, and differentiation potential*. Blood, 2004. **103**(5): p. 1662-1668.
377. Mrugala, D., et al., *Phenotypic and functional characterisation of ovine mesenchymal stem cells: application to a cartilage defect model*. Annals of the Rheumatic Diseases, 2008. **67**(3): p. 288-295.
378. Rozemuller, H., et al., *Prospective Isolation of Mesenchymal Stem Cells from Multiple Mammalian Species Using Cross-Reacting Anti-Human Monoclonal Antibodies*. Stem Cells and Development, 2010. **19**(12): p. 1911-1921.
379. Barzilay, R., et al., *Comparative characterization of bone marrow-derived mesenchymal stromal cells from four different rat strains*. Cytotherapy, 2009. **11**(4): p. 435-42.
380. Pelekanos, R.A., et al., *Comprehensive transcriptome and immunophenotype analysis of renal and cardiac MSC-like populations supports strong congruence with bone marrow MSC despite maintenance of distinct identities*. Stem Cell Research, 2012. **8**(1): p. 58-73.
381. Sun, S., et al., *Isolation of Mouse Marrow Mesenchymal Progenitors by a Novel and Reliable Method*. STEM CELLS, 2003. **21**(5): p. 527-535.
382. Jessop, H.L., B.S. Noble, and A. Cryer, *The differentiation of a potential mesenchymal stem cell population within ovine bone marrow*. Biochem Soc Trans, 1994. **22**(3): p. 248s.
383. Rhodes, N.P., et al., *Heterogeneity in proliferative potential of ovine mesenchymal stem cell colonies*. J Mater Sci Mater Med, 2004. **15**(4): p. 397-402.
384. Caminal, M., et al., *A reproducible method for the isolation and expansion of ovine mesenchymal stromal cells from bone marrow for use in regenerative medicine preclinical studies*. J Tissue Eng Regen Med, 2016.
385. Lyahyai, J., et al., *Isolation and characterization of ovine mesenchymal stem cells derived from peripheral blood*. BMC Vet Res, 2012. **8**: p. 169.
386. Letouzey, V., et al., *Isolation and Characterisation of Mesenchymal Stem/Stromal Cells in the Ovine Endometrium*. PLoS One, 2015. **10**(5).
387. Dreger, T., et al., *Intravenous application of CD271-selected mesenchymal stem cells during fracture healing*. J Orthop Trauma, 2014. **28 Suppl 1**: p. S15-9.
388. Cuthbert, R.J., et al., *Examining the Feasibility of Clinical Grade CD271(+) Enrichment of Mesenchymal Stromal Cells for Bone Regeneration*. PLoS One, 2015. **10**(3).
389. Pal, B., *In vitro Culture of Naïve Human Bone Marrow Mesenchymal Stem Cells: A Stemness Based Approach*. 2017. **5**.
390. Battula, V.L., et al., *Isolation of functionally distinct mesenchymal stem cell subsets using antibodies against CD56, CD271, and mesenchymal stem cell antigen-1*. Haematologica, 2009. **94**(2): p. 173-84.
391. Bakondi, B., et al., *CD133 Identifies a Human Bone Marrow Stem/Progenitor Cell Sub-population With a Repertoire of Secreted Factors That Protect Against Stroke*. Mol Ther, 2009. **17**(11): p. 1938-47.
392. Khan, M.R., et al., *Immunophenotypic characterization of ovine mesenchymal stem cells*. Cytometry A, 2016. **89**(5): p. 443-50.
393. Zheng, C., et al., *CD11b regulates obesity-induced insulin resistance via limiting alternative activation and proliferation of adipose tissue macrophages*. Proceedings of the National Academy of Sciences, 2015. **112**(52): p. E7239-E7248.
394. Zanoni, I. and F. Granucci, *Role of CD14 in host protection against infections and in metabolism regulation*. Front Cell Infect Microbiol, 2013. **3**.

395. Lertkiatmongkol, P., et al., *Endothelial functions of PECAM-1 (CD31)*. *Curr Opin Hematol*, 2016. **23**(3): p. 253-9.
396. Williams, K., et al., *CD44 integrates signaling in normal stem cell, cancer stem cell and (pre)metastatic niches*. *Experimental Biology and Medicine*, 2013. **238**(3): p. 324-338.
397. Nam, K., et al., *CD44 regulates cell proliferation, migration, and invasion via modulation of c-Src transcription in human breast cancer cells*. *Cellular Signalling*, 2015. **27**(9): p. 1882-1894.
398. Haig, D.M., et al., *The activation status of ovine CD45R+ and CD45R- efferent lymph T cells after orf virus reinfection*. *Journal of Comparative Pathology*, 1996. **115**(2): p. 163-174.
399. Nishimura, H., et al., *Differential expression of a CD45R epitope(6B2) on murine CD5+ B cells: Possible difference in the post-translational modification of CD45 molecules*. *Cellular Immunology*, 1992. **140**(2): p. 432-443.
400. Gao, Z., K. Dong, and H. Zhang, *The Roles of CD73 in Cancer*. *Biomed Res Int*, 2014. **2014**.
401. Kumar, A., et al., *Multiple roles of CD90 in cancer*. *Tumor Biology*, 2016. **37**(9): p. 11611-11622.
402. Nair, S., et al., *Immunohistochemical Expression of CD105 and TGF-beta1 in Oral Squamous Cell Carcinoma and Adjacent Apparently Normal Oral Mucosa and its Correlation With Clinicopathologic Features*. *Appl Immunohistochem Mol Morphol*, 2016. **24**(1): p. 35-41.
403. Swart, G.W.M., *Activated leukocyte cell adhesion molecule (CD166/ALCAM): Developmental and mechanistic aspects of cell clustering and cell migration*. *European Journal of Cell Biology*, 2002. **81**(6): p. 313-321.
404. Fujiwara, K., et al., *CD166/ALCAM Expression Is Characteristic of Tumorigenicity and Invasive and Migratory Activities of Pancreatic Cancer Cells*. *PLoS ONE*, 2014. **9**(9): p. e107247.
405. Farrell, E., et al., *Effects of iron oxide incorporation for long term cell tracking on MSC differentiation in vitro and in vivo*. *Biochemical and Biophysical Research Communications*, 2008. **369**(4): p. 1076-1081.
406. Addicott, B., et al., *Mesenchymal stem cell labeling and in vitro MR characterization at 1.5 T of new SPIO contrast agent: Molday ION Rhodamine-B(™)*. *Contrast Media Mol Imaging*, 2011. **6**(1): p. 7-18.
407. Hansen, L., et al., *Ultrastructural characterization of mesenchymal stromal cells labeled with ultrasmall superparamagnetic iron-oxide nanoparticles for clinical tracking studies*. *Scand J Clin Lab Invest*, 2014. **74**(5): p. 437-46.
408. Assis, A.C., et al., *Time-dependent migration of systemically delivered bone marrow mesenchymal stem cells to the infarcted heart*. *Cell Transplant*, 2010. **19**(2): p. 219-30.
409. Nystedt, J., et al., *Cell Surface Structures Influence Lung Clearance Rate of Systemically Infused Mesenchymal Stromal Cells*. *STEM CELLS*, 2013. **31**(2): p. 317-326.
410. Suhett, G.D., et al., *99m-Tcnetium binding site in bone marrow mononuclear cells*. *Stem Cell Res Ther*, 2015. **6**(1).
411. Guo, Y., et al., *Assessment of the green fluorescence protein labeling method for tracking implanted mesenchymal stem cells*. *Cytotechnology*, 2012. **64**(4): p. 391-401.
412. Colosimo, A., et al., *Characterization, GFP Gene Nucleofection, and Allotransplantation in Injured Tendons of Ovine Amniotic Fluid-Derived Stem Cells*. *Cell Transplantation*, 2013. **22**(1): p. 99-117.
413. Weir, C., et al., *Mesenchymal stem cells: isolation, characterisation and in vivo fluorescent dye tracking*. *Heart Lung Circ*, 2008. **17**(5): p. 395-403.
414. Hay, M., et al., *Clinical development success rates for investigational drugs*. *Nat Biotechnol*, 2014. **32**(1): p. 40-51.
415. Brodniewicz, T. and G. Gryniewicz, *Preclinical drug development*. *Acta Pol Pharm*, 2010. **67**(6): p. 578-85.
416. Spanjol, J., et al., *Surgical technique in the rat model of kidney transplantation*. *Coll Antropol*, 2011. **35 Suppl 2**: p. 87-90.

417. Bertolotti, A.M., et al., *Successful circumferential free tracheal transplantation in a large animal model*. *J Invest Surg*, 2012. **25**(4): p. 227-34.
418. Thureau, K., C. Vogt, and H. Dahlheim, *Renin activity in the juxtaglomerular apparatus of the rat kidney during post-ischemic acute renal failure*. *Kidney Int Suppl*, 1976. **6**: p. S177-82.
419. Oxburgh, L. and M.P. de Caestecker, *Ischemia-reperfusion injury of the mouse kidney*. *Methods Mol Biol*, 2012. **886**: p. 363-79.
420. Zhang, J., et al., *Administration of dexamethasone protects mice against ischemia/reperfusion induced renal injury by suppressing PI3K/AKT signaling*. *Int J Clin Exp Pathol*, 2013. **6**(11): p. 2366-75.
421. Zhang, C., et al., *Rapamycin protects kidney against ischemia reperfusion injury through recruitment of NKT cells*. *J Transl Med*, 2014. **12**: p. 224.
422. Maiga, S., et al., *Renal auto-transplantation promotes cortical microvascular network remodeling in a preclinical porcine model*. *PLoS One*, 2017. **12**(7): p. e0181067.
423. Giraud, S., et al., *Contribution of large pig for renal ischemia-reperfusion and transplantation studies: the preclinical model*. *J Biomed Biotechnol*, 2011. **2011**: p. 532127.
424. Zhao, Z., et al., *Increased peripheral and local soluble FGL2 in the recovery of renal ischemia reperfusion injury in a porcine kidney auto-transplantation model*. *J Transl Med*, 2014. **12**: p. 53.
425. Doi, A., et al., *Effect of cell permeable peptide of c-Jun NH2-terminal kinase inhibitor on the attenuation of renal ischemia-reperfusion injury in pigs*. *Transplant Proc*, 2013. **45**(6): p. 2469-75.
426. Parajuli, N., et al., *MitoQ blunts mitochondrial and renal damage during cold preservation of porcine kidneys*. *PLoS One*, 2012. **7**(11): p. e48590.
427. Grossini, E., et al., *Levosimendan protection against kidney ischemia/reperfusion injuries in anesthetized pigs*. *J Pharmacol Exp Ther*, 2012. **342**(2): p. 376-88.
428. Koyama, I., et al., *The role of oxygen free radicals in mediating the reperfusion injury of cold-preserved ischemic kidneys*. *Transplantation*, 1985. **40**(6): p. 590-5.
429. Jayle, C., et al., *Protective role of selectin ligand inhibition in a large animal model of kidney ischemia-reperfusion injury*. *Kidney Int*, 2006. **69**(10): p. 1749-55.
430. Thuillier, R., et al., *Thrombin inhibition during kidney ischemia-reperfusion reduces chronic graft inflammation and tubular atrophy*. *Transplantation*, 2010. **90**(6): p. 612-21.
431. Faddegon, S., et al., *Tadalafil for prevention of renal dysfunction secondary to renal ischemia*. *Can J Urol*, 2012. **19**(3): p. 6274-9.
432. Hunter, J.P., et al., *Ischaemic conditioning reduces kidney injury in an experimental large-animal model of warm renal ischaemia*. *Br J Surg*, 2015. **102**(12): p. 1517-25.
433. Hunter, J.P., et al., *Effects of hydrogen sulphide in an experimental model of renal ischaemia-reperfusion injury*. *Br J Surg*, 2012. **99**(12): p. 1665-71.
434. Crane, N.J., et al., *Evidence of a heterogeneous tissue oxygenation: renal ischemia/reperfusion injury in a large animal model*. *J Biomed Opt*, 2013. **18**(3): p. 035001.
435. Simone, S., et al., *Complement-dependent NADPH oxidase enzyme activation in renal ischemia/reperfusion injury*. *Free Radic Biol Med*, 2014. **74**: p. 263-73.
436. Yoon, Y.E., et al., *Preconditioning strategies for kidney ischemia reperfusion injury: implications of the "time-window" in remote ischemic preconditioning*. *PLoS One*, 2015. **10**(4): p. e0124130.
437. Behr, L., et al., *Evaluation of the effect of autologous mesenchymal stem cell injection in a large-animal model of bilateral kidney ischaemia reperfusion injury*. *Cell Prolif*, 2009. **42**(3): p. 284-97.
438. Wright, R.D., et al., *Renal autotransplantation in sheep--preparation and physiology*. *Aust J Exp Biol Med Sci*, 1982. **60**(6): p. 687-99.
439. McDougall, J.G., et al., *Renal autotransplants in sheep: investigation of renal function and renovascular hypertension*. *Clin Exp Pharmacol Physiol*, 1981. **8**(5): p. 497-501.

440. Shin, C.S., et al., *Heparin attenuated neutrophil infiltration but did not affect renal injury induced by ischemia reperfusion*. Yonsei Med J, 1997. **38**(3): p. 133-41.
441. Shin, C.S., et al., *Renal ischemia-reperfusion injury does not induce pulmonary dysfunction in sheep*. Yonsei Med J, 1997. **38**(3): p. 142-50.
442. Nilsson, K.F., et al., *The novel nitric oxide donor PDNO attenuates ovine ischemia-reperfusion induced renal failure*. Intensive Care Med Exp, 2017. **5**(1): p. 29.
443. Stubenitsky, B.M., et al., *Deleterious effect of prolonged cold ischemia on renal function*. Transpl Int, 2001. **14**(4): p. 256-60.
444. Golby, M. and H.J. White, *The operation of orthotopic renal allografting in the pig and its complications*. Br J Surg, 1971. **58**(4): p. 287-8.
445. Terblanche, J., R. Hickman, and C.J. Uys, *Renal transplantation in the unimmunosuppressed pig: an abnormal response*. Br J Surg, 1975. **62**(6): p. 474-9.
446. Scalea, J.R., et al., *Abrogation of renal allograft tolerance in MGH miniature swine: the role of intra-graft and peripheral factors in long-term tolerance*. Am J Transplant, 2014. **14**(9): p. 2001-10.
447. Mitchell, R.M., *Studies on renal transplantation in sheep*. Aust N Z J Surg, 1959. **28**(4): p. 263-73.
448. Mitchell, R.M., B.G. Stevens, and N. Langley, *LENGTHY SURVIVAL OF SHEEP-KIDNEY HOMOGRAFTS AFTER TREATMENT WITH TRIAMCINOLONE*. Lancet, 1963. **2**(7315): p. 982.
449. Pedersen, N.C. and B. Morris, *The role of the lymphatic system in the rejection of homografts: a study of lymph from renal transplants*. J Exp Med, 1970. **131**(5): p. 936-69.
450. Pedersen, N.C., E.P. Adams, and B. Morris, *The response of the lymphoid system to renal allografts in sheep*. Transplantation, 1975. **19**(5): p. 400-9.
451. Grooby, W.L., et al., *Combined anti-vascular cell adhesion molecule-1 and anti-leukocyte function-associated molecule-1 monoclonal antibody therapy does not prolong allograft survival in an ovine model of renal transplantation*. Transplantation, 1998. **66**(7): p. 920-4.
452. O'Donoghue, H., et al., *CYCLOSPORINE A IMMUNOSUPPRESSION IN SHEEP WITH RESPONSE ENHANCEMENT BY CONCOMITANT KETOCONAZOLE*. Clinical and Experimental Pharmacology and Physiology, 1996. **23**(9): p. 797-803.
453. Sun, J.H., et al., *MR tracking of magnetically labeled mesenchymal stem cells in rat kidneys with acute renal failure*. Cell Transplant, 2008. **17**(3): p. 279-90.
454. Jung, S.I., et al., *In vivo MR imaging of magnetically labeled mesenchymal stem cells in a rat model of renal ischemia*. Korean J Radiol, 2009. **10**(3): p. 277-84.
455. Hindle, P., et al., *Perivascular Mesenchymal Stem Cells in Sheep: Characterization and Autologous Transplantation in a Model of Articular Cartilage Repair*. Stem Cells Dev, 2016. **25**(21): p. 1659-1669.
456. Burk, J., et al., *Long-Term Cell Tracking Following Local Injection of Mesenchymal Stromal Cells in the Equine Model of Induced Tendon Disease*. Cell Transplant, 2016. **25**(12): p. 2199-2211.
457. Yoo, J.H., et al., *In vivo cell tracking of canine allogenic mesenchymal stem cells administration via renal arterial catheterization and physiopathological effects on the kidney in two healthy dogs*. J Vet Med Sci, 2011. **73**(2): p. 269-74.
458. Wang, Y.X., S.M. Hussain, and G.P. Krestin, *Superparamagnetic iron oxide contrast agents: physicochemical characteristics and applications in MR imaging*. Eur Radiol, 2001. **11**(11): p. 2319-31.
459. Lo Monaco, M., et al., *Stem Cells for Cartilage Repair: Preclinical Studies and Insights in Translational Animal Models and Outcome Measures*. Stem Cells Int, 2018. **2018**: p. 9079538.
460. Almeida, D., et al., *Comparison between invasive blood pressure and a non-invasive blood pressure monitor in anesthetized sheep*. Res Vet Sci, 2014. **97**(3): p. 582-6.

461. Gatson, B.J., et al., *Effects of premedication with sustained-release buprenorphine hydrochloride and anesthetic induction with ketamine hydrochloride or propofol in combination with diazepam on intraocular pressure in healthy sheep*. *Am J Vet Res*, 2015. **76**(9): p. 771-9.
462. Mlynarik, V., *Introduction to nuclear magnetic resonance*. *Anal Biochem*, 2016.
463. Tognarelli, J.M., et al., *Magnetic Resonance Spectroscopy: Principles and Techniques: Lessons for Clinicians*. *J Clin Exp Hepatol*, 2015. **5**(4): p. 320-8.
464. Koutcher, J.A. and C.T. Burt, *Principles of imaging by nuclear magnetic resonance*. *J Nucl Med*, 1984. **25**(3): p. 371-82.
465. Feng, Y., et al., *Storage of hydrogen spin polarization in long-lived (13)C(2) singlet order and implications for hyperpolarized MRI*. *J Am Chem Soc*, 2013. **135**(26): p. 9632-5.
466. Hendee, W.R. and C.J. Morgan, *Magnetic Resonance Imaging Part I—Physical Principles*. *West J Med*, 1984. **141**(4): p. 491-500.
467. Jensen, E.C., *Technical review, types of imaging, part 4--magnetic resonance imaging*. *Anat Rec (Hoboken)*, 2014. **297**(6): p. 973-8.
468. Zhang, S.X., et al., *Evaluation of the applicability of Resovist in DSC-MR perfusion-weighted imaging of rat hyperacute cerebral infarction*. *Turk Neurosurg*, 2014. **24**(3): p. 344-50.
469. Corot, C. and D. Warlin, *Superparamagnetic iron oxide nanoparticles for MRI: contrast media pharmaceutical company R&D perspective*. *Wiley Interdiscip Rev Nanomed Nanobiotechnol*, 2013. **5**(5): p. 411-22.
470. Nowacki, M., et al., *Long-term influence of bone marrow-derived mesenchymal stem cells on liver ischemia-reperfusion injury in a rat model*. *Ann Transplant*, 2015. **20**: p. 132-40.
471. Wang, W., et al., *Impact of escaped bone marrow mesenchymal stromal cells on extracardiac organs after intramyocardial implantation in a rat myocardial infarction model*. *Cell Transplant*, 2010. **19**(12): p. 1599-607.
472. Jasmin, et al., *Mesenchymal bone marrow cell therapy in a mouse model of chagas disease. Where do the cells go?* *PLoS Negl Trop Dis*, 2012. **6**(12): p. e1971.
473. Eggenhofer, E. and M.J. Hoogduijn, *Mesenchymal stem cell-educated macrophages*. *Transplant Res*, 2012. **1**: p. 12.
474. Lu, W., et al., *Exposure to supernatants of macrophages that phagocytized dead mesenchymal stem cells improves hypoxic cardiomyocytes survival*. *International Journal of Cardiology*, 2013. **165**(2): p. 333-340.
475. Eggenhofer, E., et al., *Mesenchymal stem cells are short-lived and do not migrate beyond the lungs after intravenous infusion*. *Front Immunol*, 2012. **3**.
476. Ma, T., et al., *Upregulation of CC Chemokine Receptor 7 (CCR7) Enables Migration of Xenogeneic Human Adipose-Derived Mesenchymal Stem Cells to Rat Secondary Lymphoid Organs*. *Med Sci Monit*, 2016. **22**: p. 5206-5217.
477. Fan, H., et al., *Pre-treatment with IL-1beta enhances the efficacy of MSC transplantation in DSS-induced colitis*. *Cell Mol Immunol*, 2012. **9**(6): p. 473-81.
478. Plotnikov, E.Y., et al., *Methods of detection of mesenchymal stem cells in the kidneys during therapy of experimental renal pathologies*. *Bull Exp Biol Med*, 2012. **154**(1): p. 145-51.
479. Reinders, M.E., W.E. Fibbe, and T.J. Rabelink, *Multipotent mesenchymal stromal cell therapy in renal disease and kidney transplantation*. *Nephrol Dial Transplant*, 2010. **25**(1): p. 17-24.
480. Sivanathan, K.N., et al., *Interleukin-17A-Induced Human Mesenchymal Stem Cells Are Superior Modulators of Immunological Function*. *STEM CELLS*, 2015. **33**(9): p. 2850-2863.
481. Lee, S., et al., *Activated mesenchymal stem cells increase wound tensile strength in aged mouse model via macrophages*. *Journal of Surgical Research*, 2013. **181**(1): p. 20-24.
482. Gregorini, M., et al., *Mesenchymal stromal cells reset the scatter factor system and cytokine network in experimental kidney transplantation*. *BMC Immunol*, 2014. **15**.
483. Wittwer, T., et al., *Mesenchymal stem cell pretreatment of non-heart-beating-donors in experimental lung transplantation*. *J Cardiothorac Surg*, 2014. **9**.

484. Schnapper, A., et al., *Stereological assessment of the blood-air barrier and the surfactant system after mesenchymal stem cell pretreatment in a porcine non-heart-beating donor model for lung transplantation*. *Journal of Anatomy*, 2018. **232**(2): p. 283-295.
485. Papandrinopoulou, D., V. Tzouda, and G. Tsoukalas, *Lung compliance and chronic obstructive pulmonary disease*. *Pulm Med*, 2012. **2012**: p. 542769.
486. Brown, J., et al., *GLOMERULAR NUMBER AND CAPILLARY DIMENSIONS IN THE NORMAL LAMB KIDNEY*. 2011, 2011. **21**(3): p. 8.
487. Murawski, I.J., R.W. Maina, and I.R. Gupta, *The relationship between nephron number, kidney size and body weight in two inbred mouse strains*. *Organogenesis*, 2010. **6**(3): p. 189-94.
488. Puelles, V.G., et al., *Glomerular number and size variability and risk for kidney disease*. *Curr Opin Nephrol Hypertens*, 2011. **20**(1): p. 7-15.
489. Pourgholaminejad, A., et al., *The effect of pro-inflammatory cytokines on immunophenotype, differentiation capacity and immunomodulatory functions of human mesenchymal stem cells*. *Cytokine*, 2016. **85**: p. 51-60.
490. Lim, C.Y., et al., *Evaluation of autologous bone marrow-derived mesenchymal stem cells on renal regeneration after experimentally induced acute kidney injury in dogs*. *Am J Vet Res*, 2016. **77**(2): p. 208-17.
491. De Becker, A., et al., *Migration of culture-expanded human mesenchymal stem cells through bone marrow endothelium is regulated by matrix metalloproteinase-2 and tissue inhibitor of metalloproteinase-3*. *Haematologica*, 2007. **92**(4): p. 440-9.
492. Lee, J.M., et al., *In vivo tracking of mesenchymal stem cells using fluorescent nanoparticles in an osteochondral repair model*. *Mol Ther*, 2012. **20**(7): p. 1434-42.
493. Zhao, K., et al., *Immunomodulation effects of mesenchymal stromal cells on acute graft-versus-host disease after hematopoietic stem cell transplantation*. *Biol Blood Marrow Transplant*, 2015. **21**(1): p. 97-104.
494. Friis, T., et al., *Mesenchymal stromal cell derived endothelial progenitor treatment in patients with refractory angina*. *Scand Cardiovasc J*, 2011. **45**(3): p. 161-8.
495. Wong, K.L., et al., *Injectable cultured bone marrow-derived mesenchymal stem cells in varus knees with cartilage defects undergoing high tibial osteotomy: a prospective, randomized controlled clinical trial with 2 years' follow-up*. *Arthroscopy*, 2013. **29**(12): p. 2020-8.
496. Zhang, Z., et al., *Human umbilical cord mesenchymal stem cells improve liver function and ascites in decompensated liver cirrhosis patients*. *J Gastroenterol Hepatol*, 2012. **27 Suppl 2**: p. 112-20.
497. Duijvestein, M., et al., *Autologous bone marrow-derived mesenchymal stromal cell treatment for refractory luminal Crohn's disease: results of a phase I study*. *Gut*, 2010. **59**(12): p. 1662-9.
498. Adamzyk, C., et al., *Different Culture Media Affect Proliferation, Surface Epitope Expression, and Differentiation of Ovine MSC*. *Stem Cells Int*, 2013. **2013**: p. 387324.
499. Lang, S., J.E. Murray, and B.F. Miller, *Homotransplantation of ischemic kidneys into dogs with experimentally produced impairment of renal function*. *Plast Reconstr Surg (1946)*, 1956. **17**(3): p. 211-7.
500. Murray, J.E., *The first successful organ transplants in man*. *Journal of the American College of Surgeons*, 2005. **200**(1): p. 5-9.
501. Wang, K., et al., *Pig orthotopic renal allotransplantation model*. *Transplantation Proceedings*, 2003. **35**(1): p. 191.
502. Lassiter, R., et al., *A model of acute renal allograft rejection in outbred Yorkshire piglets*. *Transpl Immunol*, 2017. **42**: p. 40-46.
503. Mundt, H.M., et al., *Optimized donor management and organ preservation before kidney transplantation*. *Transpl Int*, 2016. **29**(9): p. 974-84.

504. Herrera, M.B., et al., *Exogenous mesenchymal stem cells localize to the kidney by means of CD44 following acute tubular injury*. *Kidney Int*, 2007. **72**(4): p. 430-41.
505. Spaeth, E.L., S. Kidd, and F.C. Marini, *Tracking inflammation-induced mobilization of mesenchymal stem cells*. *Methods Mol Biol*, 2012. **904**: p. 173-90.
506. Gao, J., et al., *The Dynamic in vivo Distribution of Bone Marrow-Derived Mesenchymal Stem Cells after Infusion*. *Cells Tissues Organs*, 2001. **169**(1): p. 12-20.
507. Arutyunyan, I., et al., *Elimination of allogeneic multipotent stromal cells by host macrophages in different models of regeneration*. *Int J Clin Exp Pathol*, 2015. **8**(5): p. 4469-80.
508. Lilburn, D.M.L., G.E. Pavlovskaya, and T. Meersmann, *Perspectives of hyperpolarized noble gas MRI beyond (3)He*. *J Magn Reson*, 2013. **229**: p. 173-86.
509. Van Raemdonck, D., et al., *Machine perfusion in organ transplantation: a tool for ex-vivo graft conditioning with mesenchymal stem cells?* *Curr Opin Organ Transplant*, 2013. **18**(1): p. 24-33.
510. Karimian, N. and H. Yeh, *Opportunities for Therapeutic Intervention During Machine Perfusion*. *Current Transplantation Reports*, 2017. **4**(2): p. 141-148.
511. Uzarski, J.S., et al., *Epithelial Cell Repopulation and Preparation of Rodent Extracellular Matrix Scaffolds for Renal Tissue Development*. *J Vis Exp*, 2015(102).
512. Pezzati, D., et al., *Salvage of an Octogenarian Liver Graft Using Normothermic Perfusion: A Case Report*. *Transplant Proc*, 2017. **49**(4): p. 726-728.
513. Nicholson, M.L. and S.A. Hosgood, *Renal transplantation after ex vivo normothermic perfusion: the first clinical study*. *Am J Transplant*, 2013. **13**(5): p. 1246-52.
514. Liu, N., A. Patzak, and J. Zhang, *CXCR4-overexpressing bone marrow-derived mesenchymal stem cells improve repair of acute kidney injury*. *Am J Physiol Renal Physiol*, 2013. **305**(7): p. F1064-73.
515. Liu, N., et al., *Migration of CXCR4 gene-modified bone marrow-derived mesenchymal stem cells to the acute injured kidney*. *J Cell Biochem*, 2013. **114**(12): p. 2677-89.
516. Mundra, V., H. Wu, and R.I. Mahato, *Genetically modified human bone marrow derived mesenchymal stem cells for improving the outcome of human islet transplantation*. *PLoS One*, 2013. **8**(10): p. e77591.
517. Cao, Z., et al., *Protective effects of mesenchymal stem cells with CXCR4 up-regulation in a rat renal transplantation model*. *PLoS One*, 2013. **8**(12): p. e82949.
518. Yang, J.X., et al., *CXCR4 receptor overexpression in mesenchymal stem cells facilitates treatment of acute lung injury in rats*. *J Biol Chem*, 2015. **290**(4): p. 1994-2006.